Hydrogen bonding in organic systems: a study using x-ray and neutron diffraction and database analyses.

Clair Bilton

HYDROGEN BONDING IN ORGANIC SYSTEMS. A STUDY USING X-RAY AND NEUTRON DIFFRACTION AND DATABASE ANALYSES.

Clair Bilton

Thesis submitted in part fulfilment of the requirements for the degree of

Doctor of Philosophy

at the

University of Durham

Department of Chemistry

November 1999

Hydrogen Bonding in Organic Systems. A Study Using X-ray and Neutron Diffraction and Database Analyses

Submitted for the degree of Doctor of Philosophy, November 1999, by
Clair Bilton, University of Durham

ABSTRACT

This thesis covers three topics related to the field of crystal engineering. Three different approaches to improving the understanding of hydrogen bonding are covered; analysis of a family of related molecules, investigations of specific functional groups and a systematic, data-driven study of intramolecular hydrogen bonding patterns.

Chapters 2 to 4 and chapter 11 cover the background theory to the different methods used to obtain the data discussed in the remainder of the thesis. X-ray and neutron diffraction techniques are discussed, along with sections describing the Cambridge Structural Database, which was used as a data source throughout this work, and a brief section on intermolecular forces.

Crystal structure analyses of seventeen *gem*-alkynol molecules are given in chapters 5 to 10. The *gem*-alkynol functionality is particularly interesting for a study of intermolecular interactions as it is a combination of both a strong and weak hydrogen bonding group. The group of molecules was investigated with the aim of locating robust supramolecular motifs. The group is subdivided into sections containing molecules with similar structures and their packing patterns are discussed. The second experimental section, chapters 12 and 13, comprises statistical studies into the function of the azido and cyano functional groups as hydrogen bond acceptors. The technique used was to use the Cambridge Structural Database as a data source for the main analysis, then complement the results with simple theoretical calculations. The remaining chapter, 14, describes a systematic analysis of intramolecular hydrogen bonded motifs. A data-driven approach was designed which allows direct comparison of motifs by means of a probability ordered list.

DECLARATION

The work described in this thesis was carried out in the Department of Chemistry at the University of Durham between October 1996 and September 1999, under the supervision of Prof. Judith A. K. Howard. All the work is my own, unless otherwise stated, and has not been submitted previously for a degree at this, or any other university.

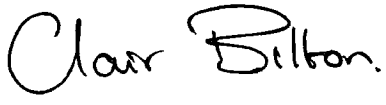

Clair Bilton

ACKNOWLEDGEMENTS

I would like to thank a number of people for a variety of things, for making this thesis possible and making its production a much easier process. Most importantly, my supervisors Prof. Judith Howard and Dr. Frank Allen, for help, support and encouragement throughout the last three years. I am also very grateful to Prof. Gautam Desiraju for his involvement in the joint project which forms a large part of this thesis. Special thanks go to Dr. Ashwini Nangia and his research student Madhavi who supplied all the crystals used for the experimental work.

Dr. Sam Motherwell, Dr. Greg Shields and Dr. Jos Lommerse have been very helpful in dealing with my questions relating to the CSD projects, thanks to Jos for teaching me what I needed to know about CADPAC. Greg deserves special thanks for the work with IMQUEST, developing the program and then fielding my endless questions, his help was invaluable. The assistance of my local contact at the ISIS facility, Dr. Chick Wilson was also appreciated.

The various members of the lab over the last three years have contributed to making it a great place to work. In particular, Claire, Charlie, Dima, John and Mike for making the lab a very happy place in the last year. Thanks also to Gus and Halima for convincing me to stick with it in the beginning.

Finally, thanks to friends and family.

TABLE OF CONTENTS

LIST OF FIGURES

CHAPTER 12 - Azides as Hydrogen Bond Acceptors

CHAPTER 13 - Organic Cyanides as Hydrogen Bond Acceptors

CHAPTER 14 - Intramolecular Hydrogen Bonding

LIST OF TABLES

LIST OF ABBREVIATIONS

BSSE	Basis Set Superposition Error
CCD	Charge-coupled device
CCR	Closed-cycle refrigerator
CSD	Cambridge Structural Database
CSDS	Cambridge Structural Database System
HFBR	High Flux Beam Reactor
ILL	Institut Laue Langevin
IMPT	Intermolecular Perturbation Theory
ICSD	Inorganic Chemical Structure Database
IUCr	International Union of Crystallography
NADB	Nucleic Acid Data Bank
PDB	Protein Data Bank
RAHB	Resonance assisted hydrogen bonding

Introduction

CHAPTER 1

1.1 Crystals as supramolecules

A crystal structure is the result of recognition processes that assemble molecules into the same structural arrangement throughout the bulk sample. It is a collection of millions of molecules arranged in a periodic fashion such that the total free energy of the system is at a minimum. The crystal structure can be described as the ideal supermolecule, the "supramolecule *par excellence*" (Dunitz, 1991). It is a near perfect assembly of molecules, ordered with high precision and held in this way by medium and long range non-covalent interactions.

If molecules are assemblies of atoms, linked by covalent bonds, supermolecules can be described as assemblies of molecules, linked by non-covalent bonds. Simply, molecules (or structural sub-units) are the 'building blocks' and the intermolecular interactions are the 'cement' holding them together. This makes supramolecular chemistry, the "chemistry of the intermolecular bond" (Lehn, 1988). Although supermolecules are built from molecules, their structure and properties are quite different from those of the constituent molecules. Supramolecular chemistry uses this to develop structures with specific properties such as second harmonic generation activity or non-linear optical properties (Ledoux & Zyss, 1997). A vibrant branch of chemistry has grown, creating 'designer molecules' with particular desired attributes.

1.2 Crystal engineering

Designing structures, deliberately built-up using non-covalent interactions, demands a thorough understanding of such interactions. Crystal engineering (Schmidt, 1971) is concerned with the understanding of intermolecular interactions, their role in crystal packing and the use of this knowledge in molecular design. The aim of crystal engineering is to perform the supramolecular equivalent of organic retrosynthesis (Desiraju, 1995). Retrosynthesis involves breaking the target molecule down into small structural units, or synthons, which can be built into the target molecule by means of synthetic reactions. Crystal engineering involves identifying equivalent 'supramolecular synthons' which can be built-up into supermolecules by means of intermolecular interactions.

The term 'synthon' in the context of organic synthesis was introduced by Corey in 1967:

> *"structural units within molecules which can be formed and/or assembled by known or conceivable synthetic operations"*

This definition was easily translated to apply to supramolecular synthons by Desiraju in 1995:

> "structural units within supermolecules which can be formed and/or assembled by known or conceivable synthetic operations involving intermolecular interactions"

Supramolecular synthons can be created by careful positioning of functional groups within the molecular skeleton in such a way that intermolecular interactions between such functional groups will lead to the formation of an extended network. The nodes of the network are the molecules and intermolecular interactions between the molecules are the nodal connections. Examples of supramolecular networks and synthons are shown in Figure 1.1.

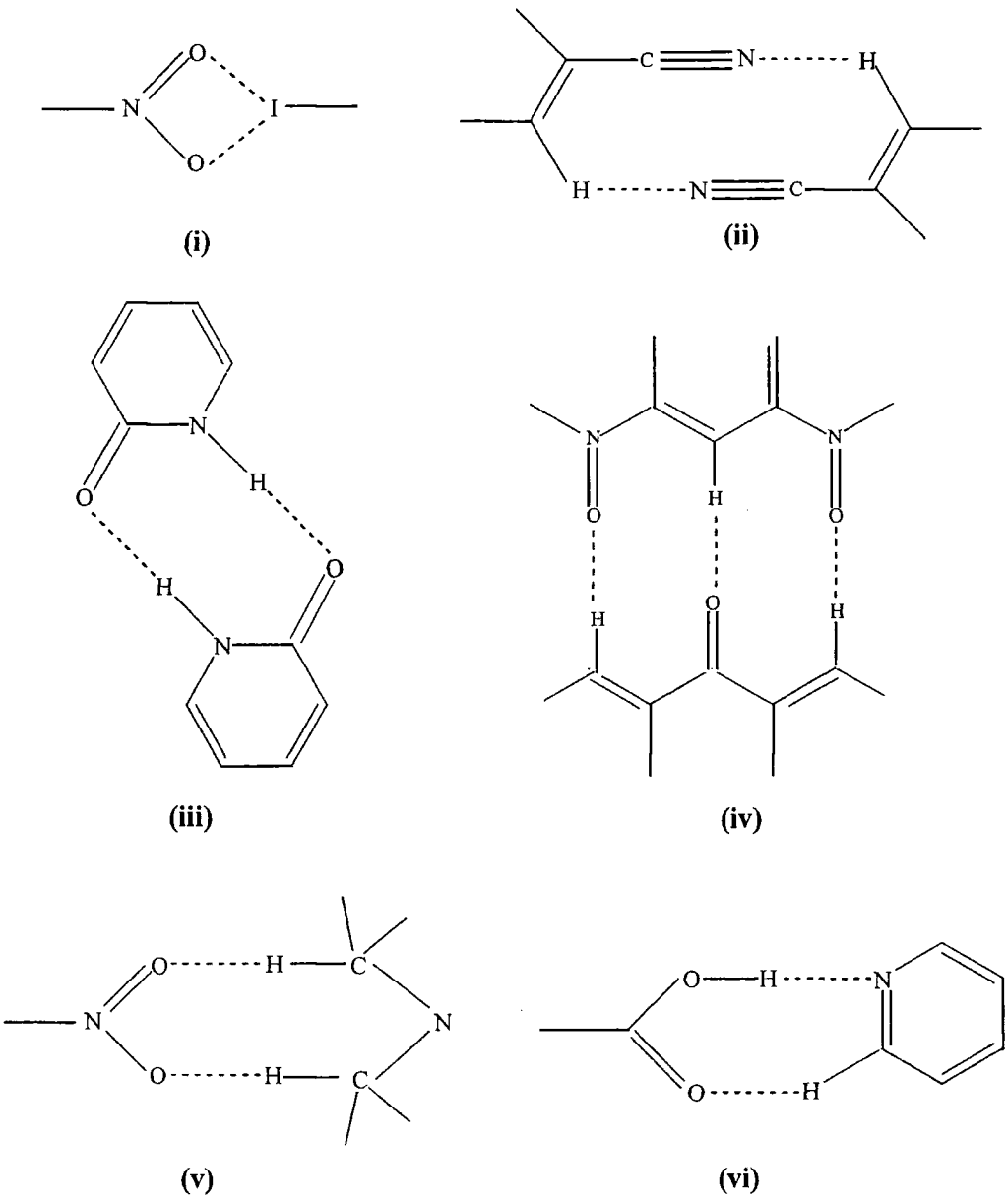

Figure 1.1 - Supramolecular synthons

(i) Pedireddi, Sarma & Desiraju, (1992); Allen, Goud, Hoy, Howard & Desiraju, (1994).

(ii) Guth, Heger & Drück, (1982).

(iii) Ducharne & Wuest, (1988).

(iv) Birada, Sharma, Panneerselvam, Shimoni, Carrell, Zacharias & Desiraju, (1993).

(v) Sharma & Zaworotko, (1996).

(vi) Sharma & Desiraju, (1994).

The ideal supramolecular synthon should be sufficiently robust to be transferred between different networks. Predictability is the key to identification of a suitable synthon, the pattern of intermolecular interactions displayed by a synthon must be consistent, if it is not reproducible in different systems then it is of limited use. Although the concept of building structures using synthons is simple, crystal structures themselves are far from simple. In theory, considering the range of possible interactions that could occur in each structure, a crystal structure could be assembled in an infinite number of ways. The fact that most crystals in a batch have crystallised in the same arrangement suggests that the molecular recognition processes which lead to stable structures are very selective. However, given a particular molecule, it is difficult to predict which of the variety of possible interactions will influence the formation of the crystal structure. It is only through increasing our understanding of intermolecular interactions themselves that can we hope to use them to our advantage in the design of functionalised molecular solids with specific properties.

Traditional, strong interactions such as O-H ---O have been used in the design of synthons with a reasonable degree of success (Aakeroy & Nieuwenhuyzen, 1994; Aakeroy & Hitchcock, 1993). Weak interactions such as C-H --- O and those involving π-electron systems such as phenyl rings and triple bonds are less well understood and generally less reproducible. However, weaker interactions still have their part to play in the greater scheme of crystal packing and it is a challenge to make use of them in the design process (Macias, Rath & Barton, 1999;. Kuduva, Craig, Nangia & Desiraju, 1999; Langley, Hulliger, Thaimattam & Desiraju, 1998).

1.3 Scope of this thesis

There are several techniques available to the crystal engineer to use to learn more about potential supramolecular synthons. Such methods include statistical analysis, theoretical work, diffraction studies and a range of spectroscopic techniques. The work presented in this thesis can be divided broadly into three sections, each using a different method to understand synthons and hydrogen bonding using single crystal diffraction.

The first method is the synthetic approach. A series of small molecules are synthesised, each containing a structural sub-unit of interest as a potential supramolecular synthon. This allows the study of the unit as a whole rather than the interactions of the individual functional groups that comprise it. The result is an overall picture of the crystal packing of that unit. The aim with a study of this type is to find a common pattern within the crystal packing of each molecule, to gauge how useful that structural unit will be as a supramolecular synthon. The structural unit

chosen has the potential to display both strong and weak intermolecular interactions and so provides an interesting study. Not only does it present the opportunity to search for reproducible hydrogen bonding patterns, the effect of competition between weak and strong interactions can be investigated along with the possibility that the interactions could work co-operatively. The series of small molecules were carefully chosen to avoid any unwanted competing potential hydrogen bonds.

The second method is the traditional study of functional groups as hydrogen bond donors and/or acceptors. Chapters 12 and 13 contain statistical surveys of two different functional groups using the information contained within the CSD (Allen & Kennard, 1993). Many other functional groups that participate in intermolecular interactions have also been studied in this way (Lommerse, Price & Taylor; Howard, Hoy, O'Hagan & Smith). The CSD is a valuable source of structural information about a large number of compounds; the October 1998 release for instance contains data for approximately 200,000 compounds. Studies of this kind provide the groundwork on which more detailed research into specific uses of the functional groups as structural design elements can be based. In order to use such groups in specific situations, it is first necessary to understand their hydrogen bonding potential in general terms. The length of a typical hydrogen bond involving the group, the directionality of the interaction and preferred acceptance site if the group has a choice of potential acceptor sites are all useful knowledge. It is only through a thorough understanding of the basics of hydrogen bonding that the crystal engineer can hope to tailor interactions for their own purposes. The two groups chosen for this study are both hydrogen bond acceptors and would be expected to form weak hydrogen bonds. They are both of interest as they contain more than one possible site for acceptance of the hydrogen

bond, atomic sites and π-electron density. Simple single point theoretical calculations with small model molecules were also performed to complement the database results.

The approach taken in the final section is quite different from the previous two. Whilst there are benefits to studying individual functional groups or potential synthons in seclusion, it is difficult to use those results to provide a direct comparison between different synthons. An ideal way to compare synthons is a general survey of all possible synthons and to obtain their probability of formation in each case. Again the CSD provides an ideal source of data for such a systematic survey, with a wealth of data on such a range of compounds, it can be used for a systematic but data driven survey. A study of intermolecular hydrogen bonding patterns has been carried out using this method by Allen, Motherwell, Raithby, Shields & Taylor, 1999. The work in this thesis is an analogous study of intramolecular hydrogen bonding patterns. Intramolecular hydrogen bonding has not received much attention in the literature other than mere observations so there is much interest in a survey of intramolecular patterns.

REFERENCES

Aakeroy, C. B. & Hitchcock, P. B., (1993). *J. Mat. Chem.*, **3**, 11, 1129-35.

Aakeroy, C. B. & Nieuwenhuyzen, M., (1994). *J. Am. Chem. Soc.*, **116**, 24, 10983-91.

Allen, F. H., Goud, B. S., Hoy, V. J., Howard, J. A. K. & Desiraju, G. R., (1995). *J. Chem. Soc. Chem. Commun.*, 2729-30.

Allen, F.H. & Kennard, O., (1993). *Chemical Design Automation News*, **8** (1), 1 & 31-37,.

Allen, F. H., Motherwell, W. D. S., Raithby, P. R., Shields, G. P. & Taylor, R., (1999). *New. J. Chem.*, **23**, 1, 25-34.

Birada, K., Sharma, C. V. K., Panneerselvam, K., Shimoni, L., Carrell, H. L., Zacharias, D. E. & Desiraju, G. R., (1993). *J. Chem. Soc. Chem. Commun.*, **19**, 1473-5.

Corey, E. J., (1967). *Pure Appl. Chem.*, **14,** 19.

Desiraju, G. R., (1995). *Angew. Chem. Int. Ed. Eng.*, **34**, 2311-27.

Ducharne, Y & Wuest, J. D., (1988). *J. Org. Chem*, **53**, 5789.

Dunitz, J. D., (1991). *Pure Appl. Chem.*, **63**, 2, 177-85.

Guth, H, Heger, G. & Drück, U., (1982). *Z. Kristallogr.*, **159**, 185.

Howard, J. A. K., Hoy, V. J., O'Hagan, D. & Smith, G. T. (1996). *Tetrahedron*, **52**, 12613-12622.

Kuduva, S. S., Craig, D. C., Nangia, A. & Desiraju, G. R., (1999). *J. Am. Chem. Soc.*, **121**, 9, 1936-44.

Langley, P. J., Hulliger, J., Thaimattam, R. & Desiraju, G. R., (1998). *New. J. Chem.*, 1307-9.

Ledoux, I & Zyss, I., (1997). *Novel Optical Materials and Applications*. Ed. I. C. Ichao, F. Simoni & C. Umeton, p 1-48, Chichester: Wiley.

Lehn, J-M., (1988). *Angew. Chem. Int. Ed. Engl*, **27**, 90-112.

Lommerse, J. P. M. Price, S. L. & Taylor, R. (1997). *J. Comput. Chem.*, **18**, 757-774.

Macias, R., Rath, N. P, Barton, L., (1999). *J. Organomet. Chem.*, **581**, 1-2, 39-44.

Pedireddi, V. R., Sarma, J. A. R. P. & Desiraju, G. R., (1992). J. *Chem. Soc. Perkin Trans.* 2, 311.

Schmidt, G. M. J., (1971). *Pure Appl. Chem.*, **27**, 647-78.

Sharma, C. V. K. & Desiraju, G. R. (1994). J. *Chem. Soc. Perkin Trans.* 2, **11**, 245-52.

Sharma, C. V. K. & Zaworotko, M. J., (1996). *J. Chem, Soc. Chem. Commun.*, 2655 -6.

CHAPTER 2

2.1 Single crystal diffraction

The first step towards the development of the field of single crystal X-ray diffraction was made in 1895 by Röntgen with the discovery of X-Rays. In 1912, Friedrich, Knipping and Laue proved that X-rays have a wavelike nature and can be diffracted by matter. Their first X-ray diffraction experiment was performed with a single crystal of copper sulphate. A single crystal is a solid with an arrangement of atoms that is periodic in all three dimensions; the smallest repeating unit is known as the unit cell. If a unit cell is thought of as a single point, the array of points that repeats regularly in all three directions is the crystal lattice. W. L. Bragg, in 1913, showed that diffraction could be used to determine the atomic arrangement in crystals. He made the analogy that, in terms of diffraction, the lattice planes within the crystal behave as mirrors and the diffracted beam appears to be 'reflected' off the lattice planes. As part of his experiments he demonstrated the relationship between the beam wavelength λ, the spacing between the lattice planes, d, and the angles of incidence of reflection θ. The relationship is expressed by the Bragg equation.

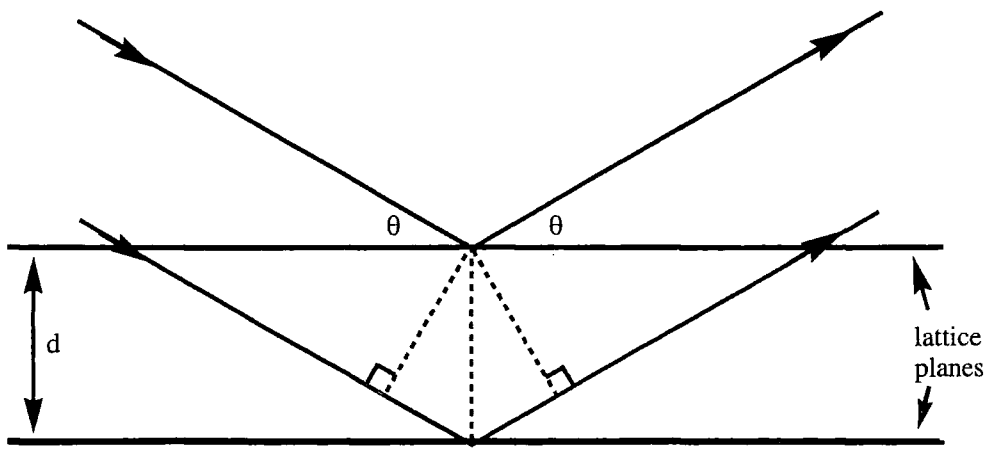

Figure 2.1 - Diffraction from parallel crystal lattice planes

Bragg's Law $n\lambda = 2d\sin\theta$

Diffraction occurs when radiation passes through a grating with dimensions comparable to the wavelength of the radiation. X-rays are ideal for use with the crystal lattice as a diffraction grating as their wavelengths are similar to the atomic spacings, of the order 10^{-9} m or 1Å.

2.2 X-ray generation

X-rays are produced by bombarding a metal target with fast moving electrons, the resulting decrease in kinetic energy is released as radiation. A continuum of radiation, white radiation, is produced due to the collision, along with sharp emission lines, specific to the type of metal target. On collision, some electrons impact with enough energy to eject electrons from the inner shells of the metal atoms and ionise the atom. Higher energy outer shell electrons drop down to replace them and emit their excess energy. This specific energy loss produces peaks in the emission spectrum characteristic of that metal atom. These characteristic X-rays are used for the diffraction experiment.

The characteristic radiation typically contains several emission lines. All but one of these lines, along with the white radiation, must be eliminated to produce a suitable monochromatic beam. The two most commonly used target materials in the laboratory are Cu-Kα with an emission line at 1.5418×10^{-10} m and Mo-Kα at 0.71069×10^{-10} m. A monochromator, for example, graphite for Mo-Kα, is used to eliminate the unwanted radiation. A collimator is then used to produce a narrow beam of radiation

of known diameter. The diameter is chosen carefully to maximise the exposure of the crystal to the beam and minimise background radiation.

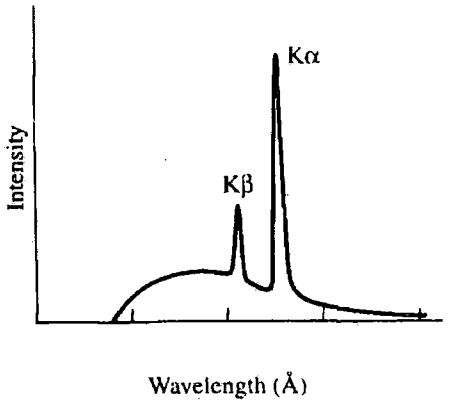

Figure 2.2 -Output from a typical X-ray tube

2.3 Diffraction geometry

In the diffraction experiment, the crystal is bathed in the beam produced by the X-ray source, the diffracted beam is collimated and measured by the detector. The remainder of the direct beam is collected by the beam stop. The set-up is represented by a simple schematic in Figure 2.3.

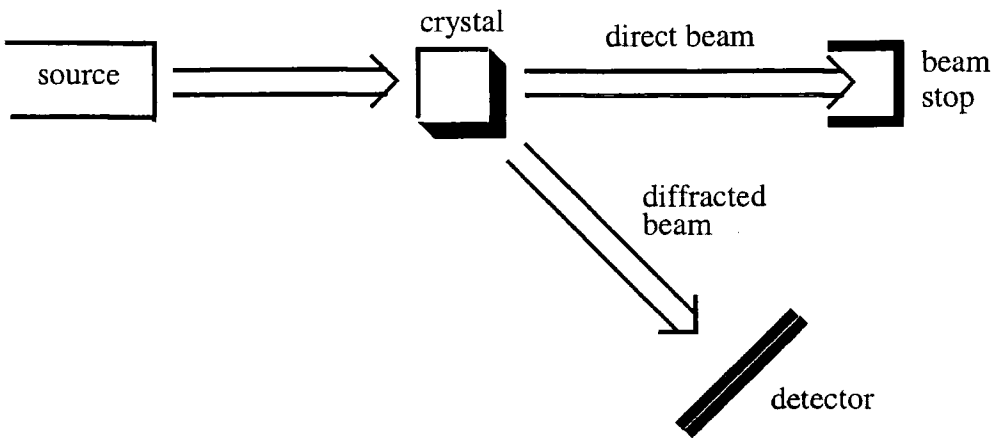

Figure 2.3 Simplified experimental set-up.

Diffractometer geometry is represented by three Eulerian angles which define three-dimensional space. ϕ, χ, and ω and a fourth, 2θ, relating to motion of the detector. ϕ is the rotation about the axis of the goniometer head, χ is the rotation of the whole goniometer head, ω is the angle of rotation about the χ circle and 2θ is the rotation of the detector about the whole assembly.

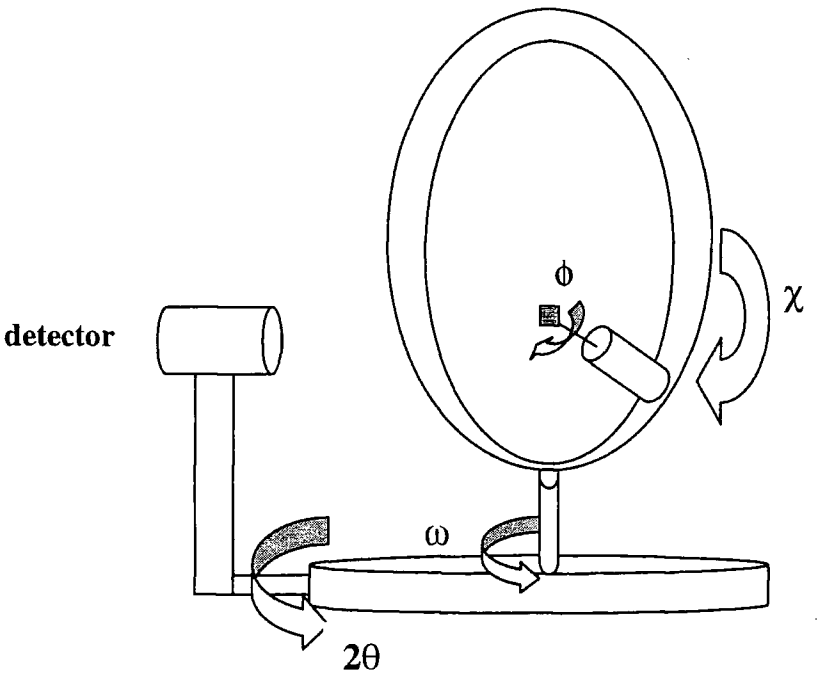

Figure 2.4 - Representation of Eulerian circles

2.4 Area detectors

The type of diffractometer used to perform all the X-ray diffraction experiments contained within this thesis was an area detector. The area detector diffractometer can be thought of as a three-circle instrument as the device used to record the diffraction image fills the role of both the 2θ and χ-circles. Unlike point detectors which are used on four-circle diffractometers, area detectors record diffraction in two dimensions. A

number of reflections are recorded simultaneously, the whole diffraction pattern is recorded, not just the Bragg reflections. Advantages of this method include much shorter experimental time due to the recording of several reflections at once. In addition, as the whole pattern is recorded it is not necessary for the detector to determine the likely position of reflections and position itself accordingly, therefore it is not necessary to determine the correct orientation matrix prior to data collection.

2.5 Experimental methods

The basic methods and principles of the single crystal X-ray diffraction experiment using a CCD area detector are outlined in the following sections. More detail about the theory and methods can be found in a variety of texts, for example Glusker and Trueblood, Woolfson or Arndt and Willis.

2.5.1 Crystal selection and mounting

Time taken in the initial stages to chose a suitable crystal can save time later in the experiment and also reflect on the quality of the final experimental solution. Crystals were screened using a polarising microscope to check for any obviously twinned samples. When rotated in the plane of polarised light, single crystals should extinguish light sharply and completely. If the change is not sharp or complete, the crystals are likely to be twinned. Care should be taken as cubic crystals will not extinguish polarised light and tetragonal or hexagonal crystals also will not when viewed along their c axis. Crystals were also screened on appearance, so that those which were curved, deformed or had large crystallites attached were rejected where

possible. The ideal crystal dimensions are dependant on the beam collimator diameter and the contents of the unit cell. The crystal should be smaller than the collimator diameter in order to immerse all the crystal in the beam but not too small as this will increase the relative level of the background radiation. A larger crystal will bring more problems with absorption but the scattering power of the crystal also increases with volume so these effects must be balanced against each other. Ideal dimensions for organic crystals are 0.1 to 0.5 mm on edge. Crystals were selected with dimensions in this range or larger crystals were cut suitably.

All crystals were mounted on glass fibres secured into brass pips with plasticine and epoxy resin. The glass fibre should be sufficiently thin to minimise absorption effects but thick enough for rigid support. The crystals were glued to the end of the glass fibre with epoxy resin. All crystals reported in this thesis were air and moisture stable, but alternative methods do exist for the mounting of crystals with such sensitivities. The mounted crystals were then attached to the goniometer head which was then screwed onto the diffractometer. The crystal was optically adjusted so that it was positioned in the centre of the path of the X-ray beam and the centre of rotation of all goniometer axes.

2.5.2 Bruker SMART CCD

All X-ray experiments discussed in this thesis were performed using a Bruker SMART CCD diffractometer. The instrument uses a graphite monochromator and typically runs with a 0.8 mm beam collimator. The diffractometer has only three

Eulerian circles, it has no χ-circle, the value of χ is fixed at 54.74°. A charge coupled device (CCD) is a semi-conductor which stores electrons. There is a phosphor screen on the front face of the detector which converts X-rays to optical photons, the photons are transmitted down fibre optic cable to the CCD chip which converts the photons to stored electrons. The detector is a 512 x 512 pixel scintillation area detector.

2.5.3 Searching and indexing

The indexing and data collection procedures using the Bruker CCD are largely automated using the control software SMART (Bruker AXS, 1998). As the detector covers a large area of reciprocal space, the initial search procedure is quite quick. Three different regions of reciprocal space are selected, two of which are orthogonal and a number of frames are measured in each region. The number of frames to be collected and exposure times are set by the user. All reflections found by this procedure are "thresholded" (ordered in terms of a specified parameter and rejected relative to a certain limit) according to the user specified I/σ limit. The program then tries to index these reflections. If this fails then extra reflections can be collected or the reflections can be manually sorted by a parameter such as intensity and the indexing procedure re-attempted. The procedure for indexing the reflections is known as the 'real space method' (Sparks, 1976, 1982; Clegg, 1984). The method involves taking the three shortest non-coplanar reciprocal lattice vectors from the list of reflections and arbitrarily assigning the indices 100, 010 and 001 to these basis vectors from which an orientation matrix and unit cell can be generated. This unit cell is not necessarily the correct cell but it must be a sub-cell of the correct lattice as all vectors in the true lattice are also vectors in the sub-cell. The program then tests the

indices of the remaining reflections against this cell, if any are found to have fractional values, new basis vectors are assigned. The cell is then refined to a final fit for the reflections using least-squares methods.

2.5.4 Data collection

Data collection using an area detector is a more simple process than when using a point detector. Due to the large volumes of reciprocal space covered simultaneously by one area detector frame, fewer factors need to be considered by the users before commencing the data collection. Data was collected using the ω scans method with a scan step size of -0.3° in ω. As data collection times are typically only a few hours, the collection of standard reflections to gauge crystal decay during the experiment are not so important. A set of 50 standard reflections was collected at the end of each experiment but no crystal decay was observed. An option exists within the software to allow the user to collect a hemisphere of data using a set of pre-determined angular settings. These settings can be altered to collect a full sphere of data if necessary. The exposure time for the frames is set by the user, after consideration of the diffracting ability of the crystal.

All data sets mentioned in this thesis were collected at 150K using an Oxford Cryostreams nitrogen cooling device (Cosier & Glazer, 1986) attached to the diffractometer. Collecting data at low temperature reduces the thermal motion of the atoms, so, in comparison with a higher temperature data collection, more intense reflections will be seen at higher scattering angles. Reduction of thermal motion is also helpful later in the structure refinement process when dealing with disorder.

2.5.5 Data reduction

Before the collected frames are integrated, the unit cell parameters can be refined further using a greater number of reflections. The number of reflections found in the indexing procedure will typically not be more than 100. The SMART software can be used, post data collection, to improve the cell parameters using the reflections collected during the data collection. SMART version 5.054 allows the user to pick up to 999 reflections to improve the model of the unit cell. The reflections can also be used to determine the appropriate average peak profile for the integration process. The reflection spots are analysed in terms of their widths in the x and y directions (plane of the detector plate) along with the full-width-half-maximum of the ω-rocking curve which gives the z direction.

Data reduction or (integration) is the process of converting the raw reflection intensities into structure factor magnitudes. Structure factor magnitudes $|F_{hkl}|$ are related to the intensities I_{hkl} by the following expression:

$$|F_{hkl}| = K\sqrt{\frac{I_{hkl}}{(Lp)(Abs)}}$$

Where L is the Lorentz correction, p is the polarisation correction, Abs is the absorption correction and K is a scale factor. The scale factor is a combination of several factors relating to the crystal and the radiation used. The Lorentz and polarisation corrections are purely geometric factors. The Lorentz correction corrects for the relative time each reflection spends in the diffracting position. The polarisation

correction accounts for the partial polarisation of the beam by the monochromator crystal.

2.5.6 Absorption correction

When X-rays pass through a crystal, the beam is attenuated as a result of absorption by the atoms in the crystal. The absorption is dependant on the wavelength of the radiation, the contents and volume of the unit cell and the path length of the diffracted beam through the crystal. An absorption correction is important for crystals containing strongly absorbing materials and those that are anisotropic in shape. A common experimental absorption correction used is a semi-empirical correction involving ψ scans. The method involves tracking the variation in intensity as the crystal is rotated about the diffraction vector. The intensity will vary with angle due to absorption effects, an absorption curve can be generated to correct for absorption as a function of the orientation of the crystal.

The absorption corrections applied as part of this work were at the post data reduction stage. The two corrections used were the ψ-scan correction available within XPREP (Sheldrick ,1997) and SADABS (Sheldrick, 1996). The ψ-scan correction uses the directional cosines of the incident and diffracted beams to calculate the mean path length through the crystal for each reflection. This is used to adjust the intensities to account for absorption. The second correction, SADABS, is a program written for CCD diffractometers. The program corrects for several factors specific to area detectors. The primary correction compares the intensities of equivalent reflections to gauge the scaling of the intensities needed to account for absorption. It is therefore

advisable to have a good data redundancy in order to even out any non-absorption related random errors.

2.5.7 Extinction correction

The effect of absorption is to attenuate the X-ray beam as it passes through the crystal but there is an additional effect that contributes to attenuation and this is extinction. There are two types of extinction, primary and secondary, their effect is to reduce the intensity of strong reflections at low 2θ angles. Primary extinction is the phenomenon of 'double reflection' of the beam as it passes through the crystal, a portion of the beam is reflected a second time by the same set of planes. This destructive interference reduces the intensity of the beam, however this effect only strongly occurs in perfect crystals, i.e., those with no mosaic spread. As very few crystals fit this description, primary extinction can largely be disregarded. Secondary extinction is more common in single crystal experiments, it occurs when the individual mosaic blocks within the crystal are perfectly aligned with respect to the incident beam. The incident beam is reflected by the first planes in the first mosaic block it encounters, the remainder of the beam travels deeper into the crystal to be reflected by the planes in another identically aligned block. The beam received by the deeper planes therefore is less intense than that received by the first planes so they diffract with less intensity. Secondary extinction is most pronounced for high intensity reflections, those at low 2θ. Mosaicity can be increased and thus the effects of extinction reduced by subjecting the crystal to thermal shock such as dipping them in liquid nitrogen.

2.5.8 Space group determination

The program XPREP (Sheldrick, 1997) was used to determine the space group symmetry of the sample. The software uses the cell parameters established prior to the data reduction process, Laue symmetry, Bravais lattice type and systematic absences to determine the correct space group. Systematic absences in a diffraction pattern show the presence of a symmetry element which causes exact destructive interference between diffracted reflections. For example a 2_1 screw axis will generate the situation where reflections with *l* odd are absent. The symmetry element generates equivalent positions at y and y + ½ thus halving the lattice spacing in that direction. Reflections from both positions will be exactly out of phase and so will be absent.

Normalised structure factors (E_{hkl}) in the form $|E^2-1|$ to test for the presence of an inversion centre. Normalised st ıcture factors are structure factors that have been corrected for the fall-off in ıntensity with increasing $\sin\theta/\lambda$ due to atomic size. Typically for a centric distribution the value of $|E^2-1|$ will tend toward 0.97 and for a centrosymmetric distribution it will tend toward 0.74. Comparison of the $|E^2-1|$ for the structure will suggest the presence, or otherwise, of an inversion centre.

2.5.9 Structure solution

The process of data reduction yields the structure factor amplitudes from the measured intensities which subsequently must be converted into an electron density distribution. This conversion is not direct or simple due to the 'phase problem'. The

problem is that the measured intensities lead to just the amplitudes of the structure factors, |F(hkl)|, but the phase information α(hkl) cannot be derived from the experimental data. The phase angles are needed to perform the Fourier synthesis to make the conversion to the electron density distribution

$$\rho(xyz) = \frac{1}{V}\sum_{h}\sum_{k}\sum_{l} |F(hkl)| \cos 2\pi\,(hx + ky + lz - \alpha(hkl)).$$

There are two methods commonly used by single crystal X-ray crystallographers to overcome the phase problem, direct methods (Harker & Kasper, 1948; Karle & Hauptmann, 1950; Sayre, 1952) and Patterson methods (Patterson, 1934).

2.5.10 Direct methods

Direct methods is a statistical method which uses the constraint that electron density is never negative and that it consists of isolated sharp peaks at atomic positions. These constraints restrict the number of possible solutions. Trial phases are assigned to a number of the strongest reflections and possible solutions for the phases of the remainder of the reflections are obtained considering the constraints. Phases that reinforce peaks of negative electron density will be rejected as will those that produce peaks of electron density too close to others. The trial procedure is repeated many times and each solution is given a figure of merit. The assignment of phases with the best figure of merit is used to generate an electron density map from which atomic positions can be found. Unless the structure is very small it is unlikely that all atomic

positions can be found from the initial solution and hydrogen atom positions are unlikely to be found at this stage.

The remainder of the atomic positions are found by means of a difference Fourier synthesis.

$$\rho_{obs} - \rho_{calc} = \frac{1}{V}\sum_{h}\sum_{k}\sum_{l}\Big|\,|F_{obs}(hkl)| - |F_{calc}(hkl)|\,\Big| \cos 2\pi\,[hx + ky + lz - \alpha_{calc}(hkl)]$$

The electron density distribution of the current model (ρ_{calc}) is calculated and this is subtracted for from the observed distribution (ρ_{obs}). The difference density is plotted as a map and the missing atoms appear as additional peaks to those seen in the first solution. Direct methods were used for all X-ray structure solutions presented in this thesis.

2.5.11 Patterson methods

Patterson methods are most commonly used for structures containing heavy atoms. The Patterson function is a Fourier synthesis that uses the squares of the structure factor amplitudes to produce a "vector" map; the expression contains no terms for the phase angle. The term V, in this case and the previous two equations is the cell volume.

$$P(uvw) = \frac{1}{V}\sum_{h}\sum_{k}\sum_{l}|F(hkl)|^2 \cos 2\pi(hu + kv + lw)$$

Unlike the density map produced by direct methods, the peaks in the Patterson map do not correspond to atomic positions but to inter-atomic vectors. The height of each peak is proportional to the product of the atomic numbers of the atoms linked by that vector, and for this reason, heavy atoms dominate the map. There is a large peak at the origin corresponding to a vector between each atom and itself. The peaks corresponding to the heavy atoms can be easily identified and so their atomic positions can be found using space group symmetry. The positions of some of the light atoms can be determined relative to the heavy atoms and a set of trial phases can be produced. The Patterson method relies on discrepancy between atomic weights so this method works best for structures with only a few heavy atoms.

2.5.12 Structure refinement

Structure solution yields an approximate model of the three-dimensional arrangement of the atoms in the structure. The precision of this model must be improved by the refinement process. The role of the refinement is to improve the agreement between the observed and calculated structure factor amplitudes, $|F_{hkl}|_{obs}$ and $|F_{hkl}|_{calc}$, by adjusting the atomic coordinates of the atoms (x, y and z) and the atomic thermal displacement parameters. The method of least squares is used to refine the model. The principle of least squares (Legende, 1805; Gauss, 1809) is to minimise the sum of the squares of the differences between the observed and calculated structure factors. The minimisation function is:

$$D = \sum_{hkl} w_{hkl} (|F_{hkl}|_{obs} - |F_{hkl}|_{calc})^2$$

where w_{hkl} is the weight of the reflection hkl, which is an indication of the precision of the measurement. The refinement is considered to be complete when there is no significant change in the values of the parameters with successive cycles of refinement, i.e. a stable refinement. Two indicators are used to gauge the quality of the refinement, a residual index, R, and a goodness of fit S:

$$R = \frac{\sum_{hkl} \left| |F_{obs}| - |F_{calc}| \right|}{\sum_{hkl} |F_{obs}|}$$

$$S = \sqrt{\frac{\sum_{hkl} w\left(F_{obs}^{\ 2} - F_{calc}^{\ 2}\right)^2}{(N-P)}}$$

where N is the number of reflections use and P is the number of parameters refined. The R-factor is a measure of the agreement between the observed and calculated structure factors, the value of R for a well determined structure should be under 0.08, in general the lower the value the better. For a perfect model, S will equal 1.0. A weighted residual index wR_2 can also be used:

$$wR_2 = \sqrt{\frac{\sum w(F_{obs}^{\ 2} - F_{calc}^{\ 2})^2}{\sum w(F_{obs}^{\ 2})^2}}$$

where w is the weighting of each reflection which is an estimate of the precision of its measurement. Simple weighting schemes such as $1/\sigma^2(|F_{hkl}|_{obs})$ can be used. The weighting scheme used in SHELX (Sheldrick, 1997) has the form:

$$w = \frac{1}{[\sigma^2(F_{obs}^2) + (aP)^2 + (bP)}$$

where $P = (F_{obs}^2 + 2F_{calc}^2)/3$ and a and b are refined during the least squares procedure.

REFERENCES

Arndt, U. W. & Willis, B. T. M. (1966). *Single Crystal Diffractometry.*, Cambridge University Press.

Bragg, W. L.,(1913). *Proc. Camb. Phil. Soc.*, **17**, 43-57.

Bruker AXS (1998). SMART, Area detector control software, Version 5.054, Bruker AXS, Madison, Wisconsin, USA.

Clegg W. (1984). *J. Appl. Cryst*, **17**, 334

Cosier, J. & Glazer, A. M., (1986). *J. Appl. Cryst.*, **19**, 105.

Friedrich, W., Knipping, P. & Laue, M., (1912). *Sitzungsberichteder mathematisch-physikalischen Klasse der Königlichen Bayerischen Akademieder Wissenschaften zu München*, 303-322. English translation : Stezowski, J. J. in *Structural Chemistry in Chemistry and Biology*, (1981), Ed. J. P. Glusker, Hutchinson & Ross, Stroudsburg, PA.

Gauss, C. F., (1809). *Theoria Motus Corporum Caelestiun in Sectionibus Conicus Solum Ambientum*, Perthes et Besser: Hamberg. Taken from *Crystal Structure Analysis for Chemists and Biologists*, (1994). J.P Glusker with M. Lewis & M Rossi, Wiley-VCH.

Glusker, J. P. & Trueblood, K. N., (1985). *Crystal Structure Analysis. A Primer*, 2nd edition, Oxford University Press.

Harker D. & Kasper J. S.,(1948). *Acta Cryst*, **1**, 70.

Karle, J & Hauptmann, H., (1950). *Acta Cryst.*, **3**, 181.

Legende, A. M., (1805). *Appendix. Sur le méthode des moindres quarrés. In : Nouvelles Méthodes pour la Détermination des Orbtites des Comètes*, 72-75,

Courcier: Paris. Taken from *Crystal Structure Analysis for Chemists and Biologists*, (1994). J.P Glusker with M. Lewis & M Rossi, Wiley-VCH.

Patterson, A. L., (1934). *Phys. Rev.*, **46**, 372-376.

Röntgen, W. C., (1895). *Sitzungsberichte der Würzburger Physikalischen-Medizinischen Gesellschaft,* 131-141. English translation: Stanton, A. (1896) *Science*, **3**, 227-231.

Sayre, D., (1952). *Acta Cryst.*, **5**, 60.

Sheldrick, G.M. (1996) *SADABS, Program for the Absorption Correction of X-ray Data,* University of Göttingen, Germany.

Sheldrick, G. M. (1998). *XPREP (in Shelxtl).* Version 5.1. Bruker Analytical X-ray Instruments.

Sparks R. A., (1976). *Crystallographic Computing Techniques*, ed. Ahmed, F.R., Munskgaard, Copenhagen, 452-267.

Sparks, R. A., (1982). *Crystallographic Computing*, ed. Sayre, D., Clarendon Press, Oxford, 1-18.

Woolfson, W. M., (1997). *An Introduction to X-ray Crystallography*, 2nd edition, Cambridge University Press.

Neutron Diffraction

CHAPTER 3

3.1 Historical development of neutron diffraction

Single crystal neutron diffraction began in 1936 when Elsasser demonstrated that the motion of neutrons could be determined by wave mechanics and so, should be diffracted by crystalline material. The first neutron diffraction experiments quickly followed this demonstration, a powder experiment by Halban and Preiswerk (1936) and, shortly after, a single crystal experiment by Mitchell and Powers (1936). Although both experiments proved conclusively that neutrons could be diffracted, the radium-beryllium sources used produced neutrons with insufficient flux to provide any quantitative data. Further progress with the technique was stalled until the development of nuclear reactors in the 1940s. The first neutron diffractometer was built in 1945 at the Argonne National Laboratory in the USA (Zinn, 1947). Since then, several other reactor sources have been established across the world. The early reactor sources were multi-purpose reactors. As the range of applications increased and more flux became necessary, high-flux reactors were design solely for scientific neutron scattering studies. The High Flux Beam Reactor (HFBR) at Brookhaven National Laboratory was opened in 1965 and in 1972 the Institut Max von Laue-Paul Langevin (ILL) started operation. The 1970s saw another major advance in the production of neutrons for use in the diffraction experiment, with the development of pulsed accelerator-based spallation sources. Currently the world's most intense pulsed source of neutrons for condensed matter science is ISIS at the Rutherford Appleton Laboratory in the UK.

3.2 Benefits of using neutron diffraction

The majority of single crystal diffraction experiments are carried out using X-rays. X-ray sources are widely available and convenient for laboratory use whereas neutron beams are only produced at large central facilities, therefore their use has been less widespread. However, the use of neutron radiation has many advantages over X-ray measurements.

In order for neutron radiation to be of use in determining the atomic arrangements, their wavelength must be comparable with atomic spacings. The wavelength of an X-ray beam is dependant on the metal target used to create the beam, characteristic wavelengths are produced such as 0.71069 Å from a molybdenum source. Thermal neutrons have wavelengths typically in the range 0.5 to 10 Å which means that neutrons can be used to study structural features in the range 0.1 to 1000Å. Thermal neutrons also have energies comparable with the energies of atomic movements and so can be used to probe molecular rotations and vibrations and electronic transitions within crystals.

The greatest advantage of using neutrons when studying hydrogen bonding is that neutrons are scattered by the nucleus rather than the electron cloud. The result is that unlike with X-ray diffraction, the scattering power of an atom is not directly related to its atomic number, it is an irregular function. (Figure 3.1). It is easier to locate 'light atoms' such as hydrogen as they scatter just as strongly as the other atoms in the molecule. Other consequences of this are that it is also easier to distinguish between neighbouring atoms in the periodic table as they will have distinctly different

scattering lengths. As scattering is dependant on the nucleus it is also of advantage in isotopic substitution as different isotopes can be easily distinguished.

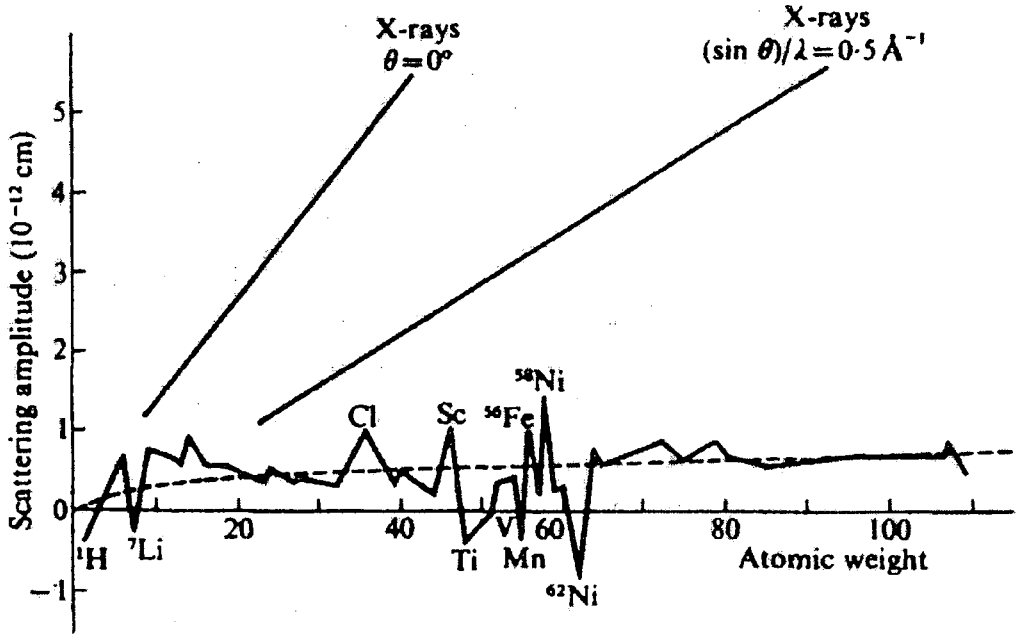

Figure 3.1 - Variation in neutron scattering length with atomic mass.

(Taken from RAL Technical Report RAL-TR-96-083, 1996.)

Neutrons are a non-destructive probe as they interact weakly with matter. As a result, delicate materials can be analysed with no damage. As neutrons are only weakly absorbed by samples, measurements can be carried out in different sample environments such as cryostats, reaction vessels and pressure cells. Neutrons are also a bulk probe, so give information about the interior of materials rather than just the surface layers. Magnetic structure can also be studied as neutrons possess a magnetic moment.

3.3 Neutron production

Many neutron diffraction experiments are carried out at reactor sources where self sustaining fission of uranium in a reactor core is used to produce neutrons. The fast neutrons produced are then passed through a moderator to slow them down to thermal and epithermal energies. The white beam produced is then monochromated and collimated. Most of the intensity is lost before the beam reaches the sample but the flux is still high enough for accurate measurements. Demand for higher flux and less controversial sources has lead to an alternative method of neutron production which is called 'spallation'. Spallation sources are pulsed sources where heavy atom nuclei are bombarded with pulses of protons from a high energy accelerator. By firing protons in batches, discrete pulses of neutrons are produced.

3.4 Spallation sources

The spallation process is based upon an accelerator rather than a reactor core, the process will be described using the ISIS facility as an example. The production of particles of high enough energy to produce spallation is a three stage process. An ion source produces H^- ions which are injected into the linear accelerator where they are accelerated up to 70MeV. As they pass into the synchotron (a circular accelerator) they are stripped of both electrons by an alumina foil to produce a circular proton beam. The beam passes round the synchotron, pushed by electromagnetic fields until it reaches 800MeV. The beam is then kicked out towards the heavy atom target. This process is then repeated 50 times a second to produce a pulsed beam.

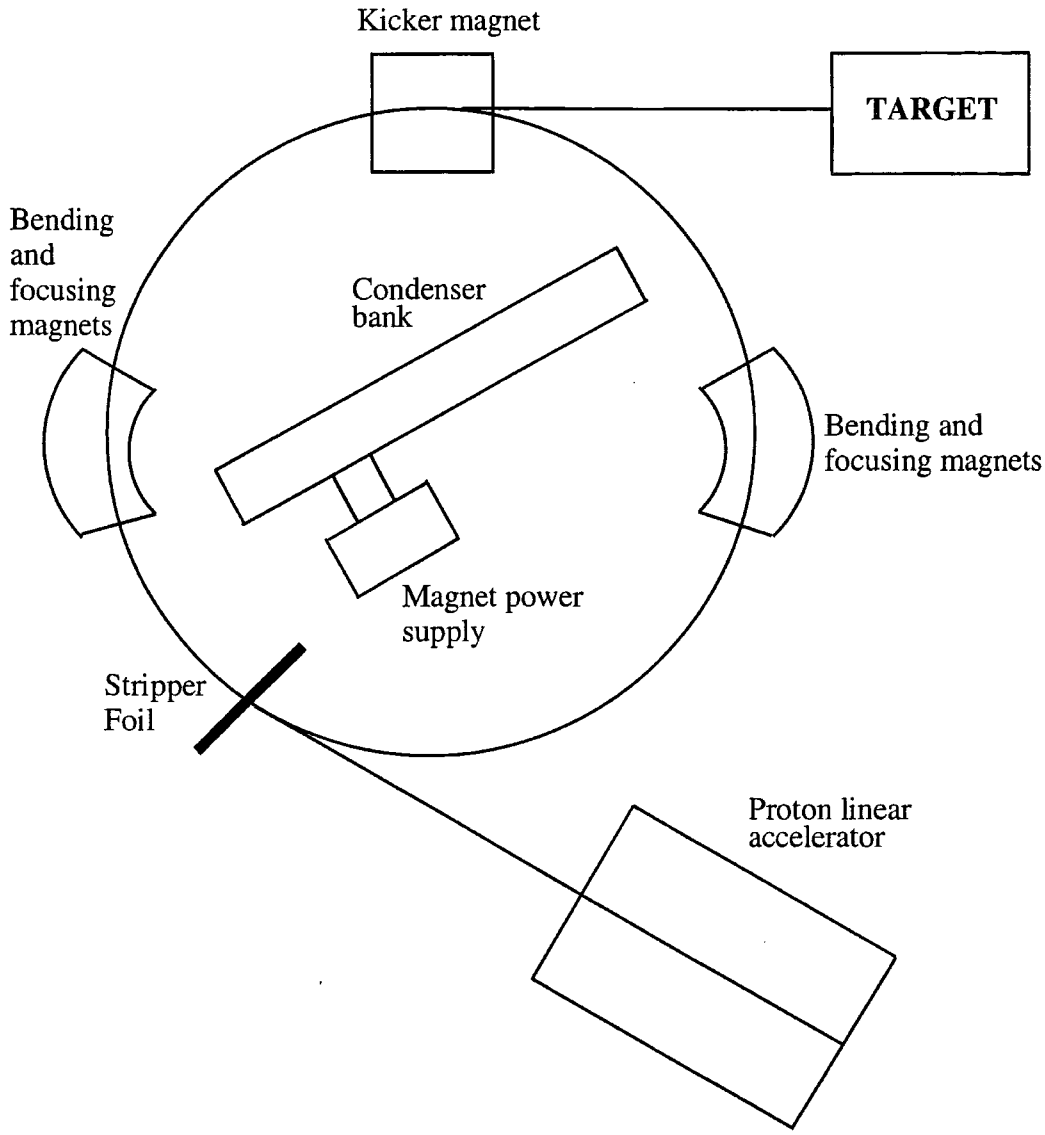

Figure 3.2 - Schematic of the proton spallation process

On impact, each proton generates tens of neutrons by chipping fragments from the heavy metal nucleus. The neutrons produced then have to be passed through a moderator to reduce then to the correct energy range (thermal or close to thermal energies) for experimental use.

Neutrons have a large collision cross-section with hydrogen atoms and therefore hydrogen is the ideal material for use as a moderator. Common materials used as

moderators are water, methane or hydrocarbons. Neutrons collide with the hydrogen atoms and as they are at higher temperature they lose energy to the hydrogen and therefore slow down. The size and temperature of the moderator can be varied to produce the desired wavelength distribution of neutrons. A distribution which contains high energy (i.e. short wavelength) neutrons will allow measurements up to high values of $\sin\theta/\lambda$ and therefore to high resolution in real space.

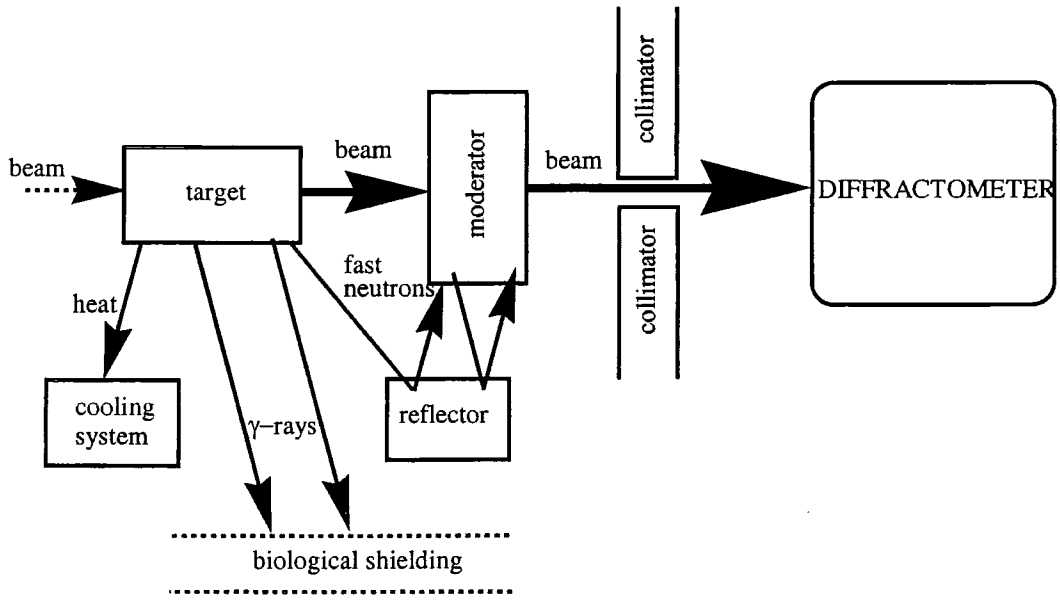

Figure 3.3 - Schematic representation of passage of neutrons from target (pulsed source)

3.5 Time-of-flight Laue Diffraction

The neutron beam emerging from the moderator is a white beam, covering a wide range of wavelengths. As the neutrons are pulsed there is a time (t_O) associated with each neutron, the production time, when the beam hits the target. By measuring the time of detection (t_D) at the instrument, the time of flight ($t_D - t_O$) can be found which

is then used to find the energy of the neutron. Since the distance travelled (L) is fixed, the velocity (v) and therefore the wavelength (λ) can be calculated using the de Broglie equation:

$$\lambda = \frac{ht}{mL}$$

which is a combination of the two equations:

$$v = \frac{L}{t} \qquad \text{and} \qquad \lambda = \frac{h}{mv}$$

where h is Planck's constant and m is the mass of the neutron.

3.6 SXD

SXD (Wilson, 1990) is a time-of-flight single crystal Laue diffractometer at the ISIS facility. The Laue diffraction method involves a stationary single crystal and a beam with a continuous spectrum of wavelengths rather than a single wavelength as with the moving crystal method. In order for diffraction to occur, Bragg's Law must be satisfied. When the incident radiation is composed of a range of wavelengths, the condition will be satisfied for many sets of crystal planes simultaneously. The method used here, time-of-flight Laue diffraction provides a wavelength sorted version of the Laue method. SXD has three large position sensitive detectors, in combination with the time sorted white neutron beam, this allows large volumes of reciprocal space, sorted in both time and space, to be surveyed in a single measurement. The collection of many Bragg reflections simultaneously allows the determination of the cell parameters from a single data frame.

The neutron beam enters SXD through a collimator made of powdered B_4C in resin ('crispy mix'). A range of collimators is available to vary the diameter of the beam between 8 and 15mm. The crystal is mounted on a crystal orientator comprised of two perpendicular circles ϕ and χ in a displex closed cycle refrigerator (CCR) helium cryostat. The cryostat can maintain temperatures from 12 to 300K, the temperature is measured by a Rh-Fe thermocouple. The diffractometer has three large position sensitive detectors each with 192 x 192mm^2 active area and 3 x 3mm^2 resolution. The detectors are fibre-optic encoded ZnS scintillation counters.

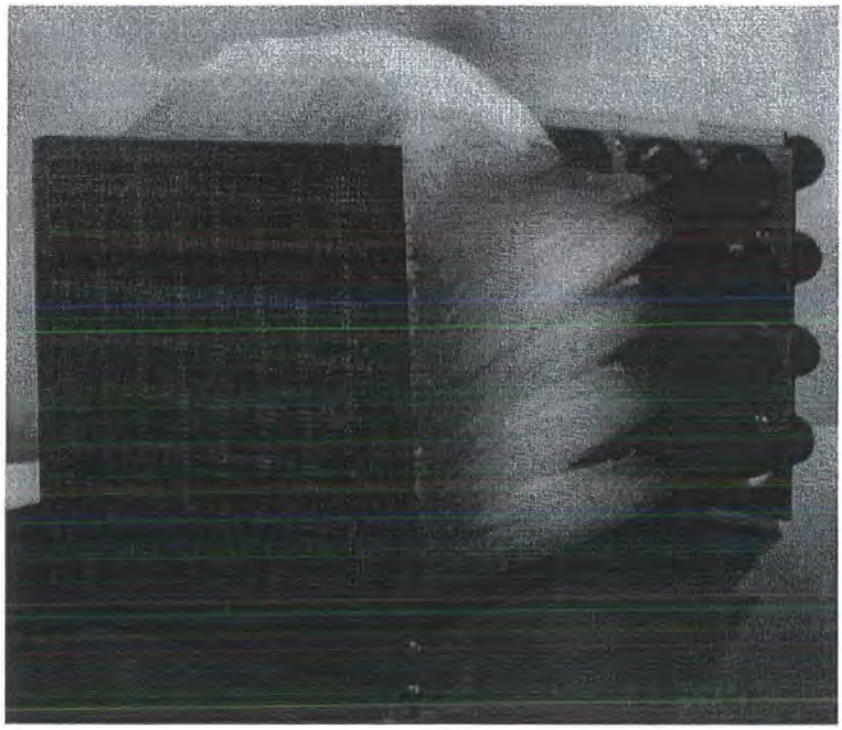

Figure 3.4 - SXD detector.

(Taken from RAL Technical Report RAL-TR-96-083, 1996.)

Only the two main detectors were used for the data collections described in this thesis, the third detector is a recent addition. The main detectors are arranged with one at low angle, 2θ for the detector centre ~ 55° and the other at high angle, 2θ for the detector centre ~ 125°. The third detector sits on the opposite side of the neutron beam to the

other two and may be located at any one of three fixed angles, 2θ for the detector centre ~ 55°, -90° or -125°. Blocks of thick borated polyethene are placed around the instrument to reduce background scattering. Figure 3.5 is a schematic drawing of SXD.

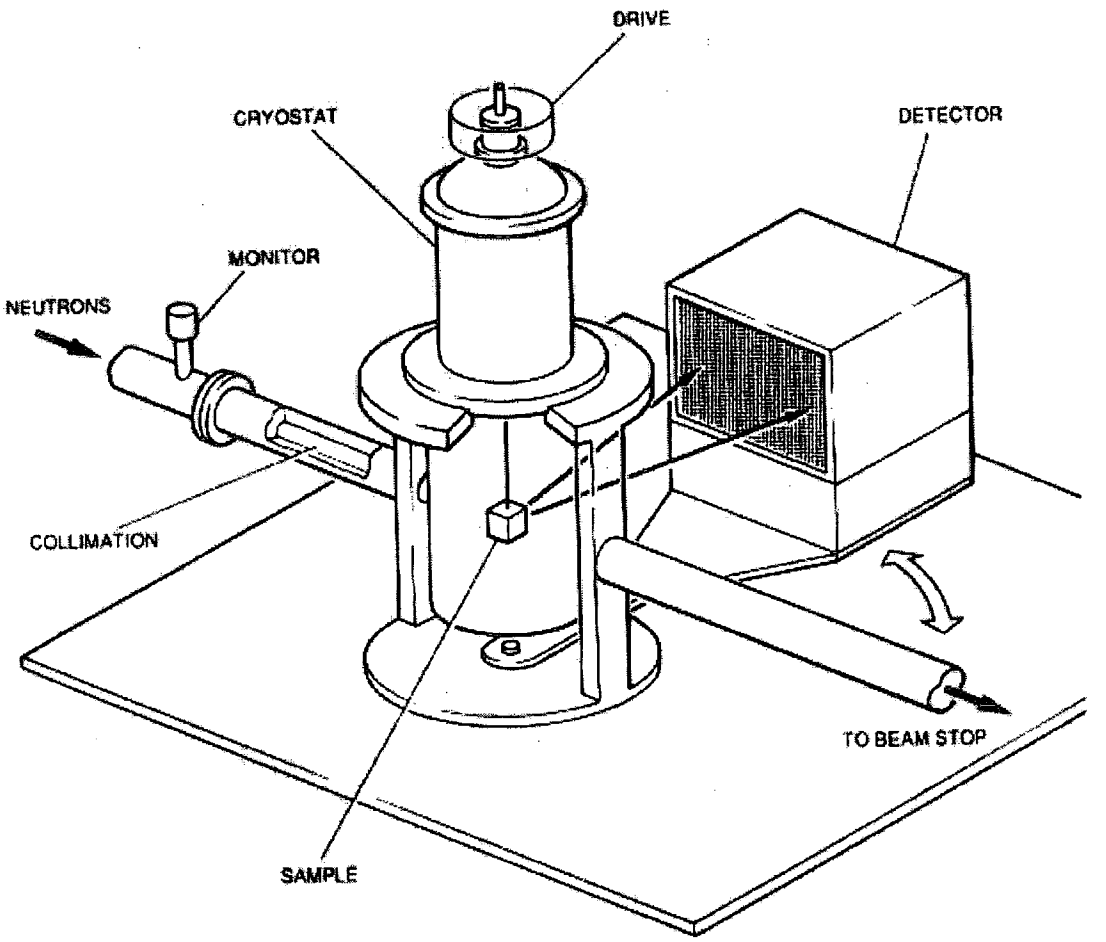

Figure 3.5 - Layout of the SXD diffractometer

(Taken from RAL Technical Report RAL-TR-96-083, 1996.)

3.7 Data collection using SXD

The flux available from the pulsed source at ISIS is much lower than that produced by a standard laboratory X-ray tube. It follows therefore that the crystals used must be

correspondingly larger. Typical size of crystals measured on SXD are between 1 and 100 mm^3 although the minimum sample size is dependant on the contents and size of the unit cell. Crystals are mounted on aluminium pins of 6mm diameter which taper down to 1mm at the sample end. The crystal is glued to the pin using quick setting epoxy resin and as much of the glue as possible is masked by cadmium to reduce hydrogen scattering. The pin is mounted into the CCR head and the position adjusted so that the centre of the sample coincides with the beam centre. As the diameter of the beam is large in comparison with the crystal, additional sample centring is not required.

Data are collected in a series of frames using each detector at a series of χ and ϕ angles to give a good coverage of reciprocal space. The crystal is rotated about 180° in ϕ in steps of 30°. This step size was chosen as 30° is slightly less than the angle subtended by the detector so it ensures that there is some overlap between frames to avoid missing any data. The χ settings used are 2, 27, 54 and 80°. Each frame is typically exposed for between 1 and 6 hours, depending on the sample. As many reflections are determined in each frame it is possible to index a crystal lattice using only one frame.

3.8 Data reduction

Reflections are located using a peak searching routine. The peaks are then integrated using a profile-fitting approach based on the known analytical shape of the reflections in the time-of-flight direction which is well understood from the characteristics of the ISIS source and moderator. The function which is known to produce a good

reproduction of peak shape is Gaussian convoluted with a decay function. This function provides a good fit for both strong and weak reflections. Any reflections for which the peak fitting procedure fails after four attempts with parameter variation are excluded from the data set. The variable parameters of the function which all vary with time-of-flight are Gaussian height and width and also the time constant.

Incoherent scattering from a polycrystalline vanadium sample is used to normalise the reflection intensities to the incident beam profile. At this stage, semi-empirical absorption corrections are applied and the resultant intensities are reduced to structure factors. The CCSL (Brown & Matthewman, 1993) least squares refinement program SFLSQ is used to apply a variable wavelength extinction correction based on the Becker-Coppens formalism (Becker & Coppens, 1974a,b). The corrected structure factors are then merged in the GSAS program (Larsen & von Dreele, 1986). The data can then be refined using a standard structure refinement package such as SHELX. The final R-factor of the refined model is generally found to be higher than that of the model refined using data collected with monochromatic radiation. This is believed to be a consequence primarily of the complex wavelength dependant corrections which have to be applied to the data.

REFERENCES

Becker, P. & Coppens, P. (1974). *Acta Cryst*, **A30**, 129.

Brown, P. J. & Matthewman, J. C. (1993). *Rutherford Appleton Laboratory Report, RAL*-93-009.

Elsasser, W. M. (1936), *C. r. hebd. Séanc. Acad. Sci. Paris*, **202**, 1029. Taken from *Crystal Structure Analysis for Chemists and Biologists*, (1994). J.P Glusker with M. Lewis & M Rossi, Wiley-VCH.

Halban, H. & Preiswerk, P. (1936), *C. r. hebd. Séanc. Acad. Sci. Paris,* **230**, 73. Taken from *Crystal Structure Analysis for Chemists and Biologists*, (1994). J.P Glusker with M. Lewis & M Rossi, Wiley-VCH.

Larsen, A.C. & von Dreele, R.B. (1986). GSAS. Los Alamos National Laboratory Report, LAUR 86-748

Mitchell, D. P. & Powers, P. N. (1936), *Phys. Rev.* **105**, 130.

Shelxtl, Sheldrick, G. M. (1998). Version 5.1. Bruker Analytical X-ray Instruments.

Wilson, C. C. (1990). *Neutron Scattering Data Analysis 1990*, ed. Johnson, M. W., IOP Conference Series Vol 107, Adam Higer, Bristol, 145-163.

Zinn, W. H. (1947), *Phys. Rev.* **71**, 752,

Crystallographic Databases

CHAPTER 4

4.1 Crystallographic databases

In the early years of crystallography, the elucidation of a crystal structure was a laborious process. Few comparative studies of crystal structures were carried out, and those could be manually analysed systematically due to the small number of available structures (Sutton, 1958). In most cases, crystallography was used to establish atomic positions and stereochemistry rather than information about crystal packing or molecular geometry. The early equivalent of the modern crystallographic database were the 'Structure Reports' (Reidel, 1929-1987) which were published by the International Union of Crystallography (IUCr). These Reports recorded bibliographic information, crystal data and atomic coordinates. Increasing automation of data collection and improvement in diffractometer design lead to a steady increase in the number of crystal structure determinations during the 1960s. The increase was further assisted by the development of computing power and the advent of direct methods as a method of structure solution. Computer development also provided the opportunity for electronic storage of crystallographic data.

4.2 Cambridge Structural Database

The Crystal Structure Database (CSD) is the largest of five computerised crystallographic databases. The Protein Data Bank (PDB) (Bernstein, Koetzle, Williams, Meyer, Brice, Rodgers, Kennard, Shimanouchi & Tasumi, 1977) was founded in 1971 and now contains over 8,000 entries. The Nucleic Acid Data Bank (NADB) (Berman, Olson, Beveridge, Westbrook, Gelbin, Demeny, Hsieh,

Srinaavasan & Schneider, 1992) contains over 700 entries, these structures were previously contained within the CSD or PDB depending on their size. The Inorganic Crystal Structure Database (ISCD) (Bergerhoff, Hundt, Sievers & Brown, 1983) with around 48,000 entries covers inorganic compounds and minerals. CRYSTMET (Wood, Rodgers, Gough & Villiars, 1996), the Metals Data File was developed in the 1970s and covers metals, alloys and intermetallics.

The Cambridge Structural Database (Allen & Kennard, 1993) originated in the University of Cambridge in 1965, the aim was to compile a computerised database containing data obtained from X-ray and neutron diffraction experiments on organic and organometallic compounds. The database initially contained around 1,500 entries and has grown rapidly, the April 1999 release contains structural data for 197, 481 compounds.

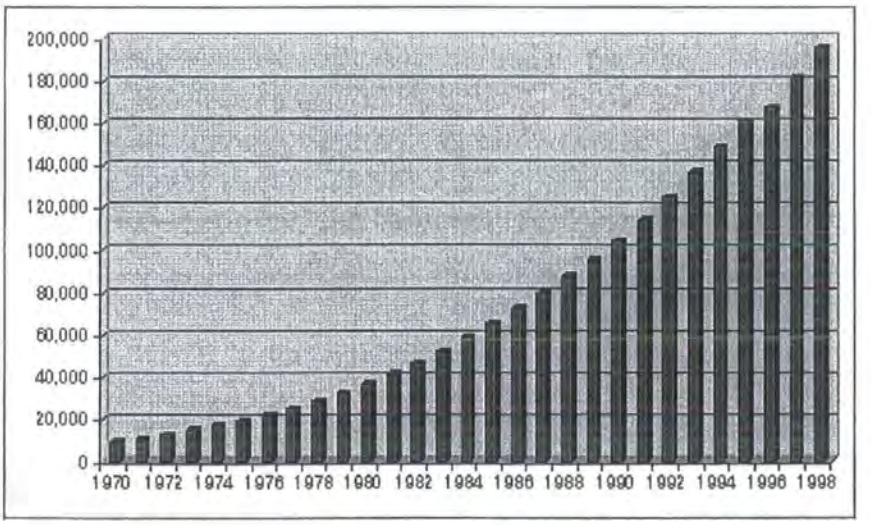

Figure 4.1 - Growth of the CSD with years on the horizontal-axis and number of database entries on the vertical axis. Taken from *http://www.ccdc.cam.ac.uk*

The CSD stores information at several levels, described by their 'dimensionality'. It holds bibliographic information such as authors, journal and R-factor, this is known as

1D information. At the next level, 2D, the chemical connectivity and structural diagram are held. Finally the 3D level contains atomic coordinates and symmetry information.

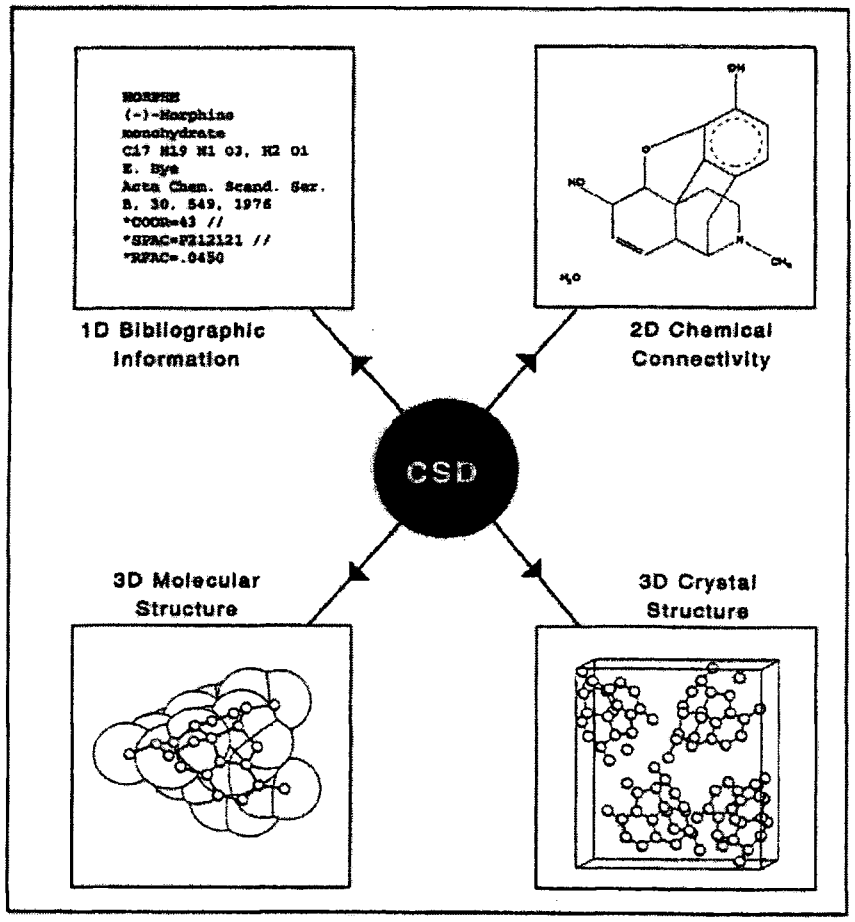

Figure 4.2 - Content of the CSD. *Taken from Getting Started with Quest*, April 1998 edition, Cambridge Crystallographic Data Centre

4.3 CSD Software

The CSDS (Cambridge Structural Database System) is not only a database of crystallographic information but also a suite of graphical software for search, retrieval and some analysis of data. The primary software packages are a search and retrieval program, a statistical analysis program and a graphics package.

QUEST 3D - this is the major component of the software package, it is used to define searches of the database. Searches can be on the 1D level e.g. text and numerical, 2D, e.g. connectivity or fragment searches or 3D level e.g. geometrical parameters, non-bonded contacts. Using Boolean logic operators, more complicated queries can be defined consisting of a combination of searches. The program searches for entries which satisfy the users requirements and displays them for the user to accept or reject. Entries can be displayed in terms of their 1D, 2D or 3D content. A number of files are output from QUEST, some of which can be read into other CSDS programs. Before initiating the search, the user has the option to specify further output formats such as postscript files and lists of accepted entries in QUEST searchable format for use in further dataset searches.

VISTA - this is a statistical analysis program which can be used if 3D parameters have been defined in a search. Vista can produce histograms, scattergrams and polar plots which can be saved in postscript format. It can also perform principal component analysis and correlation/covariance analysis. All 1D, 2D and 3D information can be viewed.

PLUTO - a graphical display program. Pluto can be used to create views and packing plots of the molecule and save them as a postscript file. Hydrogen bond networks can be located and graph set notation assigned.

The contents of the database are input using a piece of software called **PreQuest**. It is a data conversion program which accepts crystallographic information in five different file formats and converts them to searchable CSD files. The software applies

a series of data validation checks and lists problems that the user must satisfy in order for the entry to be acceptable. It is also possible to build up a personal database of structures which can be searched independently or in conjunction with the current CSD release.

In addition to the main body of software there are two other releases. **GOLD** is a protein-ligand docking program. **IsoStar** (Bruno, Cole, Lommerse, Rowland, Taylor & Verdonk, 1997) is a library of experimental and theoretical information on non-bonded interactions. This library contains information about the geometries, energies and frequencies of occurrence of thousands of different types of non-bonded contacts. Data are presented as scatterplots which are hyperlinked to the CSD and PDB.

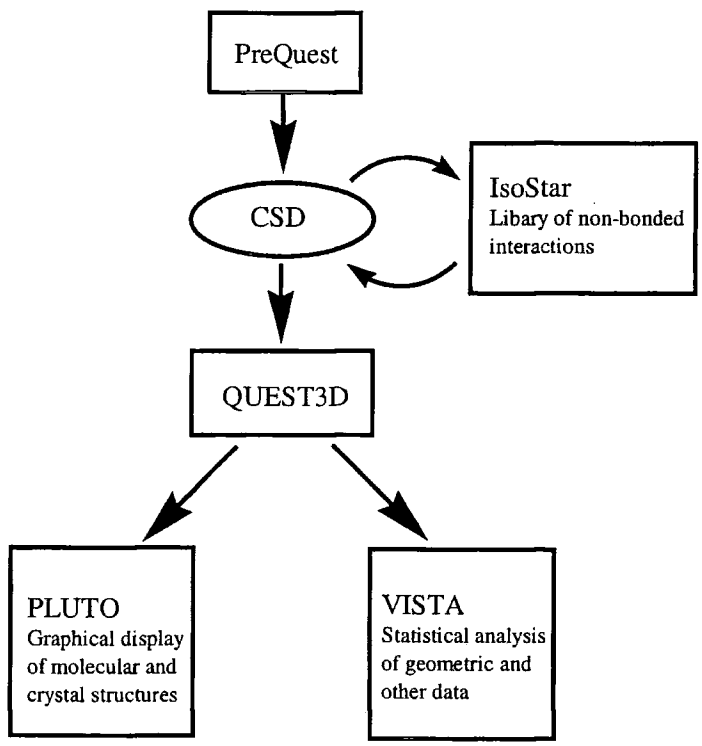

Figure 4.3 - Relationship of the individual components of the CSDS.

4.4 Research Applications

As a searchable store of a vast quantity of crystallographic data, the CSD has many uses. On a basic level it is valuable to the crystallographer as a means of checking cell parameters before collecting data from an unknown crystal to avoid wasting time with a previously analysed compound. However, work published which has involved the CSD covers a variety of topics. Several studies have been carried out into mean bond lengths and angles of particular functional groups. Allen (1980) studied the geometry of small rings, Borthwick (1980) investigated carboxylic acids, Schweizer & Dunitz (1982) covered carboxylic esters and amides and Taylor & Kennard (1982) produced an updated determination of nucleic acid base residues previously determined in 1970. A major publication was a set of updated tables of mean bond lengths and angles for both organic (Allen, Kennard, Watson, Brammer, Orpen & Taylor, 1987) and organometalllic (Orpen, Brammer, Allen, Kennard, Watson & Taylor, 1989) compounds. The nonbonded search routines available in QUEST provide the ideal opportunity to study intermolecular interactions. A variety of interactions have been researched, Taylor and Kennard (Taylor & Kennard, 1982) used the CSD to justify the existence of C-H --- O, C-H --- N and C-H --- Cl interactions as hydrogen bonds. Other interactions covered include the C-F group (Murray-Rust, Stallings, Monti, Preston & Glusker, 1983), C-X interactions where X= Cl, Br, I (Murray-Rust & Motherwell, 1979), and N-H --- O=C hydrogen bonds (Taylor, Kennard & Versichel, 1983). Other topics studied using the CSD include porphyrin sponges (Bryn, Curtis, Khan, Sawin, Tsurumi & Strouse, 1990) and systematic study of space group frequencies (Wilson, 1988).

REFERENCES

Allen, F.H., (1980). *Acta Cryst.*, B**36**, 81-96.

Allen, F. H., (1981). *Acta Cryst.*, B**37**, 890-900.

Allen, F.H. & Kennard, O., (1993) *Chemical Design Automation News*, **8** (1), 1 & 31-37.

Allen, F.H., Kennard, O., Watson, D.G., Brammer, L., Orpen, A.G. & Taylor, R. (1987). *J. Chem. Soc. Perkin Trans.* 2, S1-S19.

Bergerhoff, G., Hundt, R., Sievers, R. & Brown, I. D., (1983). *J. Chem. Inf. Comput. Sci.* **23**, 66-69.

Berman, H. M., Olson, W.K., Beveridge, D. L., Westbrook, J., Gelbin, A., Demeny, T., Hsieh, S.-H., Srinaavasan, A.R. & Schneider, B. (1992). *Biophys. J.* **63**, 751-759.

Bernstein, F. C., Koetzle, T. F., Williams, G. J., Meyer Jr., E. E., Brice, M. D., Rodgers, J.R., Kennard, O., Shimanouchi, T. & Tasumi M., (1977). *J. Mol. Biol.* **112**, 535.

Borthwick. P.W., (1980). *Acta Cryst* B**36**, 628-632.

Bruno, I.J., Cole, J.C., Lommerse, J.P.M., Rowland, R. S., Taylor, R. & Verdonk, M. L., (1997). J. *Computer-Aided Molec. Design*, **11**, 525.

Byrn, M. P., Curtis, C. J., Khan, S.I., Sawin, P.A., Tsurumi, R. & Strouse, C. E. (1990). *J. Am. Chem. Soc.*, **112**, 1865-1874.

Murray-Rust, P. & Motherwell, W.D.S., (1979). *J. Am. Chem. Soc.*, **101**, 4374-4376.

Murray-Rust, P., Stallings, W. C., Monti, C.T., Preston, R.K. & Glusker, J.P., (1983). *J. Am. Chem. Soc.*, **105**, 3206-3214.

Orpen, A.G., Brammer, L., Allen, F.H., Kennard, O., Watson, D.G. & Taylor, R. (1989). *J. Chem. Soc. Dalton. Trans*, S1-S83.

Reidel, D., (1929-1987). *Structure Reports*. Stuktur-Bericht.

Schweizer, W.B. & Dunitz, J.D., (1982)., *Helv. Chim. Acta.*, **65**, 155-1562.

Schweizer, W.B. & Dunitz, J.D., (1982)., *Helv. Chim. Acta.*, **65**, 1482-88.

Sutton, L. E., (1958).*'Tables of Interatomic Distances and Configurations in Molecules and Ions'*. Chemical Society Special Publication No. 18, Chemical Society, London.

Taylor, R. & Kennard, O., (1982). *J. Am. Chem. Soc.*, **104**, 3209-3212.

Taylor, R. Kennard, O. & Versichel, W., (1983). *J. Am. Chem. Soc.*, **105**, 5761-5766.

Taylor, R., Kennard, O. & Versichel, W., (1984). *J. Am. Chem. Soc.*, **106**, 244-248.

Wilson, A.J.C., (1988). *Acta Cryst.*, A**44**, 715-724.

Wilson, A.J.C., (1990). *Acta Cryst.*, A**46**, 742-754.

Wood, G.H., Rodgers, J. R., Gough, S.R. & Villars, P., (1996). *J. Res. Natl. Inst. Stand. Technol.*, **101**, 3, 205-215.

Gem-alkynol hydrogen bonding

CHAPTER 5

5.1 *Gem*-alkynols

The following five chapters detail work carried out on a family of small organic molecules. All 17 structures contain both an hydroxyl group and an acetylene unit, bonded to the same carbon atom as shown in Figure 5.1, i.e. they are all members of the *gem*-alkynol family.

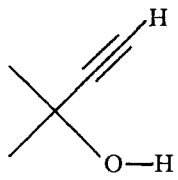

Figure 5.1 - *Gem*-alkynol unit

The aim was to investigate this unit as a potential building block for use in the design of supramolecular synthons. The molecular recognition properties of hydroxyl groups and alkynes as distinct groups have been widely researched. Alcohols were the first hydrogen bonding group to be thoroughly studied and are well understood (Pimentel & McClellan, 1960). Alkynes have also enjoyed much exposure in the literature in recent years (Steiner, 1995; Steiner, Starikov, Amado & Teixeiradias,1995; Lutz, Kanters, Van der Mass, Kroon & Steiner, 1998) as interest grows in weak hydrogen bonding. Although both functional groups are understood as individual entities in terms of their hydrogen bonding, it is interesting to study their mutual effect upon each other in cases where their separate effects may interfere with each other.

5.2 *Gem*-alkynol hydrogen bonding

The hydroxyl - acetylene combination leads to four possible competitive interactions.

(i) O-H --- O

(ii) C-H --- O

(iii) O-H --- π

(iv) C-H --- π

The OH group has the potential to act as both a hydrogen bond donor and acceptor, O-H --- O hydrogen bonds are some of the most robust of the hydrogen bonded interactions. They are widely used in crystal engineering due to their reliability and strength; they are both short (typically H --- O, 1.7 to 2.0 Å) and the O-H --- O angles are highly linear. O-H --- O interactions were the first hydrogen bonds to be discovered, by Latimer and Rodebush in 1920. The comment was made as part of a discussion of the structure of water, the interaction was termed a "weak bond". Much of the early work on the nature of hydrogen bonding was carried out on such interactions.

Alkynes can also act as both hydrogen bond donors and acceptors, but in contrast to the alcohols, the resultant interactions are far weaker (Steiner, Van der Mass & Lutz, 1997). The hydrogen atom can act as a donor and the carbon-carbon triple bond electron density can act as an acceptor. The C-H --- O hydrogen bond was first suggested by Sutor in 1962 and in 1982 Taylor and Kennard produced the first crystallographic evidence for the existence of such hydrogen bonds, along with C-H --- N and C-H --- Cl hydrogen bonds. The Taylor and Kennard study established the specific directionality of the C-H donor to the oxygen atom lone pair and also that the ability of the C-H group to form hydrogen bonds is dependant on electron

withdrawing groups adjacent to it. Interest in C-H --- O hydrogen bonding grew rapidly, studies have been carried out into both the donor and acceptor strengths of both participants in the hydrogen bond (Desiraju, 1990; Steiner, Kanters & Kroon, 1996; Steiner, 1998). A relationship was also established between the donor --- acceptor distance of such hydrogen bonds and carbon acidity (Desiraju & Pedireddi 1992). C-H --- O hydrogen bonds have also been used successfully in supramolecular design (Davidson, Hibbert, Howard, Mackinnon & Wade, 1996; Bodige, Rogers & Blackstock, 1997). In particular, the nature of C-H --- O hydrogen bonds with a terminal acetylene as the donor moiety have been thoroughly researched using both spectroscopic (Desiraju & Murty, 1987) and database analyses (Desiraju, 1990).

The hydrogen atom of a terminal alkyne can form a hydrogen bond with another alkyne group. Much of the work in this topic has been carried out by Steiner, with a comprehensive set of publications covering such topics as their long-range nature (Steiner, 1995) and also cooperativity (Steiner, Tamm, Gzegorzewski, Schulte, Veldman, Schreurs, Kanters, Kroon, van der Mass & Lutz, 1996). The interaction itself is weak in comparison with O-H donor interactions, not overly directional and unlikely to be the dominant hydrogen bonding interaction in a system which contains stronger donors such as O-H or N-H. In the optimum geometry of these hydrogen bonds, the donor-H vector points perpendicularly to the mid point of the π electron system (Steiner, 1995).

Donor groups can also interact with the electron cloud of the phenyl ring, both the C≡C-H and O-H donors can participate in this interaction. As with C≡C acceptor interactions, the optimal geometry is a perpendicular approach to the mid-point of the

π electron system, in this case the phenyl ring. However, in both cases, this geometry is easily distorted to accommodate more conventional hydrogen bonds. Theoretical calculations have shown a perpendicular approach for the N-H --- phenyl system (Levitt & Perutz, 1998; Worth & Wade, 1995). Several experimental studies have shown that the donor points towards the mid-point of an individual aromatic C-C bond (Steiner, Schruers, Kanters & Kroon, 1998) or alternatively towards an individual ring atom (Al-Juaid, Al-Nasr, Eaborn & Hitchcock, 1991).

The combination of both a weak and a strong hydrogen bonding functional group provides an interesting challenge to the crystal engineer. In addition to the one donor - one acceptor type of interaction listed on page 55 , there are several possible extended ribbons of donor-acceptor combinations resulting in cooperative interactions. Chains can be long, involving only one functional group as in Figure 5.2, or shorter and alternating between the two functional groups as shown in Figure 5.3 .

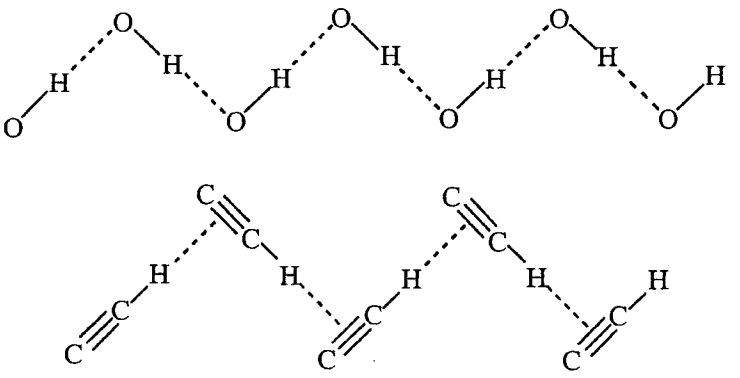

Figure 5.2 - Long repeating motifs

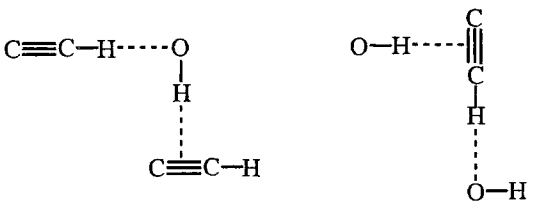

Figure 5.3 - Mixed motifs

Considering the relative strengths of the possible interactions, one would expect that the O-H --- O interaction would dominate the crystal packing. It should be noted however, that in terms of interactions of type **(ii),** the alkyne hydrogen atom is the most acidic hydrogen of the C-H species (Pedireddi & Desiraju, 1992). Therefore, in comparison with other weak hydrogen bonds, those involving the alkyne group are quite strong. The following five chapters will demonstrate that in such a flexible system, what would be expected to be the overriding interaction does not always dominate in the crystal structure.

5.3 CSD search for *gem*-alkynol functionality

The CSD (October 1998, Version 5.16, 190,307 entries) contains 94 organic molecules containing the *gem*-alkynol functionality. Bit screens -55, 57 and 153 were used to accept or reject entries accordingly. The maximum separation distance for acceptance of an interaction was the sum of the Van der Waals radii of the two interacting atoms. These structures were investigated to try to find any common pattern of hydrogen bonding patterns. Entries were manually rejected that did not contain atomic position coordinates for all hydrogen atoms, leaving 75 entries. The

structures of the remaining 75 compounds are mediated by quite different hydrogen bonding. However, of the 75 *gem*-alkynols, many have additional functional groups capable of participating in strong intermolecular interactions. This, unfortunately perturbs the effect of the *gem*-alkynol fragment alone and hinders the analysis of its hydrogen bonding. Additional functionalities include carbonyls, halogens and further hydroxyl groups. Of the remaining structures, 34 also possess a carbonyl group, removing these from the list leaves 41 for further analysis. The frequency of occurrence of the four types of hydrogen bond of particular interest are shown in Figure 5.4.

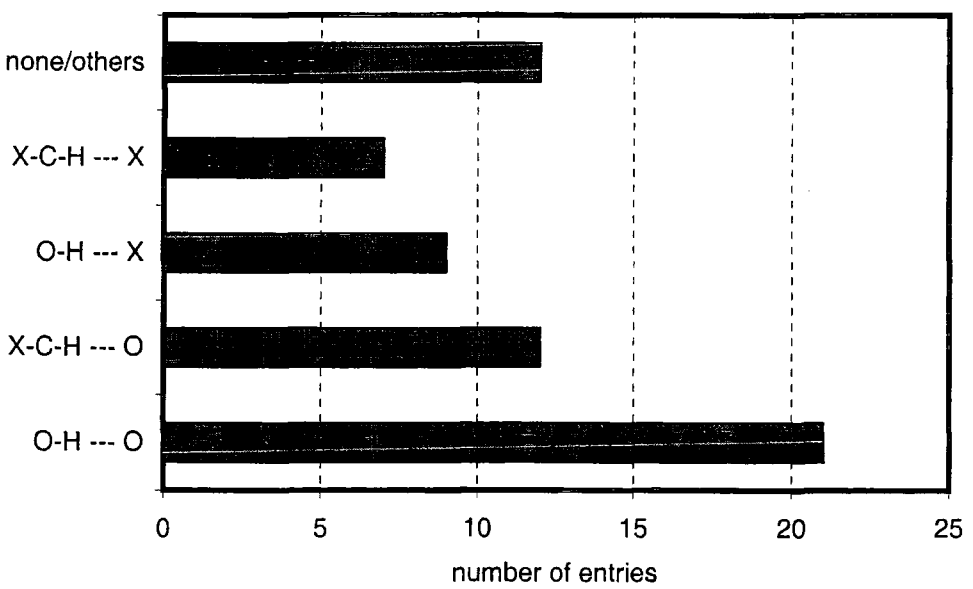

Figure 5.4 - Occurrences of the four interactions **(i)** to **(iv)** in *gem*-alkynols.

$X = \pi\ (C{\equiv}C)$

As expected, the strong O-H --- O interaction is the most frequent but there are also significant occurrences of the weaker interactions. The two most common situations are structures containing just the O-H --- O or both the O-H --- O and C≡C-H---C≡C interactions together. There are 12 structures which do not contain any of the four interactions, but in most cases the alkynol is not involved in any other strong interactions. The 75 structures show a perplexing variety of different packing patterns.

In short, *gem*-alkynols are systems with a high degree of interaction interference. That is to say, they contain several possible and very competitive intermolecular interactions. One additional complication, is the close juxtaposition of the alcohol and alkynyl functionalities. This adds the factor of steric hindrance to the problem of competition between the two functionalities, and consequently, both groups may not be equally accessible to the other potential partner in the interaction. This makes it quite difficult to predict the crystal packing of a particular *gem*-alkynol and to establish the structural repetition that is critical to its further use in crystal engineering.

5.4 *Gem*-alkynol systematic study

The analysis of the *gem*-alkynols present in the CSD was not conclusive. The sample contains a variety of different *gem*-alkynol molecules, all synthesised for different purposes other than analysing *gem*-alkynol hydrogen bonding. The ideal molecules for such structural investigations should have no other functional groups to perturb the effects of the *gem*-alkynol moiety. They should also be small in order to reduce the effects of steric hindrance from the remainder of the molecule. With such a flexible

system in terms of hydrogen bonding, the crystal packing will be very sensitive to other molecular features. A group of small organic molecules shown in Figure 5.5 was chosen to investigate the *gem*-alkynol hydrogen bonding. Aside from carefully and intentionally positioned halogen atoms, the only other groups that could effect the intermolecular interactions are the phenyl rings.

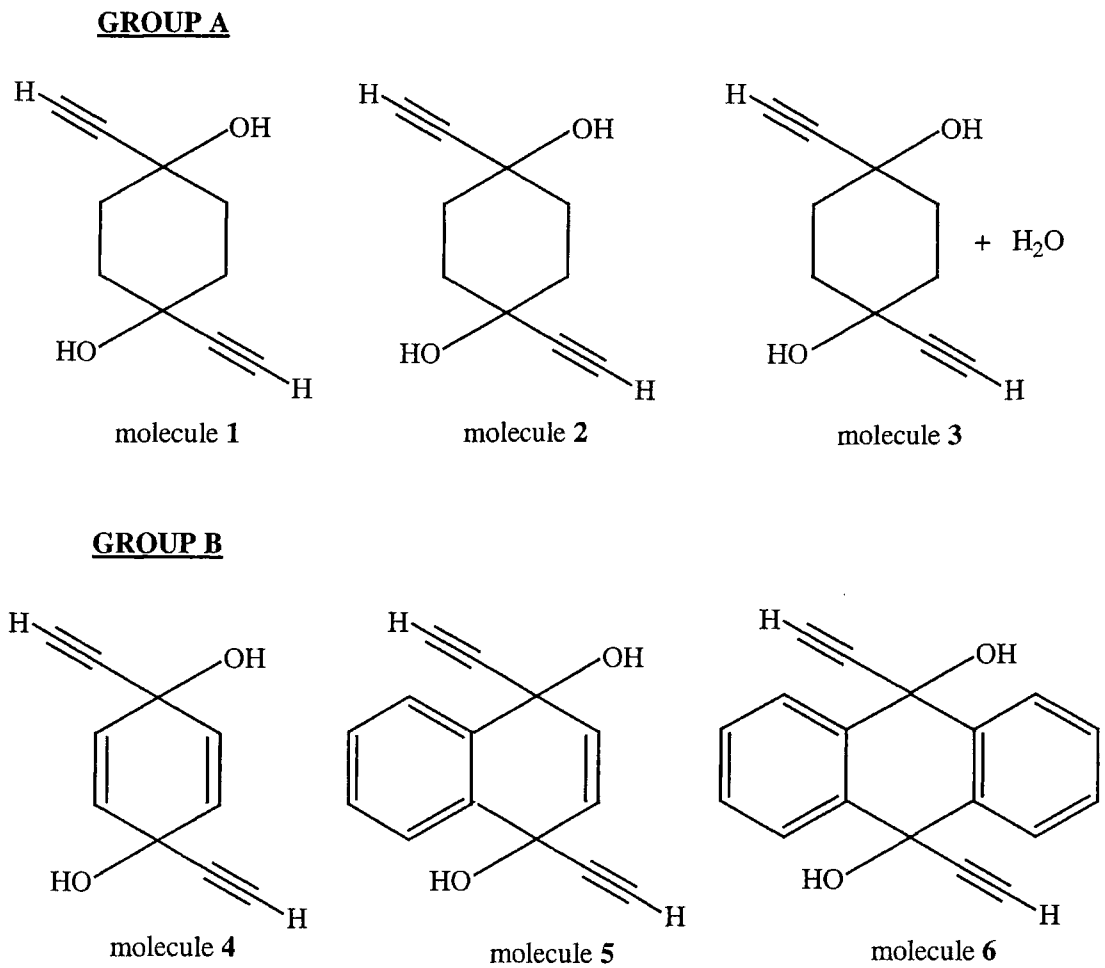

Figure 5.5 - Family of *gem*-alkynol molecules synthesised for crystal structure analysis

GROUP C

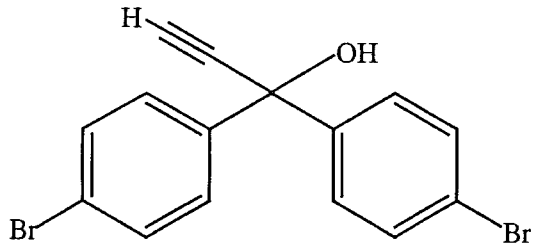

molecule **7**

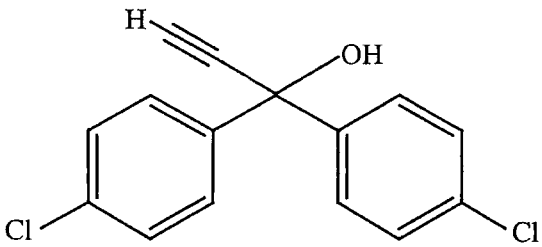

molecule **8**

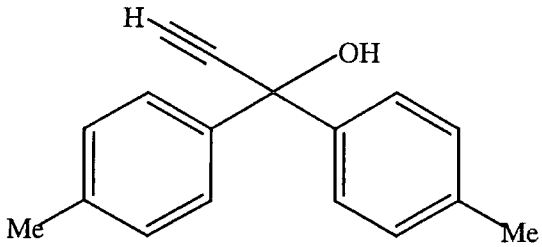

molecule **9**

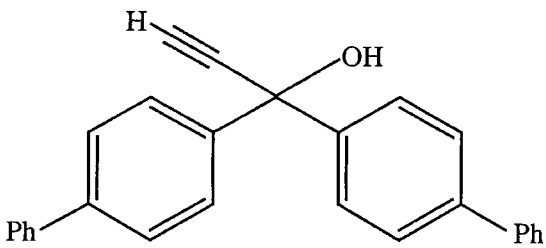

molecule **10**

GROUP D

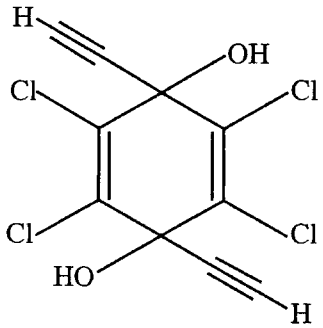

molecule **11**

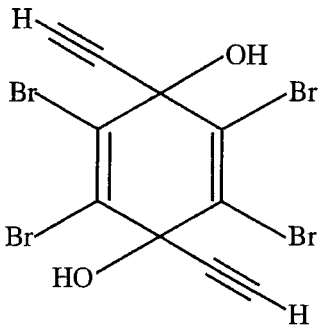

molecule **12**

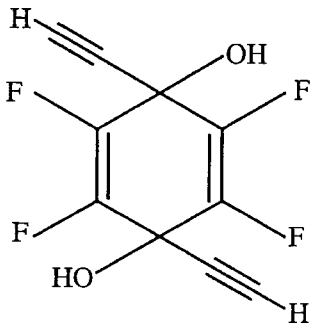

molecule **13**

Figure 5.5 (continued)

GROUP E

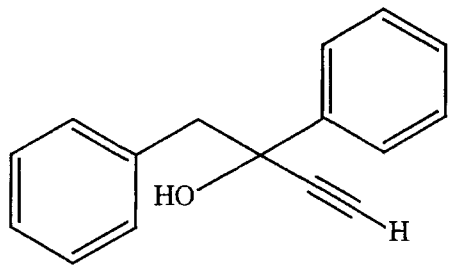

molecule 14

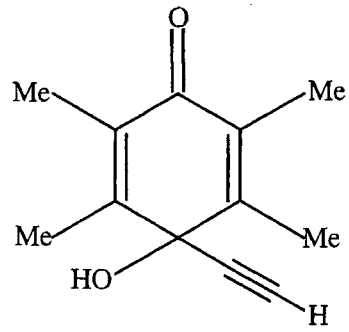

molecule 15

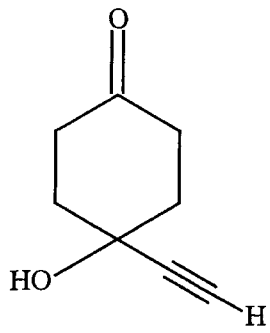

molecule 16

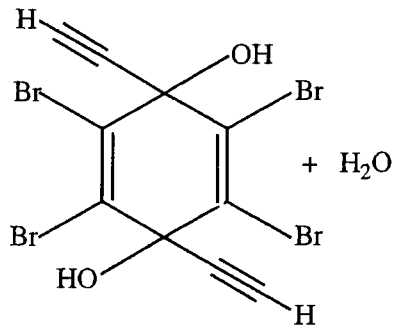

molecule 17

Figure 5.5 (continued)

Unfortunately, even after reducing the potential for competing intermolecular interactions, the 17 different molecules do not all pack in the same manner, they take advantage of different interactions in varying ratios. However, within sub-sections of the molecular family, common hydrogen bonding patterns can be identified. Four clear groups can be identified, the individual members of which display analogous hydrogen bonding patterns. Group A contains two polymorphs and one pseudopolymorph (hydrate) of 1,4-diethynyl-1,4-cyclohexanediol. Group B is based on the simple molecule 1,4-diethynyl-1,4-cyclohexenediol, the other two group members consist of the base molecule with additional phenyl rings fused to the sides.

Four halo substituted biphenyl alkynol molecules make up the third group C. The final group, D, contains three molecules based on the simple base unit of group B, with halogen atoms, fluoro, chloro and bromo, substituted at every free position. This leaves four structures unaccounted for, one of which was collected using both X-ray and neutron radiation. Two of the molecules are structurally similar, they have only one *gem*-alkynol unit and instead contain a ketone. Unlike the other sub-families, although they contain common interactions, their packing patterns are different. A further X-ray structure is structurally quite different to the other 16 and although its hydrogen bonding is very interesting, no parallels can be drawn with any of the other structures. The final molecule is the hydrate of molecule **12** but unlike the hydrate in group A, its crystal packing quite different to the non-hydrated form.

REFERENCES

Al-Juaid, S. S., Al-Nasr, A. K. A., Eaborn, C. & Hitchcock, P. B., (1991). *J. Chem. Soc. Chem. Commun.*, 1482-4

Bodige, S. G., Rogers, R. D. & Blackstock, S. C., (1997). *J. Chem. Soc. Chem. Commun.* **17**, 1669-70.

Davidson, M. G., Hibbert, T. G., Howard, J. A. K., Mackinnon, A. & Wade, K. (1996). *J. Chem. Soc. Chem. Commun.* **19**, 2285-6.

Desiraju, G. R., (1990). *J. Chem. Soc. Chem. Commun.*, 454-5.

Desiraju, G. R. & Pedireddi, V. (1992). *J. Chem. Soc. Chem. Commun.*, 988-90.

Latimer, W. M. & Rodebush, W. H. (1920). *J. Am. Chem. Soc*, **42**, 1419-33.

Levitt, M. & Perutz, M. F., (1988). *J. Mol. Biol.*, **201**, 751-4.

Lutz, B., Kanters, J. A., van der Mass, J., Kroon, J. & Steiner, T., (1998). *J. Mol. Struct.* **440**, 1-3, 81-7.

Pedireddi, V. & Desiraju, G. R., (1992). *J. Chem. Soc. Chem. Commun.*, 988.

Pimental, G. C. & McClellan, A. L. (1960). *The Hydrogen Bond.* Freeman, San Francisco.

Steiner, T. (1995). *J. Chem. Soc. Chem. Commun.*, **1**, 95-9

Steiner, T. (1998). *New J. Chem.*, 1099-1103.

Steiner, T., Kanters, J. A. & Kroon, J. (1996). *J. Chem. Soc. Chem. Commun.*, **11**, 1277-8.

Steiner, T., Schreurs, A. M. M., Kanters, J. A. & Kroon, J., (1998). *Acta Cryst.* D**54**. 25-31.

Steiner, T., Starikov, E. B., Amado, A. M. & Teixeiradias, J. J. C. (1995). *J. Chem. Soc. Perkin Trans. 2*, **7**, 1321-26.

Steiner, T., Tamm, M., Gzregorzewski, A., Schulte, N., Veldman, N., Schruers, A. M. M., Kanters, J. A., Kroon, J., van der Mass, J. & Lutz, B., (1996). *J. Chem. Soc. Perkin Trans. 2,* **11**, 2441-6.

Steiner, T., van der Mass, J. & Lutz, B., (1997). *J. Chem. Soc. Perkin Trans. 2*, 1287-91.

Sutor, D. J. (1962). *Nature* **195**, 68-9.

Taylor R. & Kennard, O. (1982). *J. Am. Chem. Soc.*, **104**, 5063-70.

Worth, G.A. & Wade, R. C. (1995). *J. Phys. Chem.*, **99**, 17473-82.

Gem-alkynol structures **1**, **2** and **3**.

CHAPTER 6

6.1 Gem-alkynol structures 1 to 3

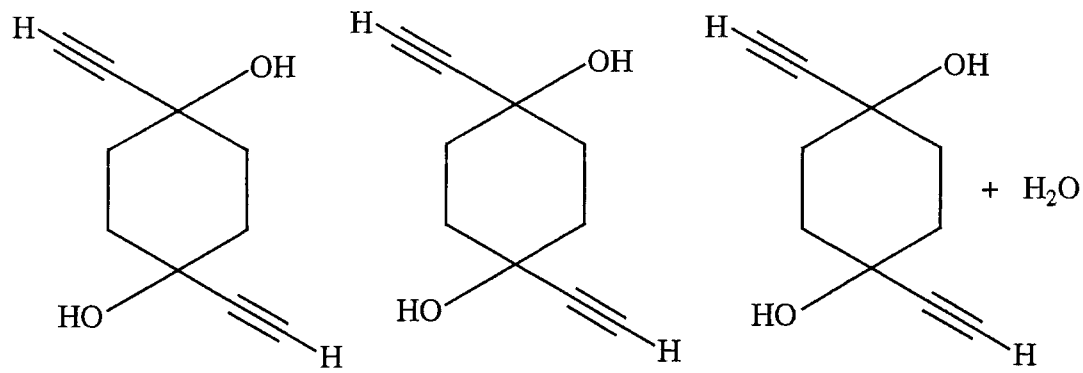

structure **1** structure **2** structure **3**

Figure 6.1 - Structural formulae, structures **1** to **3**

6.2 Polymorphism

Structures **1** to **3** raise an interesting issue that has become the bane of crystal engineers, polymorphism. Whilst they have distinctly different crystal structures, forms **1** and **2** are actually polymorphs while form **3** is a solvated form, a *pseudo*polymorph. Polymorphism was defined by McCrone in 1965 as

> *"a solid crystalline phase of a given compound resulting from the possibility of at least two different arrangements of the molecules of that compound in the solid state."*

Polymorphism was first recognised by Mitscherlich in 1822 but little work was conducted in the field until the 1960's. Early work was focused largely on the characterisation of materials such as pharmaceuticals (Haleblian & McCrone, 1969), and in recent years, emphasis has shifted to the ultimate aim of successful prediction

of polymorphs (Karfunkel & Gdanitz, 1992; Gavezzotti, 1994; Aakeröy, Nieuwenhuyzen. & Price, 1998).

The term pseudopolymorphism was coined by Threlfall in 1995 to describe two or more solvated crystalline forms of the same compound. The two polymorphs **1** and **2** and one pseudopolymorph **3** are particularly interesting as they were all obtained from the same reaction. This situation is a very good example of the problem that polymorphism poses to the crystal engineer. When trying to design molecules with specific properties, the fact that the reaction vessel or subsequent reaction vessels can conceivably contain more than one form of the same molecule is a potential problem. When synthesising a particular product with specific physical properties, difficulties arise if a different polymorph is found since its properties may be different. An added complication is that polymorphism is not particularly well understood, certainly not to the point where its occurrence can be predicted successfully and avoided. It has even been suggested that the number of polymorphs found for a particular compound, is related to the amount of time and effort devoted to obtaining them (McCrone, 1965). The proportion of structures in the CSD described as polymorphs is very small but with the advent of the age of the area detector and radically shorter data collection times, collection of data sets for more than one crystal from a given sample is becoming a more viable prospect. In line with this, the volume of publications concerning polymorphism of organic molecules should increase. The energy difference between polymorphs of molecular crystals is very small (the order of a few $kcalmol^{-1}$) so the occurrence of polymorphs **1** and **2** is hardly surprising.

6.3 Conformational polymorphism

McCrone's definition of polymorphism allows for the fact that although polymorphs are different in the crystal the state, they can be identical in the liquid or vapour state, and this leads to the definition of conformational polymorphism. Crystals which contain molecules in different conformations, fit McCrone's definition of polymorphs and so are labelled conformational polymorphs (Bernstein & Hagler, 1978). Although many organic compounds form polymorphs, in general, there is little difference in the bond lengths and angles between the structures. That is to say that they are fundamentally very similar; there is much greater potential for change in torsion angles. In comparison with the energy difference between polymorphs, the energy needed to change bond lengths and angles is large. For torsion angles it is only a matter of a few $kcalmol^{-1}$ which is comparable with the polymorphic energy difference. Therefore, for molecules with conformational (torsional) degrees of freedom there is the possibility for the occurrence of conformational polymorphism (Bernstein & Hagler, 1978).

6.4 Conformational isomerism

Interest in polymorphs **1**, **2** and pseudopolymorph **3** lie not only in the fact that they are examples of conformational polymorphism, but also that they display conformational isomerism. Conformational isomerism is the occurrence of different conformers in the same crystal structure.

6.5 Experimental Details

Data for structures **1, 2** and **3** were collected using Mo-Kα X-ray radiation. Crystals were mounted on a glass fibre and data collected on a Bruker SMART CCD diffractometer at 150K. Data were subsequently integrated using the Bruker SAINT package (Bruker AXS, 1998) and structure solution obtained by direct methods using Shelx97 (Sheldrick, 1997). The structures were then refined against F^2.

Data for structure **3** were also collected using neutron radiation. The crystal was mounted on an aluminium pin and data collected at 150K on the single crystal diffractometer SXD (Keen & Wilson, 1996) at the ISIS Spallation Source. Data were integrated using SXD97 (Wilson, 1997). Positional coordinates for carbon and oxygen atoms from the previously refined X-ray model were then used as a starting model for the refinement. Hydrogen atoms were located in the difference map.

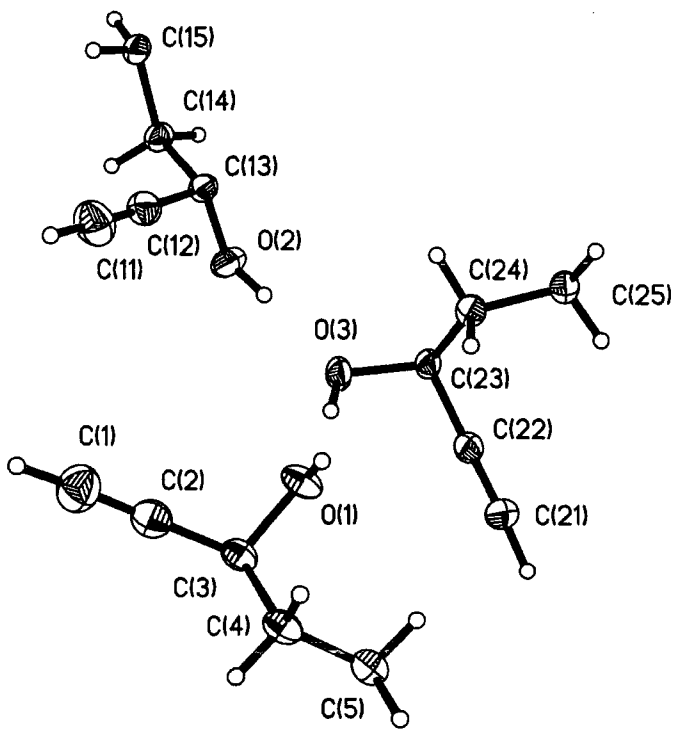

Figure 6.2 - 50 % probability ellipsoid plot of structure **1**

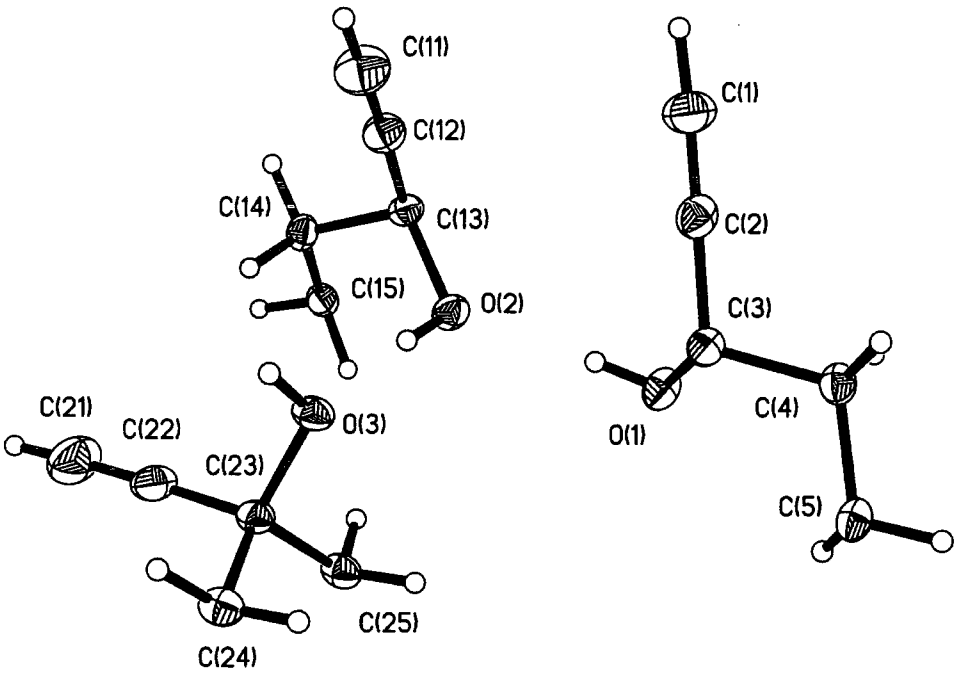

Figure 6.3 - 50 % probability ellipsoid plot of structure **2**

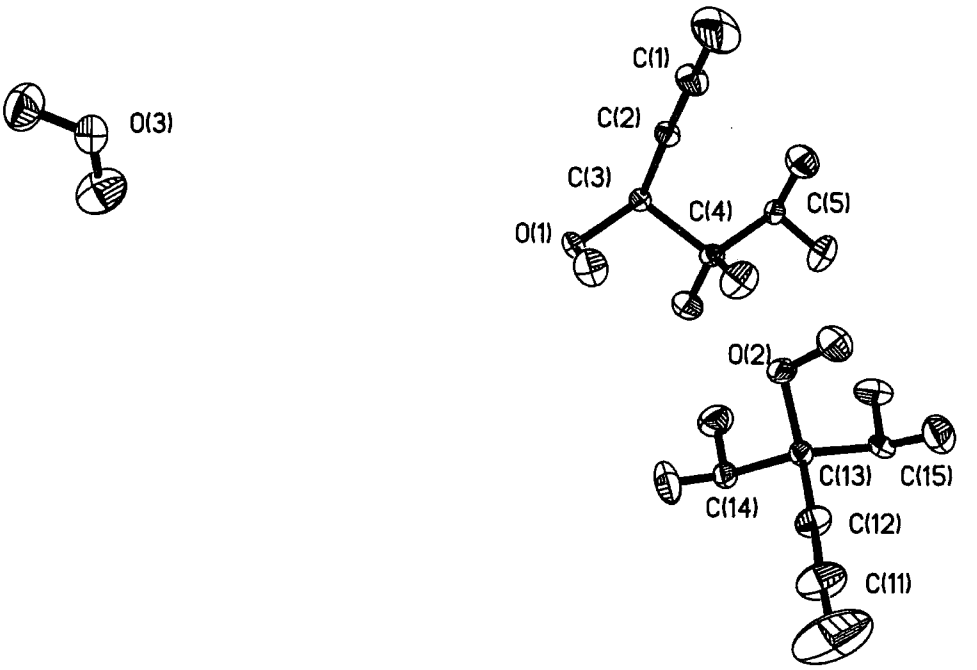

Figure 6.4 - 50 % probability ellipsoid plot of structure **3,** note hydrogen atoms

Table 6.1 - Experimental details, structure 1

Identification code	**Structure 1**
Empirical formula	C10 H12 O2
Formula weight	164.20
Temperature	150 K
Wavelength	0.71073 Å
Crystal system	Triclinic
Space group	$P\bar{1}$
Unit cell dimensions	a = 6.2074(3) Å α= 103.005(2)°.
	b = 10.0187(5) Å β= 93.424(2)°.
	c = 11.5666(5) Å γ = 94.572(2)°.
Volume	696.41(6) $Å^3$
Z	3
Density (calculated)	1.175 Mg/m^3
Absorption coefficient	0.081 mm^{-1}
F(000)	264
Crystal size	0.5 x 0.4 x 0.4 mm^3
Theta range for data collection	1.81 to 30.33°.
Index ranges	-8<=h<=8, -11<=k<=13, -16<=l<=15
Reflections collected	5564
Independent reflections	3618 [R(int) = 0.0255]
Absorption correction	Empirical
Max. and min. transmission	0.332 and 0.284
Refinement method	Full-matrix least-squares on F^2
Data / restraints / parameters	3618 / 0 / 235
Goodness-of-fit on F2	1.046
Final R indices [I>2sigma(I)]	R1 = 0.0409, wR2 = 0.1026
R indices (all data)	R1 = 0.0511, wR2 = 0.1089
Largest diff. Peak and hole	0.216 and -0.280 $e.Å^{-3}$

Table 6.2 - Experimental details, structure **2**

Identification code	**Structure 2**
Empirical formula	C10 H12 O2
Formula weight	164.20
Temperature	150 K
Wavelength	0.71073 Å
Crystal system	Triclinic
Space group	$P\bar{1}$
Unit cell dimensions	a = 6.4140(2) Å α= 105.689(2)°.
	b = 9.6367(3) Å β= 101.838(1)°.
	c = 11.7852(4) Å γ = 94.736(1)°.
Volume	678.98(4) $Å^3$
Z	3
Density (calculated)	1.205 Mg/m^3
Absorption coefficient	0.083 mm^{-1}
F(000)	264
Crystal size	0.3x 0.25 x 0.25 mm^3
Theta range for data collection	1.85 to 27.49°.
Index ranges	-7<=h<=8, -10<=k<=12, -12<=l<=15
Reflections collected	4754
Independent reflections	3061 [R(int) = 0.0234]
Absorption correction	none
Refinement method	Full-matrix least-squares on F^2
Data / restraints / parameters	3061 / 0 / 235
Goodness-of-fit on F2	1.145
Final R indices [I>2sigma(I)]	R1 = 0.0461, wR2 = 0.0966
R indices (all data)	R1 = 0.0608, wR2 = 0.1077
Largest diff. Peak and hole	0.240 and -0.229 $e.Å^{-3}$

Table 6.3 - Experimental details, structure **3**

Identification code	**Structure 3**
Empirical formula	C10 H12 O2, H2O
Formula weight	182.00
Temperature	150 K
Wavelength	0.5 - 5.0 Å
Crystal system	Monoclinic
Space group	$P2_1/c$
Unit cell dimensions	a = 9.925(2) Å α= 90.0°.
	b = 6.134(1) Å β= 104.12(3)°.
	c = 16.725(3) Å γ = 90.0°.
Volume	987.5(3) $Å^3$
Z	4
Density (calculated)	1.224 Mg/m^3
Absorption coefficient	0.226 mm^{-1}
F(000)	126
Crystal size	2 x 2 x 1.5 mm^3
Theta range for data collection	1.74 to 23.54°.
Index ranges	0<=h<=22, -0<=k<=19, -34<=l<=33
Reflections collected	2661
Independent reflections	2659 [R(int) = 0.0538]
Absorption correction	Becker-Coppens Lorentzian model
Refinement method	Full-matrix least-squares on F^2
Data / restraints / parameters	2659 / 0 / 244
Goodness-of-fit on F^2	3.792
Final R indices [I>2sigma(I)]	R1 = 0.0888, wR2 = 0.0889
R indices (all data)	R1 = 0.1270, wR2 = 0.1270

Table 6.4 - Selected bond lengths and angles for **1**.

	Length (Å)		Angle (°)
O1-H1A	0.86(2)	H1A-O1-C3	109.2(1)
O2-H2A	0.90(2)	H2A-O2-C13	112.2(1)
O3-H3A	0.86(2)	H3A-O3-C23	110.4(1)
C1-H1	0.97(2)	H1-C1-C2	177.3(1)
C11-H11	0.96(2)	H11-C11-C12	178.3(1)
C21-H21	0.98(2)	H21-C21-C22	177.3(1)
C1-C2	1.190(2)	C1-C2-C3	178.1(1)
C11-C12	1.189(2)	C11-C12-C13	178.2(1)
C21-C22	1.190(2)	C21-C22-C23	177.5(1)

Table 6.5 - Selected bond lengths and angles for **2**.

	Length (Å)		Angle (°)
O1-HA	0.86(2)	HA-O1-C3	107.2(1)
O2-HB	0.88(2)	HB-O2-C13	108.2(2)
O3-HC	0.86(3)	HC-O3-C23	112.1(2)
C1-H1	0.96(3)	H1-C1-C2	177.2(2)
C11-H11	0.96(3)	H11-C11-C12	177.8(2)
C21-H21	0.94(3)	H21-C21-C22	176.9(2)
C1-C2	1.184(3)	C1-C2-C3	177.5(2)
C11-C12	1.187(3)	C11-C12-C13	177.1(2)
C21-C22	1.186(3)	C21-C22-C23	178.1(2)

Table 6.6 - Selected bond lengths and angles for **3**

	Length (Å)		Angle (°)
O1-HA	0.993(6)	HA-O1-C3	109.4(4)
O2-HB	1.000(6)	HB-O2-C13	112.0(4)
C1-H1	1.080(6)	H1-C1-C2	178.9(5)
C11-H11	1.076(8)	H11-C11-C12	177.1(8)
C1-C2	1.203(3)	C1-C2-C3	177.3(2)
C11-C12	1.205(4)	C11-C12-C13	178.3(3)
O3-HC	0.982(8)	HC-O3-HD	108.4(6)
O3-HD	0.967(7)		

6.6 Structural variety

The structures each have three independent units in the unit-cell. Both **1** and **2** each contain three half molecules with two different conformers but in different ratios. Structure **3** contains only two half molecules, and one water molecule. There in principle are two possible conformers, one with the ethynyl group axial to the ring and the other with it equatorial.

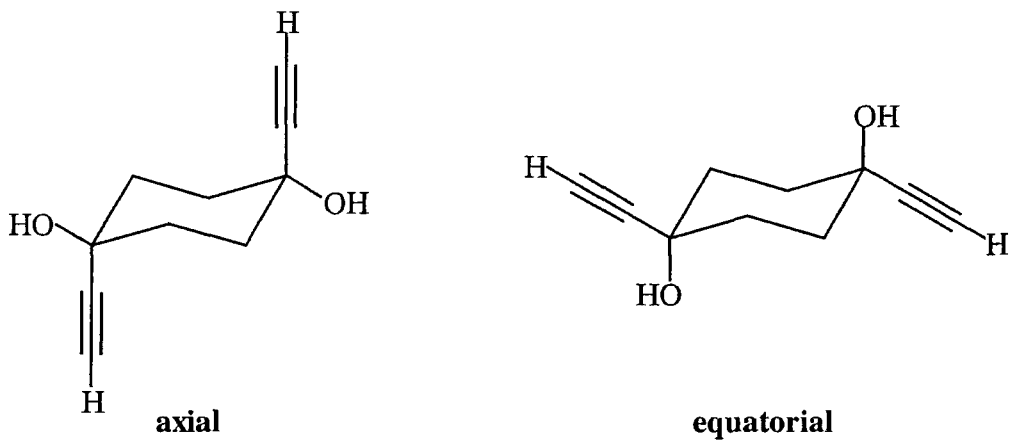

Figure 6.5 - Possible conformers

1	2 axial conformers + 1 equatorial conformer
2	1 axial conformer + 2 equatorial conformers
3	2 axial conformers + water molecule

Both **1** and **2** crystallise in space group $P\bar{1}$ with Z=3, **3** crystallises in space group P2(1)/c with Z=4. Even though the symmetry is different in the hydrated form its packing is of the same form as **1** and **2**. As the two polymorphs contain different conformers they can be described as conformational polymorphs. In addition to this, each structure also contains different conformers which makes them examples of

conformational isomorphism. The structures are a unique example of simultaneous conformational polymorphism and conformational isomorphism. All three crystalline forms are stable over time and were not found to interconvert in the solid state.

6.7 Hydrogen bonding in structures 1 to 3.

Table 6.7 - Distances and angles, O-H --- O interactions

Structure	O-H --- O distances (Å)and angles (°)			
1	1.81 (2) 176.4 (2)	1.81 (2) 173.3 (2)	1.83 (2) 164.6 (2)	
2	1.87 (2) 177 (2)	1.83 (2) 176 (2)	1.88 (3) 176 (2)	
3	1.641 (6) 176.8 (5)	1.798 (6) 170.1 (6)	1.803 (5) 163.9 (5)	1.910 (7) 174.2 (5)

Table 6.8 - Distances and angles, C≡C-H --- π (C≡C) interactions

Structure	C≡C-H --- π (C≡C) distances (Å)and angles (°)			
1	2.97 (2) 144.9 (2)	3.20 (2) 140.4 (2)	3.20 (2) 131.6 (2)	3.38 (2) 129.6 (2)
2	2.91 (3) 149 (2)	3.25 (3) 134 (2)	2.99 (3) 149 (2)	3.01 (3) 129 (2)
3	2.814 (9) 141.5 (8)	3.023 (9) 133.3 (7)	3.275 (7) 136.8 (6)	3.590 (8) 129.0 (6)

The dominant packing motif in each case is a helical trimer of O-H --- O interactions which involves both conformers. This trimer incorporates all three conformers in structures **1** and **2**. The trimer is retained in **3,** even with the loss of a conformer, as the O-H from the water molecule takes the position of the O-H from what would have been the third conformer. This trimer is a robust synthon, it is also seen in the related diol *trans*-1,4-cyclohexanediol, (Steiner and Saenger, 1998)

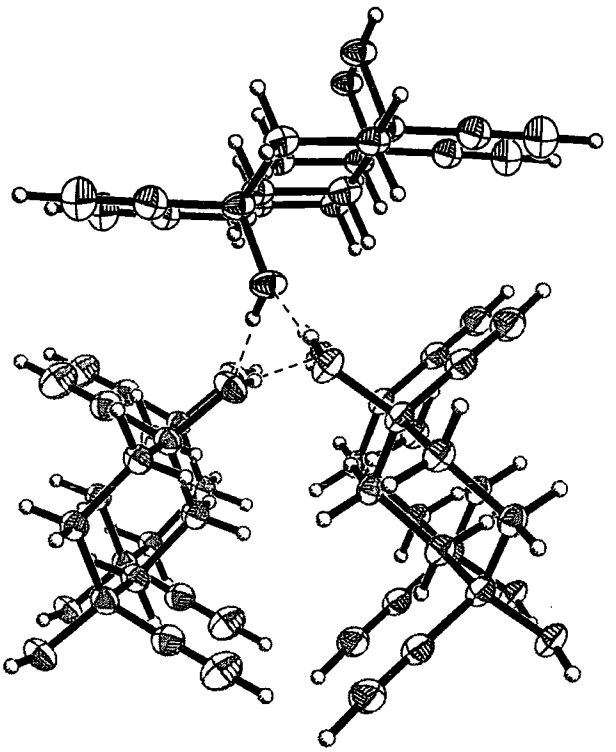

Figure 6.6 - Structure **1,** helical O-H --- O trimers

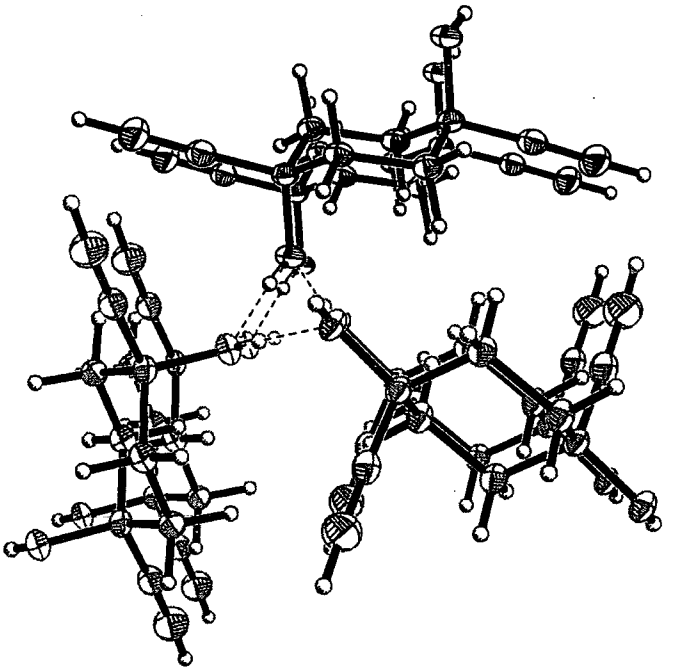

Figure 6.7 - Structure **2,** helical O-H --- O trimers

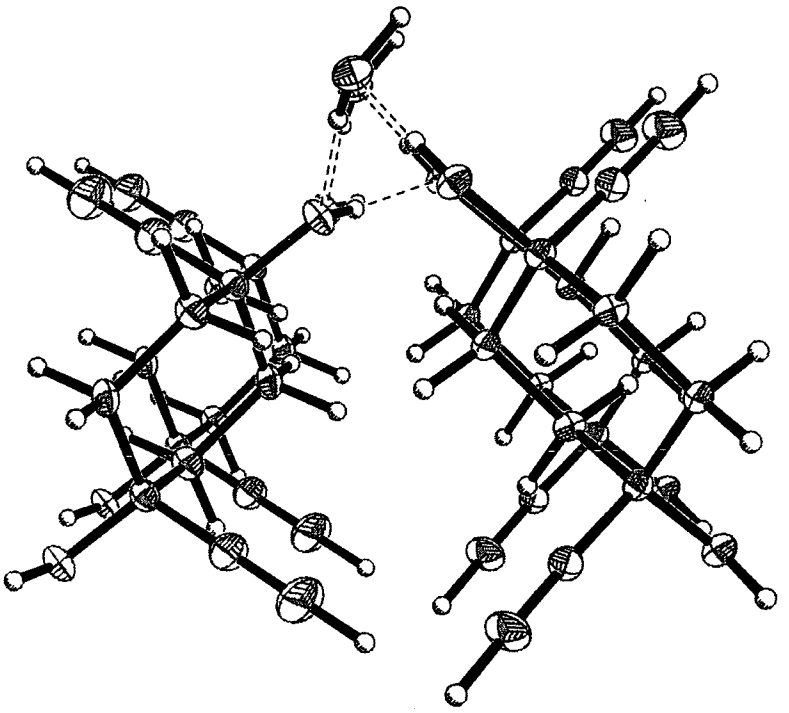

Figure 6.8 - Structure **3**, helical O-H --- O trimers

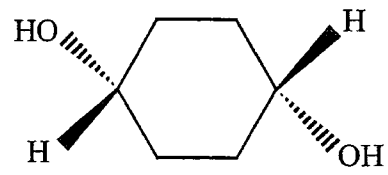

Figure 6.9 - *trans*-cyclohexane-1,4-diol

The simple diol shown in Figure 6.9 (Steiner, Saenger, 1998) crystallises in the monoclinic space group P2(1)/n with 1.5 molecules per asymmetric unit. The full molecule has both OH groups in the equatorial position, whereas the molecule on the inversion centre, has the OH group in the axial orientation. The helical O-H --- O trimer is formed from two equatorial conformers and one axial as in structure **2.**

Despite the dominant O-H --- O trimer, weaker C≡C-H --- π (C≡C) interactions are also a part of all three structures. However, even considering that such interactions are by nature weak, the interactions seen in all three structures are very long. This is understandable as the O-H --- O cooperative interactions clearly dominate the crystal packing.

It is unclear whether the presence of both conformers is necessary for the formation of the O-H --- O trimeric synthon. The cyclohexane-1,4-diols present in the CSD which exist in only one conformation do not form the synthon. It could therefore be inferred that both conformers are a necessity for trimer formation. This observation does reinforce the suggestion that the water molecule is acting as a replacement for the 'alternative' conformer in **3**, as shown by comparison of the packing plots in Figures 6.6 and 6.8.

REFERENCES

Aakeröy, C. B., Nieuwenhuyzen, M. & Price, S. L. (1998). *J. Am. Chem. Soc.*, **120**, 8986-93.

Bernstein, J. & Hagler, A. T. (1978). *J. Am. Chem. Soc.*, **100**, 673-81.

Bruker AXS (1998). SAINT, Area detector data integration software, Version 5.0, Bruker AXS, Madison, Wisconsin, USA, 1998.

Desiraju G. T. (1989) *J. Am. Chem. Soc.*, **111**, 8725.

Gavezzotti A. (1989) *J. Am. Chem. Soc.* **111**, 1835.

Gavezzotti, A. (1994). *Acc. Chem. Res.*, **27**, 309-14.

Haleblian, J. K. & McCrone, W. C. (1969). *J. Pharm. Sci.* **58**, 411.

Karfunkel, H. R. & Gdanitz, R. J. (1992). *J. Comput. Chem.*, **13**, 1171-83.

Keen, D. A. & Wilson, C. C. (1996). *Technical Report RAL-TR-96-083*. Single crystal diffraction at ISIS. User guide for the SXD instrument.

McCrone W. C. (1965) *Physics and Chemistry of the Organic Solid State*. Ed. D. Fox, M.M. Labes & A. Weissberger, Vol. 2 p. 725-767. New York:Interscience.

Mitscherlich, E., (1822). *Ann. Chim. Phys.*, **19**, 350.

Roberts K.J. (1992) *J. Phys. D: Appl. Phys.*, **26** B7-B21.

Sato K. (1992) *J. Phys. D: Appl. Phys.* **26** B77-B84.

Sheldrick, G. M. (1997). SHELX-97, Structure determination software, G. M. Sheldrick, University of Goettingen, Germany, 1997.

Steiner T. & Saenger W.(1998) *J. Chem. Soc. Perkin Trans.* 2, 371- 377.

Threlfall, T. L., (1995). *Analyst*, **120**, 2435.

Wilson, C. C. (1997). *J. Mol. Struct.*, **405**, 207-217.

Gem-alkynol structures **4**, **5** and **6**.

CHAPTER 7

7.1 Gem-alkynol structures 4 to 6

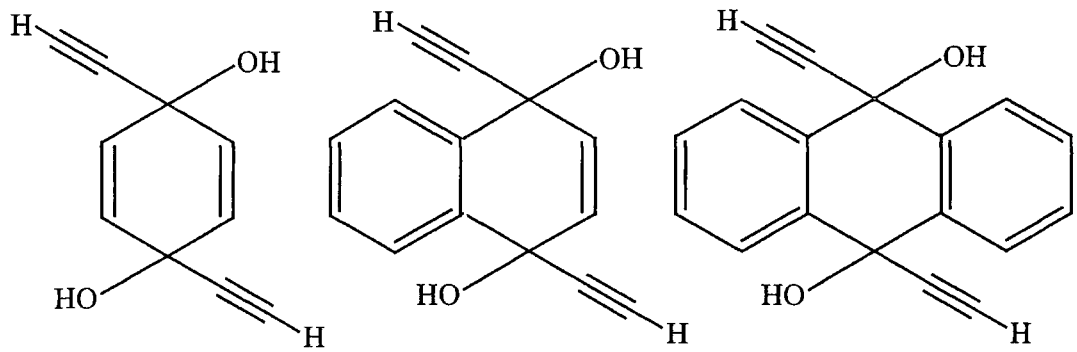

Figure 7.1 - Structural formulae, structures **4** to **6**

This group of molecules have been designed in a slightly different way to the other three related groups. Members of the other groups are related by substitution of a functional group or element consistently through all the structures. This group however are related by increasing substitution to the initial base unit. Structure **4** is the base unit for this family, the other members are constructed by fusing one ring to the side and a second on the other side.

The central framework of all three structures in this sub-family is planar so unlike the previous group, A, they have little conformational flexibility. In contrast, the next two sub-families, C and D, contain halogen atoms which introduce the possibility of additional interactions. The additional possibilities for interactions that exist for this sub-family aside from the four interactions of interest involving the gem-alkynol fragment, could stem from the interactions of the aromatic C-H or the phenyl ring centroids.

7.2 Experimental Details

Data for structures **4**, **5**, and **6** were collected using Mo-Kα X-ray radiation. In each case a suitable crystal was mounted on a glass fibre using epoxy glue. Data were collected at 150K using a Bruker SMART CCD diffractometer. The data were integrated using the Bruker SAINT package (Bruker AXS, 1998) and suitably corrected for absorption. Structure solutions were obtained by direct methods using Shelx97 (Sheldrick, 1997) and the resultant solutions were refined against F^2.

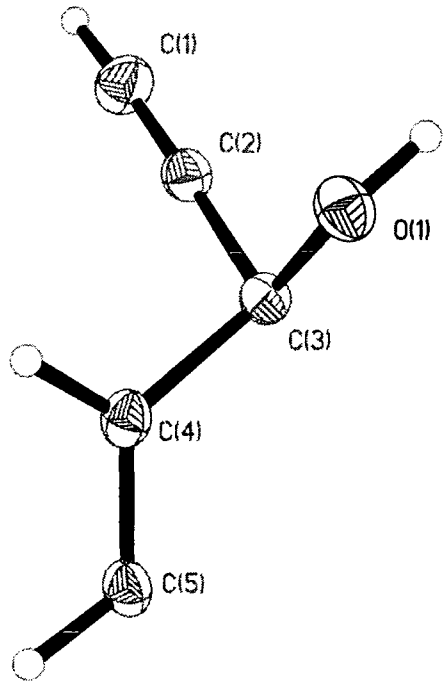

Figure 7.2 - 50 % probability ellipsoid plot of structure **4**

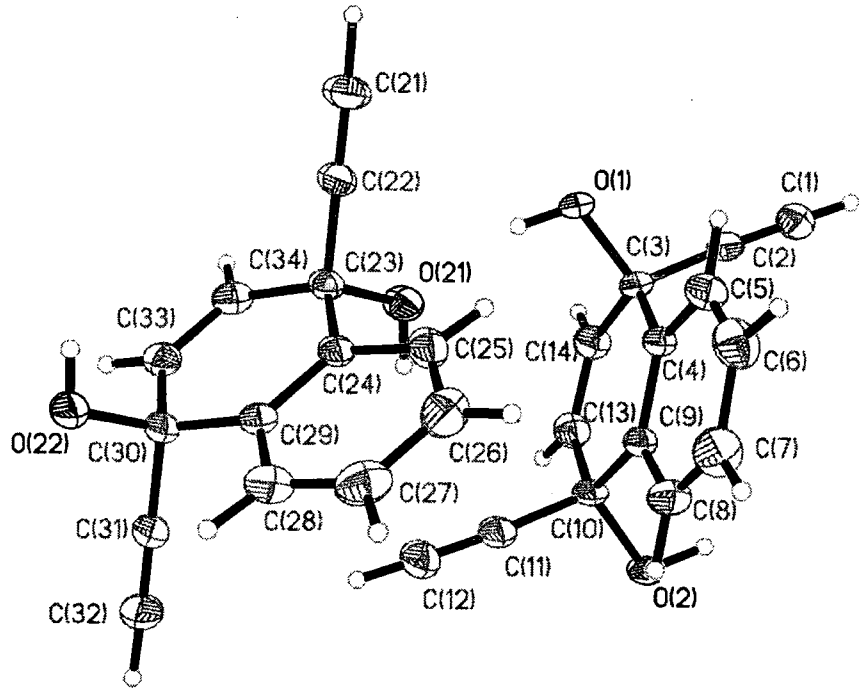

Figure 7.3 - 50 % probability ellipsoid plot of structure **5**

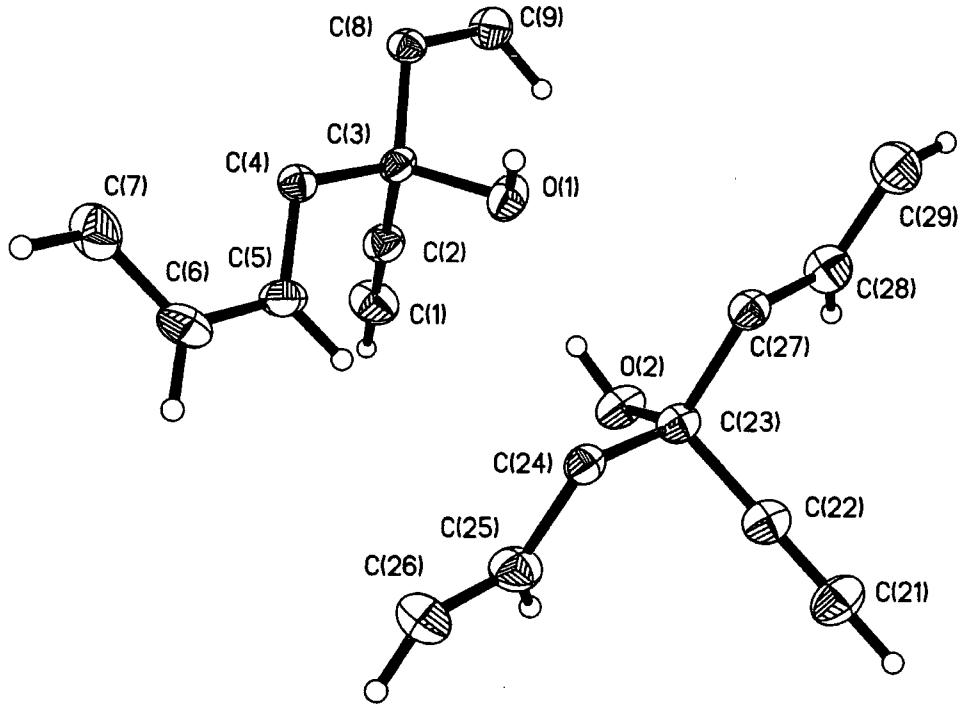

Figure 7.4 -50 % probability ellipsoid plot of structure **6**

Table 7.1 - Experimental details, structure **4**

Identification code	**Structure 4**
Empirical formula	C10 H8 O2
Formula weight	160.16
Temperature	150 K
Wavelength	0.71073 Å
Crystal system	Orthorhombic
Space group	*P*bca
Unit cell dimensions	a = 8.8316(2) Å α= 90°.
	b = 5.9003(1) Å β= 90°.
	c = 15.6123(4) Å γ = 90°.
Volume	813.54(3) $Å^3$
Z	4
Density (calculated)	1.308 Mg/m^3
Absorption coefficient	0.091 mm^{-1}
F(000)	3363
Crystal size	0.35 x 0.3 x 0.2 mm^3
Theta range for data collection	2.61 to 27.45°.
Index ranges	-11<=h<=9, -7<=k<=7, -18<=l<=20
Reflections collected	5130
Independent reflections	934 [R(int) = 0.0312]
Absorption correction	Empirical
Max. and min. transmission	0.266 and 0.236
Refinement method	Full-matrix least-squares on F^2
Data / restraints / parameters	934 / 0 / 71
Goodness-of-fit on F2	1.097
Final R indices [I>2sigma(I)]	R1 = 0.0358, wR2 = 0.0880
R indices (all data)	R1 = 0.0410, wR2 = 0.0947
Largest diff. Peak and hole	0.309 and -0.207 $e.Å^{-3}$

Table 7.2 - Experimental details, structure **5**

Identification code	**Structure 5**
Empirical formula	C14 H10 O2
Formula weight	210.22
Temperature	150 K
Wavelength	0.71073 Å
Crystal system	Monoclinic
Space group	*P*2(1)/c
Unit cell dimensions	a = 10.8247(3) Å α= 90°.
	b = 22.6384(8) Å β= 118.185(1)°
	c = 10.4783(3) Å γ = 90°.
Volume	2263.3(1) $Å^3$
Z	8
Density (calculated)	1.234 Mg/m^3
Absorption coefficient	0.082 mm^{-1}
F(000)	880
Crystal size	0.45 x 0.2 x 0.15 mm^3
Theta range for data collection	1.80 to 30.33°.
Index ranges	-15<=h<=14, -30<=k<=19, -14<=l<=13
Reflections collected	17967
Independent reflections	6159 [R(int) = 0.0628]
Absorption correction	Empirical
Max. and min. transmission	0.614 and 0.398
Refinement method	Full-matrix least-squares on F^2
Data / restraints / parameters	6159 / 0 / 369
Goodness-of-fit on F2	0.983
Final R indices [I>2sigma(I)]	R1 = 0.0596, wR2 = 0.1401
R indices (all data)	R1 = 0.1083, wR2 = 0.1597
Largest diff. Peak and hole	0.342 and -0.306 $e.Å^{-3}$

Table 7.3 - Experimental details, structure **6**

Identification code	**Structure 6**
Empirical formula	C18 H12 O2
Formula weight	260.28
Temperature	150 K
Wavelength	0.71073 Å
Crystal system	Triclinic
Space group	$P\bar{1}$
Unit cell dimensions	a = 8.7684(2) Å α= 113.78(3)°. b = 8.558(2) Å β= 102.06(3)°. c = 10.315(2) Å γ = 102.59(3)°.
Volume	682.2(2) $Å^3$
Z	2
Density (calculated)	1.267 Mg/m^3
Absorption coefficient	0.082 mm^{-1}
F(000)	272
Crystal size	0.45 x 0.3 x 0.15 mm^3
Theta range for data collection	2.29 to 30.38°.
Index ranges	-11<=h<=12, -12<=k<=12, -14<=l<=13
Reflections collected	6577
Independent reflections	3623 [R(int) = 0.0381]
Absorption correction	Empirical
Max. and min. transmission	0.412 and 0.352
Refinement method	Full-matrix least-squares on F^2
Data / restraints / parameters	3623 / 0 / 229
Goodness-of-fit on F2	1.050
Final R indices [I>2sigma(I)]	R1 = 0.0540, wR2 = 0.1084
R indices (all data)	R1 = 0.0973, wR2 = 0.1330
Largest diff. Peak and hole	0.396 and -0.228 $e.Å^{-3}$

Table 7.4 - Selected bond lengths and angles for **4**

	Length (Å)		Angle (°)
C1-C2	1.191(2)	C2-C1-H1	177.6(2)
C1-H1	0.927(2)	C1-C2-C3	178.0(2)
C2-C3	1.486(2)	O1-C3-C2	109.3(8)
C3-O1	1.453(1)	O1-C3-C4	106.05(8)
C3-C4	1.512(2)	C2-C3-C4	108.40(9)
O1-H1A	0.88(2)	C3-O1-HA	107.4(1)
C4-C5	1.3274(2)	C5-C4-C3	123.78(9)
C4-H4	0.97(2)	C3-C4-H4	114.4(8)
C5-H5	0.965(2)	C4-C5-H5	120.7(8)

Table 7.5 - Selected bond lengths and angles for **5.**

	Length (Å)		Angle (°)
C1 H1	0.93(2)	H1-C1-C2	178.91(1)
C1-C2	1.185(3)	C1-C2-C3	176.53(2)
C2-C3	1.488(2)	C2-C3-O1	106.31(1)
C3-O1	1.438(2)	C3-O1-H1A	108.40(1)
O1-H1A	0.90(2)	C14-C3-C4	113.13(1)
C12-H12	0.95(2)	H12-C12-C11	178.05(1)
C12-C11	1.183(3)	C12-C11-C10	176.43(2)
C11-C10	1.490(2)	C11-C10-O2	106.39(1)
C10-O2	1.441(2)	C10-O2-H1B	107.71(2)
O2-H1B	0.94(3)	C13-C10-C9	113.32(1)
C21-H21	1.04(3)	H21-C21-C22	177.72(2)
C21-C22	1.198(3)	C21-C22-C23	179.2(2)
C22-C23	1.484(2)	C22-C23-O21	104.57(1)
C23-O21	1.454(2)	C23 O21-H2A	109.01(2)
O21-H2A	0.90(3)	C34-C23-C24	113.46(1)
C32-H32	0.99(3)	H32-C32-C31	178.51(2)
C32-C31	1.192(3)	C32-C31-C30	179.5(2)
C31-C30	1.490(2)	C31-C30-O22	104.56(1)
C30-O22	1.450(2)	C30-O22-H2B	105.0(2)
O22-H2B	0.79(3)	C33-C30-C29	113.69(1)

Table 7.6 - Selected bond lengths and angles for **6.**

	Length (Å)		Angle (°)
C1-H1	1.00(3)	H1-C1-C2	178.8(2)
C1-C2	1.191(3)	C1-C2-C3	179.2(2)
C2-C3	1.491(3)	C2-C3-O1	104.5(1)
C3-O1	1.450(2)	C3-O1-HA	107.0(2)
O1-HA	0.99(3)	C4-C3-C8	114.5(1)
C2-C3	1.491(3)	C4-C5-C6	120.7(2)
C21-H21	0.94(3)	H21-C21-C22	178.0(2)
C21-C22	1.190(3)	C21-C22-C23	176.9(2)
C22-C23	1.494(3)	C22-C23-O2	106.0(1)
C23-O2	1.440(2)	C23-O2-HB	107.2(2)
O2-HB	0.89(3)	C24-C23-C27	114.1(1)
C28-C29	1.379(3)	C27-C28-C29	121.1(2)

7.3 Hydrogen bonding in structures 4 to 6.

Table 7.7- Interaction distances and angles, structure **4**

	Distance (Å)	Angle (°)
O-H --- O	2.22 (2)	163.0 (2)
C-H --- O	2.51 (2)	143.6 (5)
ring C-H --- C≡C[#]	2.97	128

distances and angles given to centroid of triple bond

Table 7.8- Interaction distances and angles, structure **5**

	Distance (Å)	Angle (°)
O-H --- O	1.96 (2) 1.93 (2)	164 (2) 159 (2)
O-H --- C≡C #	2.68 2.65	150 158
C≡C-H --- O	2.16 (3) 2.14 (3)	170 (3) 158 (2)
C≡C -H --- C≡C #	2.89 2.88	160 159

distances and angles given to centroid of triple bond

Table 7.9 - Interaction distances and angles, structure **6**

	Distance (Å)	Angle (°)
O-H --- O	2.00 (3)	160 (3)
O-H --- C≡C#	2.42	162
C≡C-H --- O	2.14 (3)	163 (2)
C≡C-H --- C≡C#	2.97	158

distances and angles given to centroid of triple bond

The crystal packing of **4**, the base unit, is dominated by infinite cooperative chains of O-H --- O interactions. These interactions can be seen in Figure 7.5 and are quite directional at hydrogen, O-H -- O, 163°. The O-H --- O chains are formed in the (010) plane while weaker C-H --- O interactions form in the (100) plane. Interactions in the (100) plane are shown in Figure 7.6. Along with the C≡C-H --- O interactions, there are possibly also some interactions between the ethylenic groups and the alkyne triple bond centroid. Whether the C-H --- π interaction truly is attractive and influential is

debatable. The ring C-H group is not necessarily electropositive and the acceptor group is also weak in hydrogen bonding terms. In addition to this, although the C-H --- π distance is within the bound of the usual acceptability, the approach of the C-H bond vector towards the triple bond centroid is not particularly linear, 128°.

If the ring hydrogen atom is a necessary part of the crystal packing of this molecule it would be expected that any substitution of these hydrogen atoms would change the overall packing motif. Structures **5** and **6** are substituted versions of **4** and the packing motifs of **4** are not repeated in either structure. This observation lends weight to the suggestion that the C-H --- π interactions are structurally significant. One must however, consider the steric effects of the increased size of **5** and **6** in comparison with **4**. Steric hindrance may affect the ability of the larger molecules to form the weak C-H --- π interactions.

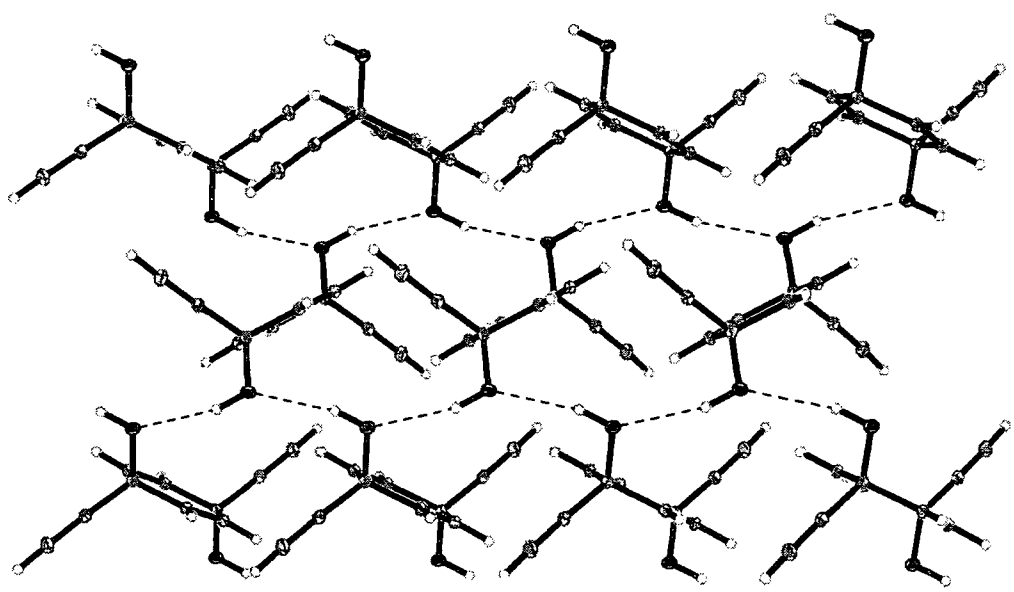

Figure 7.5 - Structure **4**, O-H --- O cooperative chains

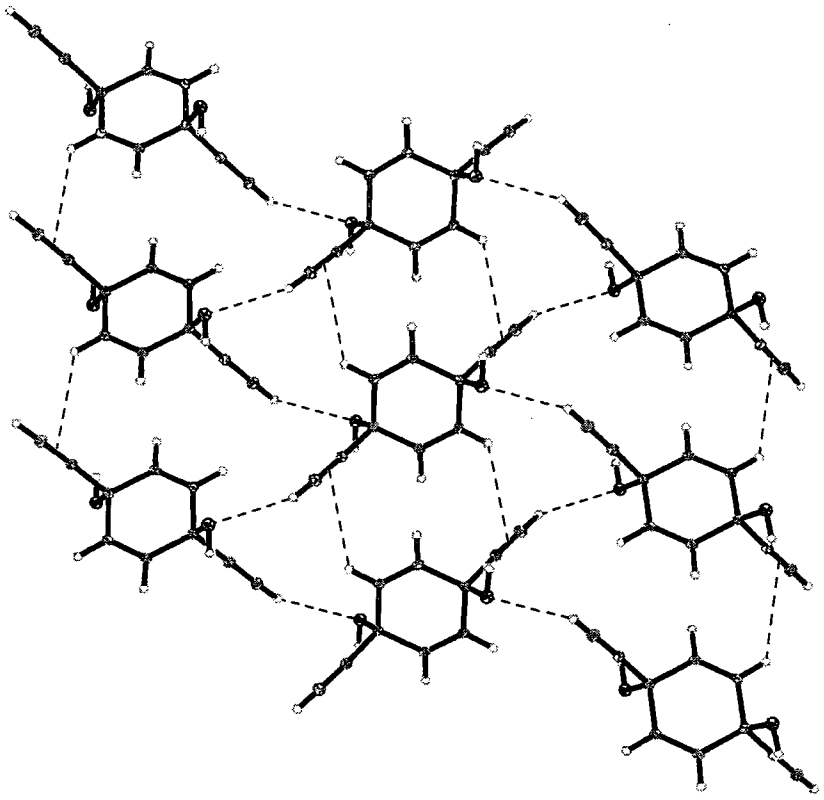

Figure 7.6 - Structure **4**, interactions in (100)

Molecule **5** consists of the base unit of molecule **4** with a phenyl ring fused to one side, **6** also has a ring fused to the other side. Both structures display quite different intermolecular interaction patterns when compared with **4** but **5** and **6** themselves have very similar packing and common hydrogen bonding networks. Each structure has two symmetry independent units in the asymmetric unit, **5** has two full molecules on general positions while **6** has two half molecules each sitting on an inversion centre. In each unit cell the two symmetry independent molecules are linked by a pattern of C≡C-H --- π, O-H --- O and O-H -- π interactions as shown in Figure 7.7.

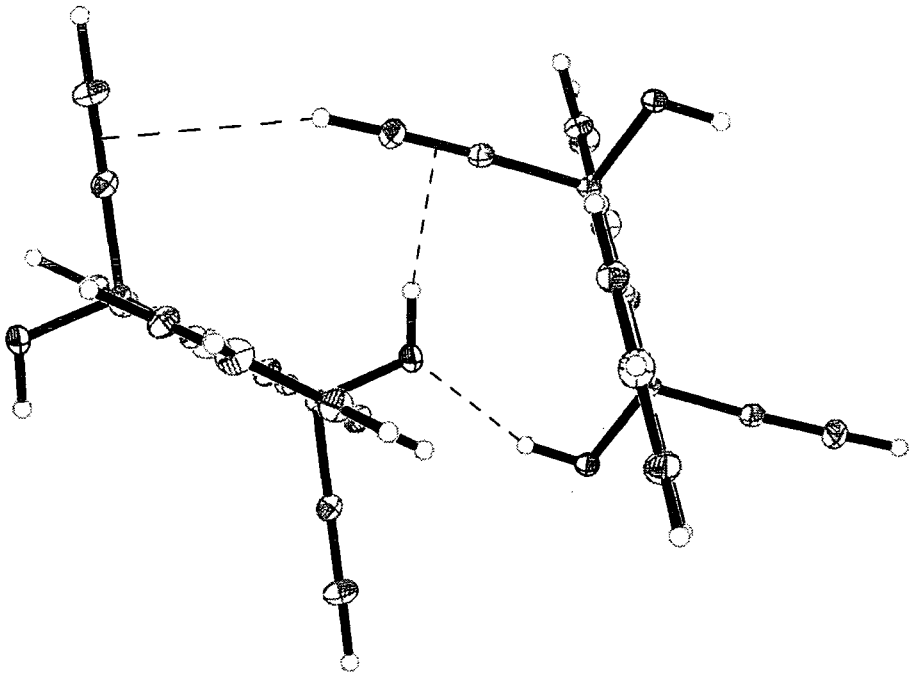

Figure 7.7 - Structure **6**, hydrogen bonding within the unit cell

Two hydrogen bonded networks can be identified which are present in both **5** and **6.** These centrosymmetric synthons involve both symmetry independent molecules. Synthon 1 consists of a loop of O-H --- O and C≡C-H --- O interactions while the second synthon is formed from O-H --- O and C≡C-H --- π hydrogen bonds.

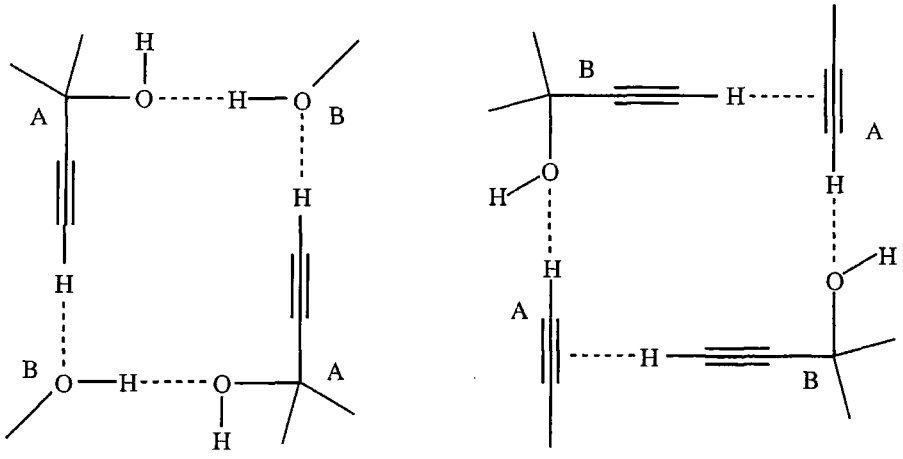

Synthon 1 Synthon 2

Figure 7.8 - tetrameric synthons present in structures **5** and **6**

The *gem*-alkynol unit alone can form four different hydrogen bonds, the formation of the two synthons requires the presence of three of these interactions. Each synthon requires two instances of two of the interactions, for example synthon 1 forms from two O-H --- O and two C≡C-H --- O hydrogen bonds. Structure **6** only has two half unique molecules so the synthons are centrosymmetric. Structure **5** has two full unique molecules so there are two distinct occurrences of each of the interactions. In each case, the synthons are made using each of the two interactions although the distances and angles are very similar. The difference is illustrated with atom labelling of synthon 1 for both structures, Figure 7.9.

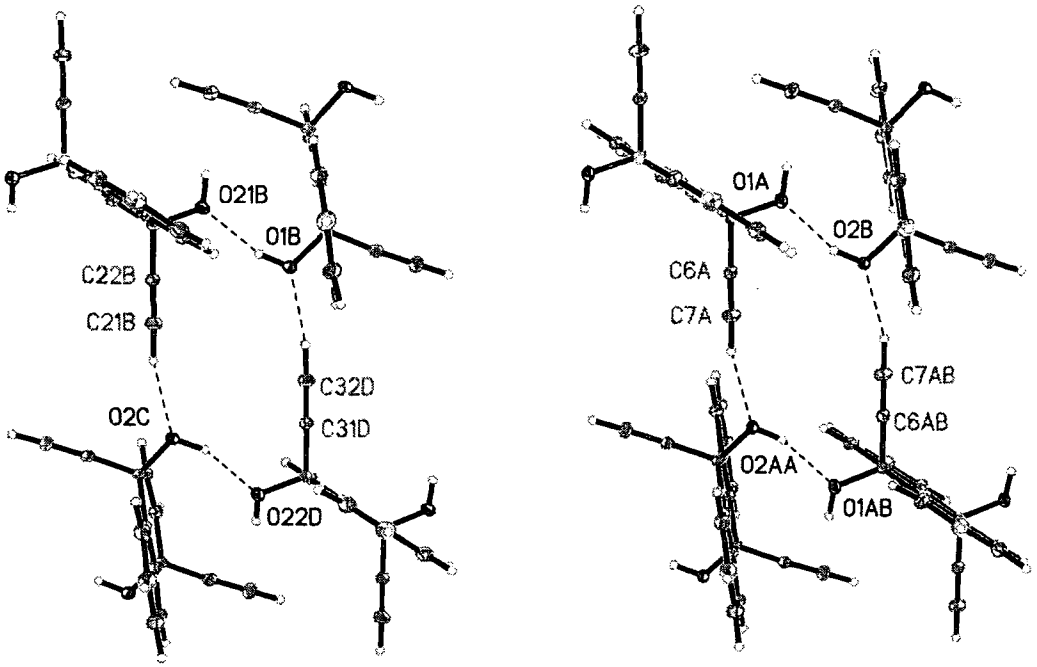

Figure 7.9 - Synthon 1, structure **5** on the left, **6** on the right

To construct synthon 1, structure **5** uses all four different oxygen atoms, O1, O2, O21 and O22, as structure **6** only has two different oxygen atoms O1 and O2, the synthon is centrosymmetric.

A feature common to both structures is that the O-H --- π (C≡C) interaction is not a part of either synthon but it does still occur. This hydrogen bond can be seen in Figure 7.7, it links the two symmetry independent molecules and provides additional stabilisation to the 3-D structure.

Synthon 1 is also seen in the structure of 2-ethynyladamantan-2-ol (Allen, Hoy, Desiraju, Reddy & Wilson, 1996), where it also forms using two symmetry independent molecules. This is an interesting observation in light of the variety of hydrogen bonding networks in the larger family of gem-alkynol structures, especially as 2-ethynyladamantan-2-ol has quite different substituent groups to both **5** and **6.** It is an instance of structural repetition of a major synthon within this family, it was hardly predictable and underlines the difficulty of categorising the hydrogen bonding of the gem-alkynol unit.

REFERENCES

Allen, F. H., Howard, J. A. K., Hoy, V. J., Desiraju, G. R., Reddy, D. S. & Wilson, C. C., (1996). *J. Am. Chem. Soc.*, **118**, 17, 4081-4.

Bruker AXS (1998). SAINT, Area detector data integration software, Version 5.0, Bruker AXS, Madison, Wisconsin, USA, 1998.

Sheldrick, G. M. (1997). SHELX-97, Structure determination software, G. M. Sheldrick, University of Goettingen, Germany, 1997.

Gem-alkynol structures 7, **8, 9** and **10**.

CHAPTER 8

8.1 Gem-alkynol structures 7 to 10

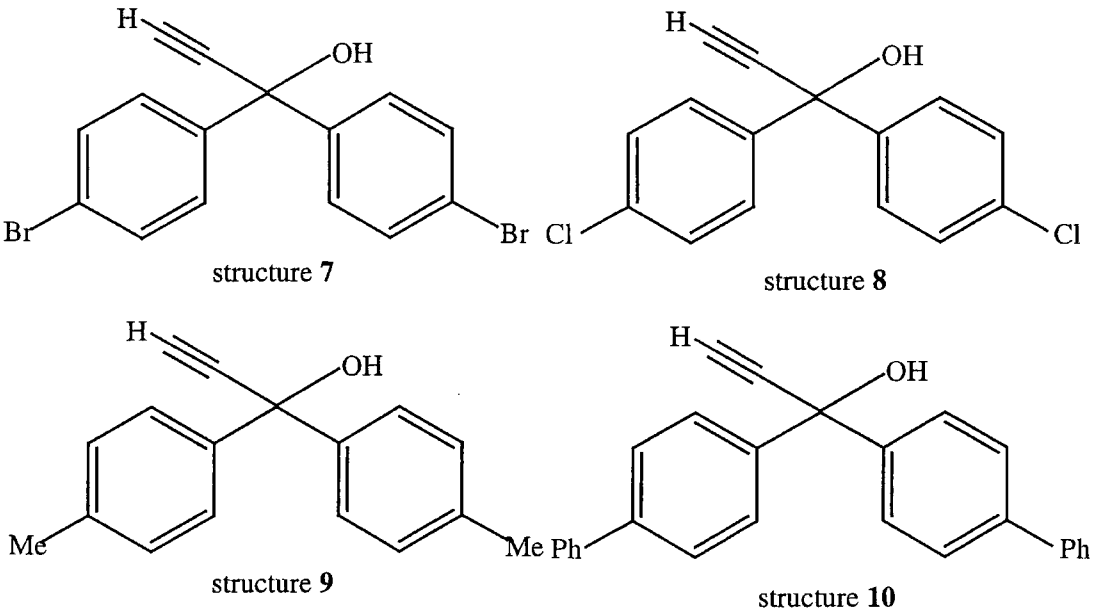

Figure 8.1 - Structural formulae, structures **7** to **10**

Intermolecular interactions involving π-electron density as the acceptor moiety have been the focus of several hydrogen bonding studies. Interactions involving alkynes have thoroughly investigated (Steiner, Starikov, Amado, Teixeiradias, 1995; Steiner, Tamm, Grzegorzewski, Schulte, Veldman, Schreurs, Kanters, Kroon, Van der Mass, Lutz, 1996) and also phenyl rings (Malone, Murray, Charlton, Docherty & Lavery, 1997; Levitt & Puretz, 1999).

The four molecules in the group (Figure 8.1) have the potential for other interactions in addition to the four interactions that can be formed by the base *gem*-alkynol unit (see page 55). All the molecules have phenyl rings, so interactions involving the rings as donors or π-acceptors are possible. The halogen substituted molecules also have the

potential for halogen --- halogen interactions. One would expect, given the relative strengths of the possible interactions, that the O-H --- O would be the dominant interactions. However, the result was completely unexpected. In fact, all four molecules pack in a similar manner and the structures are actually mediated by weak interactions involving the phenyl rings.

8.2 Experimental Details

Data for structures **7**, **8**, **9**, and **10** were collected using Mo-Kα X-ray radiation. In each case a suitable crystal was mounted on a glass fibre using epoxy glue. Data were collected at 150K using a Bruker SMART CCD diffractometer. The data were integrated using the Bruker SAINT package (Bruker AXS, 1998)and corrected appropriately for absorption. Structure solutions were obtained by Direct Methods using Shelx97 (Sheldrick, 1997) and the resultant solutions were refined against F^2.

Data for structure **8** were also collected using neutron radiation. The crystal was mounted on an aluminium pin and data collected at 150K on the single crystal diffractometer SXD (Keen & Wilson, 1996) at the ISIS Spallation Source. Data were integrated using SXD97 (Wilson, 1997). Atomic positional coordinates for carbon and oxygen atoms from the previously refined X-ray model were then used as a starting model for the least squares refinement. Hydrogen atoms were accurately located in the neutron difference map.

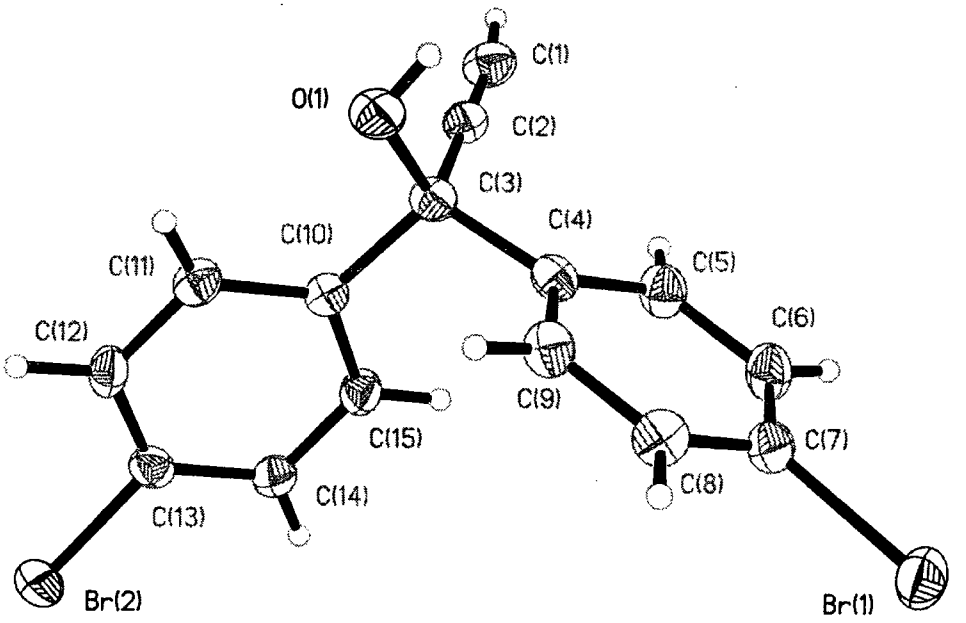

Figure 8.2 - 50% probability ellipsoid plot for structure **7**

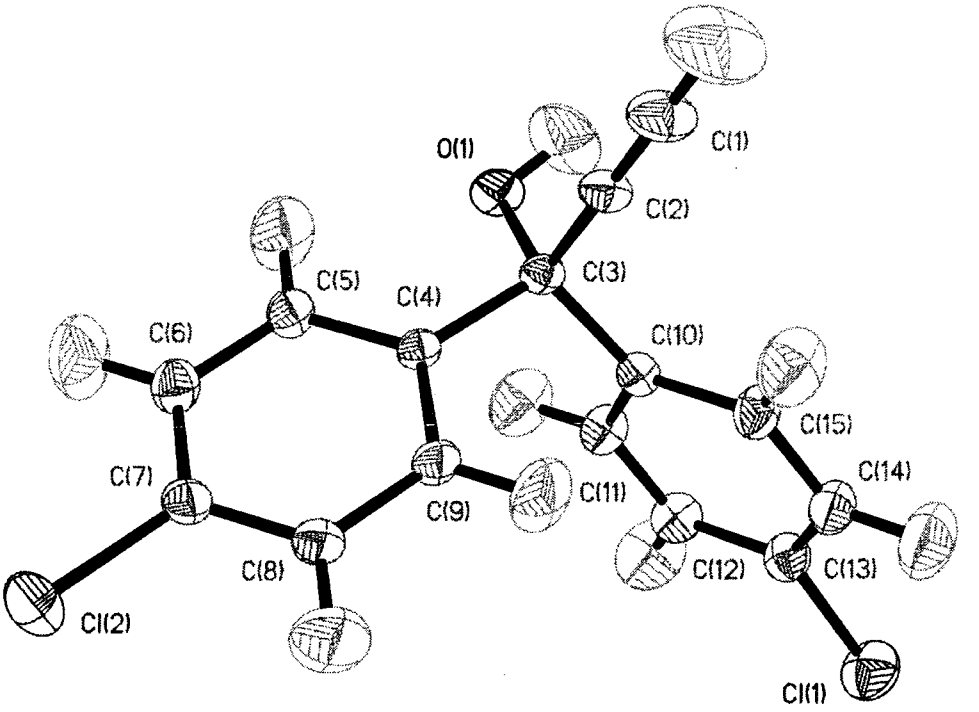

Figure 8.3 - 50% probability ellipsoid plot for structure **8**, note hydrogen atoms

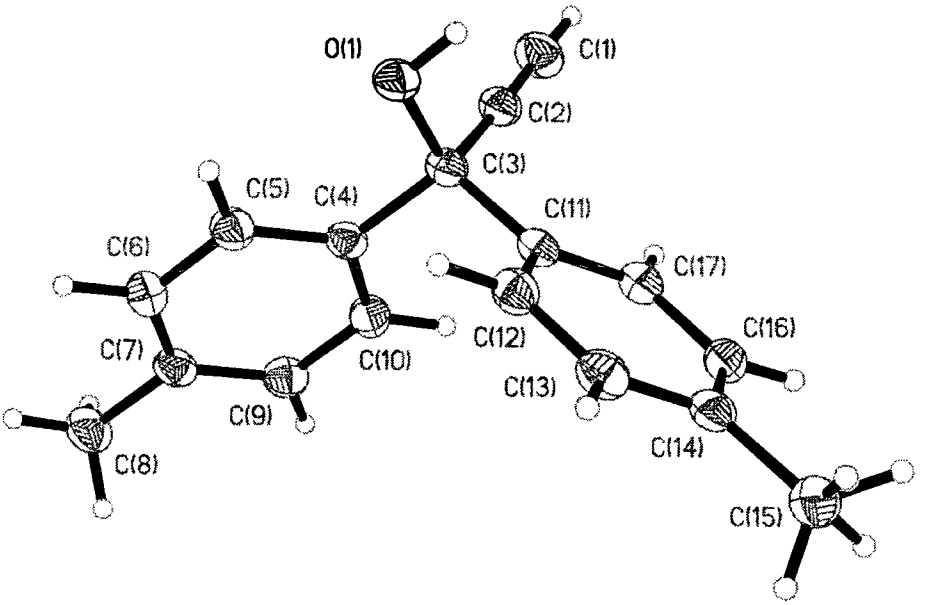

Figure 8.4 - 50% probability ellipsoid plot for structure **9**

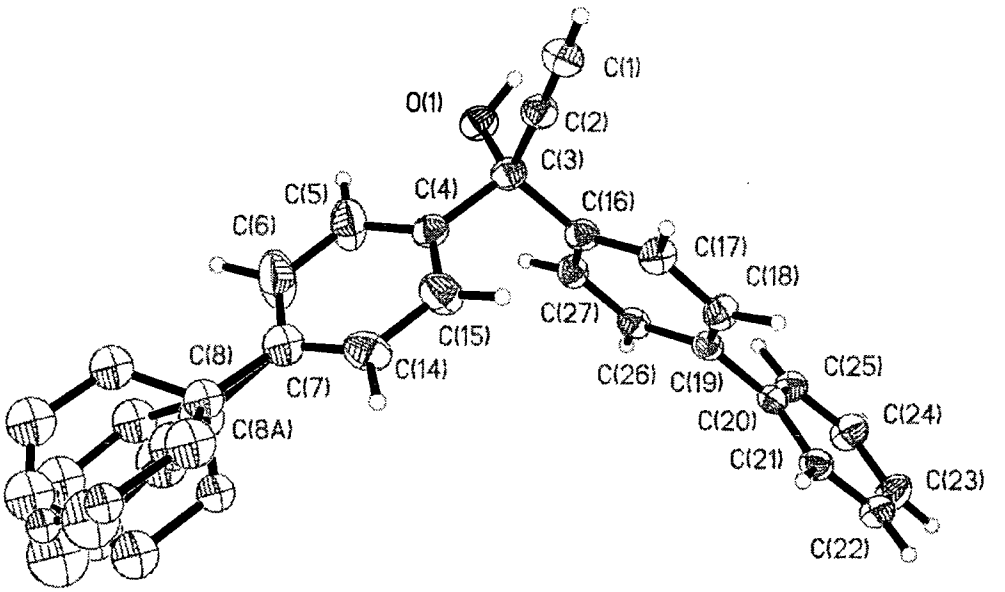

Figure 8.5 - 50% probability ellipsoid plot for structure **10**,

showing disorder of one phenyl ring over three positions

Table 8.1 - Experimental details, structure 7

Identification code	**Structure 7**
Empirical formula	C15 H10 Br2 O
Formula weight	366.05
Temperature	150 K
Wavelength	0.71073 Å
Crystal system	Triclinic
Space group	$P\bar{1}$
Unit cell dimensions	a = 5.791(1) Å α= 115.67(3)°.
	b = 11.325(2) Å β= 99.43(3)°.
	c = 11.907(2) Å γ = 97.91(3)°.
Volume	674.8(2) $Å^3$
Z	2
Density (calculated)	1.801 Mg/m^3
Absorption coefficient	5.990 mm^{-1}
F(000)	356
Crystal size	0.4 x 0.3 x 0.2 mm^3
Theta range for data collection	1.96 to 30.16°.
Index ranges	-6<=h<=8, -15<=k<=12, -15<=l<=16
Reflections collected	5364
Independent reflections	3456 [R(int) = 0.0287]
Absorption correction	Psi-scans
Max. and min. transmission	0.766 and 0.344
Refinement method	Full-matrix least-squares on F^2
Data / restraints / parameters	3456 / 0 / 203
Goodness-of-fit on F2	1.071
Final R indices [I>2sigma(I)]	R1 = 0.0276, wR2 = 0.0691
R indices (all data)	R1 = 0.0367, wR2 = 0.0718
Largest diff. Peak and hole	0.862 and -0.433 $e.Å^{-3}$

Table 8.2 - Experimental details, structure **8**

Identification code	**Structure 8**
Empirical formula	C15 H10 Cl2 O
Formula weight	277.13
Temperature	150 K
Wavelength	0.5 - 5.0 Å
Crystal system	Triclinic
Space group	$P\bar{1}$
Unit cell dimensions	a = 5.7280(1) Å α= 117.240(1)°.
	b = 11.3620(2) Å β= 99.250(1)°.
	c = 11.5210(1) Å γ = 96.800(1)°.
Volume	641.87(2) $Å^3$
Z	2
Density (calculated)	1.438 Mg/m^3
Absorption coefficient	1.450 mm^{-1}
F(000)	17.46
Crystal size	2.5 x 1.5 x 0.5 mm^3
Index ranges	$0 \leq h \leq 12$, $-20 \leq k \leq 21$, $-19 \leq l \leq 10$
Reflections collected	2929
Independent reflections	2928 [R(int) = 0.062]
Absorption correction	Becker-Coppens Lorentzian model
Max. and min. transmission	0.89 and 0.51
Refinement method	Full-matrix least-squares on F^2
Data / restraints / parameters	2929 / 0 / 253
Goodness-of-fit on F2	5.444
Final R indices [I>2sigma(I)]	R1 = 0.0668, wR2 = 0.1281
R indices (all data)	R1 = 0.0668, wR2 = 0.1281

Table 8.3 - Experimental details, structure **9**

Identification code	**Structure 9**
Empirical formula	C17 H16 O
Formula weight	236.30
Temperature	150 K
Wavelength	0.71073 Å
Crystal system	Triclinic
Space group	$P\bar{1}$
Unit cell dimensions	a = 6.829(1) Å α= 106.73(3)°.
	b = 8.241(2) Å β= 98.71(3)°.
	c = 12.658(3) Å γ = 101.39(3)°.
Volume	652.0(2) $Å^3$
Z	2
Density (calculated)	1.204 Mg/m^3
Absorption coefficient	0.073 mm^{-1}
F(000)	252
Crystal size	0.3 x 0.3 x 0.2 mm^3
Theta range for data collection	1.72 to 27.48°.
Index ranges	-8<=h<=8, -10<=k<=7, -14<=l<=16
Reflections collected	4775
Independent reflections	2964 [R(int) = 0.0176]
Absorption correction	Empirical
Max. and min. transmission	1.000 and 0.784
Refinement method	Full-matrix least-squares on F^2
Data / restraints / parameters	2964 / 0 / 231
Goodness-of-fit on F2	1.033
Final R indices [I>2sigma(I)]	R1 = 0.0478, wR2 = 0.1199
R indices (all data)	R1 = 0.0634, wR2 = 0.1317
Largest diff. Peak and hole	0.205 and -0.197 $e.Å^{-3}$

Table 8.4 - Experimental details, structure **10**

Identification code	**Structure 10**
Empirical formula	C27 H20 O
Formula weight	360.43
Temperature	150 K
Wavelength	0.71073 Å
Crystal system	Triclinic
Space group	$P\bar{1}$
Unit cell dimensions	a = 5.6413(3) Å α= 100.450(2)°.
	b = 10.2599(5) Å β= 97.790(2)°.
	c = 17.3238(9) Å γ = 95.477(2)°.
Volume	969.51(9) $Å^3$
Z	2
Density (calculated)	1.235 Mg/m^3
Absorption coefficient	0.073 mm^{-1}
F(000)	380
Crystal size	0.4 x 0.2 x 0.1 mm^3
Theta range for data collection	1.21 to 30.45°.
Index ranges	$-7 \leq h \leq 7$, $-14 \leq k \leq 13$, $-21 \leq l \leq 23$
Reflections collected	12424
Independent reflections	5270 [R(int) = 0.0426]
Absorption correction	Empirical
Max. and min. transmission	0.884 and 0.681
Refinement method	Full-matrix least-squares on F^2
Data / restraints / parameters	5270 / 0 / 322
Goodness-of-fit on F2	1.038
Final R indices [I>2sigma(I)]	R1 = 0.0759, wR2 = 0.2025
R indices (all data)	R1 = 0.1171, wR2 = 0.2336
Largest diff. Peak and hole	0.503 and -0.433 $e.Å^{-3}$

Table 8.5 - Selected bond lengths and angles for 7.

	Length (Å)		Angle (°)
H1-C1	0.90(4)	H1-C1-C2	172(3)
C1-C2	1.184(3)	C1-C2-C3	179.4(2)
C2-C3	1.483(3)	H1A-O1-C3	107(3)
C3-C10	1.543(3)	C10-C3-C4	108.9(2)
C10-C11	1.393(3)	C10-C11-C12	120.4(2)
C13-Br2	1.906(2)	C4-C5-C6	120.7(2)
C7-Br1	1.904(2)		
H1A-O1	0.76(3)		

Table 8.6 - Selected bond lengths and angles for **8**.

	Length (Å)		Angle (°)
H1-C1	0.90(3)	H1-C1-C2	179.0(2)
C1-C2	1.183(2)	C1-C2-C3	179.1(2)
C2-C3	1.479(2)	H1A-O1-C3	106.2(2)
C3-C10	1.535(2)	C10-C3-C4	108.9(2)
C10-C11	1.395(2)	C10-C11-C12	120.6(2)
C13-Cl1	1.740(2)	C4-C5-C6	120.5(2)
C7-Cl2	1.742(2)		
HA-O1	0.77(3)		

Table 8.7 - Selected bond lengths and angles for **9**

	Length (Å)		Angle (°)
H1-C1	0.95(2)	H1-C1-C2	178.4(2)
C1-C2	1.187(2)	C1-C2-C3	176.1(2)
C2-C3	1.489(2)	H1A-O1-C3	103.8(2)
C3-C4	1.544(2)	C4-C3-C11	111.2(1)
C4-C5	1.389(2)	C4-C5-C6	120.2(2)
C7-C8	1.511(2)	C11-C15-C16	120.4(1)
C14-C15	1.511(2)		
HA-O1	0.85(3)		

Table 8.8 - Selected bond lengths and angles for **10**.

	Length (Å)		Angle (°)
H1-C1	0.89(3)	H1-C1-C2	179(2)
C1-C2	1.182(3)	C1-C2-C3	177.7(2)
C2-C3	1.485(3)	H1A-O1-C3	107(3)
C3-C4	1.536(3)	C4-C3-C16	109.4(2)
C16-C17	1.396(3)	C16-C17-C18	120.3(2)
C19-C20	1.485(3)	C18-C19-C20	120.8(2)
H1A-O1	0.87(5)		

8.3 Structural similarity

All four structures crystallise in the same space group $P\bar{1}$ with comparable cell parameters. It should be noted that the cell parameters of the chloro and bromo analogues are very similar which correlates with the particular similarity of their crystal packing. All four molecules pack in a very similar fashion, however, there are differences in the overall three dimensional structures, but the dominant interactions are common to all four structures. The two main interactions both involve the phenyl rings. The first is an O-H ---π (phenyl) interaction, the second is a C≡C --- π(phenyl) interaction.

8.4 Bromo and chloro analogues

The bromo and chloro structures pack in the same manner, four different interaction motifs can be identified in both structures. The two dominant interactions are illustrated for the chloro structure in Figures 8.6 and 8.7.

Table 8.9 - Hydrogen bond distances and angles for structures **7** and **8**.

	Distance (Å)	Angle (°)
Cl --- Cl	3.394 (2)	173 (1) , 93.9 (1)
C-H --- O	2.361 (4)	150.2 (1)
Br --- Br	3.502 (1)	173.79 (7) , 93.42 (7)
C-H --- O	2.56 (31)	157 (2)

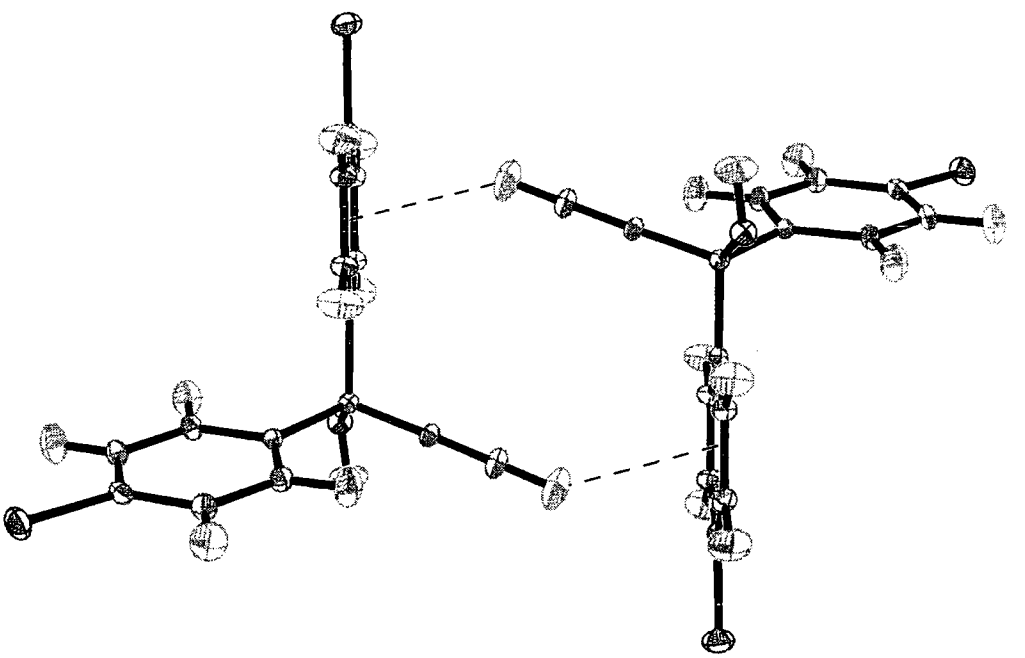

Figure 8.6 - Interaction between alkyne hydrogen atom and phenyl ring centroid

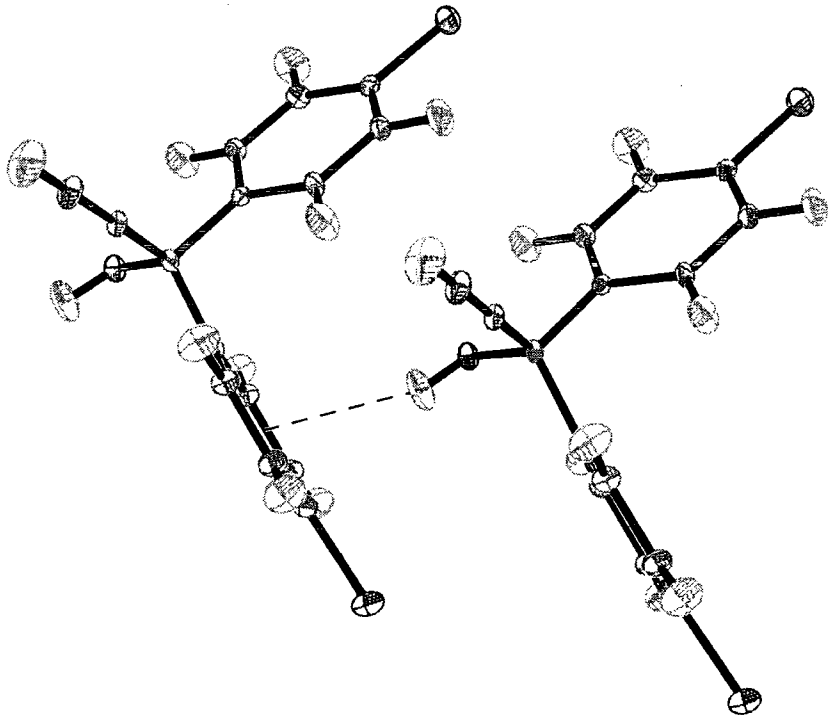

Figure 8.7 - Interaction between hydroxyl hydrogen atom and phenyl ring centroid

These interactions are also found in the bromo structure, they form in exactly the same manner. The O-H --- ring interactions form a characteristic V-shaped stack through the structure. The alkyne --- ring interactions form between pairs of molecules as illustrated in Figure 8.6. These two motifs are common to the chloro and bromo structures, slight variations are also seen in the methyl and phenyl analogues.

There are also halogen --- halogen interactions which run in ribbons down the structures. The ribbons are cross-linked in pairs by ring C-H --- O interactions and are shown for the two structures in Figure 8.8. Although the phenyl C-H --- O interaction is not typically influential, it does play a part linking pairs of molecules in these structures.

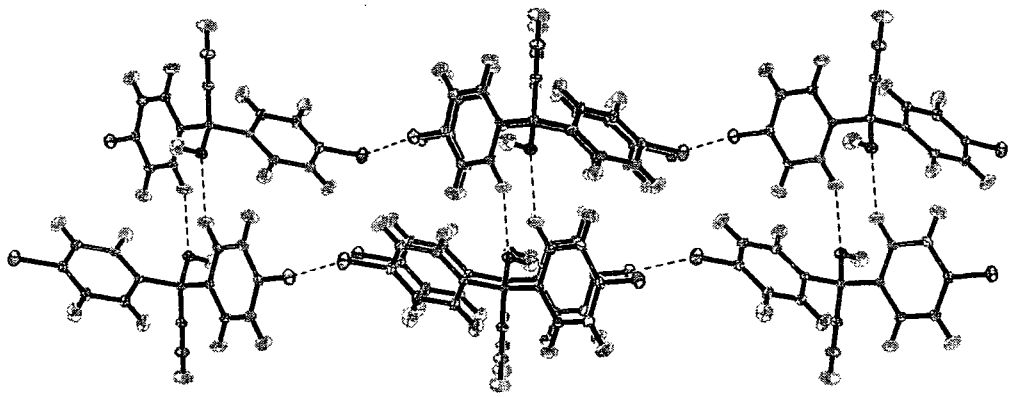

Figure 8.8 - Ribbons of chlorine --- chlorine interactions

Lommerse, Stone, Taylor & Allen (1996), quantified the nature and geometry of intermolecular interactions between halogen atoms and nitrogen or oxygen. The directionality of these contacts (a 'head-on' approach along the direction of the C-H bond) is explained by an anisotropic distribution of electron density around the halogen nucleus. This observation can be applied to the C-Hal --- Hal-C interactions found in structures **7** and **8**.

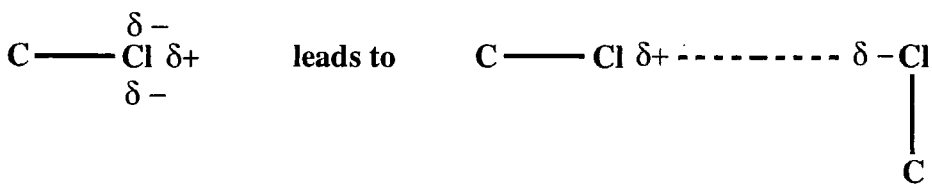

Along the C-Cl direction, the partial charge is δ+ which matches up with a δ- partial charge in an adjacent C-Cl group by a perpendicular approach. This situation is seen in structures **7** and **8**, the approach angles are ~180° and ~90°. Further discussion on the subject of Cl --- Cl interactions can be found in section 9.2.

8.5 Methyl and phenyl analogues

The methyl and phenyl structures both display the O-H --- π centroid and C≡C-H --- π centroid interactions seen in the chloro and bromo structures, however there are slight

differences. In the case of the chloro and bromo, the alkyne interactions form pairwise, while the hydroxyl interactions form V-shaped stacks. In the methyl structure, these interactions form with the opposite patterns, alkynes in a V-shape and hydroxyls pairwise. There are no interactions to replace the halogen interactions seen in the chloro and bromo structures, so this may be the reason that the packing is a little different in this structure.

The phenyl structure also makes use of the hydroxyl and alkyne to ring centroid interactions. Again the hydroxyl interactions form a V-shaped stack and the alkyne interactions form pairwise as with the halogenated structures, but the difference this time is with the choice of 'ring donor'. One feature common to the other three structures is that the hydroxyl group interacts with one ring and the alkyne group interacts with the other ring. However the phenyl substituted structure has four rings rather than two. If it followed the same pattern as the other structures, the two central rings would be involved in the interactions, but the two rings which are actually used are one central ring and its fused substituent ring. The substituent ring on the other side of the central unit is disordered over three positions. The rings that are used are down one side of the molecule rather than one either side, as a result this has a effect on the patterns of interactions. This difference can be explained by comparison of the phenyl and chloro structures. Figure 8.9 shows the unit cell for both structures.

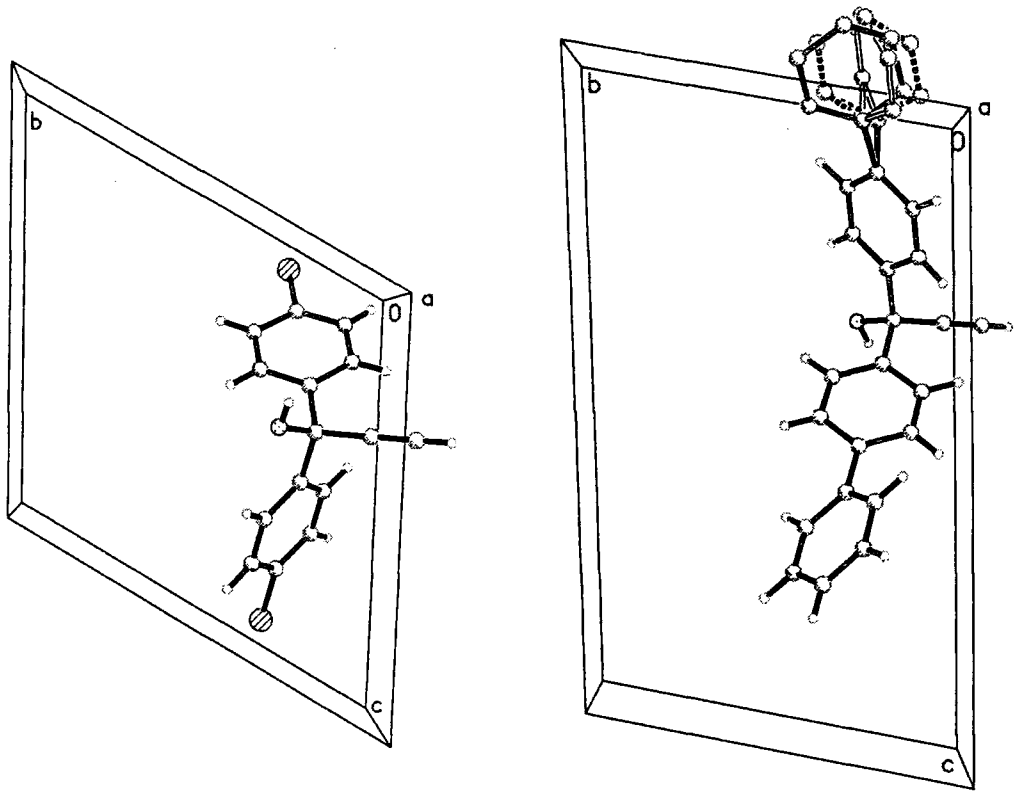

Figure 8.9 - Unit cells of chloro and phenyl substituted structures

The difference in choice of origin has an effect on the pairwise stacking of the molecules. The chloro substituted molecules form tight pairs linked by the alkyne --- π (phenyl) interactions whereas the equivalent phenyl substituted pairs are staggered further apart. The packing plots in Figures 8.10 and 8.11 illustrate this difference. The substitution of a phenyl ring for a chlorine atom increases the distance to the next *gem*-alkynol unit which affects the formation of the pairs. When this is coupled with the slight difference in origin, the alkynol units are pushed far enough apart that instead of the alkyne forming an interaction with the second central ring of one molecule, it instead interacts with the outer ring of the next molecule along the layer.

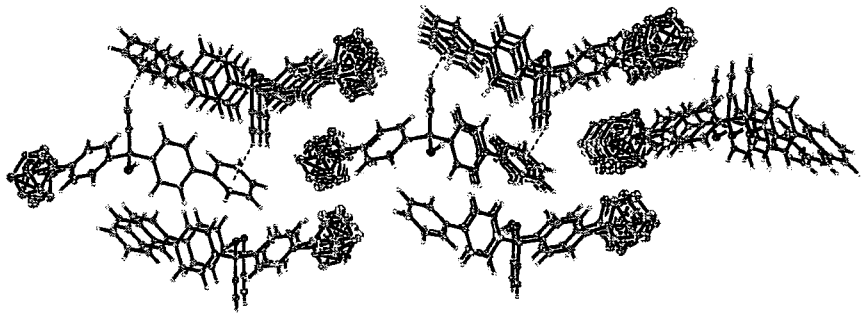

Figure 8.10 - Layers of pairs, structure **10**

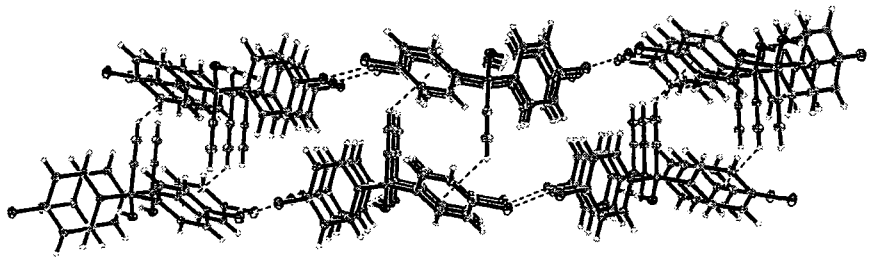

Figure 8.11 - Layers of pairs, structure **8**

Figure 8.10 also shows the channels of disordered phenyl rings running down the structure. Given that this ring is not constrained by any further substituents and is not involved in any intermolecular interactions, the disorder is perhaps not surprising.

The methyl substituted structure, **9**, is similar to the other three, but like the phenyl structure, **10**, there are slight differences. Both the hydroxyl --- centroid and phenyl --- centroid interactions are formed, one to one ring and one to the other, but the packing patterns are reversed. The unit cell of the methyl structure is depicted in Figure 8.12. A comparison of the orientation of the molecules within the unit cell with those of the chloro and phenyl structures in Figure 8.9 shows the clear difference in the relative orientations of the molecules.

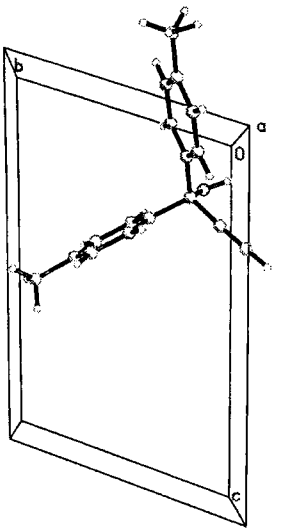

Figure 8.12 - Unit cell, structure **9**

Comparison of Figures 8.9 and 8.12 reveals that the methyl structure is orientated within the unit cell roughly perpendicular to the chloro and bromo structures. The two centroid interactions in all four structures are roughly perpendicular to each other, therefore, as the methyl molecule is oriented roughly perpendicular to the others, it follows that these two interactions form with reversed packing patterns. The hydroxyl --- centroid interactions form pairwise, the alkyne --- centroid interactions form in V-shaped stacks. The interactions are illustrated in Figure 13.

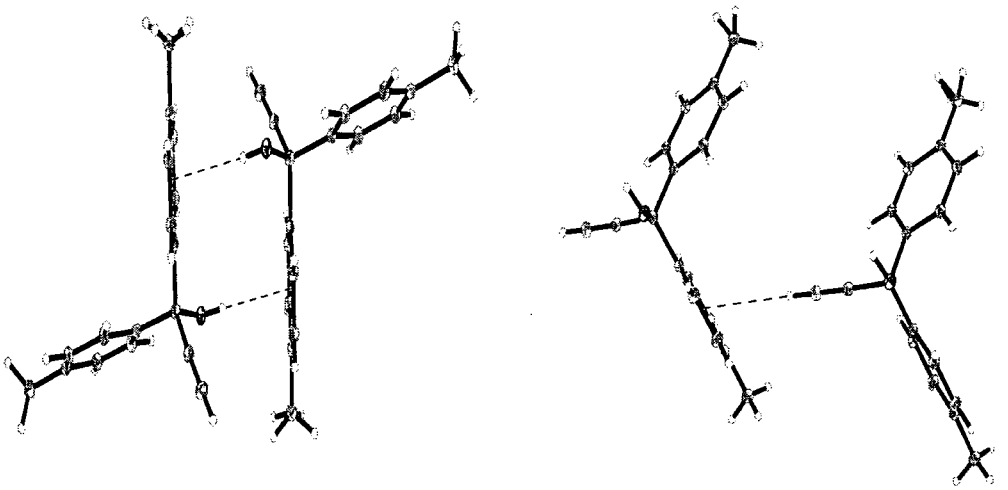

Figure 8.13 - Centroid interactions, structure **9**

8.6 Interactions involving phenyl rings

Table 8.10 - Centroid interactions for all four structures, **7, 8, 9** and **10**.

		-Cl	-Br	$-CH_3$	-phenyl
C≡C-H ---X	/ Å	2.569	2.684	3.137	2.683
Angle C-H --- X	/ ^{o}	158.4	148.1	149.5	152.3
O-H --- X	/ Å	2.637	2.835	2.484	2.623
Angle O-H --- X	/ ^{o}	137.7	159.2	167.9	154.6

X = phenyl ring centroid

The Cambridge Structural Database (CSD) Version 5.17 April 1999 release, (Allen & Kennard, 1993) contains information on 197,481 crystal structures. Searches reveal 1680 organic structures containing 2497 occurrences of the O-H --- X interaction (where X = phenyl ring centroid) under a H --- X distance of 4.0Å. There are 41 structures containing 60 occurrences of C≡C-H --- X interactions within the same distance limit. Searches were carried out for carbon bound donor groups, present only in monomeric, error free organic structures with R_1 <0.10 and no disorder. Figure 8.14 shows the distribution of hydrogen bond distances for both O-H and C≡C-H donor groups. The maximum distance of a smooth distribution would normally give an indication of the maximum distance for acceptance of the interaction as a hydrogen bond, neither distribution shows a clear group of contacts. This is understandable as they are very weak interactions, however the distances in all four crystal structures fall at the lower end of the distribution in each case.

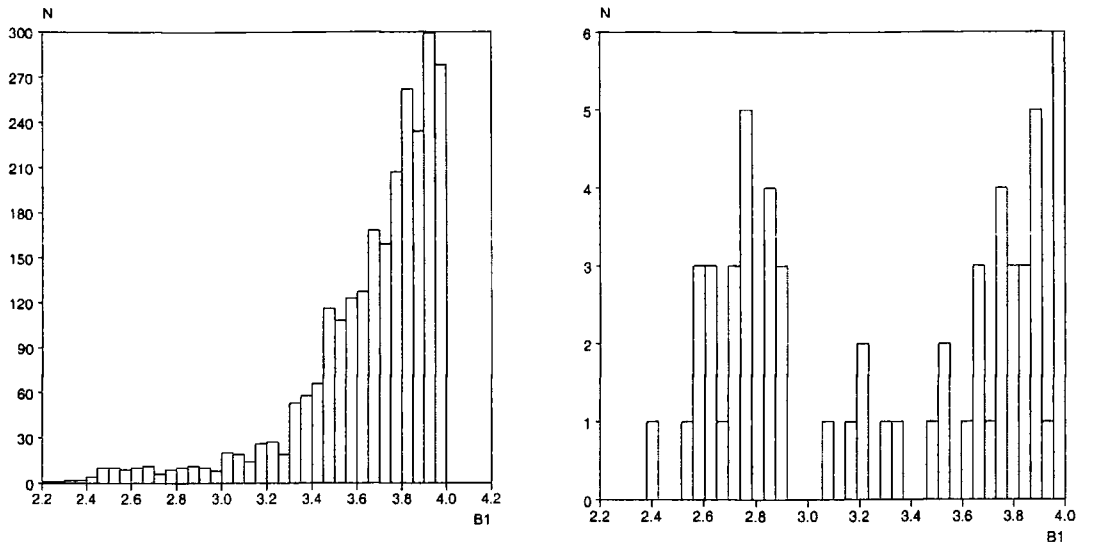

Figure 8.14 - Centroid interaction distances from CSD searches. The graph on the left corresponds to O-H --- X and that on the right corresponds to C≡C-H --X. In both cases, X is the centroid of a phenyl ring.

Comparisons can be drawn between the pairwise and V-shaped stacking motifs produced by the two centroid interactions. The O-H donor is a much stronger hydrogen bond donor than the alkyne group, hence it would be expected that the interactions formed by this group would be noticeably shorter. However, the figures in Table 8.6 show that except for the methyl structure there is actually very little difference between the two groups. The alkyne interactions form pairwise in the chloro, bromo and phenyl structures and this cooperative pairing of interactions may reinforce the interaction. In the case of the methyl structure it is the hydroxyl interactions which form pairwise and this time they are considerably shorter. Quite why the methyl structure reverses that pattern is unclear.

8.7 Neutron diffraction experiment, structure 8.

Since it is not possible the locate hydrogen atoms with the same accuracy as 'heavier' elements using X-ray diffraction experiments it is difficult to make any categorical statements about weak interactions particularly involving phenyl rings. Careful choice of small organic molecules such as those chosen here, help the situation since hydrogen atom positions can be determined with reasonable accuracy, but the length of bonds involving hydrogen atoms are systematically underestimated. Neutron diffraction experiments are the ideal solution to this problem, as the accurate positions of the hydrogen atoms involved in the hydrogen bonding can be found and thus hydrogen bonds to the centres of the phenyl rings can be defined with precision.

Single crystal neutron diffraction data were collected for structure **8**. Data were collected on the instrument SXD (Keen & Wilson, 1996) at ISIS. The crystal structure complete with hydrogen atoms modelled anisotropically is shown in Figure 8.3. Hydrogen bond distances and angles are given in Table 8.10.

As the donor hydrogen atomic positions are well defined by the neutron data, the approach of the C-H bond vector towards the phenyl ring in each case can be investigated. Figures 8.15 and 8.16 illustrate the approach towards the ring for the O-H donor and the C≡C-H donor respectively.

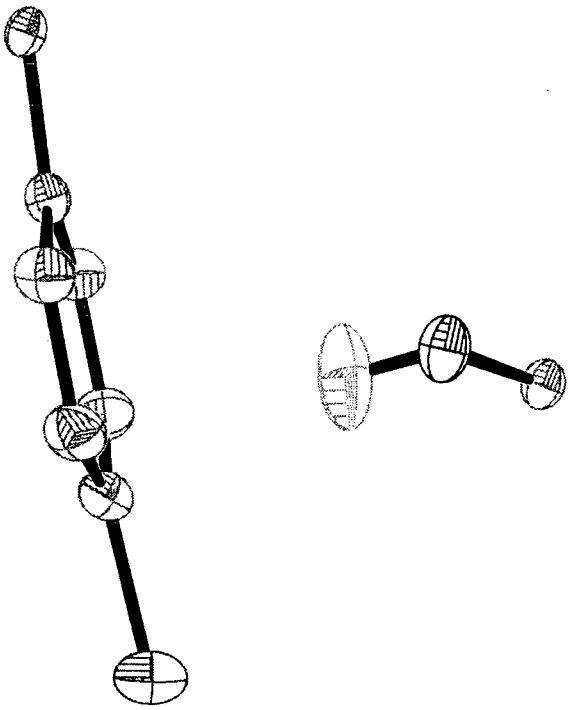

Figure 8.15- Approach of alcohol hydrogen atom to phenyl ring.

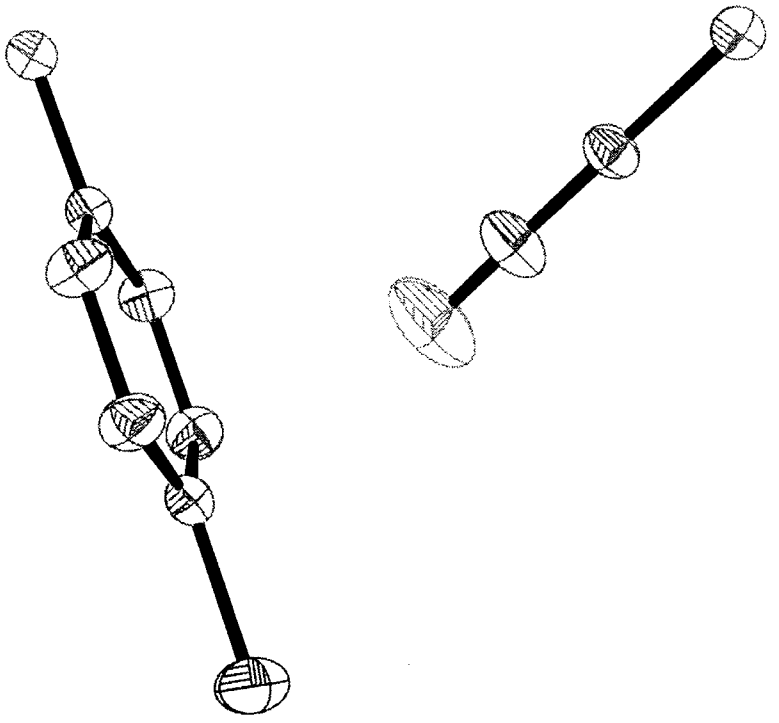

Figure 8.16- Approach of alkyne hydrogen atom to phenyl ring.

The hydrogen atoms do not approach the exact centroid of the phenyl ring and also not at 180°. However it is clear that the phenyl ring is the desired acceptor site and these interactions are not a mere geometrical coincidence. A perfectly linear approach particularly unlikely for the alkyne donor hydrogen atom due to the steric bulk of the alkyne functional group. In light of this consideration, the H --- centroid distances and the approach angles are even more remarkable. Such interactions involving phenyl rings may not be structurally determining in seclusion, but a combination as seen here can be the dominant interactions.

REFERENCES

Allen, F.H. and Kennard, O., (1993). *Chemical Design Automation News*, **8** (1), pp 1 & 31-37.

Bruker AXS (1998). SAINT, Area detector data integration software, Version 5.0, Bruker AXS, Madison, Wisconsin, USA, 1998.

Keen, D. A. & Wilson, C. C. (1996). *Technical Report RAL-TR-96-083.* Single crystal diffraction at ISIS. User guide for the SXD instrument.

Levitt, M. & Perutz, M. F. (1988). *J. Mol. Biol.*, **201**, 751-4.

Lommerse, J. P. M., Stone, A. J., Taylor, R. & Allen, F. H., (1996*). J. Am. Chem. Soc.*, **118**, 3106-16.

Malone, J. F., Murray, C. M., Charlton, M. H., Docherty, R. & Lavery, A. J. (1997). *J. Chem. Soc. Faraday Trans.*, **93**, 3429-36.

Sheldrick, G. M. (1997). SHELX-97, Structure determination software, G. M. Sheldrick, University of Goettingen, Germany, 1997.

Steiner, T., Starikov, E. B., Amado, A. M. & Teixeiradias, J. J. C. (1995). *J. Chem. Soc. Perkin Trans. 2*, **7**, 1321-6.

Steiner, T., Tamm, M., Grzegorzewski, A., Schulte, N., Veldman, N., Schreurs, A. M. M., Kanters, J. A., Kroon, J., Van der Mass, J. & Lutz, B. (1996). *J. Chem. Soc. Perkin Trans. 2*, **11**, 2441-6.

Wilson, C. C. (1997). *J. Mol. Struct.*, **405**, 207-217.

Gem-alkynol structures **11**, **12** and **13**.

CHAPTER 9

9.1 Gem-alkynol structures 11 to 13

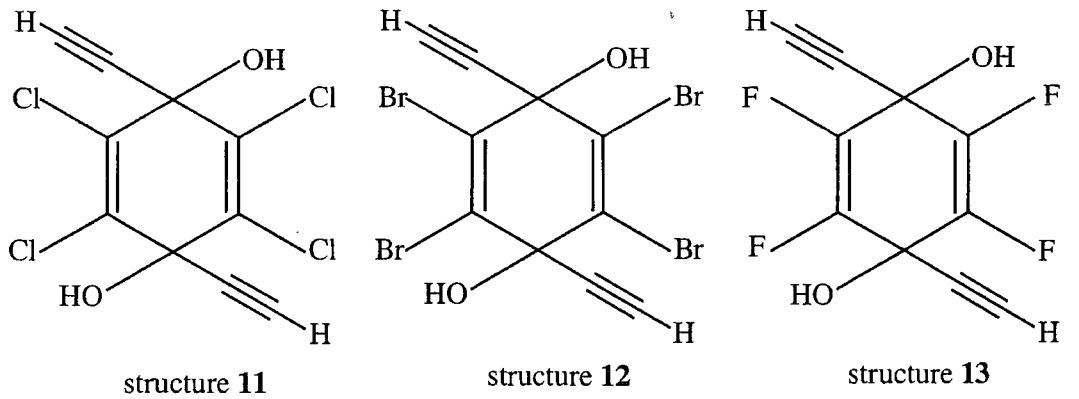

structure **11** structure **12** structure **13**

Figure 9.1 : Structural formulae, structures **11** to **13**

9.2 Halogen --- Halogen interactions

X --- X interactions where X = Cl, Br or I, have generated much interest and discussion in the chemical crystallographic community since their observation in the crystal structures of Cl_2 (Collin, 1952), Br_2 (Harris, 1928) and I_2 (Vonnegut & Warren, 1936) These structures excited particular interest, not only because they crystallised in the same space group Cmca (note: F_2 crystallises in Pm3n), but that they all contain X --- X contacts that are substantially shorter than the sum of the van der Waals radii as derived by Pauling (1947) and later revised by Bondi (1964). The structure of Cl_2 consists of layers tilted at 55^0 with respect to [010], the layers are formed by molecules linked by Cl --- Cl contacts of 3.21Å which are noticeably shorter than the van der Waals sum of 3.60 Å.

Chloro interactions in particular have been the focus of the majority of the work into halogen --- halogen close contacts. Schmidt and Green (1971) studied dichloro

substituted molecules containing such interactions and succeeded in classifying them into three types by the length of the shortest crystallographic axis and in so doing, coined the term 'crystal engineering'. The difficulty in establishing a satisfactory explanation of the nature of Cl --- Cl interactions lies in the prevalence of such interactions and the problem that the short contacts could not be modelled successfully using the usual isotropic atom potentials (Pertsin & Kitiagorodskii, 1987).

Sakurai, Sundaralingham and Jeffrey (Sakurai & Sundaralingham, 1963) noted particular angular dependence of halogen --- halogen interactions during a study of 2,5,- dichloroaniline. They noted that such short contacts fall into two distributions. The first has both C-Cl --- Cl angles equal at 160 ± 10° while the second has one angle at around 175° and the other at around 80°. These two geometries were later classified into three types, type I (θ_1 or θ_2 = 90°), type II (θ_1 or θ_2 = 180°) and type III ($\theta_1 = \theta_2$) by Parthasarathy and co-workers (Ramasubbi, Parthasarathy & Murray-Rust, 1986). These classifications were then simplified further by Desiraju and Parathasarathy (1989) to avoid the problem that a contact may be of both type I and type II. The interactions were classified as type I where $\theta_1 = \theta_2$ and the atoms are related by a centre of symmetry and type II where $\theta_1 \approx 180°$ and $\theta_2 \approx 90°$.

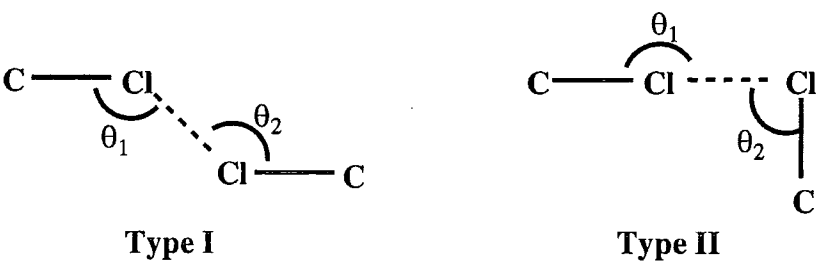

Figure 9.2 Type I and type II C-Cl interactions

Two schools of thought developed in an effort to explain the nature of such short contacts. The first which was popular with experimental crystallographers was that these short contacts with specific directionalities were a result of a specific attractive force (Desiraju, Parthasarathy & Murray-Rust, 1989). They have also been likened to a weak bond at ~3% strength of a covalent bond (Williams, 1985). The second hypothesis, popular with the theoreticians is that the atomic charge density of the chlorine atoms is anisotropic (Price & Stone, 1982) so polar flattening (Nyburg & Faerman, 1985) results in decreased repulsions between the atoms. This also correlates with the observed directionality of these close contacts. In short, these contacts are either a result of (i) specific attractive forces, (ii) close packing of non-spherical atoms (Desiraju, Parthasarathy & Murray-Rust, 1989). Two pieces of work were published in 1994 aiming at providing evidence for the anisotropy theory and the other justifying the attractive force hypothesis. Desiraju and co-workers (Pedireddi, Reddy, Goud, Craig, Rae & Desiraju, 1994) maintain that Cl --- Cl interactions have a specific attractive component. They believe that without an attractive force it is difficult to rationalise the structure of the Cl_2 dimer and also the observation that Cl substituents are known to 'steer' crystal packing towards layer structures. On the other hand, Price and co-workers (Price & Stone, 1994) disagree with the need for any attractive force. They believe that the dispersion and electrostatic contributions to the interaction energy are sufficiently anisotropic that charge transfer is not important. The chlorine charge distribution has a significant effect and there is no need for any additional attractive forces to explain either the interaction distance or any directionality. They also point out that since a large proportion of Cl --- Cl close contacts are found in heavily chlorinated compounds, any dense crystal packing will involve close contacts between chlorine atoms.

Other halogen --- halogen close contacts have unfortunately not received such depth of interest. Ramasubbu, Parthsarathy and Murray-Rust (1986) have covered Cl --- Cl , Br --- Br and I --- I contacts, Murray-Rust and Motherwell (1979) have looked at I --- I contacts.

9.3 Experimental Details

Data for structures **11**, **12**, and **13** were collected using Mo-Kα X-ray radiation. In each case a suitable crystal was mounted on a glass fibre using epoxy glue. Data were collected at 150K using a Bruker SMART CCD diffractometer. The data were integrated using the Bruker SAINT package (Bruker AXS, 1997) and suitably corrected for absorption. Structure solutions were obtained by direct methods using Shelx97 (Sheldrick, 1997) and the resultant solutions were refined against F^2.

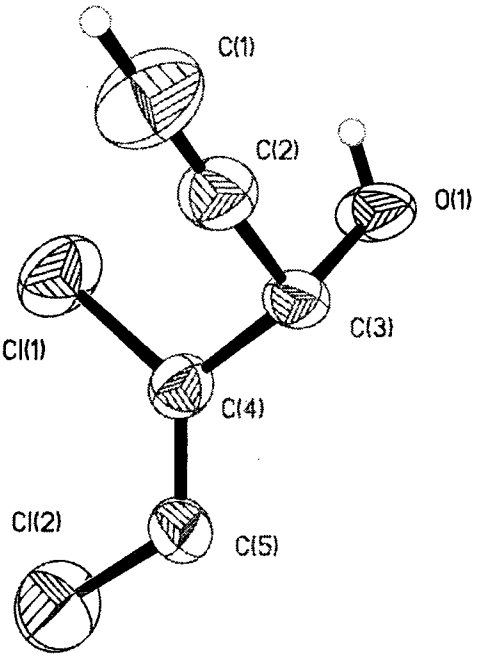

Figure 9.3 - 50% probability ellipsoid plot for structure **11**

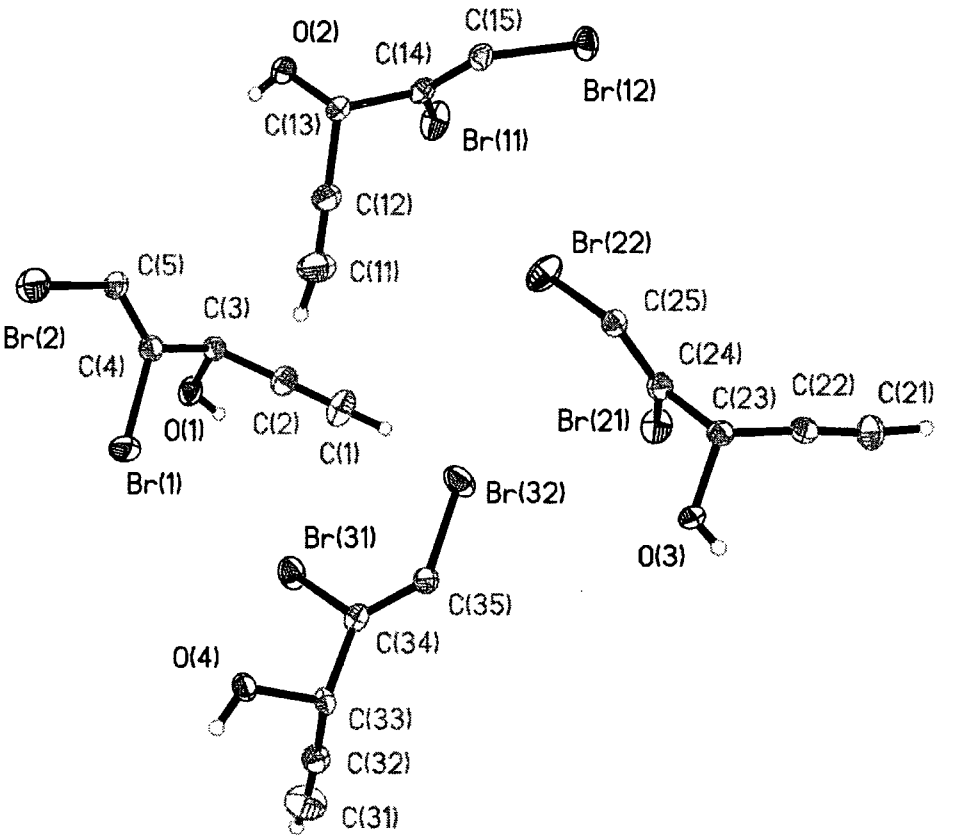

Figure 9.4 - 50% probability ellipsoid plot for structure **12**

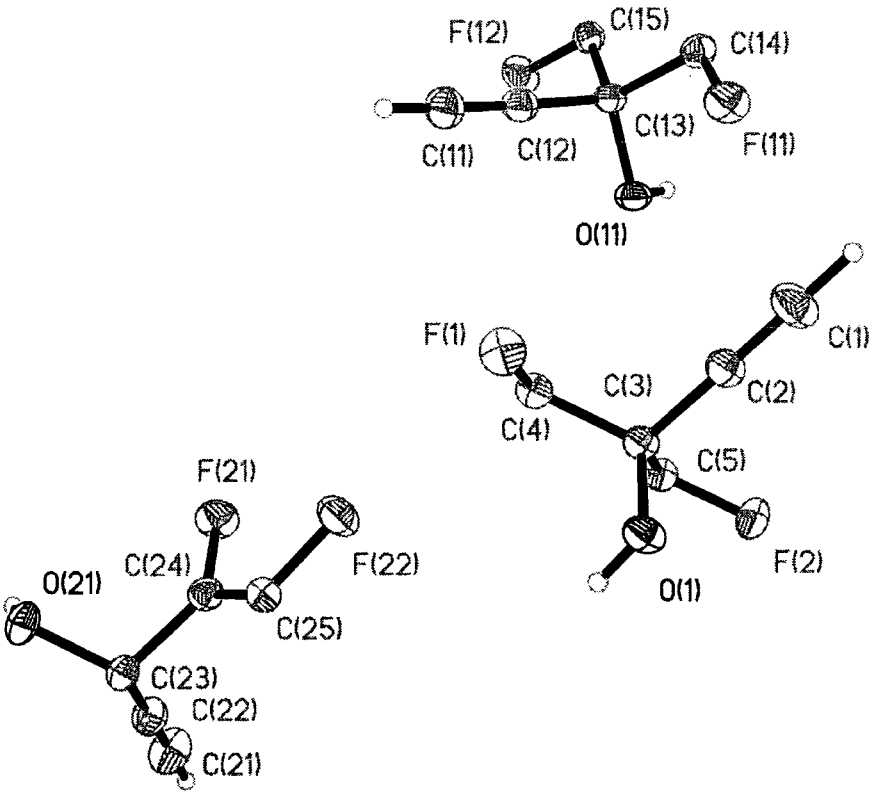

Figure 9.5 - 50% probability displacement plot for structure **13**

Table 9.1- Experimental details, structure **11**

Identification code	**Structure 11**
Empirical formula	C10 H4 Cl4 O2
Formula weight	297.93
Temperature	150 K
Wavelength	0.71073 Å
Crystal system	Tetragonal
Space group	I4(1)/a
Unit cell dimensions	a = 16.758(2) Å α= 90°.
	b = 16.758(2) Å β= 90°.
	c = 8.865(2) Å γ = 90°.
Volume	2489.6(7) $Å^3$
Z	8
Density (calculated)	1.590 Mg/m^3
Absorption coefficient	0.930 mm^{-1}
F(000)	1184
Crystal size	0.3 x 0.3 x 0.2 mm^3
Theta range for data collection	2.43 to 27.39°.
Index ranges	-21≤ h ≤20, -21≤ k ≤19, -9≤ l ≤11
Reflections collected	8404
Independent reflections	1421 [R(int) = 0.0432]
Absorption correction	Sadabs
Max. and min. transmission	0.830 and 0.665
Refinement method	Full-matrix least-squares on F^2
Data / restraints / parameters	1421 / 0 / 82
Goodness-of-fit on F2	1.064
Final R indices [I>2sigma(I)]	R1 = 0.0489, wR2 = 0.1145
R indices (all data)	R1 = 0.0590, wR2 = 0.1230
Largest diff. Peak and hole	0.588 and -0.437 $e.Å^{-3}$

Table 9.2- Experimental details, structure **12**

Identification code	**Structure 12**
Empirical formula	C10 H4 Br4 O2
Formula weight	475.77
Temperature	150 K
Wavelength	0.71073 Å
Crystal system	Triclinic
Space group	$P\bar{1}$
Unit cell dimensions	a = 8.9147(3) Å α= 85.738(1)°.
	b = 12.6402(5) Å β= 69.625 (1)°.
	c = 12.6547(5) Å γ = 72.720(1) °.
Volume	1275.76(8) $Å^3$
Z	4
Density (calculated)	2.477 Mg/m^3
Absorption coefficient	12.599 mm^{-1}
F(000)	880
Crystal size	0.3 x 0.3 x 0.2 mm^3
Theta range for data collection	5.10 to 23.72°.
Index ranges	-11≤ h ≤11, -16≤ k ≤16, -16≤ l ≤16
Reflections collected	14367
Independent reflections	1=5818 [R(int) = 0.0431]
Absorption correction	Sadabs
Max. and min. transmission	0.0737 and 0.0180
Refinement method	Full-matrix least-squares on F^2
Data / restraints / parameters	5818 / 0 / 321
Goodness-of-fit on F2	1.148
Final R indices [I>2sigma(I)]	R1 = 0.0489, wR2 = 0.1145
R indices (all data)	R1 = 0.0590, wR2 = 0.1230
Largest diff. Peak and hole	0.797 and -1.052 $e.Å^{-3}$

Table 9.3- Experimental details, structure **13**

Identification code	**Structure 13**
Empirical formula	C10 H4 F4 O2
Formula weight	228.12
Temperature	150 K
Wavelength	0.71073 Å
Crystal system	Triclinic
Space group	$P\bar{1}$
Unit cell dimensions	a = 8.900(2) Å α= 93.73(3)°.
	b = 9.239(2) Å β= 98.73 (3)°.
	c = 9.672(2) Å γ = 114.46(3) °.
Volume	708.3(2) $Å^3$
Z	3
Density (calculated)	1.619 Mg/m^3
Absorption coefficient	0.164 mm^{-1}
F(000)	342
Crystal size	0.3 x 0.3 x 0.2 mm^3
Theta range for data collection	2.15 to 29.88°.
Index ranges	$-12 \leq h \leq 12$, $-12 \leq k \leq 12$, $-13 \leq l \leq 13$
Reflections collected	8674
Independent reflections	3722 [R(int) = 0.0288]
Absorption correction	Psi-scans
Max. and min. transmission	0.382 and 0.289
Refinement method	Full-matrix least-squares on F^2
Data / restraints / parameters	3722 / 0 / 242
Goodness-of-fit on F2	1.031
Final R indices [I>2sigma(I)]	R1 = 0.0336, wR2 = 0.0895
R indices (all data)	R1 = 0.0371, wR2 = 0.0928
Largest diff. Peak and hole	0.456 and -0.239 $e.Å^{-3}$

Table 9.4 - Selected bond lengths and angles for **11**.

	Length (Å)		Angle (°)
H1-C1	0.88(5)	H1-C1-C2	179(3)
C1-C2	1.165(4)	C1-C2-C3	177.0(3)
C2-C3	1.479(3)	C2-C3-O1	110.5(2)
C3-O1	1.423(3)	C3-O1-HA	113(3)
O1-HA	0.76(4)	C2-C3-C4	109.9(2)
C3-C4	1.519(3)	O1-C3-C4	107.6(2)
C4-Cl1	1.724(3)	C3-C4-C5	124.6(2)
C4-C5	1.320(3)	C3-C4-Cl1	113.0(2)
C5-Cl2	1.722(3)	C4-C5-Cl2	121.6(2)

Table 9.5 - Selected bond lengths and angles for **12**.

	Length (Å)		Angle (°)
H1-C1	0.90(7)	H1-C1-C2	177(4)
C1-C2	1.183(7)	C1-C2-C3	176.9(5)
C3-O1	1.419(5)	C2-C3-C4	110.4(4)
O1-H1A	0.69(6)	C2-C3-O1	110.5(4)
C4-Br1	1.889(4)	C3-C4-Br1	113.5(4)
C5-Br2	1.889(4)	C4-C5-Br2	122.9(3)
H11-C11	0.83(7)	H11-C11-C12	167(5)
C11-C12	1.172(7)	C11-C12-C13	178.2(6)
C13-O2	1.429(5)	C12-C13-C14	109.0(3)
O2-H2A	0.64(9)	C12-C13-O2	107.8(3)
C14-Br11	1.889(4)	C13-C14-Br11	113.5(3)
C15-Br12	1.891(4)	C14-C15-Br12	123.3(3)
H21-C21	0.98(6)	H21-C21-C22	173(4)
C21-C22	1.185(6)	C21-C22-C23	176.0(5)
C23-O3	1.431(5)	C22-C23-C24	110.6(4)
O3-H3A	0.66(6)	C22-C23-O3	110.0(3)
C24-Br21	1.887(4)	C23-C24-Br21	113.5(3)
C25-Br22	1.888(4)	C24-C25-Br22	122.0(3)
H31-C31	0.70(7)	H31-C31-C32	175(6)
C31-C32	1.164(7)	C31-C32-C33	176.9(5)
C33-O4	1.428(5)	C32-C33-C34	110.1(3)
O4-H4A	0.78(6)	C32-C33-O4	109.9(3)
C34-Br31	1.892(4)	C33-C34-Br31	114.2(3)
C35-Br32	1.886(4)	C34-C35-Br32	122.3(3)

Table 9.6 - Selected bond lengths and angles for **13**.

	Length (Å)		Angle (°)
H1-C1	0.97(2)	H1-C1-C2	176(3)
C1-C2	1.183(2)	C1-C2-C3	177.8(1)
C3-O1	1.435(1)	C2-C3-C4	110.09(9)
O1-H1A	0.88(2)	C2-C3-O1	107.20(9)
C4-F1	1.346(1)	C3-C4-F1	114.12(9)
C5-F2	1.346(1)	C3-C5-F2	113.89(9)
H11-C11	0.94(2)	H11-C11-C12	178.4(1)
C11-C12	1.183(2)	C11-C12-C13	178.1(1)
C13-O11	1.438(1)	C12-C13-C14	109.47(9)
O11-H11A	0.85(2)	C12-C13-O11	107.14(9)
C14-F11	1.338(1)	C13-C14-F11	114.0(9)
C15-F12	1.345(1)	C13-C15-F12	113.36(9)
H21-C21	0.96(2)	H21-C21-C22	177.2(1)
C21-C22	0.186(2)	C21-C22-C23	178.1(1)
C23-O21	1.436(1)	C22-C23-C24	110.27(9)
O21-H21A	0.81(2)	C22-C23-O21	111.66(9)
C24-F21	1.339(1)	C23-C24-F21	113.84(9)
C25-F22	1.349(1)	C24-C25-F22	120.8(1)

9.4 Chloro and bromo structures

Table 9.7 - Hydrogen bonding in **11**

	Distance (Å)	Angle (°)
O-H --- O	1.93(4)	161(4)
Cl --- Cl	3.605(1) 3.731(1) 3.935(1)	161.86(9), 78.48(9) 166.0(1), 80.8(1) 132.6(1)
C-H --- Cl	3.13(5)	123.8(2)

Table 9.8 - Hydrogen bonding in **12**

	Distance (Å)	Angle (°)
O-H --- O	2.08(7)	154(7)
	2.00(6)	158(6)
	2.08(6)	165(7)
	2.13(1)	146(2)
Br --- Br	3.421(2)	163.0(1), 40.6(1)
	3.515(2)	172.6(1), 86.1(1)
	3.839(2)	152.3(1), 116.6(1)
C-H --- Br	3.02(6)	130(5)

Both molecules are symmetrical and take advantage of this by sitting on centres of symmetry. The bromo structure crystallises with four unique half molecules in space group P-1 while the chloro structure only has one unique half molecule but crystallises in a space group with a four fold axis of rotation, I4(1)/a. The crystal packing of the structures is very similar and there are three common synthons. The primary synthon is formed from O-H --- O hydrogen bonds. In the case of the chloro structure it is formed around the four-fold axis so it is a four sided synthon of symmetry related interactions. The bromo structure however has four independent OH groups and uses all of these to form the four membered O-H --- O synthon. Distances and angles of this interaction are not exceptionally short in either structure, chloro, 1.93 (4) Å, 161 (4)°, bromo 2.00(6) to 2.13(1) Å, 146 (2) to 165 (7)°, but they are still within the bounds of acceptability for such interactions.

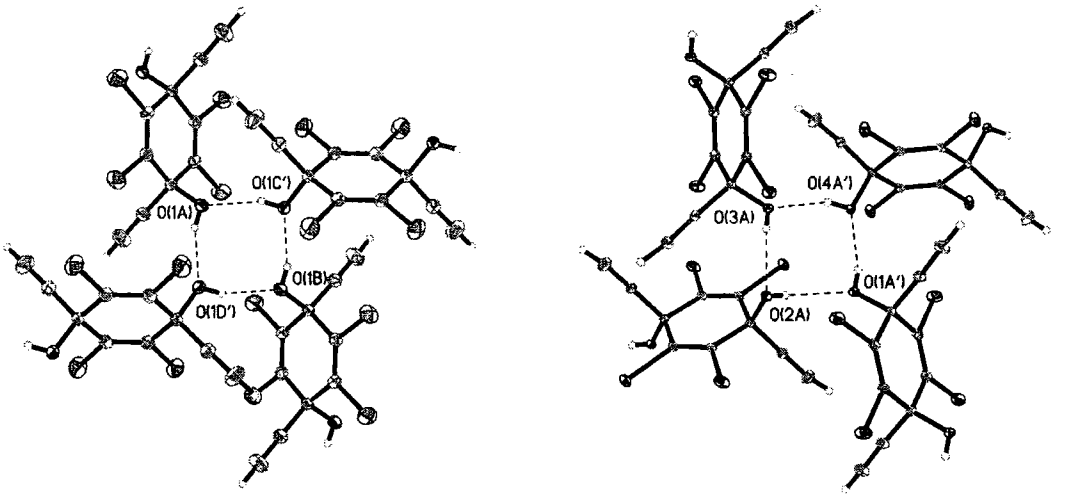

Figure 9.6 - O-H -- O synthons, chloro structure on the left, bromo on the right

Halogen --- halogen close contacts are found in both structures. The pattern in each case is triangular, they have two short sides whilst the third is significantly longer. Cl --- Cl (3.731, 3.731, 3.935 Å), Br --- Br (3.421, 3.515, 3.839 Å). The sum of the van der Waals radii of the interacting atoms are 3.50 and 3.60 Å respectively.

The only remaining significant group available to participate in hydrogen bonding is the triple bond. The alkyne does not have a role as an acceptor, instead it functions as a hydrogen donor. Each structure has a residual halogen atom which is not involved in the trimeric halogen --- halogen interactions, this atom takes part in C≡C-H --- Halogen interactions, C≡C-H --- Cl (3.13(5) Å, 123.8°); C≡C-H --- Br (3.02(6)Å, 130 (5)°). A search of the CSD (April 1999 release) reveals very few instances of such interactions. A search was carried for all entries containing both the alkyne group and carbon bound chlorine atom. Entries were considered which were 'organic', with no disorder, not polymeric, R-factor <0.10 and error free at the 0.05Å level. C-H distances were normalised to the mean value as established by neutron diffraction of

1.083Å and 'hits' were accepted which had an H --- Cl separation distance of under 3.5Å. An analogous search was carried out for interactions involving bromine and fluorine, the same criteria were used.

The search results are shown in the form of scattergrams (Figures 9.7 and 9.8) of B1 (H --- Hal) versus A1 (angle C-H --- Hal). The corresponding interactions in the chloro and bromo structure are highlighted in red. Neither interaction is significantly short, nor are they particularly directional. The bromo interaction may play some small part in the overall structure but it is unlikely that the chloro interaction is important.

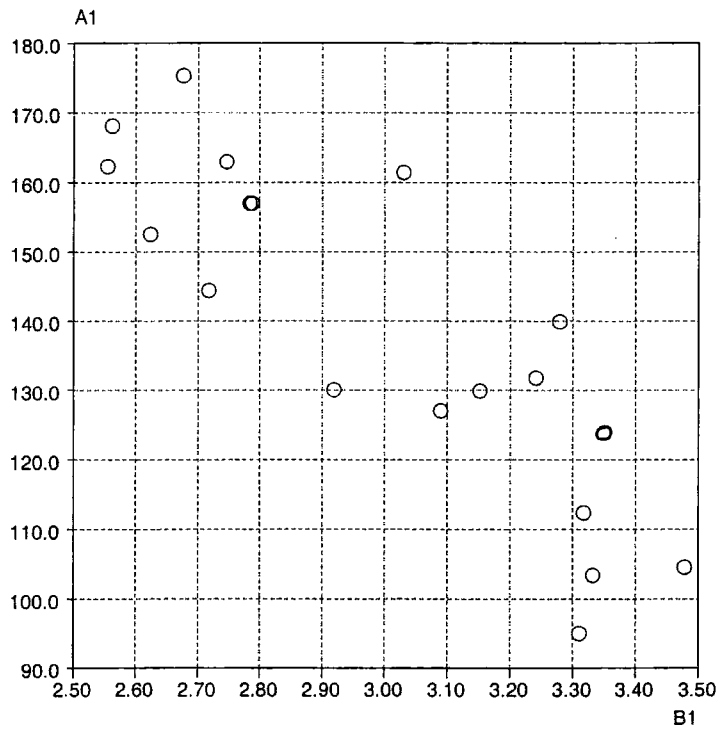

Figure 9.7 - CSD search results for C-H --- Cl

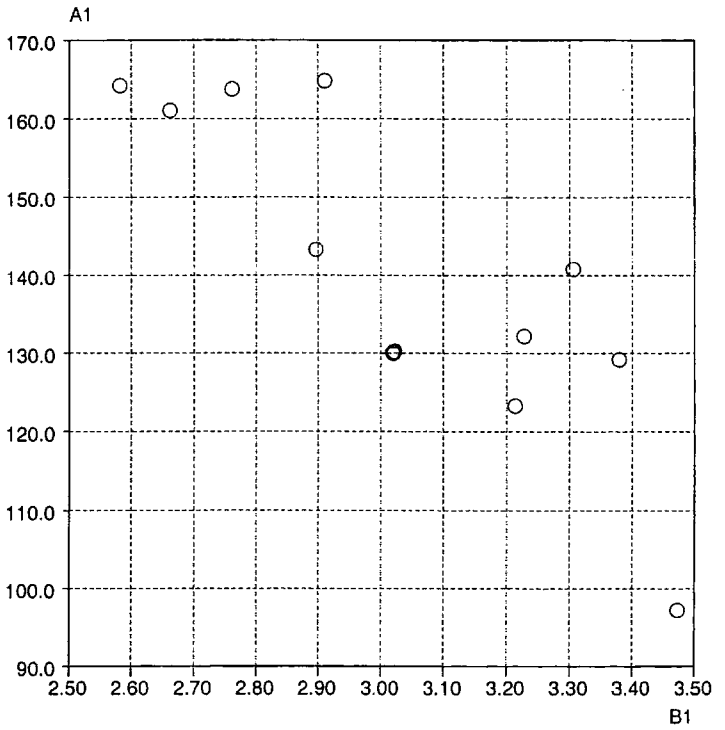

Figure 9.8 - CSD search results for C-H --- Br

9.5 Fluoro structure

Table 9.9 - Hydrogen bonding in **13**

	Distance (Å)	Angle (°)
O1-H1a --- O11	1.88(2)	174(2)
O11-H11a --- O21	1.87(2)	179(2)
O21-H21a --- O1	1.95(2)	163(2)
F1--- F22	2.865(2)	90.55(6), 173.72(7)
F1 --- F11	2.953	134.32(2), 122.52(2)
C11-H11 --- F2	2.48(2)	171.2(2)

The fluoro substituted structure is broadly similar to the chloro and bromo structures but there are significant differences. The molecule crystallises in space group $P\bar{1}$ with three unique half molecules. A distinctive pattern of O-H --- O hydrogen bonds is formed, in contrast to the four-sided pattern of the chloro and bromo structures, the pattern formed is six-membered. Again this interaction pattern sits around an inversion centre with three of the six interactions unique. The four sided motifs in the chloro and bromo structures are slightly puckered but this six-sided interaction forms a characteristic chair shape as seen in cyclohexane rings.

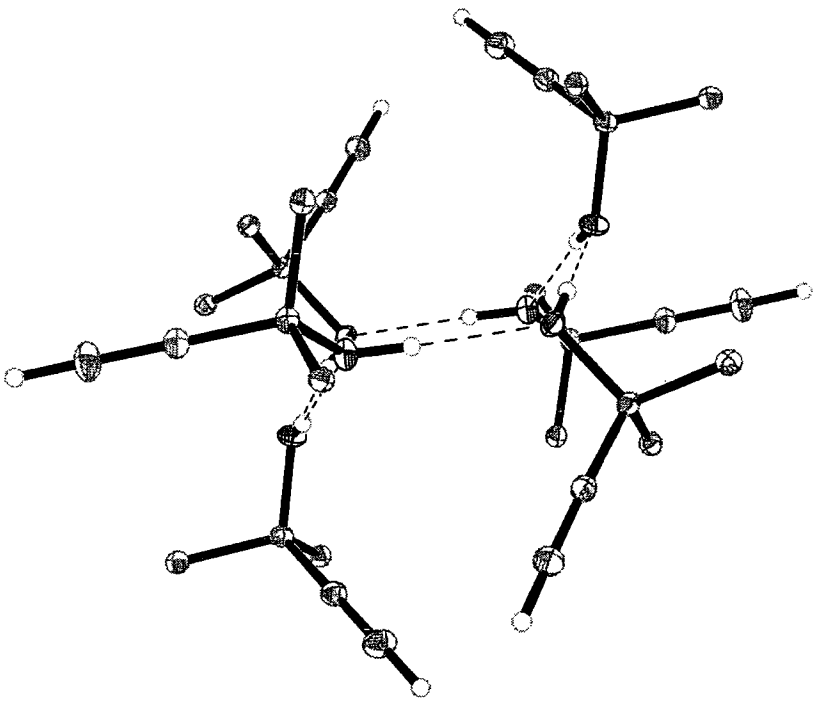

Figure 9.9 - Chair shaped motif, all fluorine and some carbon atoms removed for clarity

There are close contacts between neighbouring fluorine atoms ranging between 2.69 and 2.95 Å but these are not significantly lower than the sum of the van der Waals radii of the two atoms, 2.96 Å, and occur in isolation so are unlikely to be of

importance. There is also a C≡C-H --- Hal interaction as seen in both the two previous structures and in this case it is more significant. The CSD search for interactions of this type involving fluorine provided an equally small dataset to the chloro and bromo searches. Again the interaction for this structure is highlighted in red.

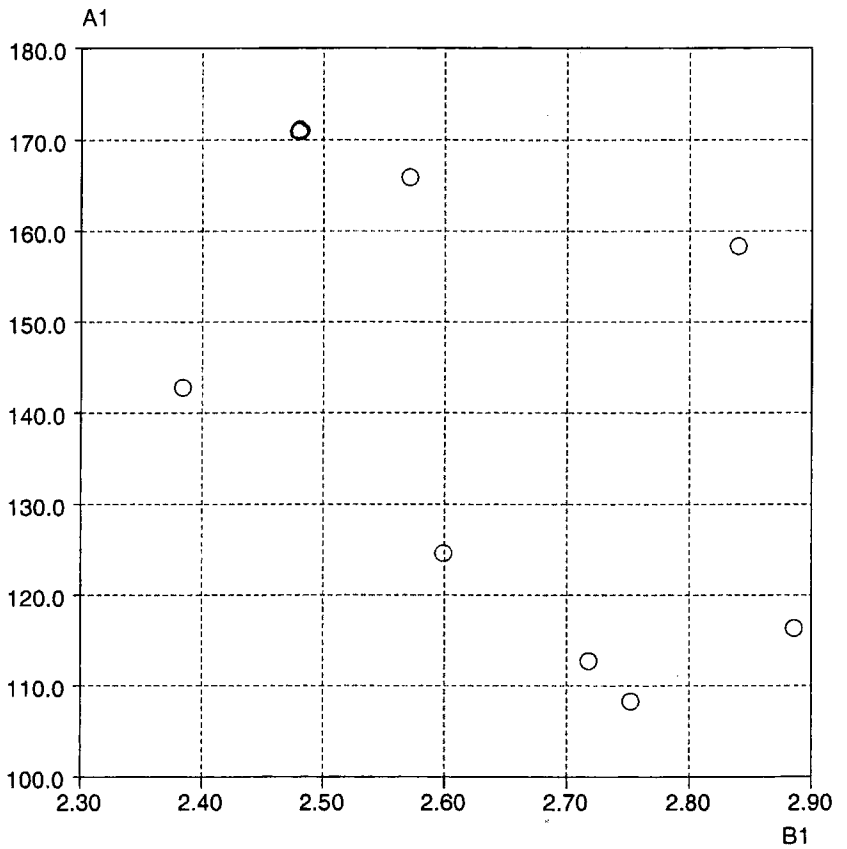

Figure 9.10 - CSD search results for C-H --- F

This interaction is much more important to the structure as a whole than its equivalents in the other two structures. The H --- F distance, 2.48(2)Å, is well within the van der Waals limit but also it is very directional C-H --- F 171(2)° especially considering that energetically this is expected to be a comparatively weak interaction.

9.6 General discussion on the structural family

Several interesting observations can be made about this structural sub-family. The first is the variety of intermolecular interactions displayed by these molecules. The primary synthon is formed solely from O-H --- O cooperative interactions, unlike the other structural sub-families, there are no C≡C-H --- π interactions at all. The chloro and bromo structures form similar four sided hydroxyl synthons whereas the equivalent in the fluoro structure is six-membered. All three structures contain close contacts between halogen atoms but they are not exceptionally short in any of the structures. The F --- F distances are marginally below the sum of the van der Waals radii, the Cl --- Cl contacts are a little over the limit, it is only the Br --- Br interactions that are noticeably short. The third type of interaction common to all three structures is C≡C-H --- Halogen. Again, the chloro interaction is over the van der Waals limit, the bromo interaction is just under the limit but the angular approach is not ideal. The C≡C-H --- F interaction is well below the sum of the radii and it is also exceptionally directional, C-H --- F 171(2)°.

The fluoro structure is significantly different to the chloro and bromo structures, which would be expected considering their relative polarisability. As we move down the halo series from F to Cl to Br, the atoms become less electronegative and more polarisable. This affects the type of interactions formed by the halogens. Br and Cl are more polarisable so Br --- Br and Cl ---- Cl interactions will from in preference to Br --- H or Cl --- H. Fluorine is more electronegative than bromine or chlorine, so as F --- H is strongly dipolar it is formed in preference to F --- F. Fluorine --- fluorine interactions are not stabilising , they may even be repulsive and probably only form as

a result of close packing. In structures **11** and **12**, none of the interactions involving Cl or Br are likely to be structure determining, these two structures are mediated almost entirely by the O-H --- O synthon, the other interactions just provide a slight degree of additional stabilisation. The C≡C-H --- F interaction is the only halo interaction of this type of any real significance. Work by Murray-Rust (16) and co-workers concluded that the C-F bond can form significant interactions but are generally weak. Shimoni and Glusker (1994) stated that "the C-F group competes unfavourably with a C-O$^-$, C-OH or C=O group". Studies by J. A. K. Howard et al.(1996) and Dunitz and Taylor (1997) both concluded that the C-F group is a poor hydrogen bond acceptor. Dunitz and Taylor commented that "covalently bonded F hardly ever acts as a hydrogen bond acceptor and than only in exceptional molecular and crystal environments". They attribute its poor hydrogen bonding capability to its low proton affinity (tightness of electron shell) and also as it only forms single bonds it is unable to take advantage of electron density delocalisation to attract electrons through a π-system.

Other halo systems have been reported which crystallise with isomorphous structures, including 1,4-dihalogenobenzenes (Wheeler & Coulson, 1976; Nguygen-Ba-Chanh, Haget & Cuevas-Diatre, 1984) and 4-halogenoethynylbenzenes (Weiss, Boese, Smith & Haley, 1997). In each case the fluoro structure does not fit the patterns established by the other structures.

Questions still remain about this structural sub-family. While the chloro and bromo structures pack in a similar fashion they crystallise in quite different space groups, bromo in low symmetry triclinic $P\bar{1}$ and chloro in higher symmetry tetragonal I4(1)/a. The bromo interactions are a little shorter than the chloro interactions so one could

postulate that the choice of the higher symmetry has a positive effect on the structure which offsets the slightly less optimised weaker interactions. The cell volume of the bromo structure is ~2.4% larger than the chloro, which even accounting for the larger size of bromine with respect to chlorine, this small decrease in cell volume may be enough to push the structure into the higher symmetry space group.

REFERENCES

Boese, R., Weiss, H.-Chr & Kirchner, M., unpublished results.

Bondi, A., (1964). *J. Phys, Chem.*, **68**, 441.

Bruker AXS (1998). SAINT, Area detector data integration software, Version 5.0, Bruker AXS, Madison, Wisconsin, USA, 1998.

Collin. R. l., (1952). *Acta Cryst.*, **5**, 431.

Desiraju, G. R., Parthasarathy, R. & Murray-Rust, P., (1989). *J. Am. Chem. Soc.*, **111**, 8725.

Dunitz, J. D. & Taylor, R., (1977). *Chem. Eur. J.*, **3**, 89-98.

Green, B. S., Schmidt. G. M., (1971). *J. Israel Chemical Society Annual Meeting Abstracts, Israel Chemical Society*, 190.

Harris, P. M., Mack. E., (1928). *J. Am. Chem. Soc*, **50**, 1583.

Howard, J. A. K., Hoy, V. J., O'Hagan, D. & Smith, G. T., (1996). *Tetrahedron*, **52**, 12613- 12622.

Murray-Rust, P. & Motherwell, W. D. S.,(1979). *J. Am. Chem. Soc.*, **101**, 4374.

Murray-Rust, P., Stallings, W. C., Monti, C. T., Preston, R. K. & Glusker, J. P., (1983).*J. Am. Chem. Soc.*, **105**, 3206.

Nguygen-Ba-Chanh, A. M., Haget, Y. & Cuevas-Diatre, M. A., (1984). *J. Appl. Crystallogr.*, **17**, 210.

Nyburg, S. C., Faerman, C. H., (1985). *Acta Cryst.*, B**41**, 274-279.

Pauling. L., (1947). '*The Nature of the Chemical Bond*', Cornell University Press, UAS, 1947.

Pedireddi, V. R., Reddy, D. S., Goud, B. S., Craig, D. C., Rae, A. D. & Desiraju, G. R., (1994). *J. Chem. Soc. Perkin Trans., 2*, 2353-2360.

Pertsin, A. J., Kitiagorodskii, A. I., (1987). *'The Atom-Atom Potential Method'*, Springer-Verlay, Berlin, 105-112.

Price, S. L. & Stone, A. J., (1982). *Molecular Physics*, **47**, 6, 1457-1470.

Price, S. L. & Stone, A. J., (1994). *J. Am. Chem. Soc.*, **116**, 4910-4918.

Ramasubbi, N., Parthasarathy, R., Murray-Rust, P., (1986). *J. Am. Chem. Soc.*, **108**, 4308.

Sakurai, T., Sundaralingam, M., Jeffrey, G. A., (1963). *Acta Cryst.*, **16**, 354-363.

Sheldrick, G. M. (1997). SHELX-97, Structure determination software, G. M. Sheldrick, University of Goettingen, Germany, 1997.

Shimoni, L. & Glusker, J. P., (1994). *Struct. Chem.*, **5**, 383.

Vonnegut, B., Warren. B. E., (1936). *J. Am. Chem. Soc*, **58**, 2459

Weiss, H-Chr, Boese, R., Smith, H. L. & Haley, M. M., (1997). *Chem. Commun.*, 2403-2404.

Wheeler, G. L.& Coulson. S. D., (1976). *J. Chem. Phys.*, **65**, 1227.

Williams, D. E., Hsu L.-Y., (1985). *Acta Cryst.*, A**41**, 296.

Gem-alkynol structures **14**, **15, 16** and **17**.

CHAPTER 10

10.1 Gem-alkynol structure 14

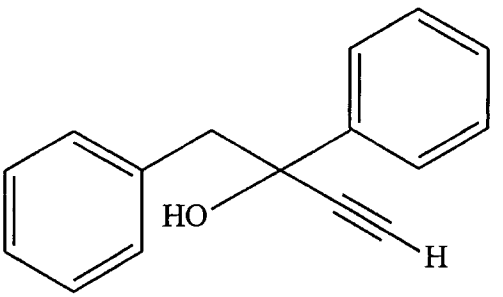

Figure 10.1.1 - Structural formula, structure **14**

10.1.1 Experimental Details

Data for structure **14** were collected using Mo-Kα X-ray radiation. A suitable crystal was mounted on a glass fibre using epoxy glue. Data were collected at 150K using a Bruker SMART CCD diffractometer. The data were integrated using the Bruker SAINT package (Bruker AXS, 1998) and suitably corrected for absorption. Structure solutions were obtained by direct methods using Shelx97 (Sheldrick, 1997) and the resultant solutions were refined against F^2.

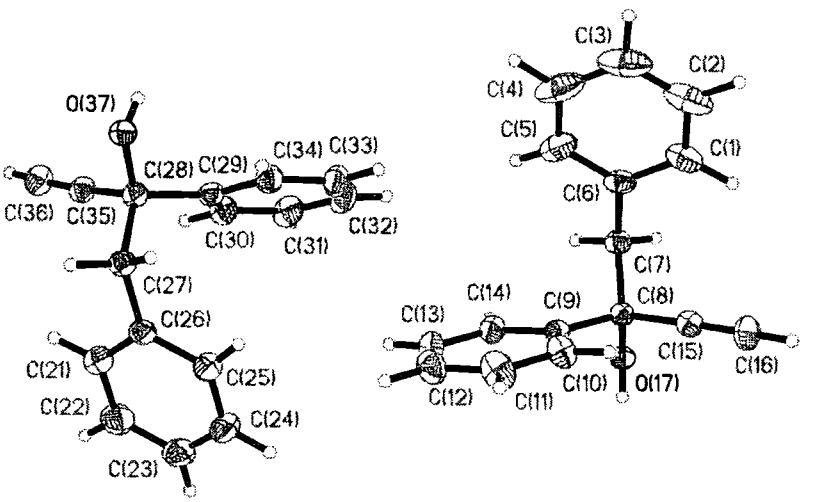

Figure 10.1.2 - 50% probability ellipsoid plot for structure **14**

Table 10.1.1 Experimental details, structure **14**

Identification code	**Structure 14**
Empirical formula	C16 H14 O
Formula weight	222.27
Temperature	150 K
Wavelength	0.71073 Å
Crystal system	Tetragonal
Space group	P-4
Unit cell dimensions	a = 19.8403(4) Å α= 90°.
	b = 19.8403(4) Å β= 90°.
	c = 6.5068(2) Å γ = 90°.
Volume	2561.32(11) $Å^3$
Z	8
Density (calculated)	1.153 Mg/m^3
Absorption coefficient	0.070 mm^{-1}
F(000)	944
Crystal size	0.4 x 0.3 x 0.3 mm^3
Theta range for data collection	1.03 to 30.35°.
Index ranges	-27<=h<=23, -27<=k<=25, -9<=l<=8
Reflections collected	20665
Independent reflections	7018 [R(int) = 0.0237]
Absorption correction	Empirical
Max. and min. transmission	0.239 and 0.258
Refinement method	Full-matrix least-squares on F^2
Data / restraints / parameters	6166 / 0 / 419
Goodness-of-fit on F2	1.024
Final R indices [I>2sigma(I)]	R1 = 0.0366, wR2 = 0.0872
R indices (all data)	R1 = 0.0452, wR2 = 0.0921
Largest diff. Peak and hole	0.244 and -0.204 $e.Å^{-3}$

Table 10.1.2 - Selected bond lengths and angles for **14**.

	Length (Å)		Angle (°)
H16-C16	0.93(2)	H16-C16-C15	177.4(1)
C16-C15	1.183(2)	C16-C15-C8	177.64(1)
C15-C8	1.481(2)	C15-C8-O17	108.16(9)
C8-O17	1.455(1)	C8-O17-H17	106.5(1)
O17-H17	0.83(2)	C7-C8-C9	112.41(9)
C8-C7	1.554(2)	C6-C7-C8	114.5(1)
H36-C36	0.90(2)	C14-C9-C10	118.7(1)
C36-C35	0.189(2)	H36-C36-C35	175.6(1)
C35-C28	0.486(2)	C36-C35-C28	173.5(1)
C28-O37	1.452(1)	C35-C28-O37	107.30(9)
O37-H37	0.82(2)	C28-O37-H37	105.7(1)
C25-C26	1.398(2)	C27-C28-C29	110.21(9)
		C26-C27-C28	114.42(9)
		C21-C26-C25	118.2(1)

10.1.2 Crystal packing

This compound crystallises in the tetragonal space group P-4 with two independent molecules in the asymmetric unit, which have slightly different conformations, the twisting of the phenyl rings with respect to the central straight chain unit.

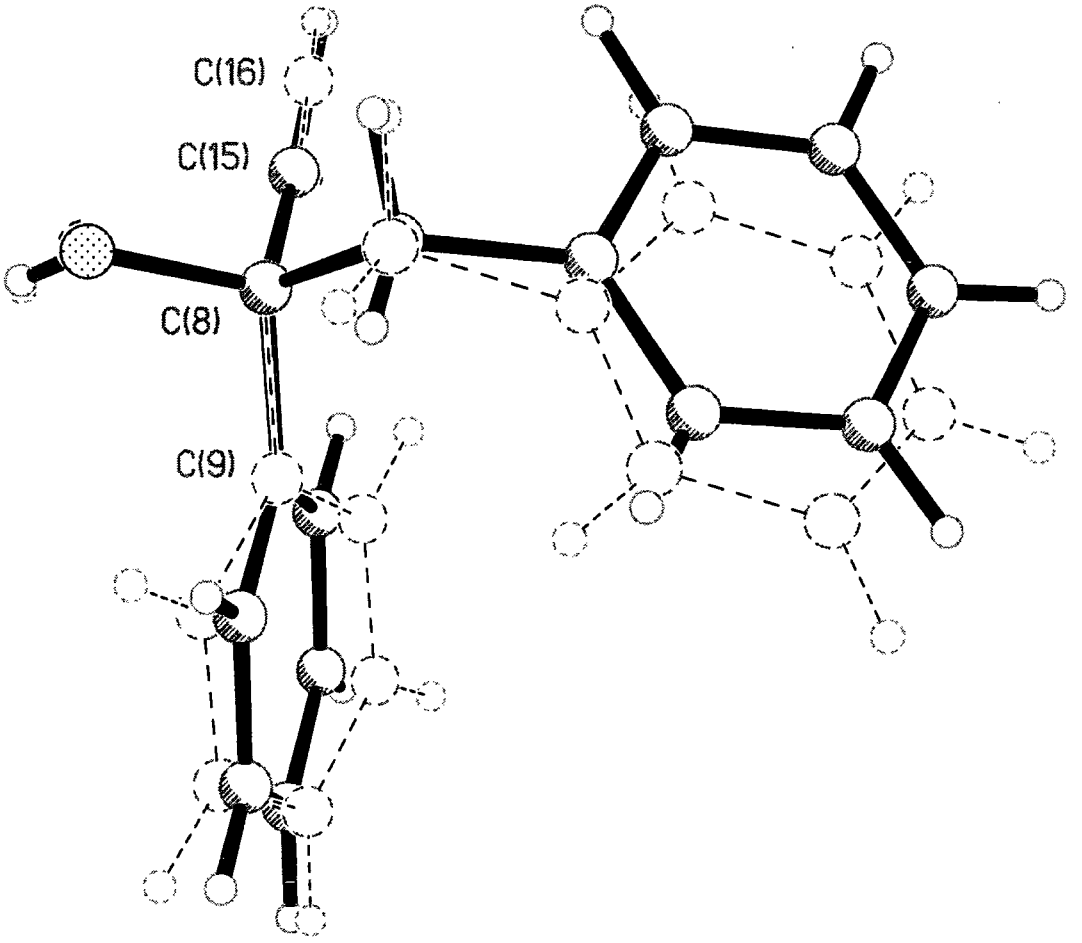

Figure 10.1.3 - Superposition of the two independent molecules

Figure 10.1.3 was obtained by inverting the model of one of the independent molecules and overlaying the positions of atoms C28 C29 C35 and C36 to that of C8 C9 C15 and C16. It is clear that the orientations of the two molecules are slightly different. The central sections of the two molecules fit quite well but neither of the two rings superimpose neatly. The two rings on the right of Figure 10.3.1 (C1 C2 C3 C4 C5 C6 and C21 C22 C23 C24 C25 C26) are only twisted by a few degrees relative to each other, 4.7°, instead the difference is seen within the plane of the atoms. The distance between the ring centroids is 0.73 Å. The other rings overlap well within the

plane of the atoms but the rings themselves are twisted by 17.5°. The comparison is illustrated in Figure 10.1.4.

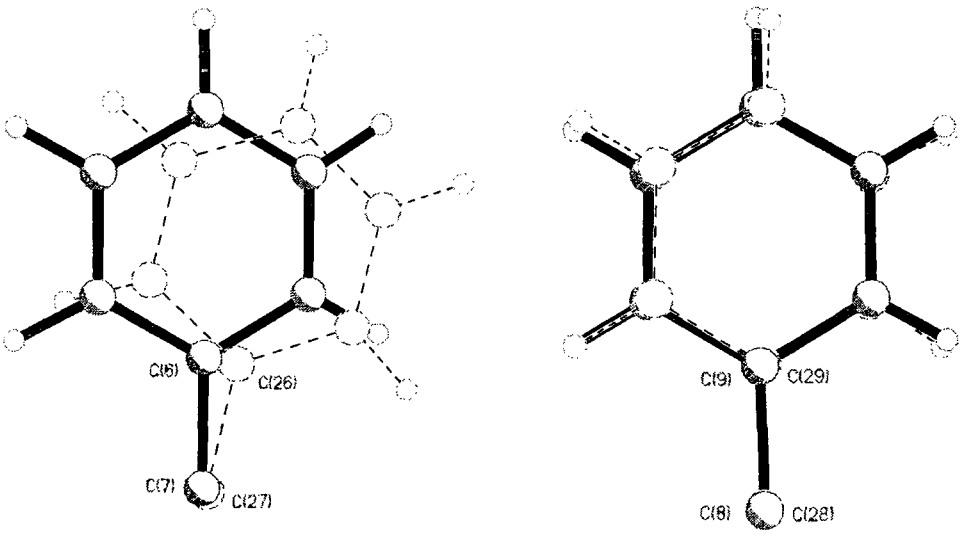

Figure 10.1.4 - superposition of individual rings

Two interactions dominate the hydrogen bonding of this compound. The first is the synthon seen in the halo series, group D. Each independent molecule takes advantage of the four fold rotation axis to form tetramers linked by O-H --- O hydrogen bonds. There is little difference between the hydrogen bond distances and angles of the two tetramers, 2.01(2) Å, 169 (2)°; 2.05 (2) Å, 166(2)°. The second major interaction links the stacks of tetramers via C≡C-H --- O hydrogen bonds with the C-H from one tetramer making a close contact with the O(H) of the next tetramer in the stack, 2.31(2) Å, 156 (1)°; 2.45(2) Å, 156(2)°. Interestingly these interactions run in opposite directions in the two tetramers, they run 'upwards' in one stack and 'downwards' in the other.

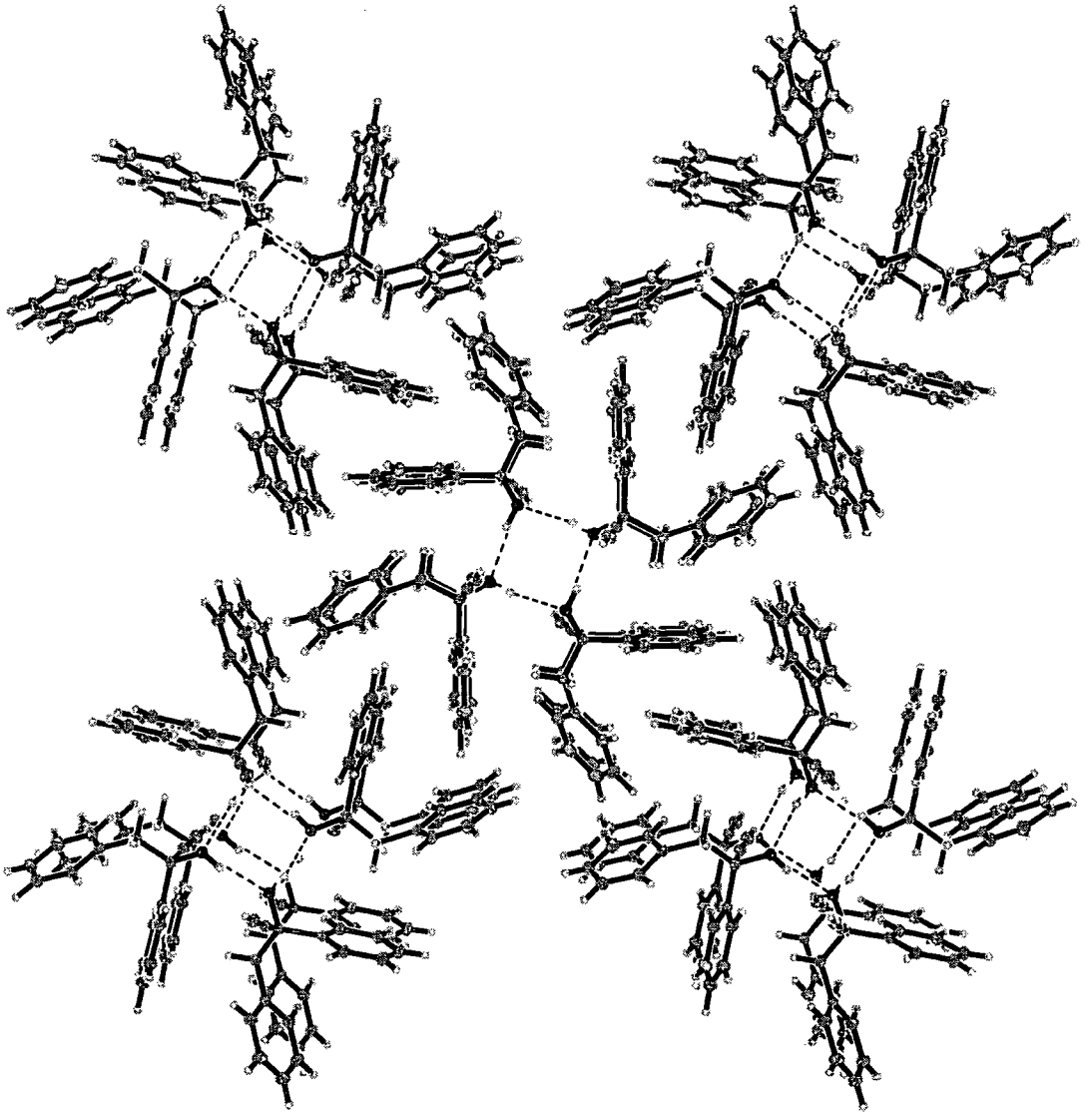

Figure 10.1.5 - Stacks of tetramers formed by O-H --- O interactions

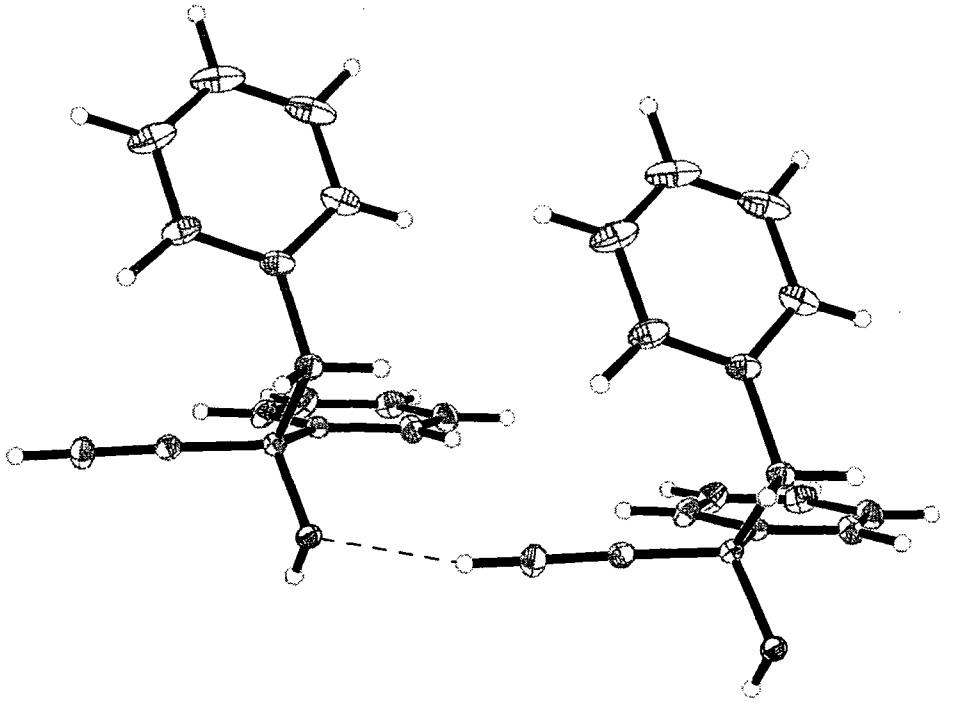

Figure 10.1.6 - C≡C-H --- O interaction

This combination of O-H --- O tetramers and columns of C≡C-H --- O interactions have been observed in another *gem*-alkynol. 3-phenylpenta-1,4-diyn-3-ol, (Steiner, Tamm, Grzegorzewski, Schulte, Veldman, Schreurs, Kanters, Kroon, Mass & Lutz, 1996). This compound also crystallises in a tetragonal space group I-4 but with only one independent molecule. The O-H --- O tetramer was also seen in structures **11** and **12**, structure **12** is also in a tetragonal space group.

There are also close contacts between methylene C-H groups and phenyl rings (2.63 Å, 2.69 Å; 160°, 172°) and phenyl C-H groups and ring centroids (2.60 Å, 168°). As always with such weak donors, it is possible that the short distance between such groups is merely a consequence of geometry.

10.2 Gem-alkynol structure 15

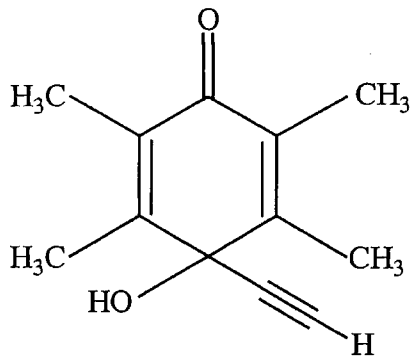

Figure 10.2.1 - Structural formula structure **15**

This compound provides an interesting example of just how fragile the *gem*-alkynol moiety is in terms of participation in major hydrogen bonding patterns.

10.2.1 Experimental Details

Data for structure **15** were collected using Mo-Kα X-ray radiation. A suitable crystal was mounted on a glass fibre using epoxy glue. Data were collected at 150K using a Bruker SMART CCD diffractometer. The data were integrated using the Bruker SAINT package (Bruker AXS, 1998) and suitably corrected for absorption. Structure solution was obtained by direct methods using Shelx97 (Sheldrick, 1997) and the resultant solutions were refined against F^2. Two of the methyl groups (C7, C12) were constrained as idealised CH_3 groups with tetrahedral angles. The coordinates of the

hydrogen atoms were set to 'ride' on the coordinates of the parent carbon atoms but the site occupancy factors were refined freely.

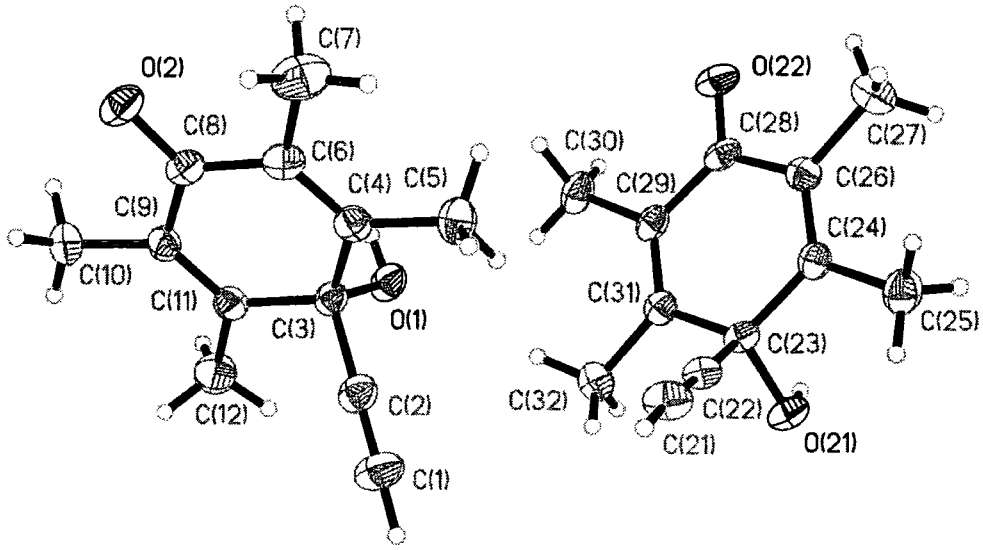

Figure 10.2.2 - 50% probability ellipsoid plot for structure **15**

Table 10.2.1 Experimental details, structure **15**

Identification code	**Structure 15**
Empirical formula	C12 H14 O2
Formula weight	190.23
Temperature	150 K
Wavelength	0.71073 Å
Crystal system	Monoclinic
Space group	P2(1)/c
Unit cell dimensions	a = 9.020(2) Å $\alpha = 90°$.
	b = 14.010(3) Å $\beta = 93.56(3)°$.
	c = 16.612(3) Å $\gamma = 90°$.
Volume	2095.2(7) $Å^3$
Z	8
Density (calculated)	1.206 Mg/m^3
Absorption coefficient	0.081 mm^{-1}
F(000)	816
Crystal size	0.3 x 0.25 x 0.2 mm^3
Theta range for data collection	1.90 to 27.49°.
Index ranges	$-11 \leq h \leq 11$, $-18 \leq k \leq 17$, $-21 \leq l \leq 21$
Reflections collected	14728
Independent reflections	4796 [R(int) = 0.0501]
Absorption correction	Empirical
Max. and min. transmission	0.802 and 1.000
Refinement method	Full-matrix least-squares on F^2
Data / restraints / parameters	4796/ 0 / 329
Goodness-of-fit on F2	1.006
Final R indices [I>2sigma(I)]	R1 = 0.0515, wR2 = 0.1244
R indices (all data)	R1 = 0.0932, wR2 = 0.1447
Largest diff. Peak and hole	0.288 and -0.205 $e.Å^{-3}$

Table 10.2.2 - Selected bond lengths and angles for **15**.

	Length (Å)		Angle (°)
H1-C1	0.93(3)	H1-C1-C2	176.5(2)
C1-C2	1.173(3)	C1-C2-C3	178.7(2)
C3-O1	1.439(2)	C2-C3-O1	105.7(1)
O1-H1A	0.82(3)	C3-O1-H1A	108(2)
C4-C5	1.505(3)	C3-C4-C6	121.3(2)
C8-O2	1.236(2)	C3-C4-C5	114.8(2)
H21-C21	0.96(3)	H21-C21-C22	174.5(2)
C21-C22	1.181(3)	C21-C22-C23	177.7(2)
C23-O21	1.443(2)	C22-C23-O21	106.6(1)
O21-H21A	0.89(3)	C23-O21-H21A	103.4(2)
C24-C25	1.507(3)	C23-C24-C26	121.7(1)
C28-O22	1.241(2)	C23-C24-C25	115.0(2)

10.2.2 Crystal packing

This structure crystallises with two independent molecules in the asymmetric unit. The structure consists of alternating layers of the symmetry independent molecules. The layers are formed by molecules linked in pairs by O-H --- O=C interactions (1.96(3) Å, 179(3)°; 1.94(3) Å, 172(2)°) and the pairs are linked by C≡C-H --- O=C hydrogen bonds (2.44(3) Å, 149(3)°; 2.21(3) Å, 168(2)°). The layers of symmetry independent molecules are lined by close contacts between methyl hydrogen atoms and the alcohol groups. C-H --- O (2.86(2) Å, 171(2)°; 2.55(3) Å, 155(2)°).

The carbonyl group is deeply involved in the hydrogen bonding displayed by this molecule, there are no interactions between the two fragments of the gem-alkynol moiety. One can conclude that the carbonyl group has a much greater effect on the resulting hydrogen bonding pattern of this molecule than the gem-alkynol portion.

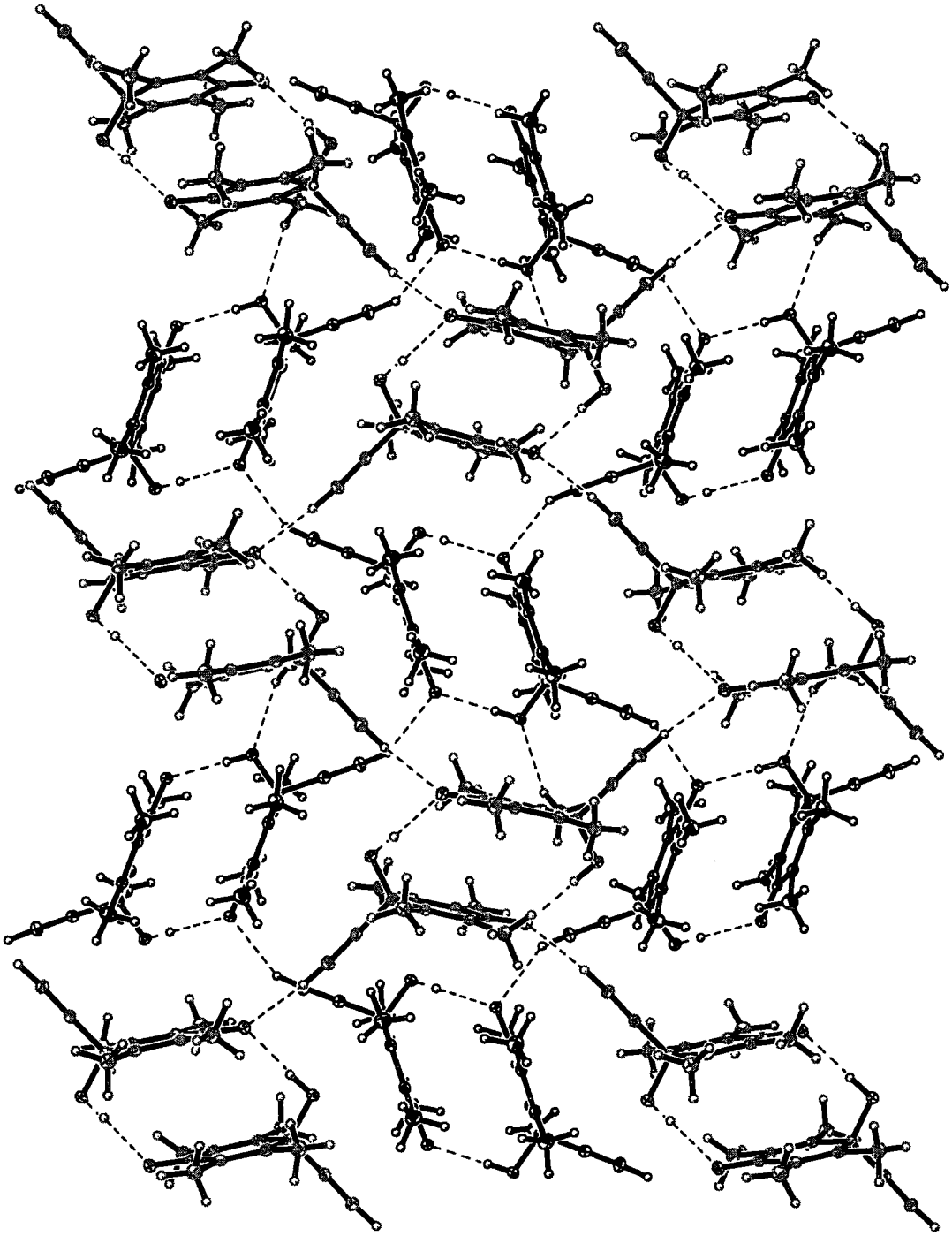

Figure 10.2.3 - Layered packing,

10.3 Gem-alkynol structure 16

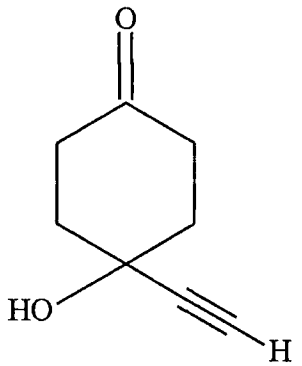

Figure 10.3.1 - Structural formula, structure **16**

10.3.1 Experimental Details

Data for structure **16** were collected using Mo-Kα X-ray radiation. A suitable crystal was mounted on a glass fibre using epoxy glue. Data were collected at 150K using a Bruker SMART CCD diffractometer. The data were integrated using the Bruker SAINT package (Bruker AXS, 1998)and suitably corrected for absorption. Structure solutions were obtained by direct methods using Shelx97 (Sheldrick, 1997) and the resultant solutions were refined against F^2.

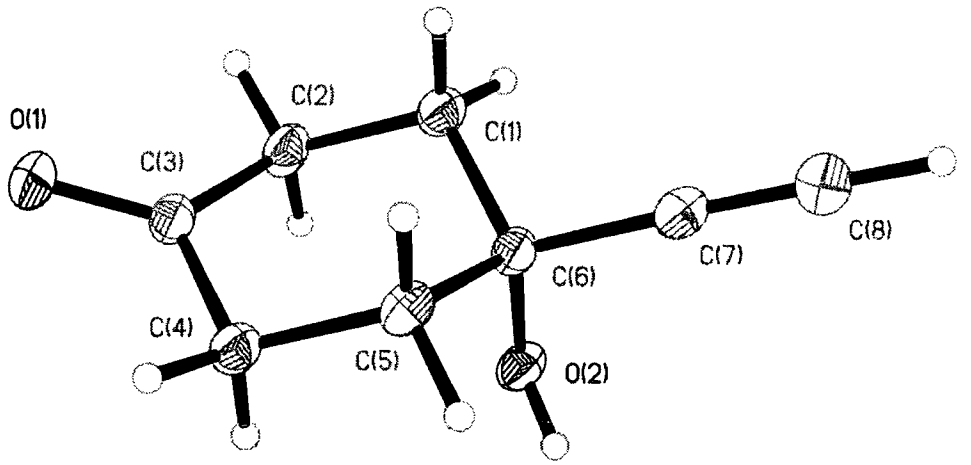

Figure 10.3.2 - 50% probability ellipsoid plot for structure **16**

Table 10.3.1 - Experimental details, structure **16**.

Identification code	**Structure 16**
Empirical formula	C8 H10 O2
Formula weight	222.27
Temperature	150 K
Wavelength	0.71073 Å
Crystal system	Monoclinic
Space group	P2(1)/c
Unit cell dimensions	a = 6.550(1) Å α= 90°.
	b = 16.931(3) Å β= 95.42(3)°
	c = 6.493(1) Å γ = 90°.
Volume	716.9(2) $Å^3$
Z	4
Density (calculated)	1.280 Mg/m^3
Absorption coefficient	0.091 mm^{-1}
F(000)	296
Crystal size	0.4 x 0.1 x 0.05 mm^3
Theta range for data collection	2.41 to 27.49°.
Index ranges	-8<=h<=8, -21<=k<=16, -8<=l<=8
Reflections collected	5018
Independent reflections	1657 [R(int) = 0.0601]
Absorption correction	None
Refinement method	Full-matrix least-squares on F^2
Data / restraints / parameters	1657 / 0 / 131
Goodness-of-fit on F2	1.099
Final R indices [I>2sigma(I)]	R1 = 0.0550, wR2 = 0.1037
R indices (all data)	R1 = 0.1017, wR2 = 0.1269
Largest diff. Peak and hole	0.213 and -0.240 $e.Å^{-3}$

Table 10.3.2 - Selected bond lengths and angles for **16**.

	Length (Å)		Angle (°)
C1-C2	1.535(3)	C1-C2-C3	112.7(2)
C2-C3	1.505(3)	C2-C3-C4	116.6(2)
C3-O1	1.231(2)	C2-C3-O1	122.3(2)
C3-C4	1.507(3)	O1-C3-C4	121.1(2)
C4-C5	1.537(3)	C3-C4-C5	113.3(2)
C5-C6	1.535(3)	C4-C5-C6	111.1(2)
C6-O2	1.436(2)	C5-C6 C1	109.6(2)
O2-HA	0.84(3)	C5-C6-O2	110.2(2)
C6-C7	1.490(3)	C6-O2-HA	150(2)
C7-C8	1.188(3)	C5-C6-C7	111.3(2)
C8-H8	0.97(3)	C6-C7-C8	175.7(2)
		C7-C8-H8	179.2(2)

10.3.2 Hydrogen bonding in structure 16 (comparison with structure 15)

Table 10.3.3 - Distances and angles of intermolecular interactions.

	Distance	**Angle**
O-H --- O=C	1.99 (3) Å	175 (3)°
C-H --- O-H	2.51 (2) Å	175 (2)°
C≡C-H ---O=C	2.65 (3) Å	132 (2)°

This compound crystallises in the monoclinic space group P2(1)/c with one molecule in the asymmetric unit. This structure contains a carbonyl group in addition to the gem-alkynol unit so the range of possible interactions is extended. Considering their structural similarity one might expect that the crystal packing of this structure would

be similar to that of the closely related molecule, **16**. Molecule **16** crystallises in the same space group as the related structure **15** but while their packing patterns are similar there are important differences. The packing differences are largely as a result of the different shape of the two molecules. The ring carbon atoms of molecule **16** are sp^2 hybridised which makes the ring planar. Conversely the ring carbon atoms of molecule **16** are sp^3 hybridised so the ring adopts a chair formation. The dominant synthon in structure **15** consists of two molecules lying head to tail with their rings parallel forming O-H --- O=C interactions. The same interactions are formed by structure **16,** but the interaction exist in chains running down the structure. These chains of interactions are cross-linked by C-H --- O-(H) interactions. Such interactions are also seen in structure **15** but they cross-link the O-H ---- O=C linked pairs.

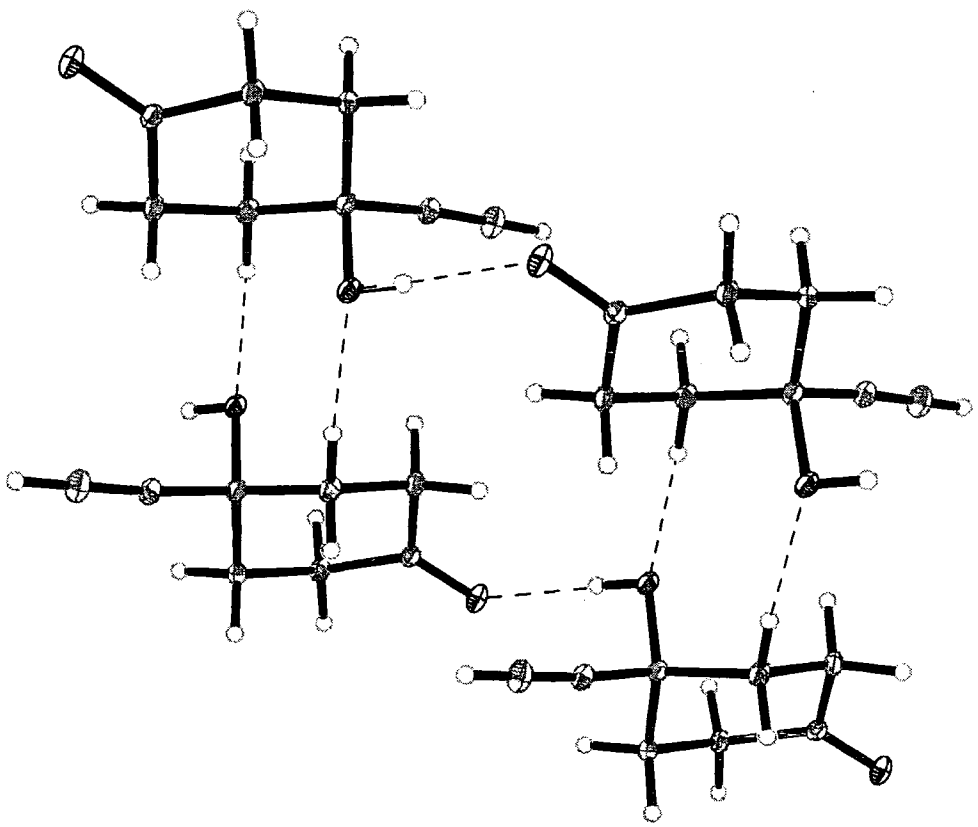

Figure 10.3.3 - O-H --- O=C and C-H --- O interactions, structure **16**

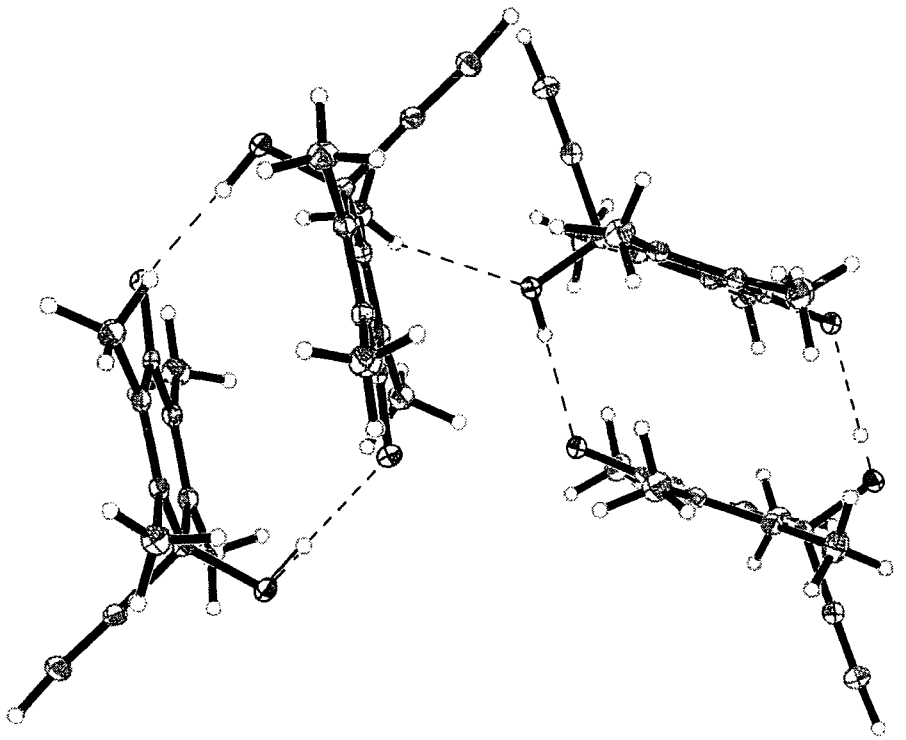

Figure 10.3.4 - O-H --- O=C and C-H --- O interactions, structure **15**

The third interaction in **16** is also common to structure **15**. C≡C-H --- O=C interactions play a minor role in providing a link between the individual layers in the stacked chains of O-H --- O=C interactions.

Both structures **16** and **15** are mediated by the same three intermolecular interactions, the differences lie in the patterns formed and the relative importance of the three interactions. The O-H ---- O=C interaction is the primary interaction in both structures but the importance of the remaining two interactions are reversed. The C-H --- O=C interaction plays a minor role linking pairs in structure **15** whereas in structure **16** the hydrogen atoms are better hydrogen bond donors (ring hydrogen atoms rather than CH_3 substituent hydrogen atoms) and play a more dominant part in the crystal packing.

Structures **16** and **15** are a good example of the problems faced when trying to design a robust, reproducible supramolecular synthon. Although the same interactions are formed in both structures, the change in shape of the central portion of the molecule from planar to chair formation effects the way that these interactions form. The influence of the carbonyl group is clear when structure **16** is compared with the two polymorphs, molecules **1** and **2**, structurally the only difference is the carbonyl group in place of the second *gem*-alkynol fragment. The interactions formed by these two structures are very different, the polymorphs are mediated primarily by trimeric O-H --- O interactions which are not present at all in structure **16.** It is clear therefore that the carbonyl group has a greater influence on the crystal packing of the molecules than the *gem*-alkynol unit.

10.4. Gem-alkynol structure 17

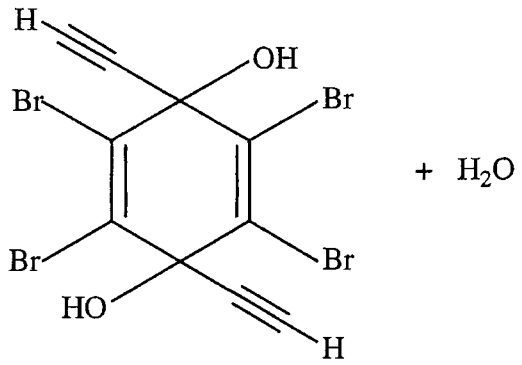

Figure 10.4.1 - Structural formula, structure **17**

10.4.1 Experimental Details

Data for structure **17** were collected using both X-ray and neutron radiation. The crystal was mounted on an aluminium pin and data collected at 150K on the single crystal diffractometer SXD (Keen & Wilson, 1996) at the ISIS Spallation Source. Data were integrated using SXD97 (Wilson, 1997). Positional coordinates for carbon and oxygen atoms from the X-ray model were used as a starting model for the refinement. Hydrogen atoms were located in the difference map.

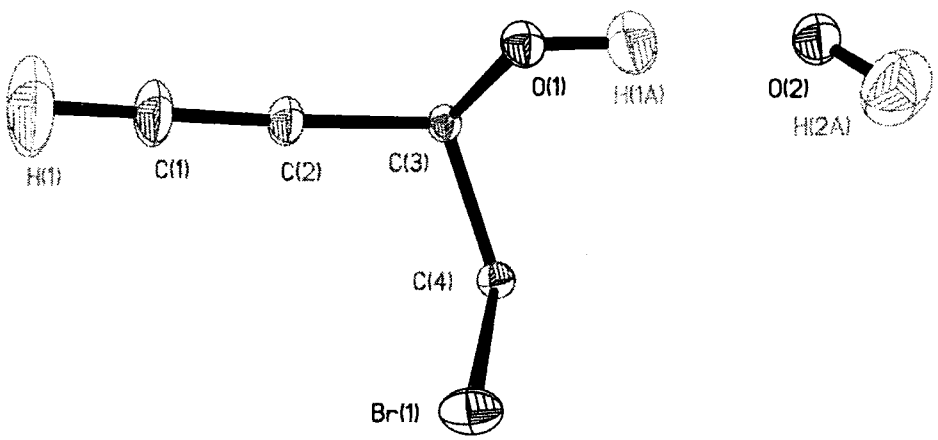

Figure 10.4.2 - 50% probability ellipsoid plot for structure **17**

Table 10.4.1 - Experimental details, structure **17**.

Identification code	**Structure 17**
Empirical formula	C10 H8 Br4 O4
Formula weight	292.00
Temperature	150 K
Wavelength	0.5 - 5.0 Å
Crystal system	Tetragonal
Space group	P4(2)ncm
Unit cell dimensions	a = 12.655(2) Å α= 90°.
	b = 12.655(2) Å β= 90°.
	c = 8.734(2) Å γ = 90°.
Volume	1398.8(4) $Å^3$
Z	4
Density (calculated)	1.387 Mg/m^3
Absorption coefficient	0.990 mm^{-1}
F(000)	34.78
Crystal size	3 x 2.5 x 2 mm^3
Index ranges	0<=h<=28, 0<=k<=18, 0<=l<=26
Reflections collected	1655
Independent reflections	1655 [R(int) = 0.052]
Absorption correction	Becker-Coppens Lorentzian model
Refinement method	Full-matrix least-squares on F^2
Data / restraints / parameters	1654 / 0 / 70
Goodness-of-fit on F2	6.188
Final R indices [I>2sigma(I)]	R1 = 0.0607, wR2 = 0.0819
R indices (all data)	R1 = 0.0607, wR2 = 0.0819

Table 10.4.2 - Selected bond lengths and angles for **17**.

	Length (Å)		Angle (°)
H1-C1	1.061(2)	H1-C1-C2	179.5(3)
C1-C2	1.197(1)	C1-C2-C3	175.4(1)
C2-C3	1.464(1)	C2-C3-C4	109.75(4)
C3-C4	1.524(7)	C2-C3-O1	105.52(7)
C3-O1	1.426(1)	C3-O1-H1A	109.7(1)
O1-H1A	0.987(2)	O1-C3-C4	110.18(4)
C4-Br1	1.8817(9)	C3-C4-Br1	113.93(5)
O2-H2A	0.951(2)		

10.4.2 Structural details

This structure is particularly interesting as it takes advantage of the highest possible symmetry of the molecule and crystallises in a tetragonal space group. There is one quarter molecule in the asymmetric unit, one fully occupied carbon and bromine atom with the remainder of the atoms all at half occupancy. In addition there is one half water molecule with a fully occupied hydrogen atom and a half occupied oxygen atom. It is possible for the molecule to have four fold symmetry if both the hydroxyl and alkyne groups are planar with the plane perpendicular to the core of the molecule. Structure **12** is the unsolvated version of this structure, there the molecule crystallises in $P\bar{1}$ only taking advantage of the inversion centre present in the molecule, there are four half molecules in the asymmetric unit.

Elucidation of this structure, **17** relies on location of the hydrogen atom positions. The hydroxyl and alkenic hydrogen atoms need to be lying within the plane in order to maintain the four-fold symmetry. For this reason, neutron diffraction was an ideal

method to use for this structure as the hydrogen atom positions could be identified accurately. The four half molecules in structure **12** do not come close to planarity, the torsion angles, (H1A-O1-C4-C3) are -12.4°, 37.1°, 13.0° and 29.1°.

10.4.3 Hydrogen bonding in structure 17

Table 10.4.3 - Distances and angles of intermolecular interactions

		Distance (Å)	Angle (°)
1	**O-H --- O-(H_2)**	1.700 (2)	179.4 (2)
2	**(H)-O-H --- O**	2.141 (2)	159.7 (2)
3	**C≡C-H --- O-(H_2)**	2.354 (3)	150.4 (3)
4	**(H)-O-H --- Br**	2.995 (2)	121.2 (2)
5a	**Br --- Br**	3.708 (1)	155.26 (4)
5b		3.847 (1)	122.19 (4)

There are five different intermolecular interactions in this structure, all except one involving the solvent water. Nangia and Desiraju (1999) have commented that multi-point recognition of the solvent is important in the formation of solvated structures. They argue that when solvent molecules become involved in hydrogen bonds with the solute, the extrusion of the solvent becomes enthalpically disadvantageous. This multi-point recognition is clearly the situation in this structure, the solvent water is involved in both hydrogen bond acceptor and donor roles.

The strongest interaction runs along the 2_1 symmetry axis on which the alkyne and hydroxyl groups lie. The hydroxyl hydrogen atom makes a close contact with the solvent water oxygen atom which also sits on the symmetry axis.

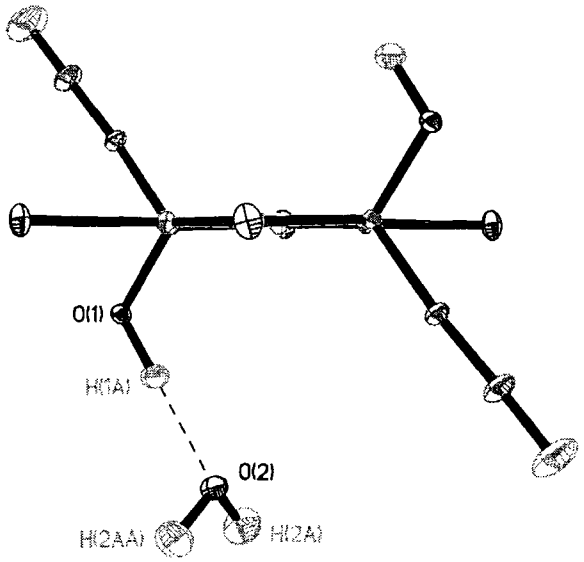

Figure 10.4.3 - Short O-H --- O interaction

The oxygen atom of the water molecule is a bifurcated acceptor, not only does it form the short contacts with the hydroxyl hydrogen atom as shown in Figure 10.4.3, it also interacts with the hydrogen atom of the alkyne group. The hydroxyl oxygen atom is also involved in two interactions but they are symmetry related across the 2_1 axis. The final three interactions involve the bromine atom, one involves the water molecule and the other two are bromine --- bromine interactions. The pattern of interactions is described schematically in Figure 10.4.4 and their labels correspond to those given in Table 10.4.2.

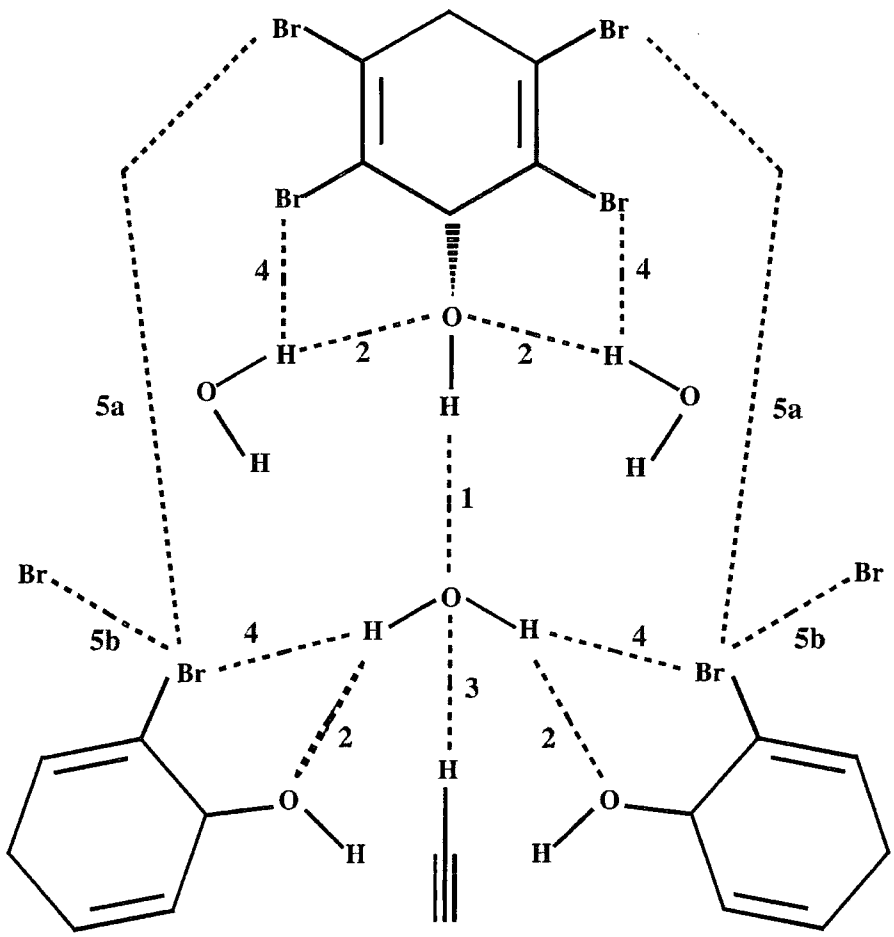

Figure 10.4.4- Schematic representation of interactions

The pattern of interactions is complex, it is best described as a spider's web of criss-crossing interactions. When viewed down 001, channels of molecules and interactions are seen. Two four-sided channels of interactions exist, one consisting purely of Br --- Br interactions and the other comprised of O-H --- O interactions involving the water molecule. O-H --- Br interactions provide additional stabilisation between the channels. The C≡C-H --- O hydrogen bonds lie perpendicular to the plane of the paper.

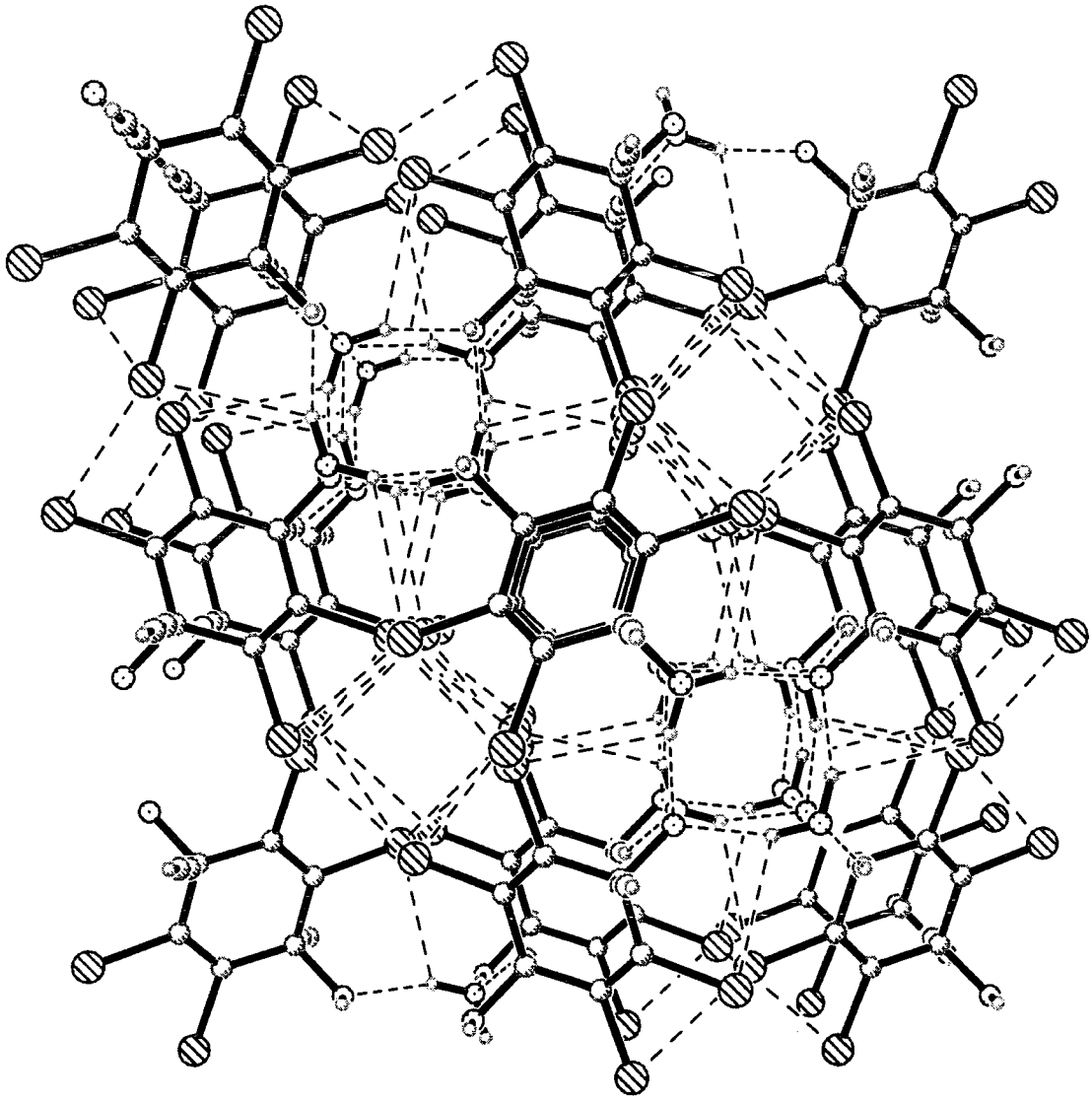

Figure 10.4.5 - Wealth of interactions in structure **17**.

REFERENCES

Bruker AXS (1998). SAINT, Area detector data integration software, Version 5.0, Bruker AXS, Madison, Wisconsin, USA, 1998.

Keen, D. A. & Wilson, C. C. (1996). *Technical Report RAL-TR-96-083*. Single crystal diffraction at ISIS. User guide for the SXD instrument

Nangia, A & Desiraju, G. R., (1999). *Chem. Commum*, 605-606.

Sheldrick, G. M. (1997). SHELX-97, Structure determination software, G. M. Sheldrick, University of Göettingen, Germany, 1997.

Steiner. T., Tamm, M., Grzegorzewski, A., Schulte, N., Veldman, N., Schruers, A. M. M., Kanters, J. A., Kroon, J., Mass, J. & Lutz, B., (1996). *J. Chem. Soc Perkin Trans.* 2, 2441-6.

Wilson, C. C. (1997). *J. Mol. Struct.*, **405**, 207-217.

Intermolecular Forces

CHAPTER 11

11.1 Intermolecular forces

Intermolecular forces are responsible for the attraction and repulsion between molecules. These forces are very weak in comparison with typical chemical bonds, their energies range form around 10 to 65 $kJmol^{-1}$ (Aakeröy & Seddon, 1993). Each intermolecular force is a balance between attractive and repulsive energetic contributions. These forces can be divided into short and long range terms however the major contribution to the overall force comes from the electrostatic contribution.

Long range

Electrostatic	coulombic interaction of charge distributions between the molecules. It is strongly dependant on the relative orientation of the molecules and can be attractive or repulsive.
Induction/ polarisation	distortions of the charge distribution of each interacting molecule due to the presence of the charge distributions of the other. Always an attractive force as such distributions only occur if they are energetically favourable.
Dispersion	arises due to the fluctuating charge distributions in molecules as a result of the constant motion of their electrons. The electron motion in both molecules becomes correlated to favour lower energy configurations and disfavour those of higher energy. The average effect is lowering of the energy. As

molecules get closer, the correlation energy becomes stronger so the result is an attractive force.

There are also resonance and magnetic contributions to the long-range energy but they are not present in all molecular systems. Their contributions are very small in comparison with the electrostatic, induction and dispersion terms.

Short range

Short range forces begin to take effect in the region where the molecular wavefunctions of the molecules begin to overlap slightly.

Exchange-repulsion this is the dominant contribution at very short range. It is the sum of the energy lowering due to exchange of electrons of parallel spin between molecules, and repulsion as a result of the Pauli Exclusion Principle which prohibits electrons with parallel spin from occupying the same region in space.

Charge transfer attractive interaction between donor and acceptor atoms.

Penetration this term describes the strong repulsions that occur when closed-shell systems begin to interpenetrate. The form of this expression is dependant on the adequacy of the approximate description of the molecular wavefunctions.

The major contribution to the total intermolecular force comes from the electrostatic interaction energy between the two molecules.

11.2 IMPT

The method used here to calculate interaction energy was Intermolecular Perturbation Theory (IMPT) (Hayes & Stone, 1984) within the CADPAC 6.0 (Amos, 1996) package. The IMPT method provides estimates of the significant contributions to the intermolecular interaction energy, electrostatic energy E_{es}, exchange-repulsion E_{er}, polarisation E_{pol}, charge transfer E_{ct} and dispersion energy E_{disp}. This method is free from Basis Set Superposition Error (BSSE). BSSE leads to an overestimation of the charge transfer term as the description of the electronic interactions of one molecule are enhanced relative to those of the isolated molecule by the basis set of the second molecule. BSSE is a major problem when calculating interaction energies, as such calculations are typically performed on small model systems using small basis sets and the effect of BSSE is more pronounced when small basis sets are used, as the electronic configuration is described less thoroughly.

IMPT is computationally too expensive to be used for the large number of geometrical calculations needed to define a potential energy surface, but it is ideal for calculations at a limited number of interaction geometries. As a result, IMPT is ideal for use in conjunction with CSD studies. The CSD can be used to ascertain statistically favourable interaction geometries which can then be used as a starting point for a series of IMPT calculations. The two studies described in this section were carried out using this CSD/IMPT combination. The number of CSD entries in each case is quite small, which makes it difficult to draw decisive conclusions as a small data set will have a large associated statistical error. However when taken in

conjunction with a complementary set of energetic calculations more definite conclusions can be drawn.

This combination of statistical analysis using the CSD and energetic calculations using IMPT is a powerful tool for studying intermolecular interactions. This method has been used to study various systems including C-Cl --- O=C interactions (Lommerse, Stone, Taylor & Allen, 1996), halogen --- O(nitro) supramolecular synthons (Allen, Lommerse, Hoy, Howard & Desiraju, 1997) and carbonyl, ether, ester --- OH interactions (Lommerse, Price & Taylor, 1996).

In order to investigate interaction energies between donor and acceptor groups, a model system must be chosen for the calculations. Model molecules must be chosen to represent the donor and acceptor fragments. The molecules chosen should be representative of the type of interactions of interest and ideally quite small to minimise calculation time. The method used in the work described here was first to establish an initial model of each molecule using bond length and angular data form the CSD and International Tables and then to calculate a minimum energy model using this starting point. The calculation optimises the gradient of the energy, it is said to be optimised when the largest component of the gradient is lower than the required tolerance. The geometry optimised molecules were then placed at certain distances and orientations relative to each other and the energy of their mutual interaction was calculated. As the molecules are modelled quite simply it would be unwise to make any comment on the values of the energies obtained from the calculations. However internal comparisons can be made confidently, within the set of values taken as a whole.

REFERENCES

Aakeröy, C. B. & Seddon, K. R. (1993). *Chem. Soc. Rev.*, 397-407.

Allen, F.H., Lommerse, J.P.M., Hoy, V.J., Howard, J.A.K. & Desiraju, G.R., (1997). *Acta Cryst* **B**53, 1006-1016.

Amos, R. D. (1996). *CADPAC6.0. The Cambridge Analytical Derivatives Package. Issue 6.0. A Suite of Quantum Chemistry Programs*. University of Cambridge, England.

Hayes, I. C. & Stone, A. J., (1984). *J. Mol. Phys.*, **53**, 83-105.

Lommerse, J.P.M., Price, S.L. & Taylor, R. *J.*, (1996). *Comput. Chem.*, **18**, 6, 757-774.

Lommerse, J.P.M., Stone, A. J., Taylor, R. & Allen, F.H., (1996). *J. Am. Chem. Soc.*, **118**, 3108-3116.

Azides as Hydrogen Bond Acceptors

CHAPTER 12

12.1 Azide chemistry

The first azide, phenyl azide, was prepared in 1864 by Greiss. Azide chemistry has been of interest ever since due to the wide range of reactivity of the compounds and their unusual structures. However work is difficult due to their instability and their explosive nature. This branch of chemistry has been extensively reviewed. Inorganic azide chemistry has been covered by Audreith (1934) and Gray (1963) while a review by Evans, Yoffe and Gray (1959) dealt with their physical properties. Organic azides have been covered albeit less thoroughly by Boyer and Canter (1954) and Lieber, Curtice and Rao (1966). Metal azide chemistry or 'coordinated azides' were reviewed by Dori and Ziolo (1973). A thorough review of many aspects of azide chemistry and structure can be found in a volume of the "Chemistry of the Functional Groups" series (Patai, 1971).

12.2 Electronic Structure

Originally azides were thought to have a structure based on pentavalent central nitrogen atom with double and triple bonds linking the three atoms (Samuel, 1944). It is now accepted that this is not the case and that covalent azides can be written as two canonical structures (Pauling, 1967).

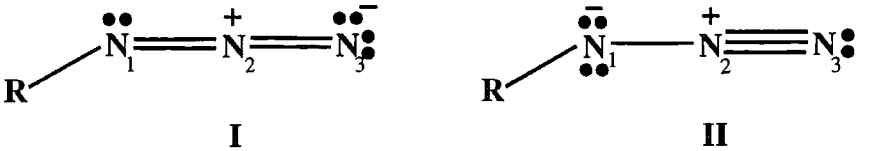

Figure 12.1 - Azide resonance forms

When considered as equal contribution resonance hybrids, formal charges are -1/2, +1, -1/2 on N1, N2 and N3 respectively with bond order 1.5 for bond N1-N2 and 2.5 for bond N2-N3. This model takes account of the significant delocalisation of π electrons. The linearity of the azido group is a result of the sp hybridisation of the central atom N2. The σ orbitals of N1 are not truly sp^2 hybridised, they consist of three non-equivalent hybrids formed from the s, p_z and p_x orbitals. There is an sδp orbital, largely of s character which is occupied by a lone pair of electrons. There are also two remaining orbitals of pδs character which take part in the bonding of R and N2. The third nitrogen atom N3 uses a p_z orbital for bonding to N2 and also has a lone pair in an s orbital, however this orbital is also likely to have some s character. A localised πorbital is formed by the p_x orbitals of N2 and N3 while the p_y orbitals of all three nitrogen atoms form three delocalised π orbitals.

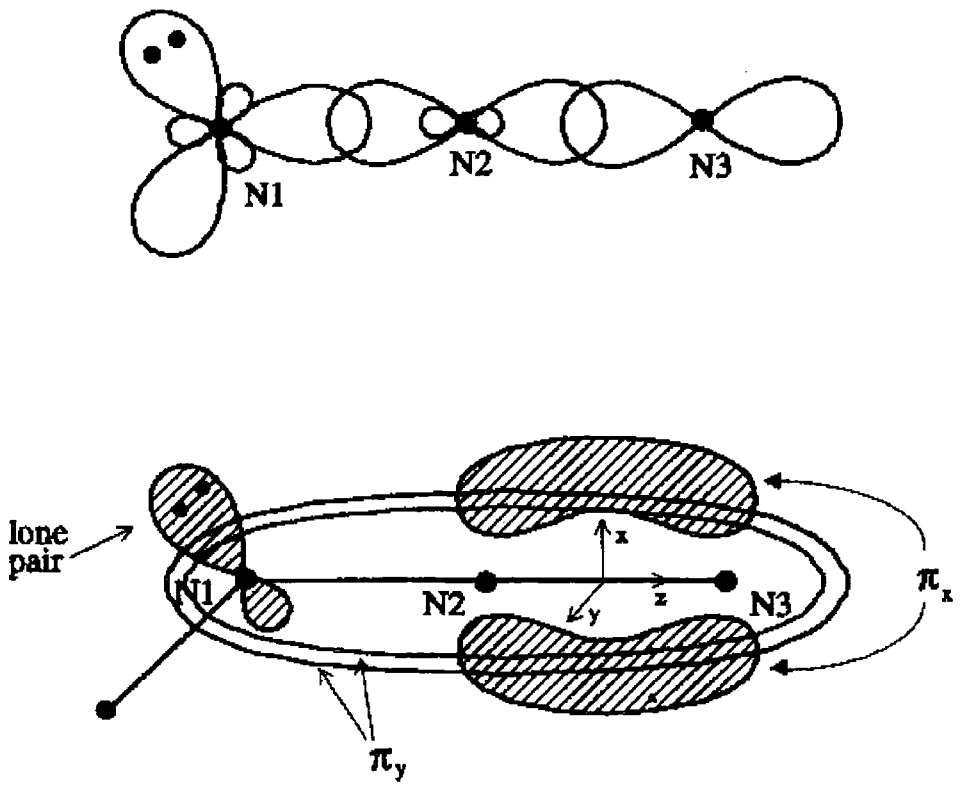

Figure 12.2 - Electronic structure

There are two lone pairs in the valence shell of the azido group, the lone pair in the sδp hybrid orbital of N1 is of higher energy than that in the s orbital of N3 and can be more readily excited

The azido group was chosen for study in light of recent interest in intermolecular interactions involving π-electron systems. Alkynes have been widely studied as both weak hydrogen bond donors and acceptors. There is much interest in phenyl rings as hydrogen bond acceptor moieties, opinion varies as to whether they are genuine stabilising interactions or merely a consequence of geometry. Interest also lies in whether, if indeed such interactions are attractive, the preferred acceptance site of the donated hydrogen atom electron density is the centroid of the phenyl ring or the atomic sites themselves (Malone, Murray, Charlton, Docherty & Lavery, 1997) The azide group is interesting in this way, as due to its electronic structure, there are two possible 'types' of acceptor site, the atoms or the multiple bond electron densities.

12.3 Search methodology

A search of the Cambridge Structural Database, October 1996 issue (Allen & Kennard, 1996) was carried out for all entries containing the azide group. Searches were carried out for both organic and organometallic compounds. Since the azide group exists in resonance forms, a rough search of the database was carried out to check which particular form dominated. All azides were accepted and the bond lengths N1N2 and N2N3 were tabulated.

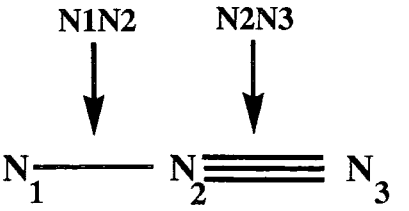

Figure 12.3 - Bond lengths N1N2 and N2N3.

The array of publications containing azide crystal structures, draw the azide unit in a variety of different ways, some of which are depicted below.

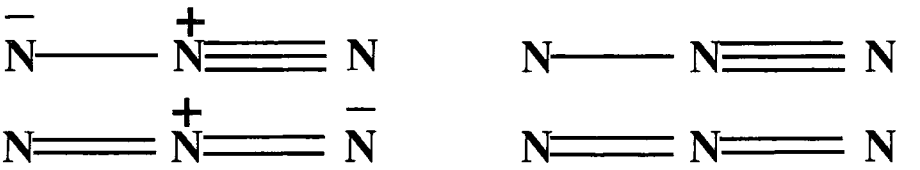

Figure 12.4 - Variety of depictions of the azide group

The bond length distributions N1N2 and N2N3 are shown in Figure 12.5. The mean values of the two distributions are 1.192(2) and 1.144(1) Å respectively which suggest that the most common resonance form contains a single bond N1N2 and a triple bond N2N3.

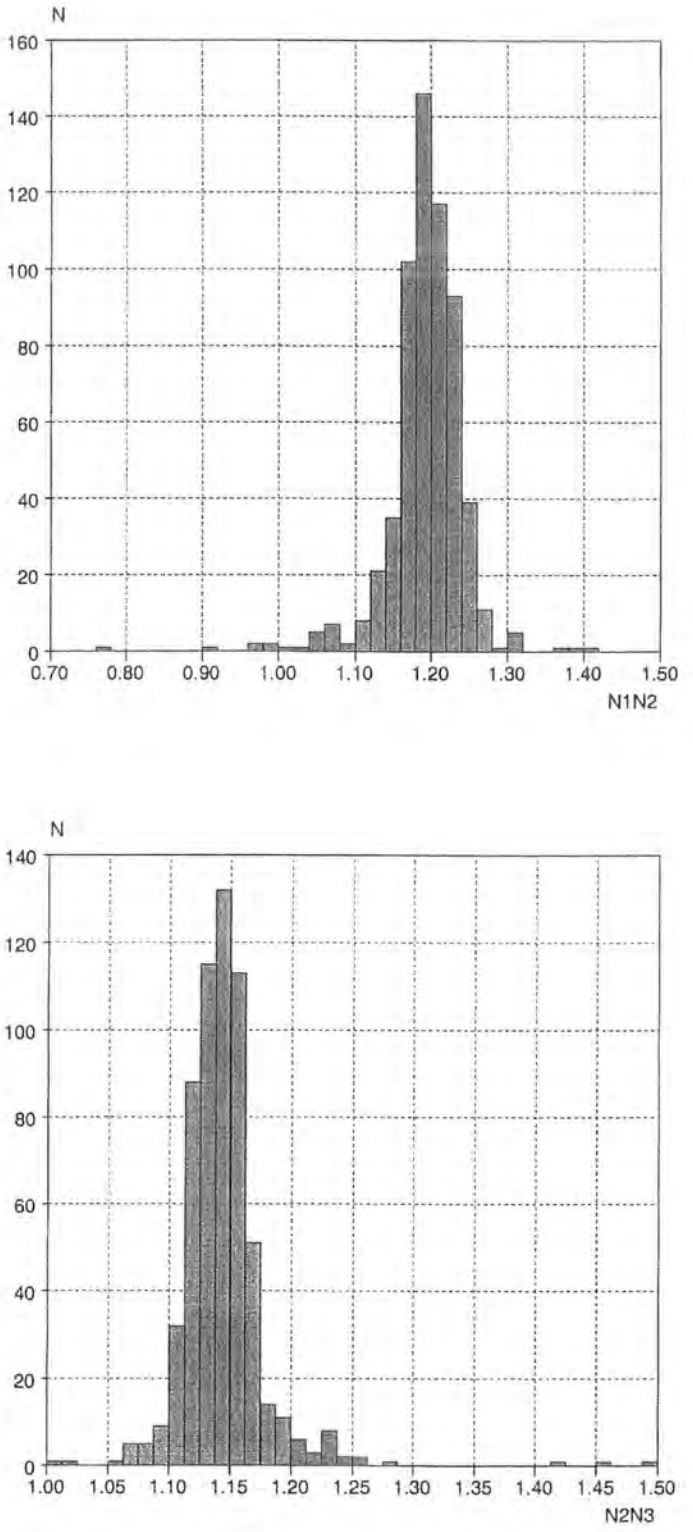

Figure 12.5 - Bond length distributions in the azide group.

However not all these entries were suitable for the systematic hydrogen bonding survey.

The following constraints were applied to the structures in the search:

- 3-D coordinates must be present
- no disorder
- no polymers
- R-factor ≥ 10%
- Error free at the 0.05Å level

The refined search was defined as shown in Figure 12.6.

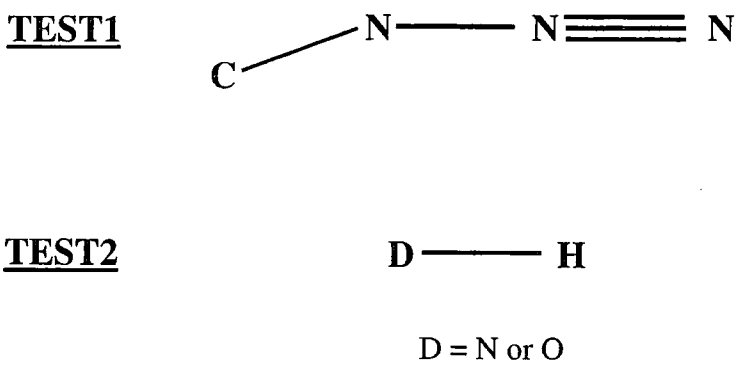

Figure 12.6 - Test definitions to locate suitable azides

Both TEST1 and TEST2 must be satisfied for any entry to be accepted. This ensures that all entries also contain a suitable donor group so they that are capable of forming the necessary hydrogen bond. Results showed that the database contained information for 63 organic and 56 organometallic azides. The basic search was then modified to sub-search this list for instances where the H --- N distance was less than the sum of

the Van der Waals radii of the two interacting atoms, which is 2.75Å. Several bond lengths and angles were tabulated to describe the geometry of the interactions.

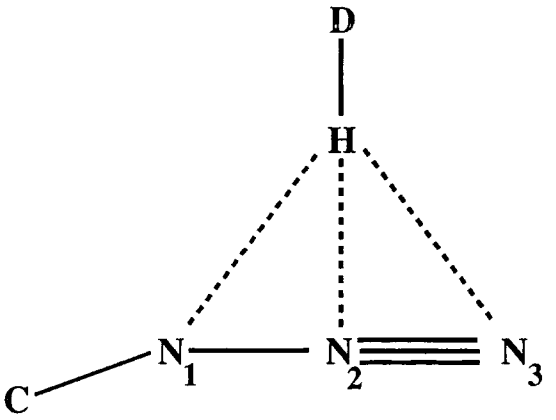

A1 = angle D-H --- N1
A2 = angle D-H --- N2
A3 = angle D-H --- N3

B1 = length H --- N1
B2 = length H --- N2
B3 = length H --- N3

ANG1 = angle N2-N1 --- H
ANG2 = angle N3-N2 --- H

Figure 12.7 - Definition of tabulated parameters

12.4 Search results

From a total of 63 organic molecules capable of forming the required hydrogen bond, 11 contain an interaction within the distance limits set. There are also interactions within 21 of the 56 organometallic molecules.

Table 12.1 - Search results for organic molecules

	Number of contacts	Shortest contact (Å)	Longest contact(Å)	Mean length (Å)
N1	8	2.069	2.693	2.53 (7)
N2	2	2.368	2.716	2.5 (2)
N3	9	2.457	2.701	2.57 (3)

Table 12.2 - Search results for organometallic molecules

	Number of contacts	Shortest contact (Å)	Longest contact (Å)	Mean length (Å)
N1	18	1.887	2.672	2.16 (6)
N2	9	2.423	2.740	2.67 (4)
N3	28	1.880	2.533	2.13 (5)

12.4.1 Hydrogen bond distances

The shortest contact to any of the three nitrogen atoms in the organic molecules involves N1. This interaction is far shorter than the shortest contacts to either of the other two nitrogen atoms. There are far fewer contacts to the central nitrogen atom N2. The resonance forms of the azide group as shown in Figure 12.4, show this nitrogen atom to carry a positive charge and no lone pairs. As this atom is not a site of localised electron density unlike the other two sites, it is understandable that it is a less favoured site for acceptance of the donated hydrogen. The average length of the interactions involving the organometallic azides are significantly shorter than those involving the organic molecules. This is understandable when one considers the effect of the π overlap and the back donation from a filled d orbital on the metal into a vacant antibonding π^* orbital on the azide ligand. This extra donated electron density makes the azide ligand more attractive to the approaching hydrogen atom. However the organic and organometallic results are broadly similar, since both show that N2 is less favoured but the distinction between N1 and N3 is less clear although the number of contacts involving N3 is greater and significantly so for the organometallic

compounds. As the difference between the two data sets is slight and the number of entries in each is small, no distinction was made between organic and organometallic azides for the remainder of the analysis.

12.4.2 Angular approach

A characteristic of strong hydrogen bonds is the relationship between the length of the hydrogen bond and the angle of approach of the D-H bond vector to the acceptor group or atom. It is recognised that in shorter contacts, D-H makes a more linear approach to the acceptor than in longer contacts. This effect is less pronounced for interactions between weak hydrogen bonding systems.

A1, A2 and A3 describe the approach of the D-H bond vector towards N1, N2 and N3 respectively. The three graphs of interaction distances B1, B2 and B3 versus D-H --- N angle A1, A2 and A3 show that for B1 and B3 the interactions follow this trend with the shorter interactions closer to linearity. In contrast, the graph of B2 versus A2 has no such trend, this is to be expected if this atom does not function as a hydrogen bond acceptor.

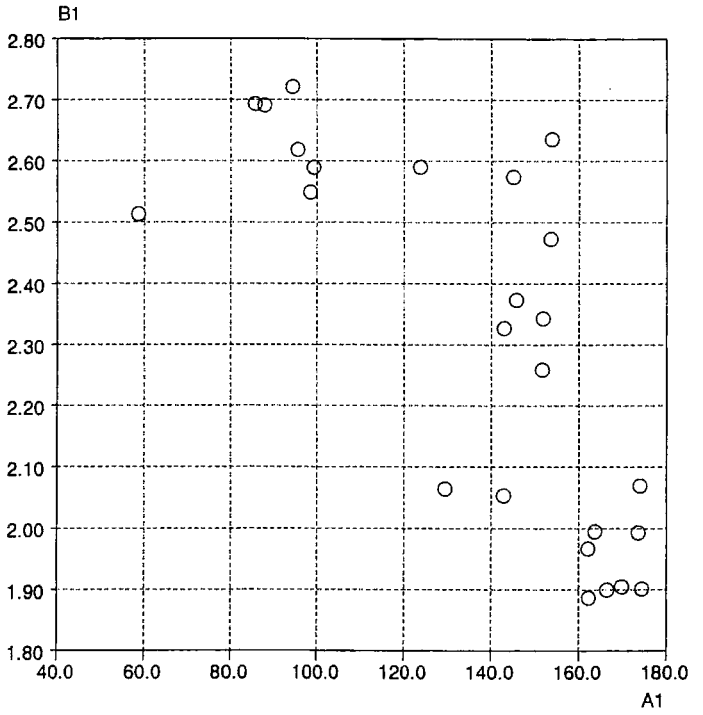

Figure 12.8 - Interaction distance B1 versus angle A1

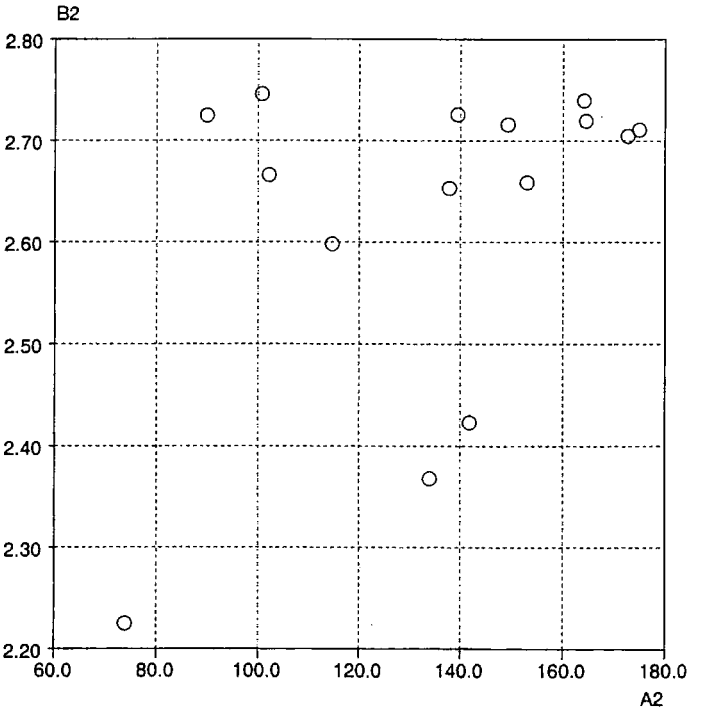

Figure 12.9 - Interaction distance B2 versus angle A2

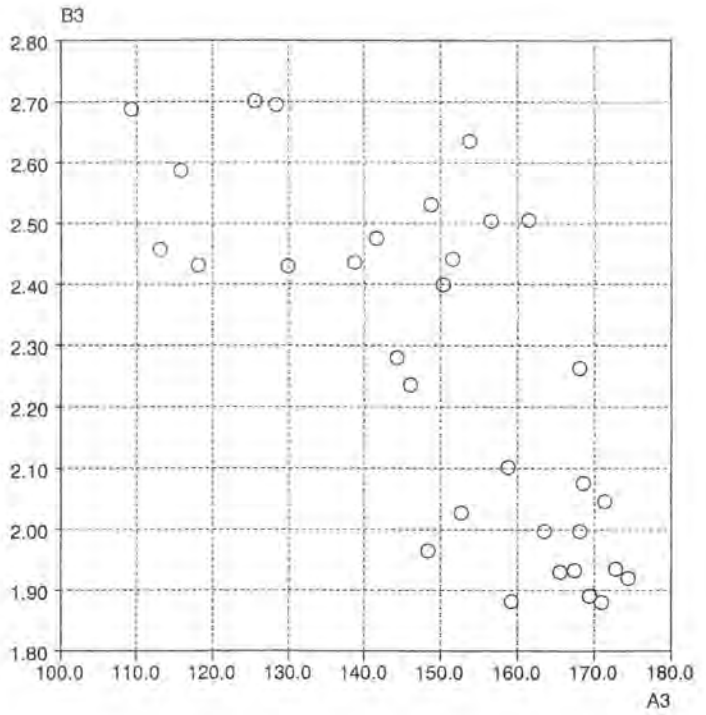

Figure 12.10 - Interaction distance B3 versus angle A3

A cone angle correction (Kroon & Kanters, 1974) can be applied to this data in order to correct for frequency distribution effects. Although the optimum hydrogen bond angle for a system may be linear, the frequency distribution of angles may have its maximum at less than 180°. This occurs because the number of possible hydrogen bond configurations at any angle θ is proportional to θ. Therefore at a less than linear angle θ there will be a greater number of possible configurations than when θ is 180° so the frequency maximum will move away from linearity. Application of a sine or cone angle correction will correct for this problem. The CSD program VISTA includes an option to apply a cone angle correction to angular histograms. Every histogram bar is multiplied by $N/\sin\theta$ where θ is the average of the upper and lower limits of the bar and N is a normalisation constant. Figure 12.11 illustrates this effect for the A3 angles. The distribution of angles shifts towards 180° leaving the genuinely smaller angles unaffected.

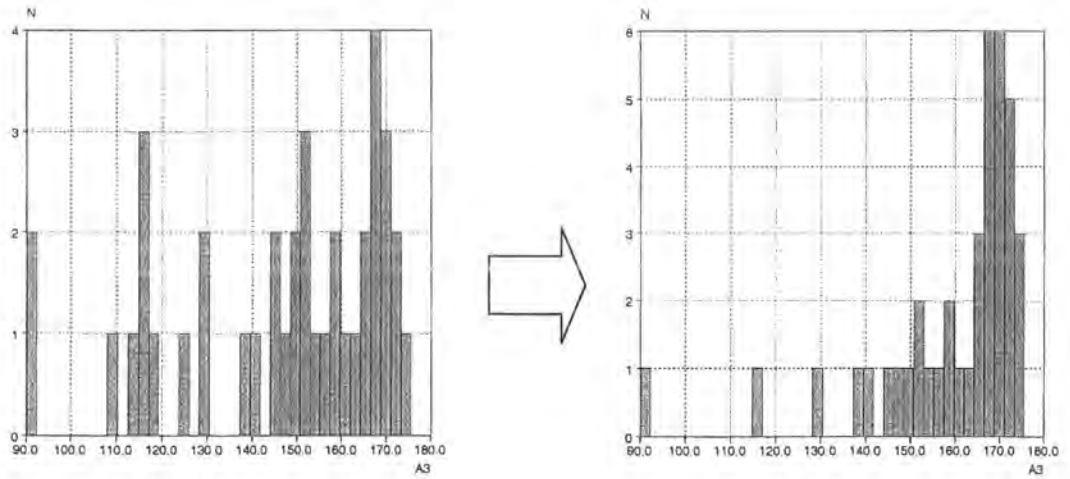

Figure 12.11 - application of conical correction. Uncorrected data to the left, corrected to the right.

A further set of angles were tabulated, ANG1 and ANG2, which describe the approach of the hydrogen atom towards the azide group. The angular approaches correlate with the position of the lone pairs at N1 and N3. The mean angle of approach to N1 is 113(4)° which suggests that the hydrogen atom is drawn to the sδp lone pair at this site. The equivalent angle for N3 (167°) is not quite linear as would be expected.

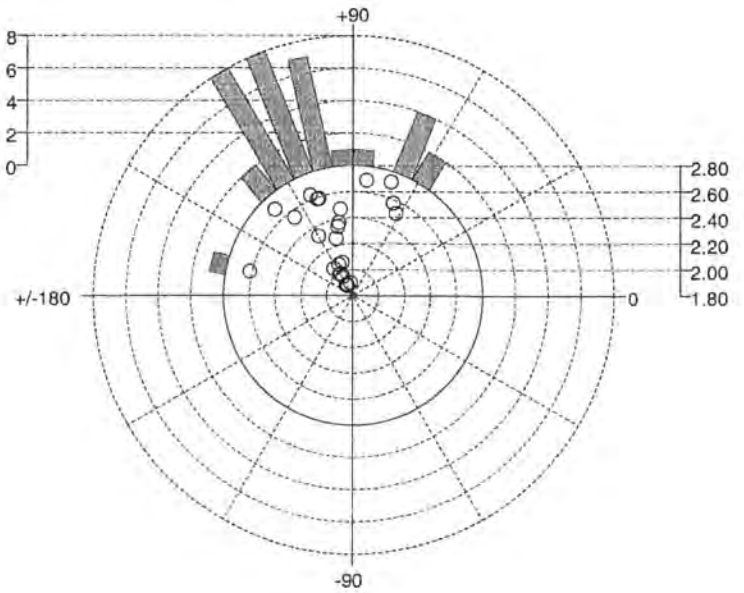

Figure 12.12 - Polar scattergram of B1 versus ANG1.

In Figure 12.12, the centre of the graph represents N1 with the N1-N2 bond vector lying along the horizontal axis towards 0.

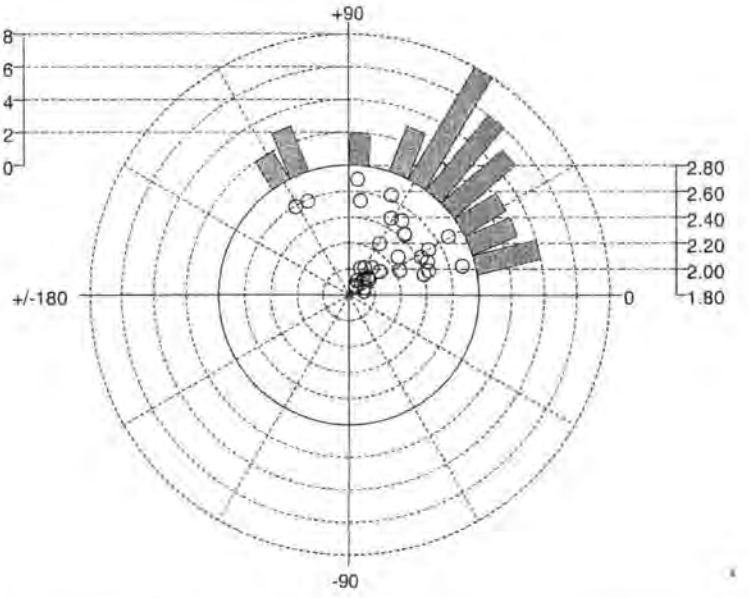

Figure 12.13 - Polar scattergram of B3 versus ANG2.

In Figure 12.13, the centre of the graph represents N3 with the N2-N3 bond vector lying along the horizontal axis to the left. The graph plotted is [180 - ANG2] to aid visualisation

The fact that the angular approach of the hydrogen atom towards N3 is significantly less than linear could be a result of steric influences involving the molecular packing. The azide group is quite long in comparison with other functional groups that are recognised as hydrogen bond acceptors. It is possible that as the interactions are unlikely to be the most significant interactions in the structure, the energetic cost in orienting the molecule for an idealised 'end-on' approach is too great. Another possibility is orbital overlap between the π orbital between N2 and N3 and the s-

character lone pair at N3. If any significant overlap does occur then this will extend the region of likely hydrogen atom approach away from the N2-N3 bond vector.

12.5 Summary of CSD analysis

In summary, it is clear from the CSD search results that the lone pairs at N1 and N3 are good hydrogen bond acceptor sites and N2 is not favoured. However, it is not possible to distinguish between these two sites to ascertain the preferred acceptor due to the small data set.

12.6 IMPT calculations

Methyl azide and methanol were chosen as a model system for the interaction energy calculations. Initial models for each molecule were obtained using data sources such as International Tables and the CSD. These models were then optimised to produce a final model system. All calculations were performed at the 631G** level of theory. The geometrical details of the optimised methyl azide molecule are shown in Figure 12.14. The NNN angle is described in the literature as linear and the angle optimised by CADPAC was 175.39°. For the purposes of these calculations the NNN fragment was treated as a cylinder.

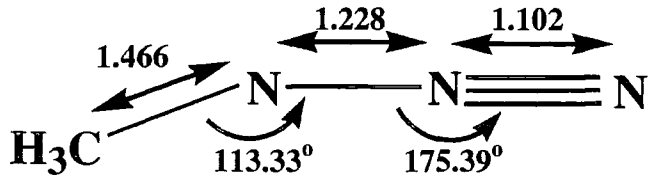

Figure 12.14 - Optimised geometry of methyl azide, all distances in angstrom.

12.6.1 Interactions involving N3

The information gleaned from the CSD analysis was used as a starting place for the energy calculations. The shortest hydrogen bond to an organic azide molecule in the CSD was 2.201Å so calculations were performed with the molecules separated by 2.1Å then increasing the separation in 0.1Å increments to a maximum separation of 2.9Å.

The methanol molecule was aligned along the N2N3 bond vector with the CH_3 group oriented out of the plane of the NNN fragment. Results are given in graphical form in Figure 12.15. The total interaction energy is given as the sum of five energy terms, electrostatic, electron-repulsion, polarisation, charge transfer and dispersion. All five contributions are plotted individually along with the total energy. It can be seen that electron-repulsion is high at short interaction distances but its influence fades as the separation grows. The dominant term is the electrostatic contribution.

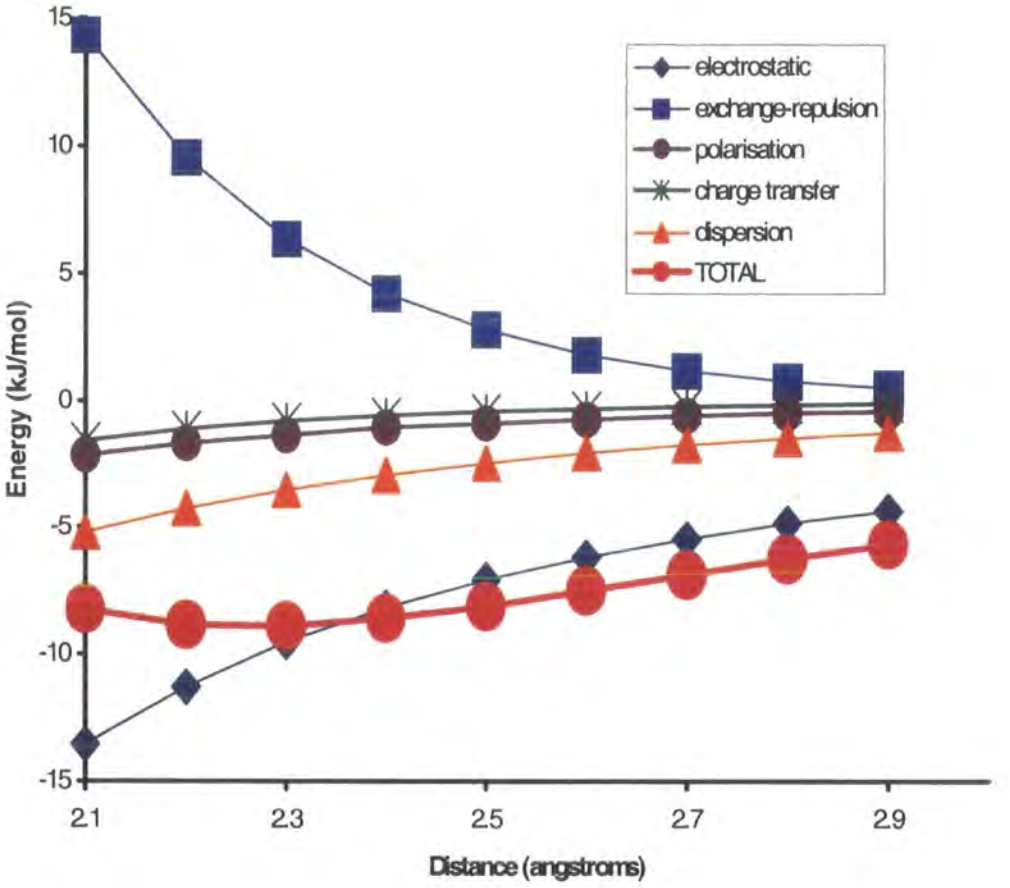

Figure 12.15 - Individual components of the interaction energy versus distance of methanol H from N3

The optimum separation distance was found to be 2.3Å, this was then probed by calculating the energy at 0.01Å increments at either side of this value. The interaction energy is at a maximum at a separation of 2.26Å.

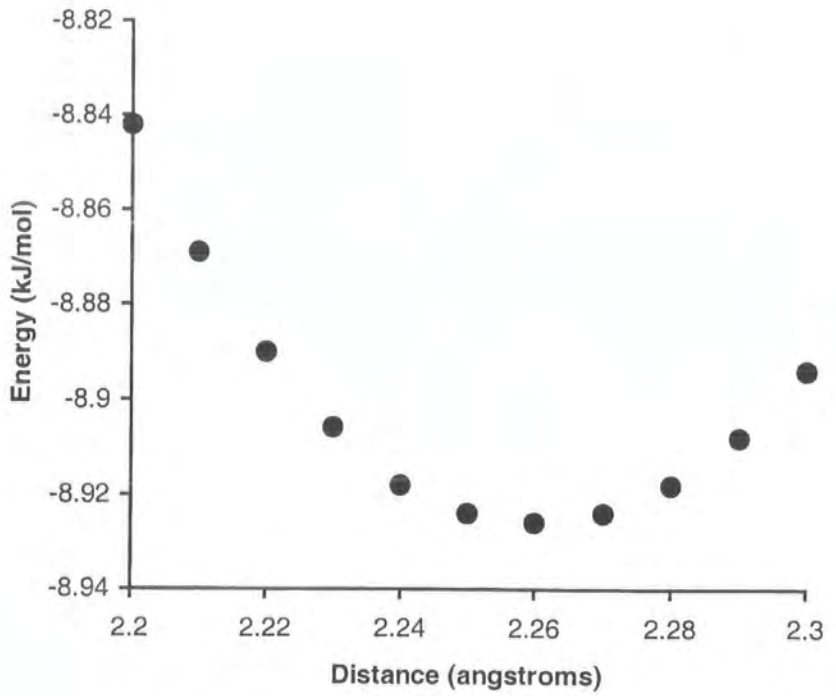

Figure 12.16 - Energy versus distance of methanol H from N3

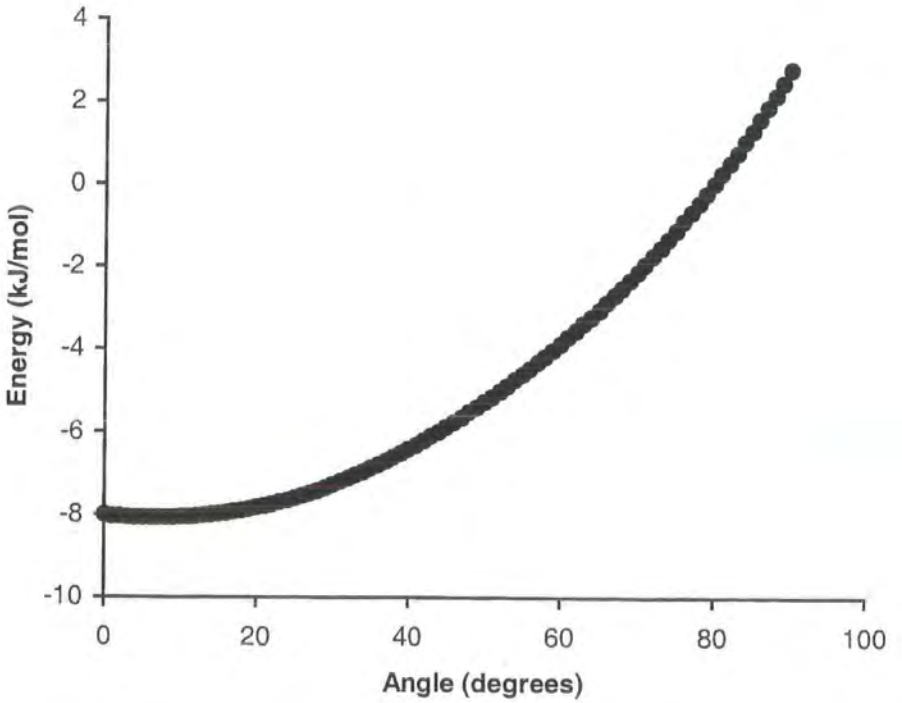

Figure 12.17 - Energy versus angular deviation from N2N3 bond vector

The optimum angle of approach of the methanol towards the terminal nitrogen atom N3 was then calculated. The distance between N and H was fixed at 2.26Å and the angle was varied in one degree increments. These results which are displayed in Figure 12.17 show that the optimum angle of approach of O-H towards N3 is not along the N2-N3 bond axis as would be expected. The maximum attractive interaction energy occurs at 9° to the N2-N3 bond axis. However the energy range between a linear approach and 20° is quite small (0.176 $kJmol^{-1}$) so it is likely that the ideal approach angle is quite diffuse as suggested by the CSD results.

12.6.2 Interactions involving multiple bonds and N1

The methanol molecule was then rotated fully 90° so the O-H group was perpendicular to the N2-N3 bond. The methanol was then moved relative to the methyl azide in 0.1A increments at a separation of 2.26Å. The interaction energy is repulsive all the way along this bond. It grows steadily more repulsive until the O-H passes the mid-point of the bond and nears the central nitrogen atom N2. At this point the energy becomes a little less repulsive but only slightly. The interaction energy when the O-H is perpendicular to the N2-N3 bond and positioned 2.26Å directly above N2 is +5.285 kJ.

The same treatment was then applied with the methanol perpendicular to the N1-N2 bond. Again the interaction at N2 is repulsive but it rapidly becomes decreasingly repulsive as the methanol is moved further towards the mid-point of the bond. The interaction becomes attractive and the energy increases swiftly to a maximum above N1 itself.

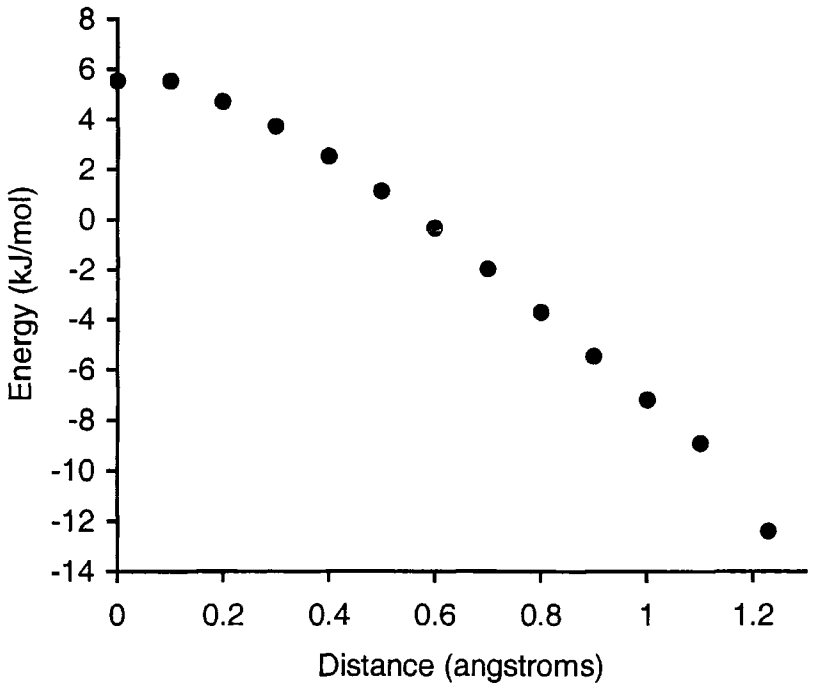

Figure 12.18 - Energy versus distance of methanol along N1-N2 bond measured from N2

The maximum attractive interaction energy was obtained with the O-H positioned directly above N1, the energy was -12.407 $kJmol^{-1}$. This interaction is far more attractive than the best results that were obtained when probing the area around N3.

12.7 Summary

Using the CSD search results and the IMPT calculations together, a more complete picture of the involvement of the azide group in hydrogen bonding can be drawn. The conclusions that can be made from the search results are that both N1 and N3 can act as hydrogen bond acceptors although no clear distinction can be drawn between them.

The central nitrogen atom N2 on the other hand is disfavoured as an acceptor site. These observations agree well with the results of the simple single point calculations. N2 is clearly not a good site for hydrogen bonding, the interaction energies at and around the atom are repulsive. The calculations however do allow us to make a distinction between atoms N1 and N3. Both sites are acceptable in hydrogen bonding terms but the interaction energies at N1 are more attractive by a significant amount, -12.4 $kJmol^{-1}$ compared with -8.93 $kJmol^{-1}$. As the sδp lone pair at N1 is of higher energy than the s-nature lone pair at N3 it is likely that it is a more attractive site for acceptance of hydrogen bonds.

REFERENCES

Allen, F.H. and Kennard, O. (1993) *Chemical Design Automation News*, **8** (1), 1 & 31-37.

Audreith, L. F, (1934).*Chem. Rev.*, **15**, 169.

Boyer, J. H. & Canter, F. C., (1954). *Chem. Rev.*, **54**, 1.

Dori, Z. & Ziolo, D. F., (1973). *Chem. Rev.*, **73**, 247.

Evans B. L., Yoffe, A. D., & Gray, P., (1959). *Chem. Rev.*, **59**, 515.

Gray, P., (1963). *Quart Rev. Chem. Soc.*, **17**, 441.

Greiss, P., (1964). *Phil. Trans. Roy. Soc. London*, **13**, 377.

Kroon, J & Kanters, J. A. (1974). *Nature (London),* **248**, 667

Lieber, E., Curtice, J.S. & Rao, C. N. R., (1966). *Chem. Ind.*, 586.

Malone, J. F., Murray, C. M., Charlton, M. H., Docherty, R. & Lavery, A. J. (1997). *J. Chem. Soc. Faraday Trans.* **93**, 3429-36.

Patai, S., (1971). *"The Chemistry of the Azido Group"* Interscience Publishers.

Pauling, L., (1967). *'The Nature of the Chemical Bond'*, Cornell University Press, Ithaca, N.Y.

Samuel, R. J., (1944). *J. Chem. Phys.*, **12**, 167, 180.

Organic Cyanides as Hydrogen Bond Acceptors

CHAPTER 13

13.1 Electronic structure

The cyano group consists of nitrogen and carbon atoms that are sp hybridised. The atoms are bound by a σ-bond and there are a further two π-bonds at right angles to each other. The group R-C≡N is linear with a lone pair centred on the nitrogen atom and directed along the C≡N bond axis. This lone pair leads to a large dipole moment of approximately 3.5D, the electron density of the π-orbitals is displaced towards the nitrogen atom so partial charges δ+ and δ- can be assigned to the carbon and nitrogen atoms respectively. Due to the lone pair, complexation largely occurs at the nitrogen atom, however, weak complexes can be formed using the π-electrons.

The C≡N group can be described a rod surrounded by a cylindrical cloud of π-electrons. The sp lone pair sits at the end of the cylinder oriented along the bond axis.

13.2 Hydrogen bonding studies

The crystal structure of HCN was published in 1951 by Dulmage and Lipscomb. The structure exists in two different temperature dependant forms, each consisting of linear chains of C≡N --- H interactions with an N --- H separation of 2.2Å. Cyano intermolecular interactions play an important role in the structure of tetracyanoquinodimethane and its function as an organic superconductor. For discussions of TCNQ salts see for example Melby, Harder, Mahler, Benson & Mochel (1962) and Acker & Blomstron (1962).

Much of the work on intermolecular interactions involving cyanides has been carried out on the C≡N --- Halogen system, these interactions were noted by Hassell in 1958 as part of a study into donor-acceptor complex formation. Interactions with halogens were reviewed comprehensively by Britton in 1967 as part of a detailed review of cyanide chemistry in general. The work by Britton included interactions within the structure of halogen cyanides and other simple cyano molecules, interactions were found to be considerably shorter than the sum of the van der Waals radii of the two interacting atoms. Interactions were discussed in terms of the effect on the C≡N bond length and were found to form linear or nearly linear chains of molecules. A short review of cyano hydrogen bonding was presented by Grundes and Klaboe (1970) as part of a wider work on the chemistry of the cyano group. C≡N --- Br and C≡N --- Cl interactions in the structures of 4-Halobenzonitriles were studied systematically by database analysis and some crystal structure analysis. Reddy, Panneersevlvam, Pilati and Desiraju (1993) later showed that C≡N --- Cl interactions can be used successfully in supramolecular design, reporting work on molecular tapes based on these interactions. Reddy, Goud, Panneerselvam and Desiraju (1993) used C≡N --- H-C interactions to design a hexagonal network in the 1:1 complex of 1,3,5-tricyanobenzene and hexamethylbenzene. Linear arrays of C≡N --- H-C≡C interactions were successfully predicted in 4-cyano-4'ethynylbiphenyl (Langley, Hulliger, Thaimattam & Desiraju, 1998).

There has also been a brief analysis of C-C≡N --- H-O-C as part of work by Sarma, Dhurjati, Bhanuprakash and Ravikumar (1993) into strategies for the design of non-centrosymmetric structures. Statistical analysis was carried out on organic molecules

within the June 1990 release of the CSD. 19 instances of the C-C≡N --- H-O-C fragment had a mean N --- H distance of 2.07 and mean O-H --- N angle of 160°.

13.3 CSD search

A search of the Cambridge Structural Database, October 1996 issue was carried out for all entries containing the cyano group. Searches were restricted to accept only 'organic' compounds with the cyano fragment bound to a carbon atom. The donor groups chosen for investigation of the hydrogen bonding were O-H and N-H. Entries were accepted which passed the checks listed below and which also contained one or both of the donor groups.

- 3-D coordinates present
- no polymers
- error free at the 0.05Å level
- no disorder
- R-factor ≤ 10%

The search was set-up as shown in Figure 13.1.

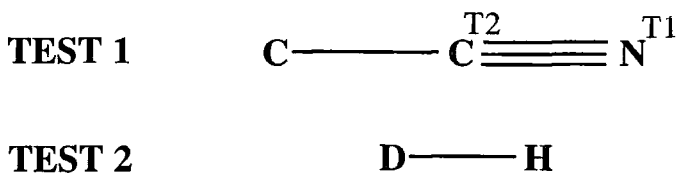

Figure 13.1 - Initial search for cyanide compounds with donor groups.

The total number of molecules found that have the donor and acceptor fragments was 642.

13.3.1 Interactions at the nitrogen atom

The search was then constrained to find those entries with a close contact between the donor hydrogen atom and the acceptor atom. The distance limits were set to be less than or equal to the sum of the Van der Waals radii of the two atoms concerned, i.e. 2.75Å.

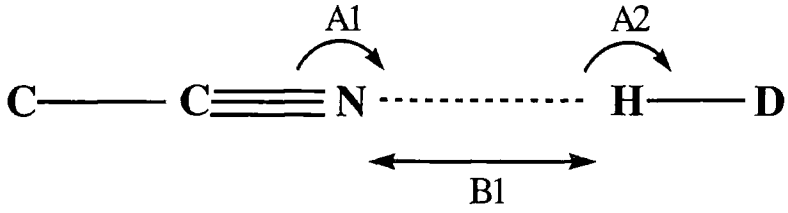

Figure 13.2 - Angular and distance definitions

The number of molecules containing close contacts within the limits was 257. The 257 molecules contain a total of 377 different cyano interactions. The shortest interaction was 1.733 Å (N --- H) with the mean of the distribution at 2.20(1) Å.

The bulk of the distribution is found between 1.9 and 2.3 Å, see Figure 13.3. The shape of the distribution suggests that these interactions may be reasonably strong. The majority of the distances are far shorter than the 2.75 Å maximum limit, this is typical of a relatively strong interaction. The distribution of distances for a weak interaction will not have such a well defined peak of short distances, instead, the distribution would be more uniform with the bulk of the interactions at longer distance. A cone angle correction (Kroon & Kanters, 1974) was applied to the angular

data A2 in Figure 13.4. The distribution tends towards 180° but there is a large proportion in the 170 to 180° range. The ideal linear approach is favoured but as there is a large proportion of contacts making a slightly less than linear approach this suggests that these interactions are not exceedingly strong.

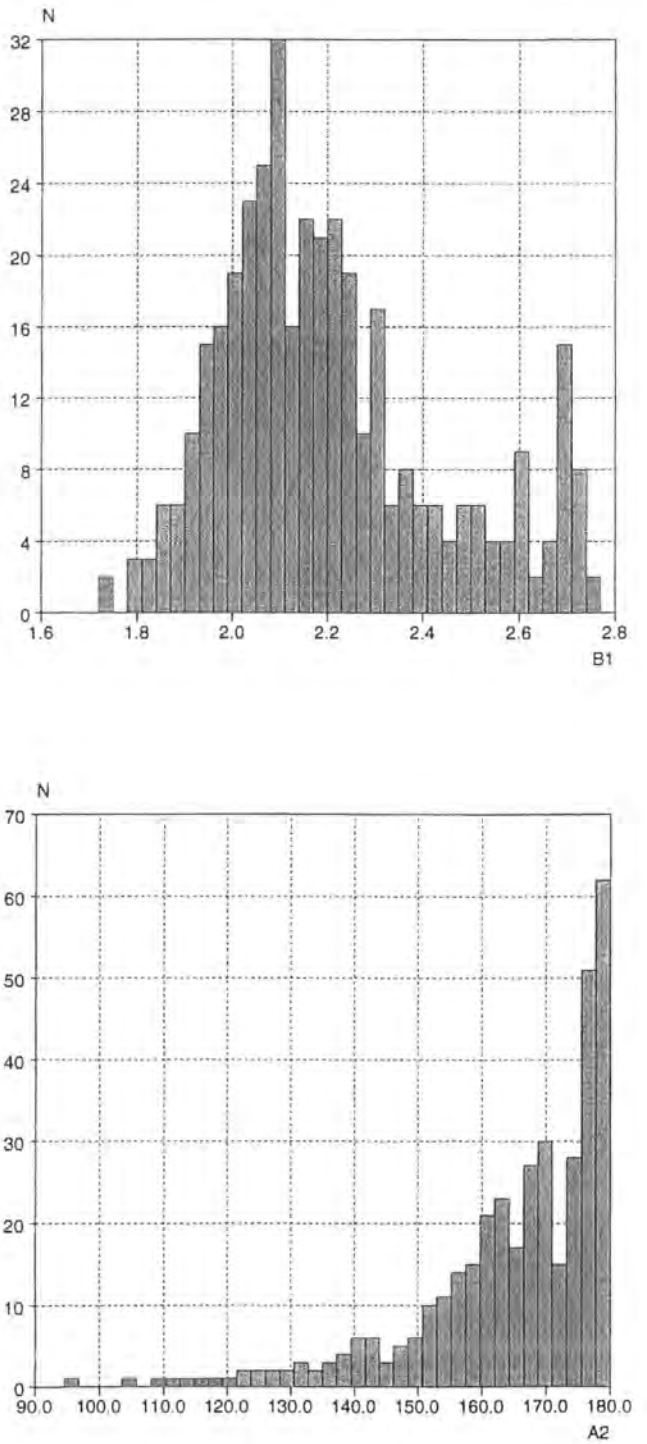

Figure 13.4 - Distribution of angle A2, cone angle correction applied

The second angle tabulated was the angle of approach of the hydrogen atom to the axis of the C≡N bond, A1, see Figure 13.5.

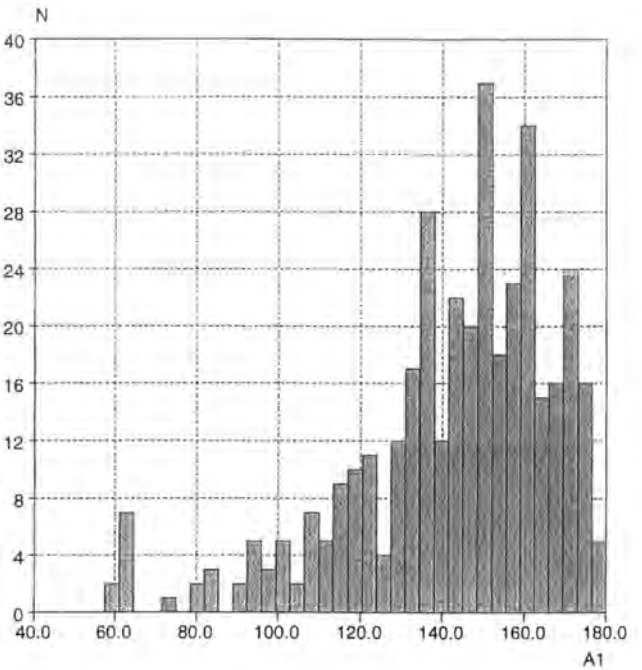

Figure 13.5 - Distribution of approach angle A1

Considering the electronic structure of the cyano fragment, it would be expected that the most favoured site for acceptance of a hydrogen bond would be the sp lone pair sited at the nitrogen atom. Therefore, the idealised angle of approach should be 180° if the lone pair is indeed the favoured site. There are very few entries at 180°, the bulk of the instances are in the 130° to 175° range. This observation does still correlate with the suggestion that the sp lone pair is the favoured approach site but the influence of the lone pair is possibly more diffuse than previously thought.

13.3.2 Nature of the acceptor.

The electronic structure of the acceptor group is responsible for the 'strength' of any hydrogen bonds it is involved in. The nature of the atom to which the acceptor is directly bonded can influence the hydrogen bond by effecting the electronic structure of the acceptor group. The 377 cyano interactions were subdivided by the nature of the carbon atom to which they were directly bonded, sp^2, sp^3, and aromatic carbon atoms, results are given in Table 13.1. The difference between the three groups is small, the group with the shortest length is the sp^2 group but the difference is very small. The greatest difference is in the C≡N --- H angle B2. The mean angle of the sp^2 bound cyanides is largest, closest to the expected 180° approach towards the nitrogen atom sp lone pair. These two observations taken together suggest that the interaction involving sp^2 carbon bound cyano groups are slightly stronger but the differences between the three groups are slight when taking into account the standard deviations so it is not possible to make and categorical distinction.

Table 13.1 - Search results, subdivided by nature of carbon atom to which cyano group is bonded.

	Number of hits #	B1 (Å)	A1 (°)	A2 (°)
TOTAL	257	2.20 (1)	151 (1)	143 (1)
AROMATIC	47	2.23 (3)	153 (2)	140 (3)
SP^3	90	2.22 (2)	151 (2)	139 (3)
SP^2	130	2.18 (2)	151 (1)	145 (1)

some molecules contain more than one cyano group which are bonded to different 'types' of carbon atom.

13.3.3 Triple bond

It was necessary to perform a further search to investigate the involvement of the carbon atom and the triple bond in hydrogen interactions. The search was set up as shown in Figure 13.6, the C≡N fragment was defined as a non-bonded group, hits were accepted within distance criteria of 2.75Å with the centroid of the group set as the acceptor site. Distances and angles were tabulated relating to both cyano atoms and the triple bond centroid.

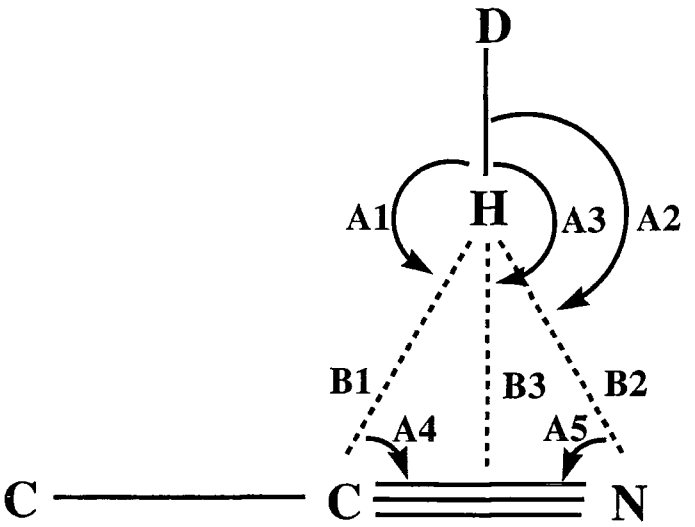

Figure 13.6 - Definition of search parameters

The scattergram of H --- C distance versus D-H --- C angle, Figure 13.7, reveals that the carbon atom is not a site involved in any hydrogen bonding involving the cyano atom. The bulk of the interaction distances are longer than 2.8 Å, there are only a handful shorter which could possibly be significant. The angular distribution of these distances is also not typically of a group hydrogen bonds. The trend of distance versus angle does not follow the expected behaviour of more shorter distances with more linear interactions.

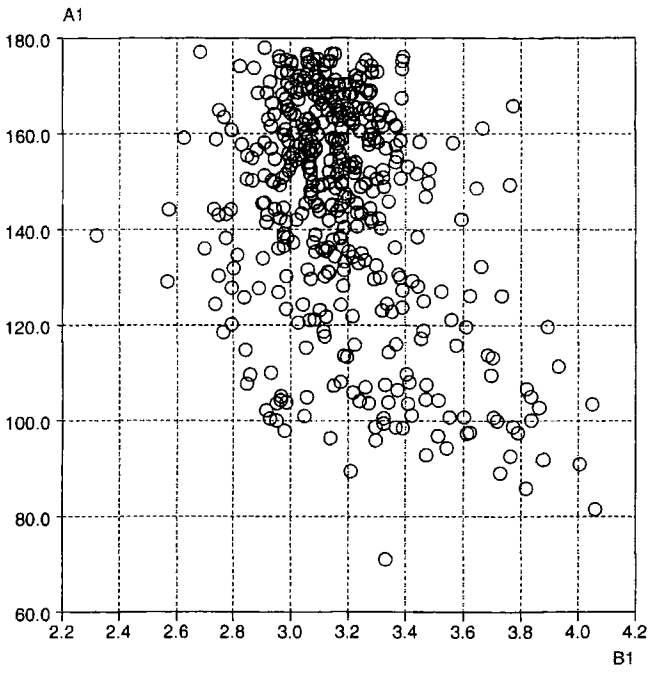

Figure 13.7 - Scattergram of interaction distance to carbon atom, B1, versus donor-H approach angle A1

The triple bond is also an electronically viable site for acceptance of donated hydrogen electron density. Figure 13.8 is a plot of B2 versus B3, there are many instances of reasonably short distances between the hydrogen atom and the triple bond centroid but in fact in the majority of cases, the distance from that hydrogen atom to the nitrogen atom is actually shorter. So the short contacts to the bond centroid are actually interactions to the nitrogen atom. The contacts that are actually shorter to the bond centroid are highlighted in red on the graph, however, these are not significantly short distances.

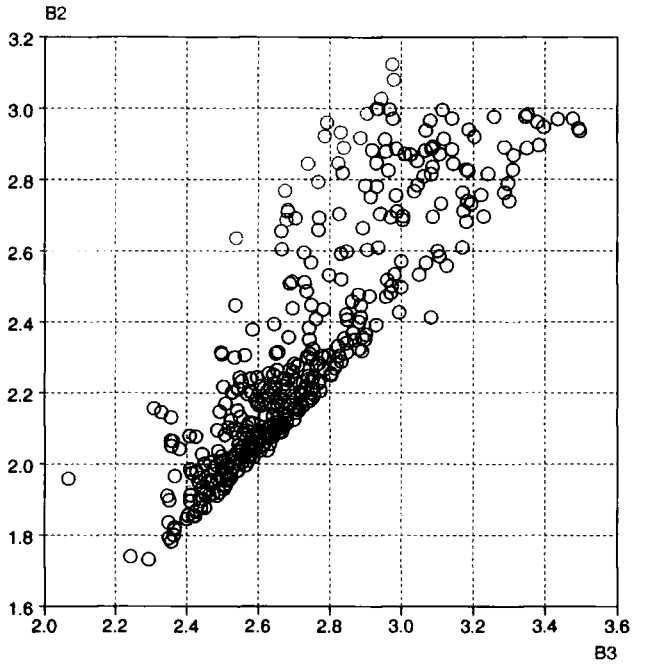

Figure 13.8 - DistanceB2 versus B3

Angles A4 (Figure 13.9) and A5 (Figure 13.10) describe the approach of the hydrogen atom towards the C≡N bond axis. There are clear angular preferences of both bond length distributions B1 and B2. Hydrogen atoms that appear within 3.0Å of the carbon atom all fall to the side of the carbon atom which is bonded to the nitrogen atom. It is likely that these distances correspond to the small number of instances of the hydrogen atom oriented towards the triple bond and the shorter contacts to the nitrogen atom. The instances where A4 is close to 0° correspond to A1 angles of close to 180°, i.e. contacts to the nitrogen atom. The distribution of B2 against A5, Figure 14.10, has a large group of points with small values of B2 and values of A5 in the range 140° to 180° which corresponds to the interactions involving the nitrogen sp lone pair. There are few instances of A5 under 90° which would correspond to interactions with the triple bond.

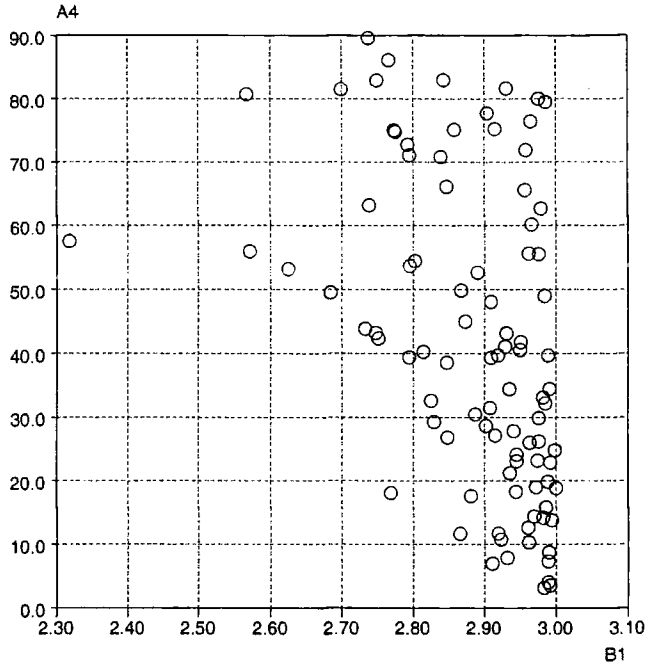

Figure 13.9 - Distribution of angle A4 versus distance B1

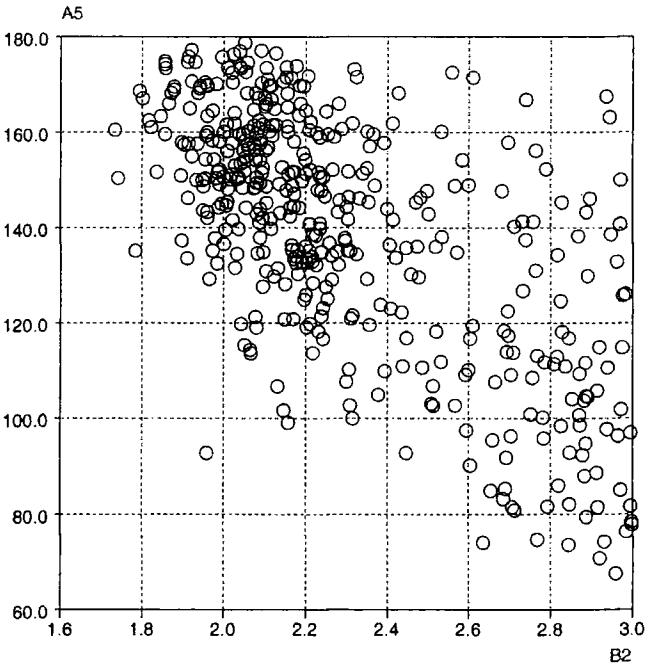

Figure 13.10 - Distribution of angle A5 versus distance B2

13.4 IMPT calculations

Methyl cyanide and methanol were chosen as a model system for the interaction energy calculations. Initial models for each molecule were obtained using International Tables and the CSD as data sources. The geometries of these models were then optimised to produce a final model system. All calculations were performed at the 631G** level of theory The geometrical details of the optimised methyl azide molecule are shown in Figure 13.11.

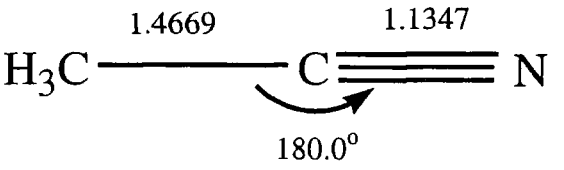

distances in angstrom

Figure 13.11 - Optimised methyl cyanide geometry

13.4.1 Interactions involving N1

The nitrogen atom of the cyano molecule was fixed as the origin of the coordinate system. The C≡N fragment was treated as a cylinder with the bond lying along the x axis of the reference coordinate system.

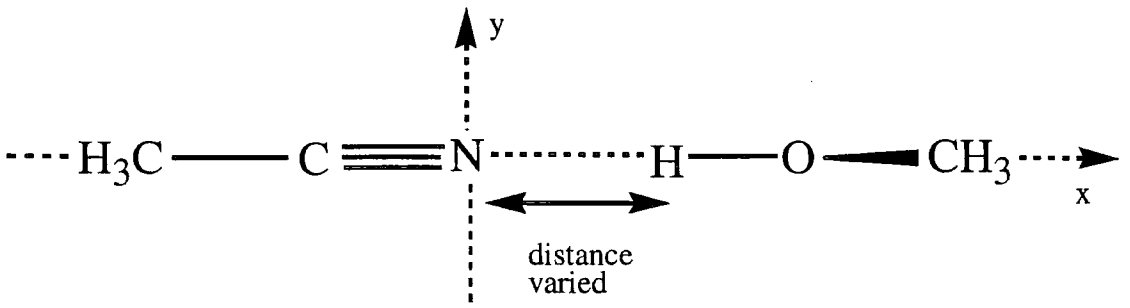

Figure 13.12 - Position of model molecules relative to reference axis

The methanol was oriented with the O-H group lying along the x axis and the CH_3 fragment sitting out of the plane of the C≡N group, along the z axis. The starting N --- H separation distance was 2.00 Å, this distance was increased in 0.01Å increments up to a maximum of 2.20 Å with the interaction energy calculated at every point. Results are displayed in Figure 13.13. The interaction energy reaches a clear energy minimum at 2.11Å.

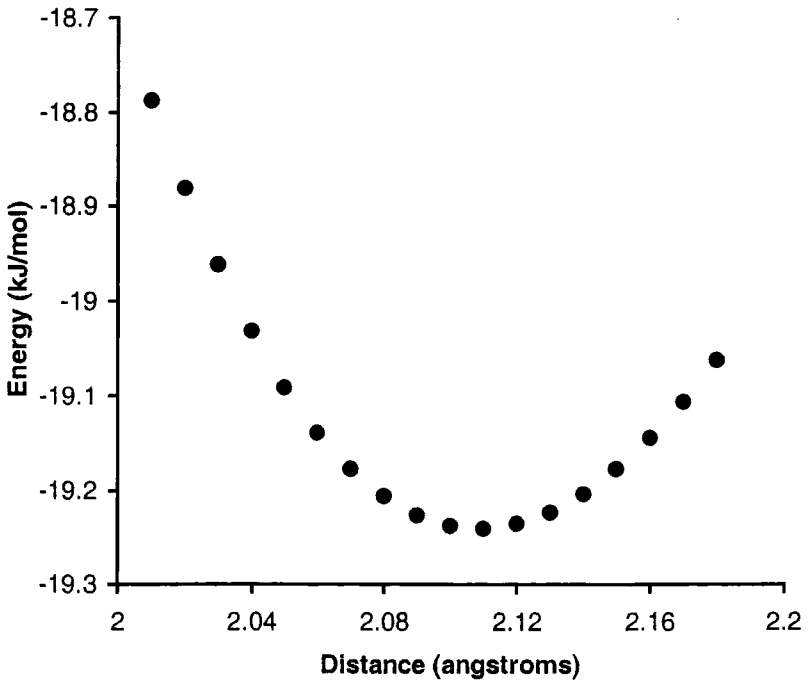

Figure 13.13 - Variation of interaction energy with N --- H separation.

The methanol molecule was then rotated about the origin, in the xy plane, to calculate the optimum angle of approach of the OH group relative to the C≡N bond. The distance between H and N was maintained at 2.11 Å. Rotation away from a linear 'end-on' approach towards the nitrogen atom has a detrimental effect on the interaction energy. There is only a slight decrease in interaction energy between a 0° and a 5° rotation. However as the rotation angle increases, the energy becomes steadily less attractive. It is clear that the region covered by a 5° angle either side of the C≡N bond vector is the optimum region for the donor group, see Figure 13.4.

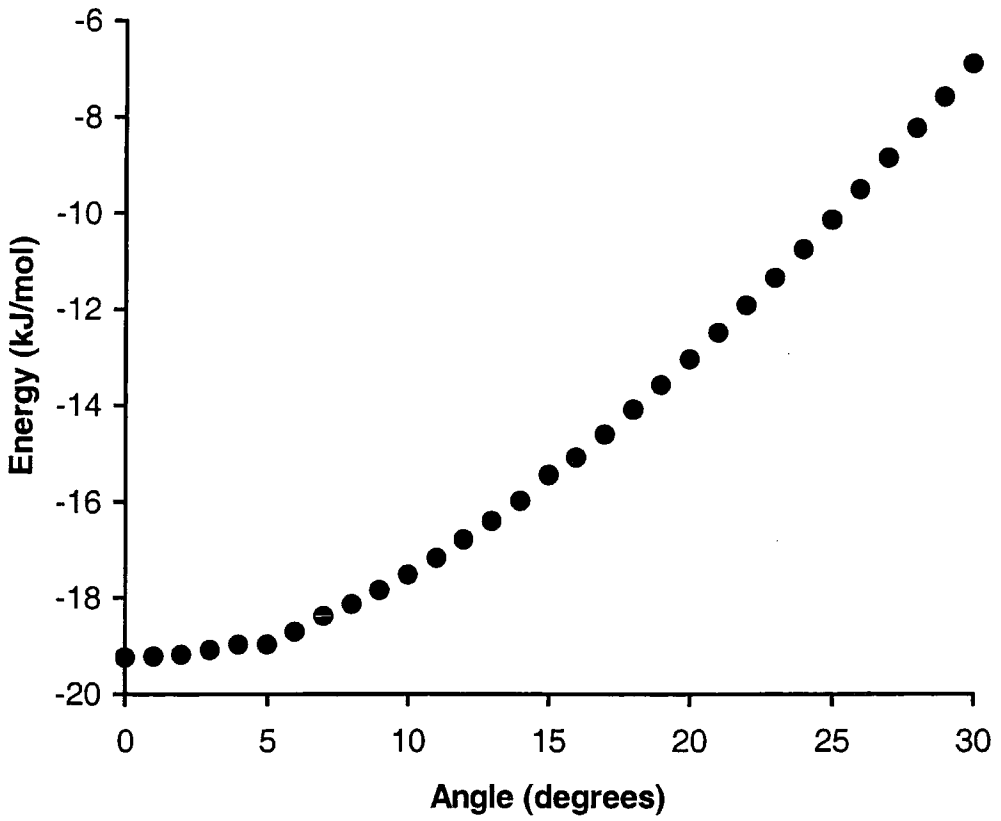

Figure 13.4 - Variation of interaction energy with angle of O-H rotation about N

13.4.2 Interactions involving C≡N

The final set of calculations was run with the O-H group aligned perpendicular to the C≡N group. The distance between H and the C≡N bond was maintained at 2.11 Å

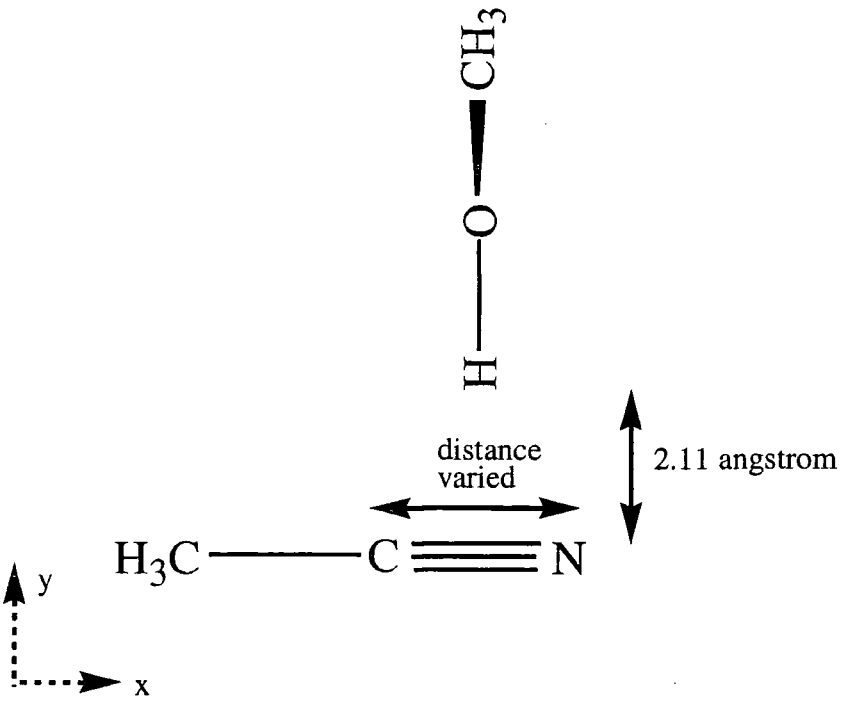

Figure 13.15 - Methanol perpendicular to C≡N bond

The methanol molecule was moved along the length of the bond from N along to C with the energy calculated at 0.1Å intervals, see Figure 13.15. The energy becomes steadily attractive as the OH is moved further from N. Half-way along the bond, the energy becomes repulsive and continues to grow more repulsive as it is moved towards the carbon atom, see Figure 13.16.

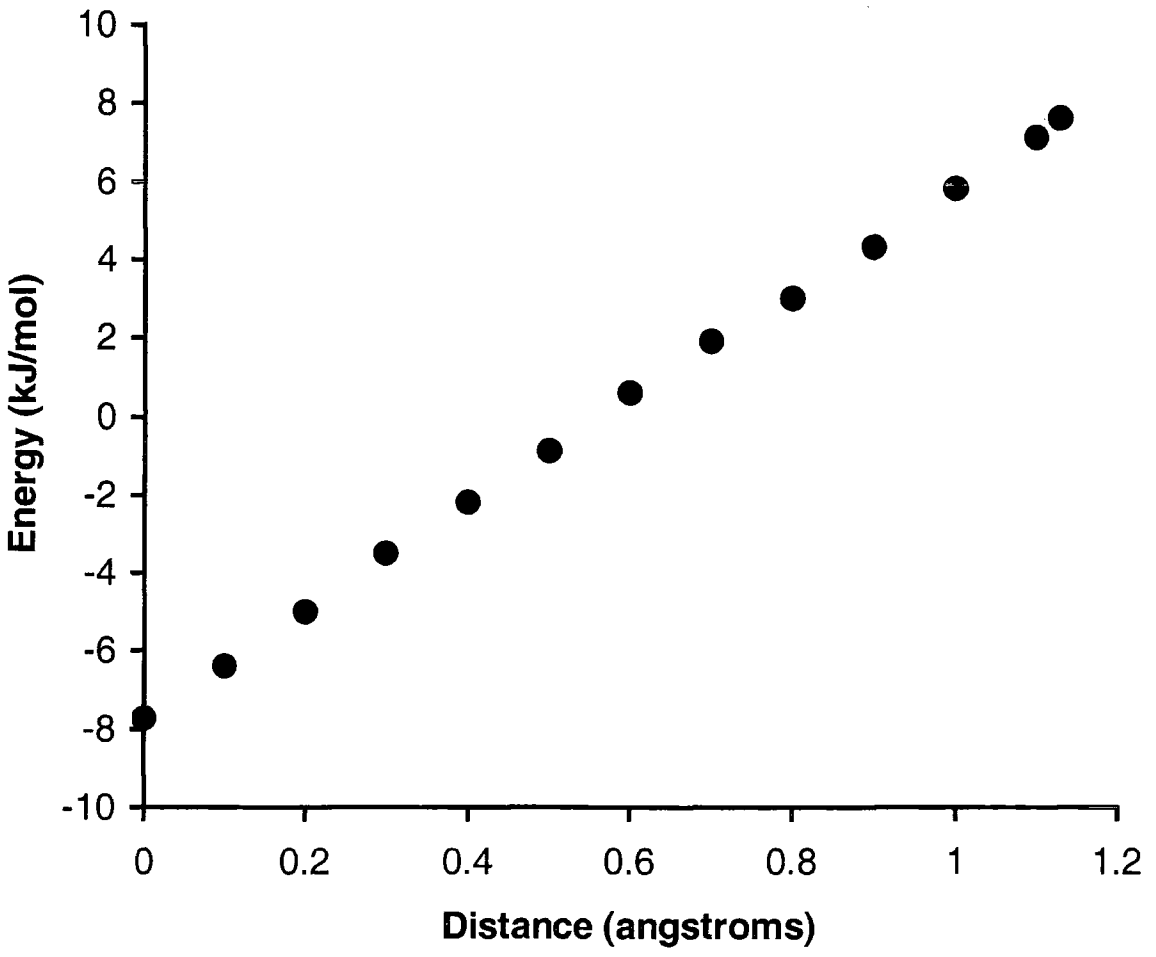

Figure 13.16 - Variation of interaction energy with distance of OH along C≡N bond. Measured from nitrogen atom.

13.5 Conclusions

In conclusion, the IMPT results show the interaction between methanol and methyl cyanide to be most attractive when the H-O group makes a linear approach to the cyanide nitrogen atom. This observation is consistent with the location of the sp lone pair at the nitrogen atom, directed away from the carbon atoms. These results agree well with the CSD analysis which showed a linear or close to linear approach to be

most favoured. The IMPT and CSD results also agree well about the optimum N --- H separation for maximum attraction. The optimum distance from IMPT results was 2.11 Å which is also the peak of the distribution of distances from the CSD search.

REFERENCES

Acker, D. S. & Blomstrom, (1962). D. C. US. Patent No. 3162641.

Britton, D., (1967). *'Perspectives in Structural Chemistry'* Vol 1. Ed. J. D. Dunitz & J. A. Ibers. Wiley, New York.

Dulmage, W., J., Lipscomb & W. N., (1951). *Acta Crystallogr.*, , **4**, 330-4.

Grundes, J. & Klaboe, P., (1970). *'The Chemistry of the Cyano Group'*. Ed. Z. Rappoport. Wiley, New York.

Harlow, R. L.& Desiraju, G. R., (1989). *J. Am. Chem. Soc.*, **111**, 6757-6764.

Hassell, O., (1958). *Mol. Phys*, **1**, 241.

Kroon, J & Kanters, J. A. (1974). *Nature (London),* 248, 667

Melby, L.R., Harder, R. J., Hertler, W. R., Mahler, W., Benson, R. E. & Mochel, W. C., (1962). *J. Am. Chem. Soc.*, **84**, 3374.

Reddy, D. S., Goud, B. S., Panneerselvam, K. & Desiraju, G. R., (1993). *J. Chem. Soc., Chem. Commun.,* 663-664.

Reddy, D. S., Panneerselvam, K., Pilati, T., & Desiraju, G. R., (1993). *J. Chem. Soc., Chem. Commun.,* 661-662.

Sarma, J. A. R. P., Dhurjati, M. S. K., Bhanuprakash K. & Ravikumar, K., (1993). *J. Am. Chem. Soc., Chem. Commun,* 440-443.

Torrance, J. B., (1979). *Acc. Chem. Res.*, **12**, 79-86.

Williams, J. M., Beno, M. A., Wang, H. H., Leung, P. C. W., Emage, T. J., Geiser, U. & Carlson, K. D., (1985). *Acc. Chem. Res.*, **18**, 261-267.

Intramolecular Hydrogen Bonding.

CHAPTER 14

14.1 Intramolecular hydrogen bonds

> ... meta- *and* para-*compounds ... differ markedly from the* ortho-*compounds (a) in being less volatile, (b) in being more miscible (in the liquid state) with water, and (c) in being less miscible with benzene ... this change depends on the simultaneous presence of two substituents of reactive character, it must be due to some interaction between them; and as we find that it occurs only in the* ortho- *position, we may conclude that it is due to ring formation.*
>
> N. V. Sidgwick & R. K. Callow, 1924.

Sidgwick and Callow (1924) commented on the possibility of ring formation between adjacent, reactive, ring substituents to explain the differing properties of *-ortho* substituted rings, in comparison with *-meta* and *-para* substituted compounds. They noted that, for phenols, when certain substituents are in the *-ortho* position, there is an abnormally large effect on their physical properties, in particular, solubility and volatility. A series of substituents were considered in the study, these were ordered in terms of the "abnormality" of the physical properties of the molecule.

$$CH_3 < Cl < Br < I < NO_2 < CO_2R < CHO < NH_2 < CO_2H < OH$$

They concluded that the hydrogen atom of the OH group of the phenol must form a "co-ordinate link" with an atom of the *-ortho* substituent and that this atom must have a lone-pair of electrons to offer. Examples of this ring formation listed were hydroxybenzoic acids, their esters and aldehydes and also nitrophenols. Ring

formation was denoted by an arrow pointing towards the atom which "receives" the lone-pair of electrons. It was suggested that favourable ring geometry would be six-membered with two conjugate double bonds. Five-membered rings were also noted but said to be less common.

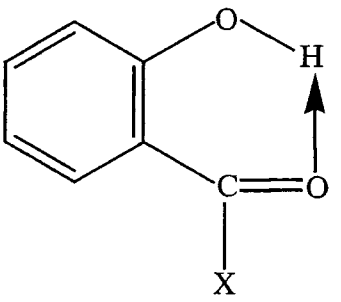

Figure 14.1 - Intramolecular ring formation as depicted by Sidwick & Callow (1924)

Using a series of molecules that were known to form intramolecular hydrogen bonds, Pimental and McClellan (1960), made observations about the formation of the interactions. They commented that the two hydrogen bonding functional groups must be ortho to each other and that O-H, N-H and C=O groups commonly participated in the ring formation. Their third comment was in relation to the size of ring formed, the rings are usually constructed using five, six or seven atoms, the exception to this is proteins.

In comparison with intermolecular hydrogen bonds, intramolecular hydrogen bonds receive far less attention in the crystallographic community. Intermolecular interactions are of widespread interest as they have a direct effect on the long-range extended molecular structure and cause readily observable effects on the physical properties of the molecule.

Prior to the development of X-ray diffraction to a sufficient level to be used for the identification of hydrogen bonds, several techniques were used to investigate intramolecular interactions. Electric moments were used by Curran (1945) to study the conformations of ortho-substituted phenols and anisoles. Curran suggested that resonance played a part in the formation of intramolecular rings. Runner, Kilpatrick and Wagner (1947), used polarography to study the restriction of tautomerism of amidines as a result of intramolecular hydrogen bonding. They commented that the formation of the intramolecular hydrogen bond removed the freedom of the proton to migrate or to participate in intermolecular hydrogen bonding. Kuln (1952) used spectroscopic methods to investigate inter- and intramolecular hydrogen bonds in alcohols. The crystal structure of maleic acid was determined in 1952 by Shahat, it was not possible to locate the hydrogen atoms but a an O --- O distance of 2.46 Å was found.

Intramolecular hydrogen bonds have now been identified in a variety of different compounds and have been studied using several different techniques. Vibrational spectroscopy was used to investigate o-hydroxybenzoyl compounds (Palomer, DePaz & Catalan, 1999). In addition, nitroresorcinols (Chung, Kwon & Kwon (1997), fluorophenol derivatives (Kovacs, Macsari & Hargittai, 1999) and carbohydrates (Luque, Lopez, de la Paz, Vicent & Orozco, 1998) were investigated using ab initio calculations, while X-ray diffraction was used to study 4,5-dicarboxyimidazoles (Harmon, Gill, Rasmussen & Hardgrove, 1999). Other sets of molecules studied include beta-ketols (Fakhraian, Cossebarbi & Doucet, 1991) and polyamides (Gung, Mackay & Zou, 1999). Some work has also been carried out into the competition

between inter- and intramolecular hydrogen bonding (Missopolinou & Panayiotou, 1998; Furlani & Garvey, 1997).

A review of the early progress into theoretical studies of intramolecular hydrogen bonds can be found in a chapter of a series of volumes covering many aspects of hydrogen bonding (Schuster, 1976). Here the distinction is made between two different 'types' of intramolecular hydrogen bonds, distinguished by their π-electron character. The first type consists of those where the donor and acceptor groups are separated by at least one sp^3 hybridised carbon atom, thus there is no possibility for π-delocalisation along the "molecular backbone". These hydrogen bonds are found to be weaker than an intermolecular hydrogen bond formed by the same functional groups. The second type of hydrogen bond is characterised by a planar π-electron system between the donor and acceptor groups. This type of hydrogen bond was found to be considerably stronger than the intermolecular equivalent. The reason given for this difference is that the charge transfer occurring in the hydrogen bond is compensated for by inverse electron flow along the π-electron system.

14.2 Supramolecular synthons

Well-defined and robust hydrogen bonded motifs which occur frequently in crystal structures can be described as 'supramolecular synthons' (Desiraju, 1995). Crystal engineering is dependant on the identification of such synthons. Classical, strong interactions such as O-H --- O or N-H --- O have been used successfully in supramolecular design and weaker interactions such as C-H --- O are increasing in application. The results from surveys of limited sets of crystal structures contained

within the Cambridge Structural Database (CSD) are often used to develop an understanding of the hydrogen bonds that constitute supramolecular synthons. Families of related compounds can also be synthesised in order to analyse hydrogen bonds and this approach is often used in conjunction with database analysis. Systematic studies are typically centred on specific hydrogen bonds or particular functional groups. While these methods are beneficial, it is difficult to make a direct comparison of the robustness of individual hydrogen bonded motifs. A study of a large range of hydrogen bonded motifs is of great value as it allows the crystal engineer to compare and contrast different motifs to find those which occur with higher probabilities, and whose incorporation into an extended structure are therefore most likely, thus generating supramolecular structures in a predictable fashion.

14.3 Classification methods : graph sets

A method exists to describe the topology of hydrogen bonded motifs systematically, that is, the graph-set approach. Most methods used to categorise hydrogen bonded motifs are based on the physical or geometric properties of the interactions (Taylor & Kennard, 1984; Murray-Rust & Glusker, 1984). The beauty of the graph-set method is that it does not simply focus on the atoms directly involved in the interaction, but can be used to describe the hydrogen bond patterns throughout the structure. The importance of the patterns produced by the formation of hydrogen bonds was first noted by Wells (1962). Wells considered molecules as single points and the hydrogen bonds connecting them as lines between these points, he used this idea to develop a scheme for classifying hydrogen bonds in inorganic structures. Hamilton and Ibers (1965) took this idea a little further by considering the number of

hydrogen bonds per point molecule and the number of hydrogen bonds emanating from the point. The connection between these classification schemes and graph theory (Harary, 1967) which is a formal mathematical method of analysing graphs and networks, was made by Kuleshova and Zorky (1980). Kuleshova and Zorky devised symbols to describe the graph sets and used the method to analyse organic polymorphs in terms of their hydrogen bonding. The graph set methodology was further developed by Etter (1990) to analyse many organic crystal structures and she used this information to develop a set of "rules" for the formation of hydrogen bonds in organic structures. The graph set notation adopted in that paper has now been extended into an accepted formalism (Etter, MacDonald & Bernstein, 1990; Bernstein, Davis, Shimoni & Chang, 1995; Bernstein & Davis, 1999). Thus:

$G_d^a(n)$ where a = number of acceptors used in the motif

d = number of donors used in the motif

n = number of atoms involved in the motif

G is the descriptor of the form of the motif, it can be one of four possibilities, C (chain), R (ring), D (dimer) or S (self = intramolecular). By their nature, all intramolecular patterns form rings.

14.4 Systematic study[#]

A systematic study of intermolecular hydrogen bonded motifs (Allen, Motherwell, Raithby, Shields & Taylor, 1999) has been carried out using the CSD (Allen & Kennard, 1993) as a data source. This list enables the crystal engineer to contrast a

variety of motifs formed by N-H or O-H donors and N or O acceptors, and ordered in terms of their probability of formation. Several factors can affect the formation of an intermolecular motif: (a) steric accessibility of donors and acceptors and (b) also stoichiometric availability of the donors and acceptors, which is affected by competition for the formation of alternative intermolecular or intramolecular hydrogen bonds. If it is possible for the donor and/or acceptor to be involved in a strong intramolecular motif, this may reduce their ability to participate in intermolecular motifs. To our knowledge, no fully systematic study has been carried out into intramolecular hydrogen bonding using X-ray diffraction data.

The work described in the remainder of this chapter describes a systematic study of intramolecular hydrogen bonding motifs, using the information contained within the CSD as a source of data. The CSD is ideal for conducting such a study as it contains structural data for a large number of crystal structures (197,481, April 1999 release) which can be searched using user-specified chemical and geometrical constraints.

Although the CSD can be used to investigate all intramolecular hydrogen bonds i.e., any donor or acceptor and any size of pattern, this study concentrated only on a restricted set of donors and acceptors and a maximum pattern size. Restrictions were made so that the patterns were only located if they contained N-H or O-H donors and N or O acceptors, that is, donor-acceptor pairings that form short hydrogen bonds, that occur frequently and are particularly robust. Thus, the work concentrated on the motifs that were most likely to be structurally significant, formed by interactions with attractive energies of > 20kJmol^{-1}.

[#] this work, and the following analysis, was carried out in conjunction with Dr. G. P. Shields, CCDC.

A modified version (IMQUEST, Shields, 1998) of the QUEST3D search program (Allen & Kennard, 1993) was used to locate intramolecular motifs. Donor-H (D-H) and acceptor (A) atoms are initially specified by the user, along with any distance and angular constraints to be used in the definition and location of suitable D-H --- A hydrogen bonds. The D-H distances were all normalised to the ideal values as derived from neutron diffraction studies (Allen, Kennard, Watson, Brammer, Orpen & Taylor, 1987). This was done in order to even out discrepancies in hydrogen atom treatment throughout the vast range of crystal structures used and to compensate for the very short D-H distances observed in X-ray work due to atomic asphericity effects (Allen, 1986). The standard distances are 1.009 and 0.983 Å for N-H and O-H respectively. The program checks each CSD entry for contacts within the specified distance limits. Once the hydrogen bond has been located, the path between the two interacting atoms is traced and the atomic path length is recorded. Symmetry equivalent motifs are rejected. The pattern is assigned a number and each subsequent pattern is cross-referenced against all previous patterns and is only assigned its own code number if it is entirely different to all others. The program produces a series of data files that can be used to analyse the results. The motifs are described in terms of an atomic sequence and bond types connecting them, from which a unique identifier is generated for the motif. This file can be post-processed to give the number of CSD entries in which the motif occurs and the total number of occurrences of the pattern. A second file lists each pattern in numeric form with CSD element code number and atomic coordination numbers, this file is created for further use by other programs. The final file of interest is a list of which motifs are found in each refcode. Additional programs are available to process the initial output files. Database subset files can be generated for each motif, containing a list of all refcodes in which the motif can be found. The

output files can also combined to generate QUEST input search query files for each motif.

14.5 Intramolecular hydrogen bond distances

Whilst intermolecular hydrogen bonds have been widely researched and reviewed in the literature, intramolecular hydrogen bonds have received comparatively little attention, so ideal interaction distances are not immediately obvious. Clearly, using the sum of the Van der Waals radii of the two atoms concerned would not be a suitable maximum distance limit for acceptance of a contact as an intramolecular hydrogen bond. Intramolecular hydrogen bonds can be typically quite short in comparison to intermolecular hydrogen bonds. Basic CSD searches were set up for each of the four donor-acceptor combinations to be considered. The following constraints were applied to each search:

- D-H --- A distance 1.0 to 3.5 Å.
- Organics only
- 3-D coordinates present
- No disorder
- No polymers
- Error free at 0.02 Å level
- R-factor < 0.10
- Symmetry equivalents rejected

No constraints were placed on the nature and connectivity of the defined atoms themselves. Results are shown in Table 14.1.

Table 14.1 - Search results for general intramolecular searches

	Number of refcodes	Number of fragments
O-H --- O	3075	7615
O-H --- N	899	1372
N-H --- O	2643	5745
N-H --- N	1499	3424

The distance histograms for the four searches are shown in Figures 14.2 to 14.5, each accompanied to the right by a histogram of those entries where the D-H --- A angle was greater than 90°.

In each case, the ideal distance cut-off is not immediately clear. Decisions were taken based on groupings of entries within the distance histogram and also the effect of the angular restraint on the histogram. The application of a minimum angle mostly affects the longer contact distances. It is also difficult to find a distance that is suitable for a range of oxygen atoms in different chemical environments, it is safer to err slightly on the side of generosity rather than risk losing significant interactions. The four interactions were separated into two groups on the basis of the donor group. 2.3Å was chosen as the upper limit for all interactions involving O-H donors. A slightly longer limit of 2.35Å was selected for the N-H donors as these donors are weaker then the O-H donors and so the hydrogen bonds formed are likely to be a little longer on average.

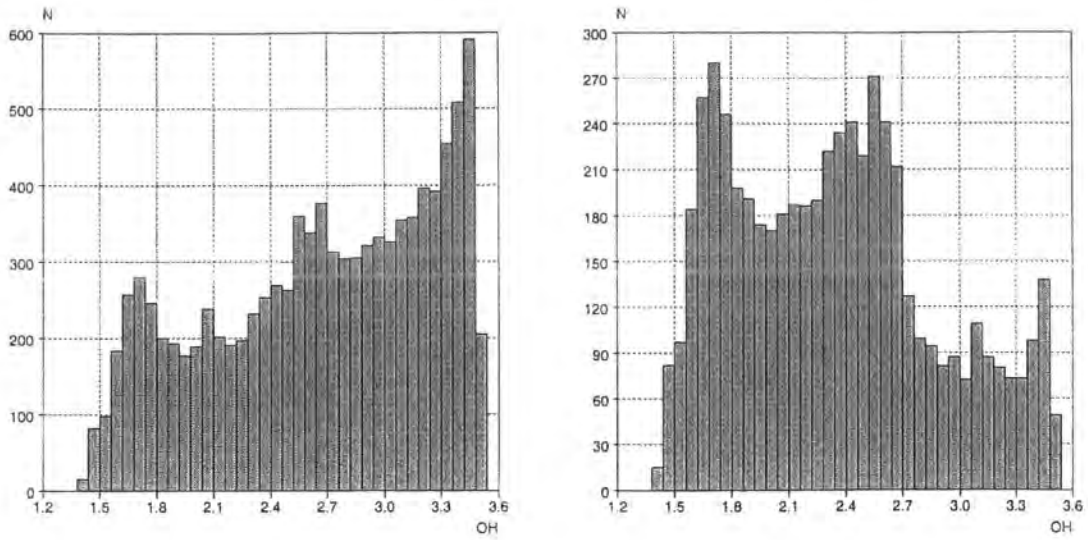

Figure 14.2 - O-H --- O contacts in the CSD. All contacts on the left, restriction of O-H --- O angle > 90° applied on the right.

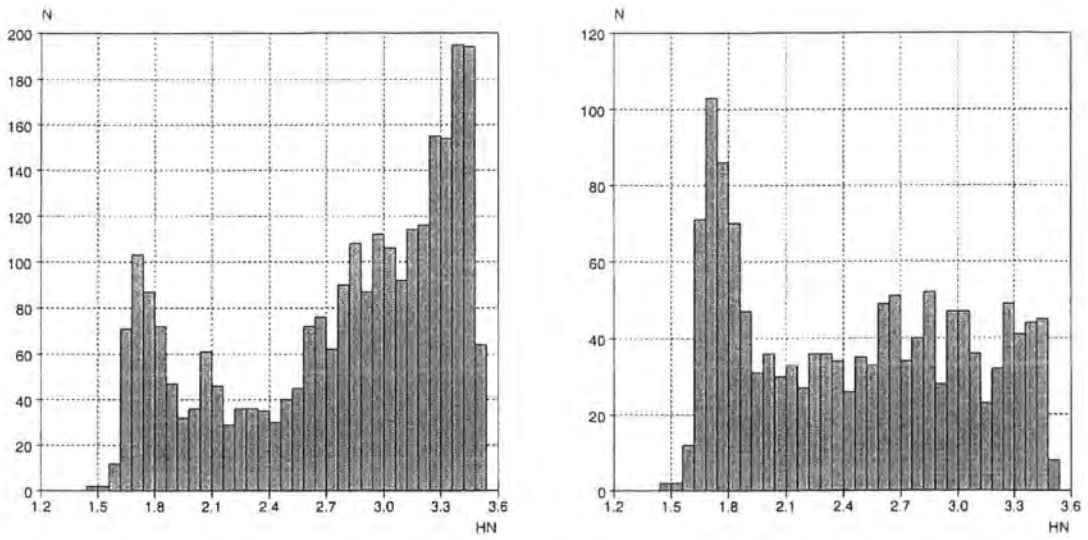

Figure 14.3 - O-H --- N contacts in the CSD. All contacts on the left, restriction of O-H --- N angle > 90° applied on the right.

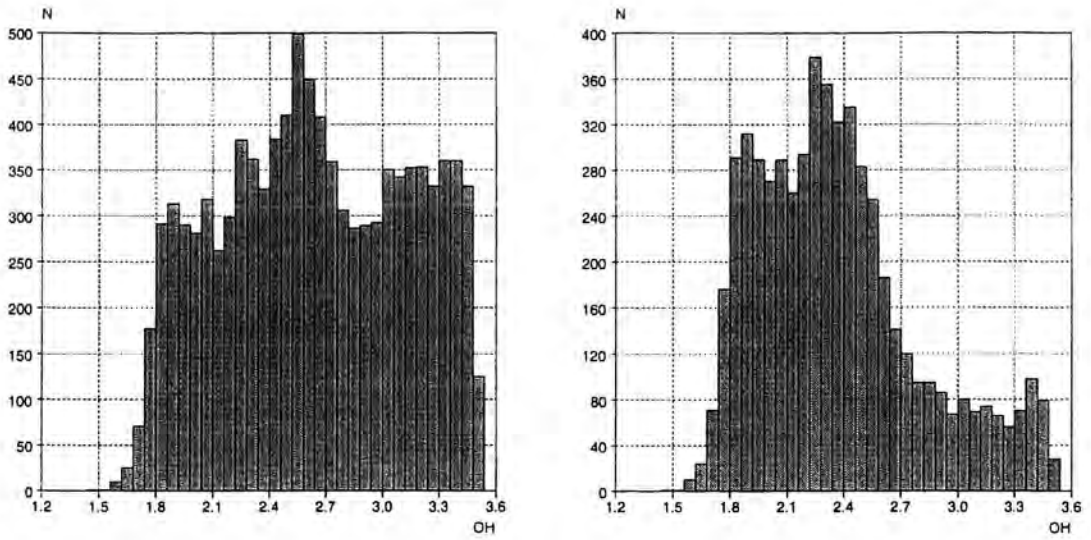

Figure 14.4 - N-H --- O contacts in the CSD. All contacts on the left, restriction of N-H --- O angle > 90° applied on the right.

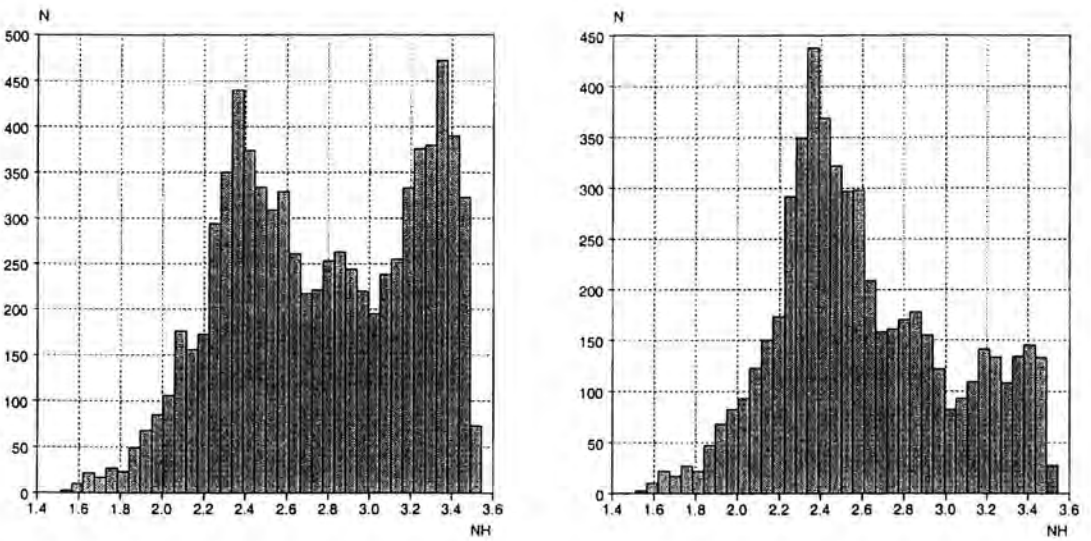

Figure 14.5 - N-H --- N contacts in the CSD. All contacts on the left, restriction of N-H --- N angle > 90° applied on the right.

14.6 IMQUEST search

The CSD search using the IMQUEST program was carried out using the following search constraints:

- Atom coordinates field present
- Chemical and crystallographic connectivity perfectly matched
- Error free at 0.02Å level
- C, N, O, H, D, S, P, Cl, Br, F, I accepted, all other elements rejected.
- No polymers
- R-factor <0.10
- Duplicate refcodes rejected
- O-H and N-H distances normalised to standard values
- O/N-H --- O/N angle >75°
- O-H --- O/N distance minimum 1.0Å, maximum 2.30Å
- N-H --- O/N distance minimum 1.0Å, maximum 2.35Å
- Path length around ring from H to O/N ranges from 4 to 10 atoms.

As IMQUEST makes no assumptions about the motifs located, other than that they satisfy the chemical and statistical constraints and also the simple geometrical constraints placed upon the spatial relationship of the donor-H and acceptor atoms, some of the motifs found are geometrically unrealistic. Figure 14.6 illustrates the affect on the geometry of the motif when the two torsion angles which are determined by the geometry of the bulk of the molecule itself are allowed to vary to extremes.

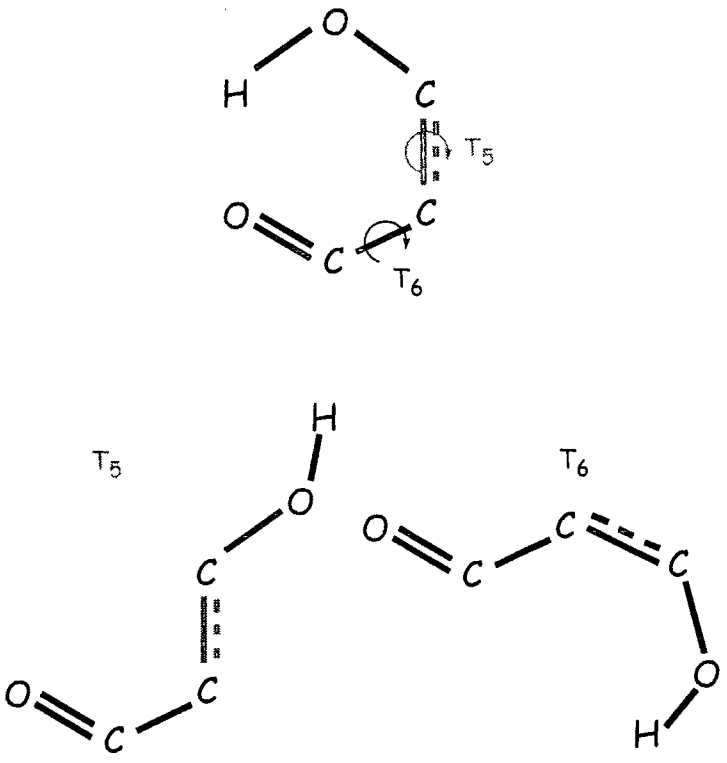

Figure 14.6 - Effect of unrestrained torsion angles

When T_5 and T_6 are greater then 90° it becomes impossible for the donor and acceptor to interact. Inclusion of such situations will lower the number of motifs formed relative to the number expected, when the donors and acceptors are free to interact and so will produce an artificial statistical result. In order to remove all geometrically unrealistic situations, motifs were only accepted if the torsion angles about cyclic and acyclic unsaturated bonds and cyclic single bonds between two sp^2 centres fell in the range $-90° < T < +90°$

14.7 Probability of motif formation

The difficulty when making a general survey of a limited set of data (however large) is determining a means of providing an unbiased comparison between individual

results. The problem is that although the CSD is now a vast resource of crystallographic data for a diverse range of structures, there are some inherent biases within the database. The database does not contain an even proportion of individual families of structures, the relative proportions are determined by the chemists and crystallographers who generate the data sets. For example, there may be a huge interest in a particular structural family due to its interesting properties and so there will be many examples of related structures, in contrast, there may be only one or two examples of other structural families as they may pose no continuing interest to their original investigator. The result is that the motifs cannot be compared fairly in terms of their occurrence alone, as the number of occurrences of individual motifs varies widely. One cannot comment on the robustness of a motif purely because it has the largest number of occurrences. To compare the motifs on a more even basis, the probability of formation of each motif has to be established, that is, the number of occurrences relative to the number of times the motif *could* be formed. The probability of formation of a particular motif (Pm) is defined as:

$$Pm = \frac{Nobs}{Nposs}$$

where Nobs is the total number of motifs that actually occur and Nposs is the total number of motifs that *could* have occurred (i.e., where the correct atomic arrangement exists to enable formation of the motif). A structural probability can also be found (Ps) with probabilities based on the number of structures rather than numbers of fragments:

$$Ps = \frac{Sobs}{Sposs}$$

where Sobs is the number of structures in which the motif is found and Sposs is the number of structures in which the motif *could* form.

The IMQUEST program produces Nobs and Sobs for each motif, however, further CSD searches are needed to establish Nposs and Sposs. A QUEST search was run for each motif, the search being conducted with the same constraints as the IMQUEST search, aside from the distance restriction between donor-H and the acceptor. Thus, these CSD searches gave the number of instances where the atomic arrangement was such that the motif could form. Pm and Ps could then be calculated and the motifs ordered in terms of their probabilities of formation.

14.8 Results

The list of the top 50 motifs is given in Table 14.2, the list is ordered by probability of formation Pm. The top 50 motifs are also listed in Table 14.3, in order of Nobs, their raw occurrence; values of Nobs, Nposs, Pm, Sobs, Sposs and Ps are also given. Note the lack of correlation between motif occurrence and motif probability. The motifs are also shown pictorially in Figure 14.7.

Key to motif bond description:

--	single bond	==	double bond
c	cyclic bond	()	aromatic bond

Tn total coordination number of that atom

Motif Number	Pm	Ps	Motif
1	100	100	H--N--N==C c-C==O
2	98.9	98.5	H--N--C==C--C==O
3	97.7	97.2	H--N--C==C c-C==O
4	97.6	97.0	H--O--C c=C c-C==O
5	97.3	97.1	H--O--C ()C c-C==O
6	97.1	98.0	H--O--C==C--C==O
7	95.1	93.6	H--N--C ()C--N==O
8	94.8	93.6	H--O--C ()C--C==N
9	93.7	91.7	H--N--C ()C--C==O
10	90.8	91.0	H--O--C c=C--C==O
11	88.0	88.1	H--N--C c=C--C==O
12	86.0	83.8	H--O--C ()C--C==O
13	79.2	76.8	H--N--C ()C--O
14	76.3	74.4	H--O--C ()C--N==O
15	73.2	70.1	H--N--C--C--O
16	70.0	82.8	H--N--C--N--N
17	67.1	89.1	H--O--C ()C c-C c-C ()C--O
18	62.1	65.5	H--N--C--C ()C--O
19	60.6	93.6	H--N c-C c-C c=C c-N
20	57.8	87.8	H--N c-C c=C c-C c=N
21	56.3	61.9	H--N--C--C--N--C--C--N--C==O
22	56.1	56.7	H--N--N==C--C==O
23	55.0	55.4	H--N c-C--C==O
24	54.2	54.7	H--O--C c-C==O
25	53.6	63.1	H--N--C--C--N--C--C--N--C==O
26	51.5	56.9	H--N--C c-C==O
27	40.6	69.8	H--N--C--N--C==O
28	39.7	33.7	H--N--C--C==O
29	37.9	54.5	H--O--C ()C--O
30	35.9	64.8	H--O--C--C c-C--C--O
31	26.8	30.2	H--O--C c-C--O--C c-O
32	23.4	28.8	H--O--C--C==O
33	22.2	24.3	H--O--C c-C==O
34	22.2	31.1	H--N--C--C--N
35	20.0	20.7	H--O--C c-C--C==O
36	19.1	22.2	H--N--C--C c-N
37	19.0	48.5	H--N c-C c-C c-N c-C c-C c-N c-C==O
38	16.9	14.6	H--N--C--C--O
39	14.4	16.3	H--N--C--C==O
40	12.7	17.5	H--N c-C c-C c-N
41	8.9	10.0	H--O--C--C--C==O
42	8.7	14.5	H--N--C--C==O
43	7.6	16.9	H--O--C c-C c-C--O
44	7.4	8.2	H--O--C c-C c-C==O
45	7.2	16.7	H--O--C c-C--O
46	5.2	15.2	H--O--C--C--C--O
47	2.8	6.4	H--O--C--C--O
48	2.5	3.5	H--O--C c-C c-C c-C--O
49	2.4	3.5	H--O--C c-C c-O
50	2.4	3.5	H--O--C c-C c-C c-O

Table 14.2 - Top 50 motifs, ordered on Pm

Motif Number	Nobs	Nposs	*Pm*	Sobs	Sposs	Ps
5	287	295	*97.3*	199	205	97.1
12	259	301	*86.0*	186	222	83.8
45	239	3323	*7.2*	206	1230	16.7
7	235	247	*95.1*	147	157	93.6
29	228	602	*37.9*	165	303	54.5
34	212	956	*22.2*	147	473	31.1
25	199	371	*53.6*	99	157	63.1
43	155	2031	*7.6*	133	786	16.9
42	147	1688	*8.7*	123	849	14.5
8	147	155	*94.8*	102	109	93.6
32	143	611	*23.4*	122	423	28.8
20	126	218	*57.8*	86	98	87.8
19	126	208	*60.6*	88	94	93.6
16	119	149	*70.0*	101	122	82.8
9	118	126	*93.7*	77	84	91.7
33	114	514	*22.2*	106	436	24.3
17	106	158	*67.1*	41	46	89.1
24	97	179	*54.2*	75	137	54.7
39	96	666	*14.4*	82	503	16.3
40	92	725	*12.7*	65	372	17.5
10	89	98	*90.8*	71	78	91.0
2	86	87	*98.9*	67	68	98.5
15	71	97	*73.2*	54	77	70.1
6	67	69	*97.1*	50	51	98.0
11	66	75	*88.0*	59	67	88.1
49	65	2758	*2.4*	52	1502	3.5
37	65	343	*19.0*	49	101	48.5
30	61	170	*35.9*	46	71	64.8
13	61	77	*79.2*	43	56	76.8
18	59	95	*62.1*	55	84	65.5
50	58	2420	*2.4*	52	1467	3.5
28	58	146	*39.7*	33	98	33.7
38	52	307	*16.9*	33	226	14.6
14	45	59	*76.3*	32	43	74.4
41	44	497	*8.9*	35	350	10.0
3	43	44	*97.7*	35	36	97.2
1	42	42	*100*	37	37	100
36	40	209	*19.1*	35	158	22.2
21	40	71	*56.3*	39	63	61.9
4	40	41	*97.6*	32	33	97.0
47	38	1378	*2.8*	35	547	6.4
46	38	732	*5.2*	34	224	15.2
31	38	142	*26.8*	29	96	30.2
22	37	66	*56.1*	34	60	56.7
48	35	1410	*2.5*	25	724	3.5
44	35	473	*7.4*	33	403	8.2
35	35	175	*20.0*	30	145	20.7
26	34	66	*51.5*	33	58	56.9
23	33	60	*55.0*	31	56	55.4
27	28	69	*40.6*	30	43	69.8

Table 14.3 - Top 50 motifs, given in order to total number of occurrences

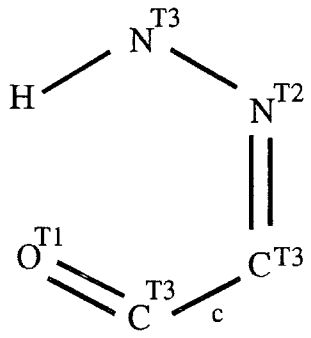

motif 1

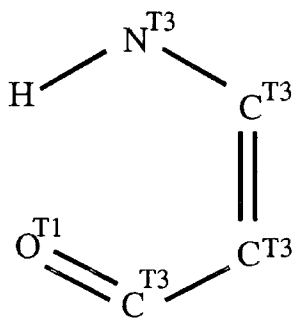

motif 2

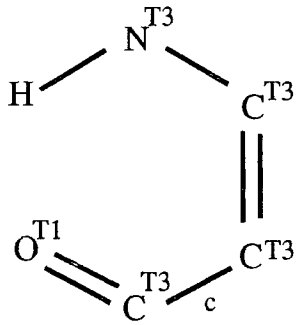

motif 3

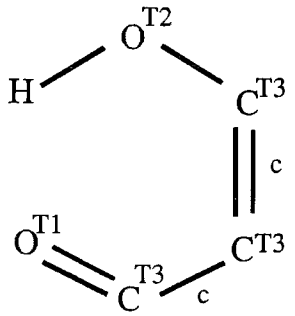

motif 4

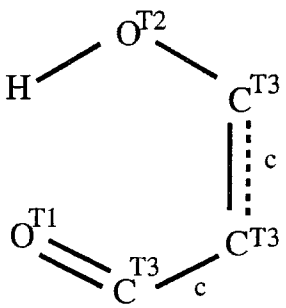

motif 5

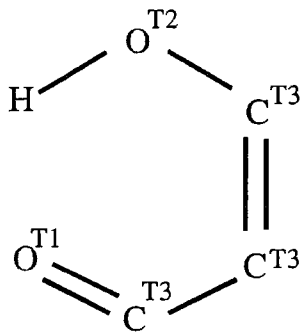

motif 6

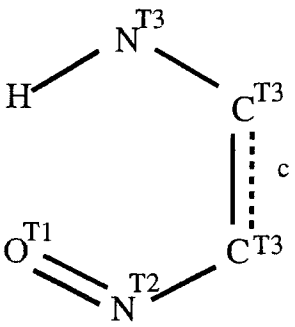

motif 7

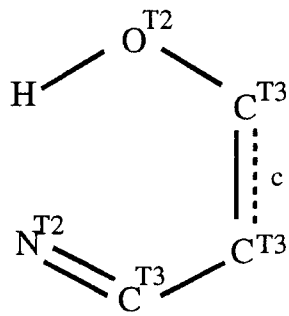

motif 8

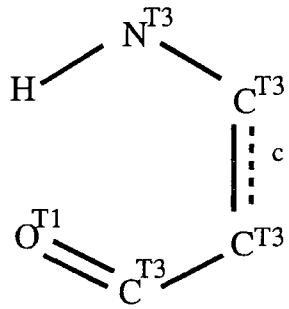

motif 9

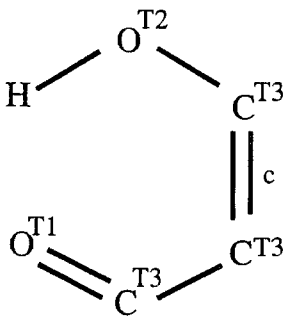

motif 10

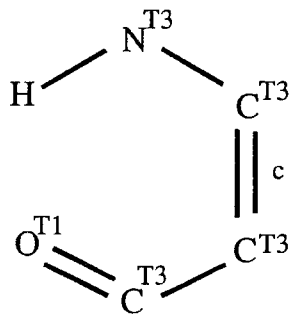

motif 11

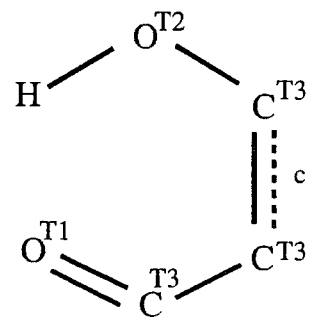

motif 12

Figure 14.7 - Motifs **1** to **50**

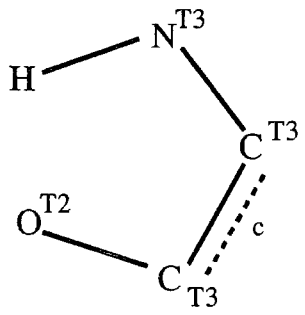

motif 13

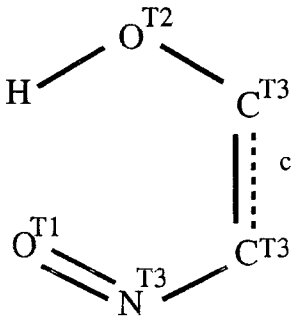

motif 14

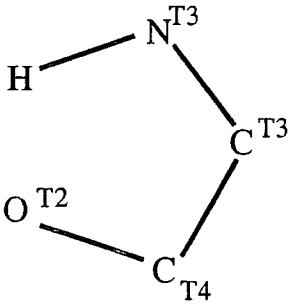

motif 15

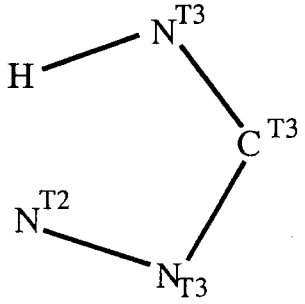

motif 16

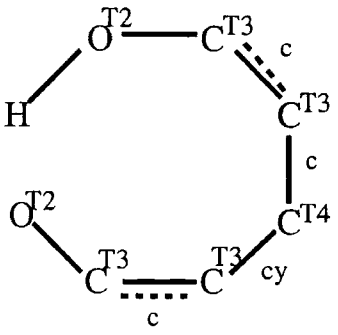

motif 17

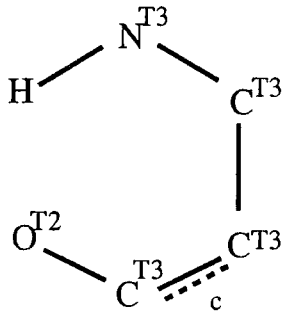

motif 18

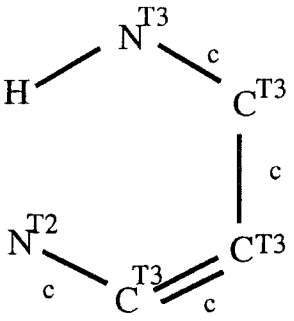

motif 19

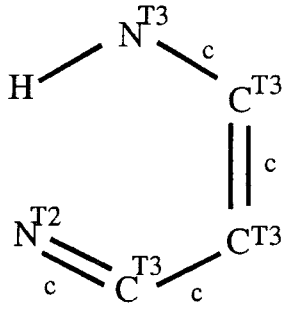

motif 20

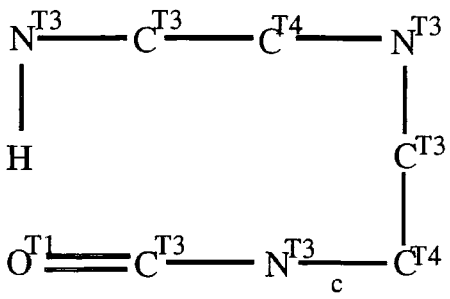

motif 21

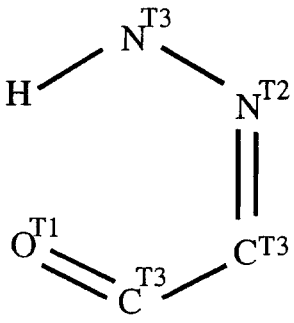

motif 22

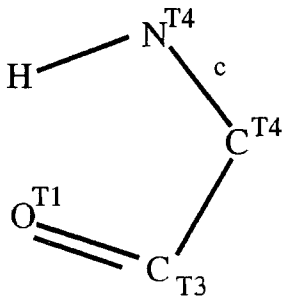

motif 23

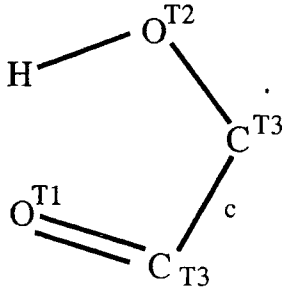

motif 24

Figure 14.7 - Motifs **1** to **50**, continued

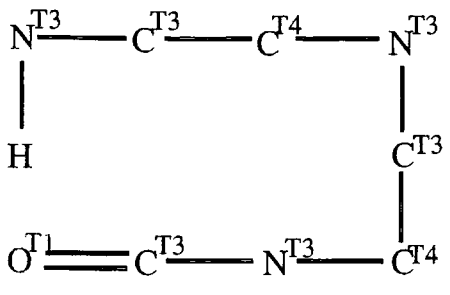

motif 25

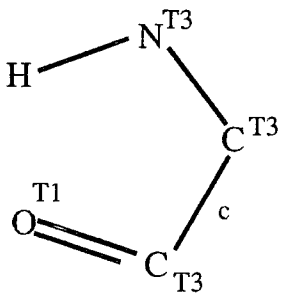

motif 26

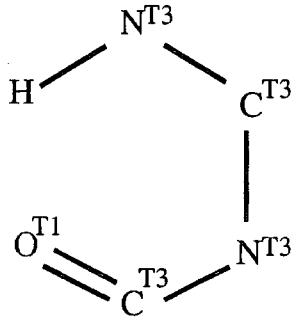

motif 27

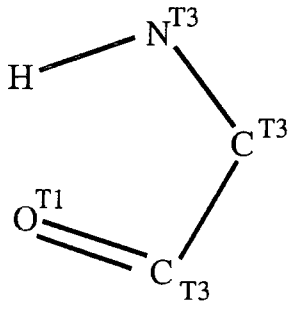

motif 28

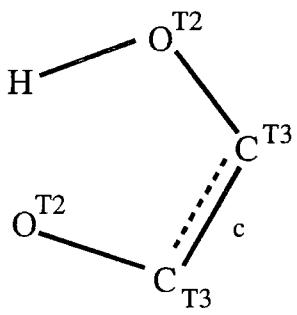

motif 29

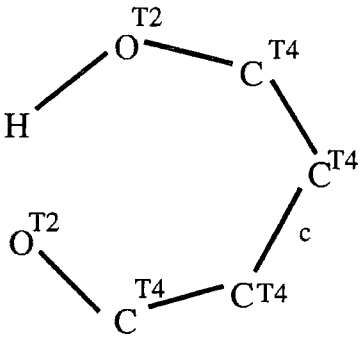

motif 30

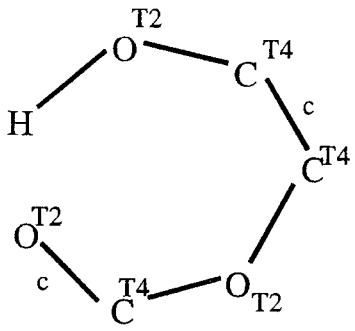

motif 31

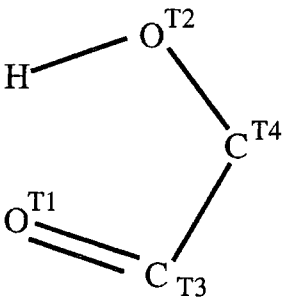

motif 32

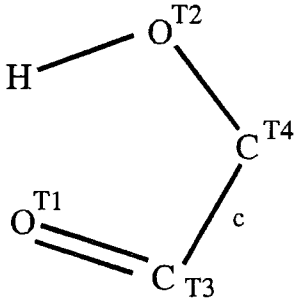

motif 33

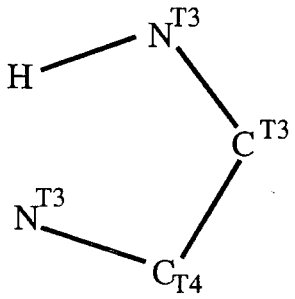

motif 34

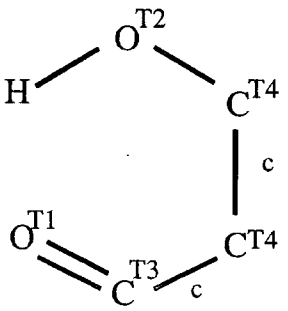

motif 35

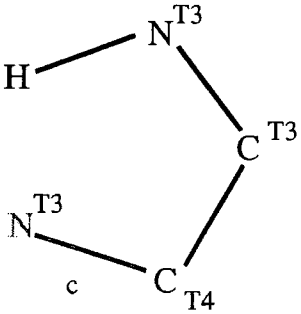

motif 36

Figure 14.7 - Motifs **1** to **50**, continued

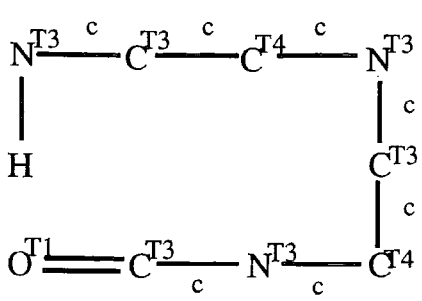
motif 37

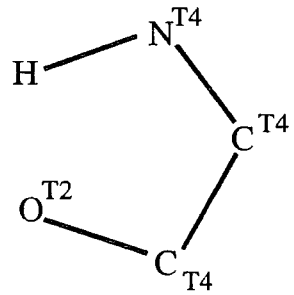
motif 38

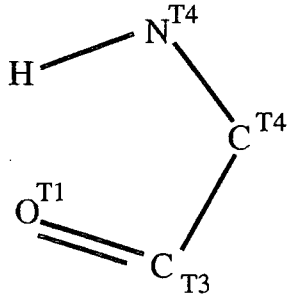
motif 39

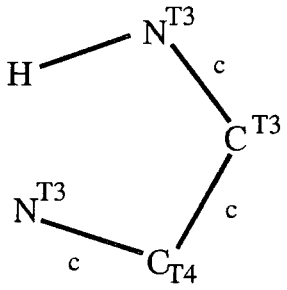
motif 40

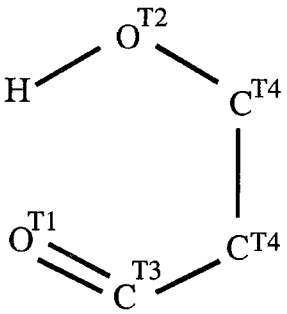
motif 41

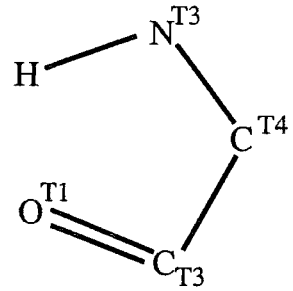
motif 42

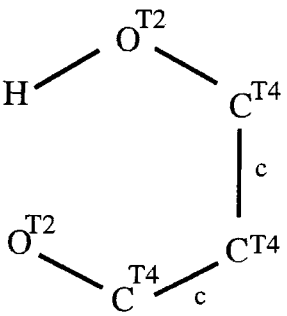
motif 43

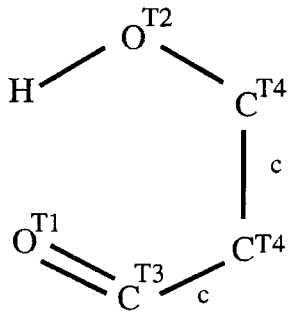
motif 44

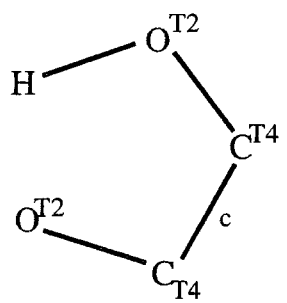
motif 45

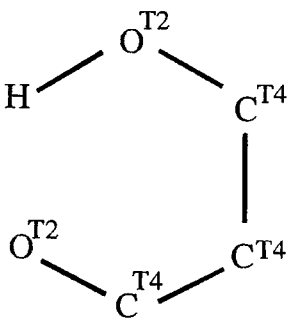
motif 46

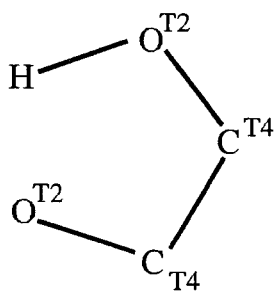
motif 47

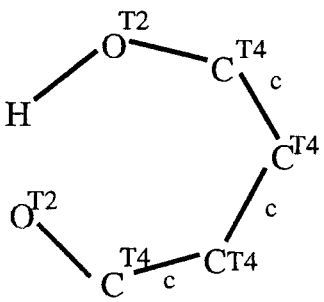
motif 48

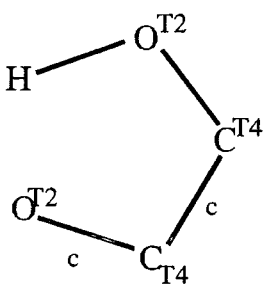
motif 49

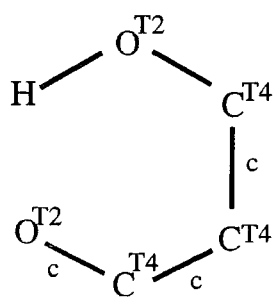
motif 50

Figure 14.7 - Motifs **1** to **50**, continued

14.8.1 Comparison of low and high probability motifs

Histograms of the H --- A distances clearly illustrate the difference between high and low probability motifs. The groupings of contacts in the histograms of the top two most probable motifs, **1** and **2**, have similar patterns, see Figures 14.8 and 14.9 for Pm 100% and Pm 98.9% respectively. The bulk of the contacts are below the defined cut-off limit (verifying that the choice was suitable), the next shortest contact is far longer, the group of significant contacts is clear and well-defined. The longer contacts in each case are between the second hydrogen atom of NH_2 donor groups and the acceptor atom. In contrast, the distinction between short, significant, contacts is far less clear for the lower probability motifs. Figure 14.10 shows the histogram of contacts for the fortieth most probable motif, **40**, at 12.7%. Although there is a peak of contacts at short distances, they are longer than the shortest groupings in the other two graphs. The tail-end of the shortest peak is 'smeared-out' to longer distance, there is no definite distinction between hydrogen bonds and distances which result purely from the configuration of the molecule.

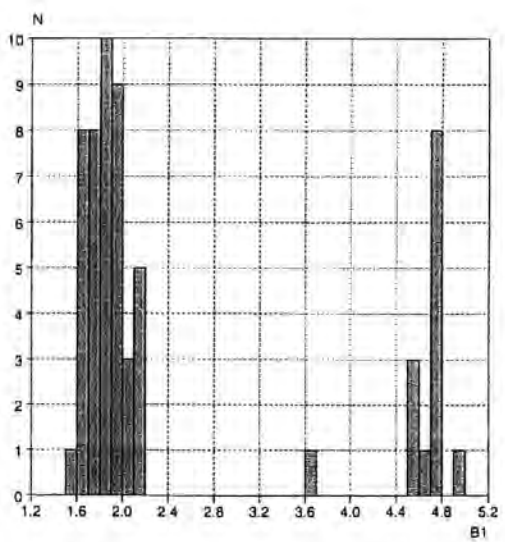

Figure 14.8 - Histogram of contact distances for motif **1**

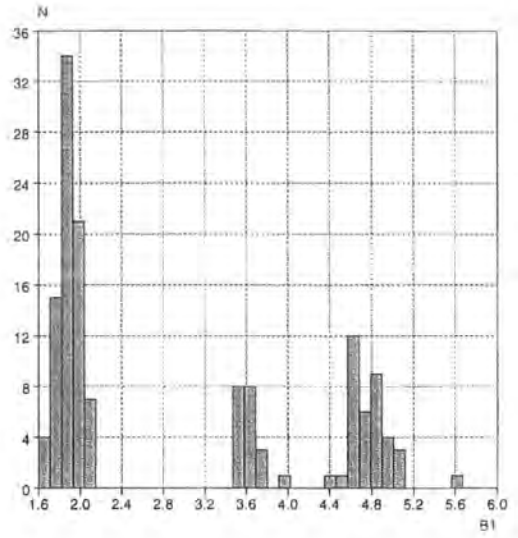

Figure 14.9 - Histogram of contact distances for motif **2**

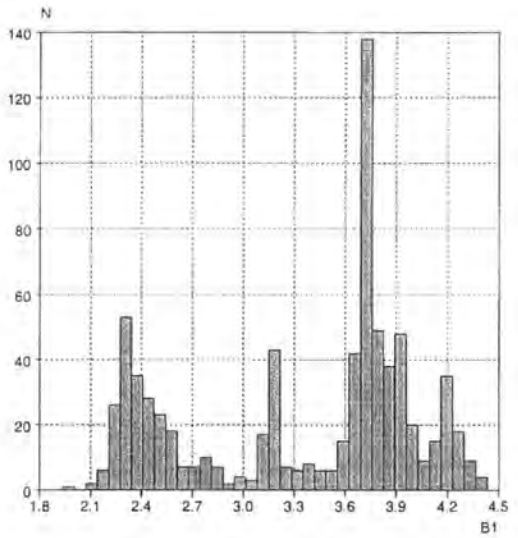

Figure 14.10 - Histogram of contact distances for motif **40**

14.8.2 Robustness of strong motifs

The most probable motif, **1**, occurs in 100% of possible structures. The second, third and fourth most probable motifs each form in every possible structure except one. However, in all three instances, either the donor, the acceptor, or both, are involved in

the formation of alternative ring motifs. Figures 14.11, 14.12 and 14.13 show the alternative intramolecular motifs that are formed instead of motifs **2**, **3**, and **4** respectively. The atoms which would be involved in the expected motif are highlighted with circles. The alternative intramolecular motifs formed are illustrated by hashed lines.

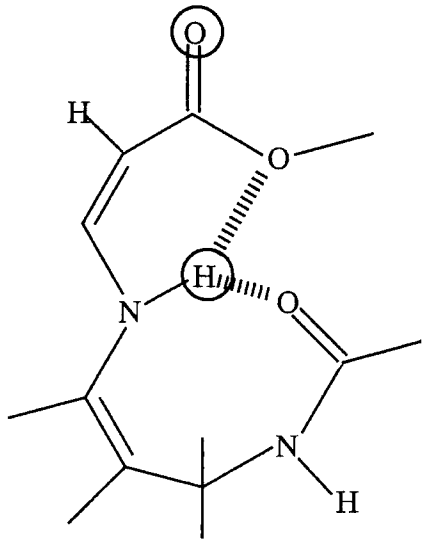

Figure 14.11 - Alternative hydrogen bonding to motif **2**

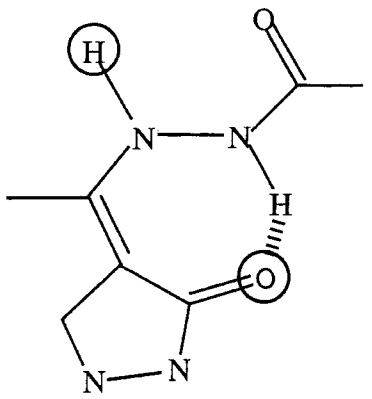

Figure 14.12 - Alternative hydrogen bonding to motif **3**

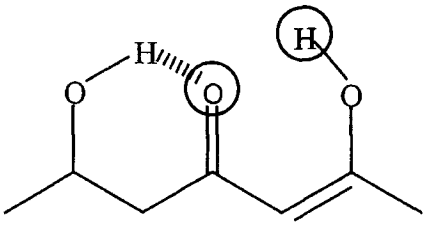

Figure 14.13 - Alternative hydrogen bonding to motif **4**

14.8.3 Benefit of cyclic bonds

The presence of a cyclic bond in the 'backbone' i.e., section of the motif not directly involved in the intramolecular hydrogen bond, aids motif formation by reducing the conformational flexibility of the molecule. A cyclic bond fixes part of the motif so that it cannot twist away from the remainder of the atoms in the motif. The ideal geometry for a motif is for the whole ring to be as close to planar as possible, the strongest motifs deviate from planarity by no more than a few degrees. Cyclic bonds reduce the potential for the section of the molecule to flex away from planarity. The difference is illustrated by comparison of motifs **1** and **22**. The only difference between the two motifs is a cyclic bond adjacent to the donor O=C bond. The probability of formation , Pm, for motif **1** is 100%, whereas that of motif **22** is only 56.1%.

14.8.4 Resonance assistance

β-diketones, in the enol form, participate in intramolecular O-H --- O hydrogen bonds. When these hydrogen bonds are formed, the π-conjugated system is found to be

partially delocalised. The effect of hydrogen bond formation in the perturbation of the lengths of the bonds involved in the intramolecular ring fragment has been investigated and a model proposed to explain this phenomenon, resonance assistance hydrogen bonding, RAHB (Gilli, Bellucci, Ferretti & Bertolasi, 1989). The RAHB model is shown schematically in Figure 14.14.

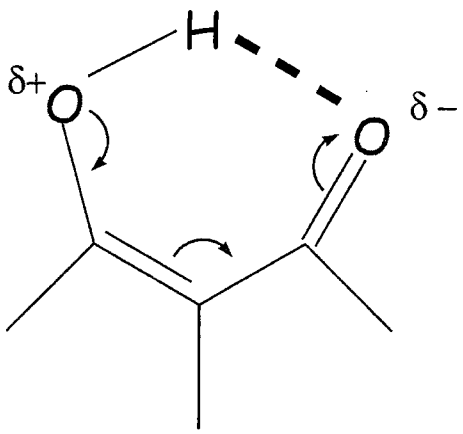

Figure 14.14 - Schematic representation of resonance assisted hydrogen bonding

The model involves transfer of partial charge around the ring from one oxygen atom to the other. Zero partial charges on the two oxygen atoms are maintained by a shift of the proton towards the oxygen atom with the negative partial charge. This proton shift is a strengthening of the hydrogen bond. The RAHB model can also be considered in terms of the lone pairs of the oxygen atoms. The out-of-plane lone pair (π) is donated from the hydroxyl oxygen atom to the carbonyl oxygen atom which results in resonance around the ring. Due to the π-system resonance, the carbonyl oxygen atom is less electronegative and so the energy of the in-plane lone pair (π') is increased. As it is the π' lone pair donation to the carbonyl oxygen atom that forms the hydrogen bond, the interaction is stronger.

Inspection of the list of the top 50 most probable intramolecular ring motifs in Figure 14.7 reveals the importance of resonance assistance in the formation of strong, robust, intramolecular ring motifs. In order to take advantage of resonance assistance, the central bond (between the middle two atoms in the ring) must have pi-electron character, a double bond or be part of an aromatic system. Motifs **1** to **12**, along with **14**, **20** and **22** all fit the resonance assistance definition. The observation that the top 12 most probable motifs, which are all found in over 85% of cases are resonance assisted, shows the beneficial effect of the ability to assist the formation of an intramolecular hydrogen bond by π-system resonance.

14.8.5 Generic motifs

Generic patterns can be identified from the list of top 50 motifs, six-membered and five-membered motifs are common. There are two major geometric patterns based on six-membered and five membered rings, all have C=O acceptors. Results are shown in Figures 14.15 and 14.16 and Tables 14.4 to 14.7.

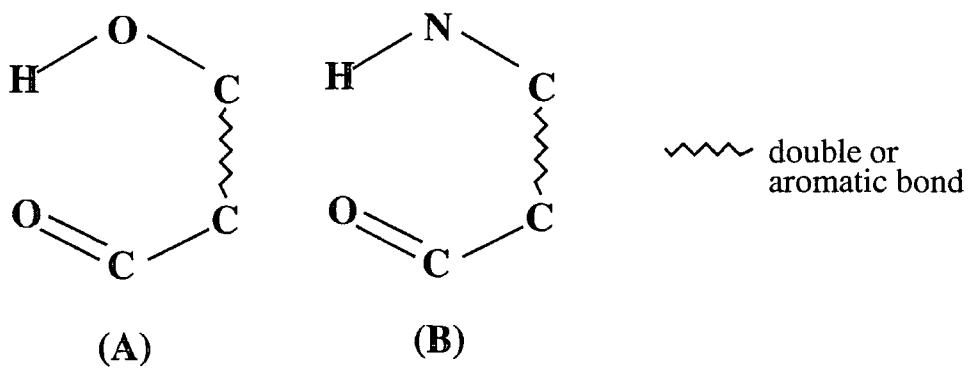

Figure 14.15 - Generic patterns (A) and (B)

Generic pattern (A)	
Motif	Pm
4	97.6
5	97.3
6	97.1
10	90.8
12	86.0

Table 14.4 - Generic pattern (A)

Generic pattern (B)	
Motif	Pm
2	98.9
3	97.2
9	93.7
11	88.0

Table 14.5 - Generic pattern (B)

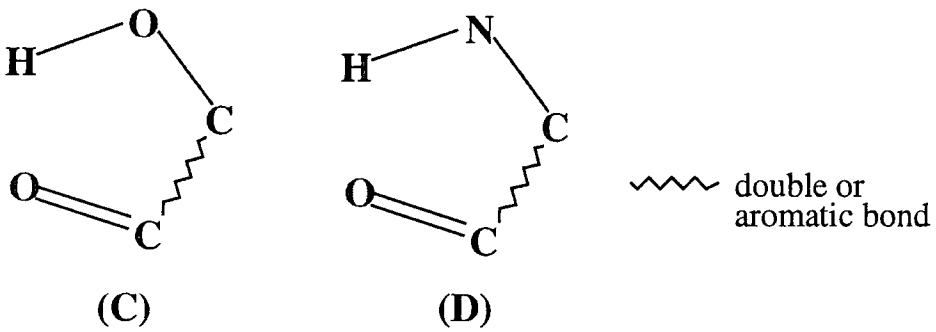

Figure 14.16 - Generic patterns (C) and (D)

Generic pattern (C)	
Motif	Pm
24	54.2
32	23.4
33	22.2

Table 14.6 - Generic pattern (C)

Generic pattern (D)	
Motif	Pm
23	55.0
26	51.5
28	39.7
39	14.4
42	8.7

Table 14.7 - Generic pattern (D)

When separated into generic groups, the distinction between five- and six-membered motifs is clear. The six-membered motifs have a higher probability of formation than the five-membered, however, no distinction can be made between the O-H and N-H donors on a probability criterion.

14.8.6 Comparison with intermolecular motifs

Possibly the most striking result of this analysis is the number of motifs with a high probability of formation, Pm. Twenty-six motifs have Pm over 50% and the top 10 motifs have probabilities over 90%. This is quite a contrast to the study of intermolecular motifs (Allen, Motherwell, Raithby, Shields & Taylor, 1999) where the probabilities were calculated in an analogous manner and so they can be compared directly. The intermolecular study found only two motifs with Pm over 90% and eight with Pm over 50%. One can draw the conclusion that intermolecular ring motifs are far less robust and predictable than intramolecular motifs. However, this difference could be explained by the increased competition for strong donors and acceptors in the intermolecular situation.

14.9 Bifurcation

Crystal engineering is concerned with the use of molecular fragments to construct robust, reproducible synthons. When considering the hydrogen bonds that might be formed by a particular molecule, one must consider the competition effects between

possible intermolecular interactions. It is usually assumed that all donors and acceptors are free to participate in intermolecular hydrogen bonds. However, if the donor or acceptor is also involved in an intramolecular interaction, does this have a detrimental effect on the formation of an intermolecular interaction? A series of CSD searches was devised to test this hypothesis. These searches are of a preliminary nature but, even so, reveal some interesting possibilities for further work.

14.9.1 Bifurcation at the donor

Motifs **5** and **12** were chosen as the model system to investigate the occurrence of bifurcation at the hydrogen atom.

TEST 1 : combined search for motifs **5** and **12** with an intramolecular hydrogen bond distance < 2.6Å. See Figure 14.17.

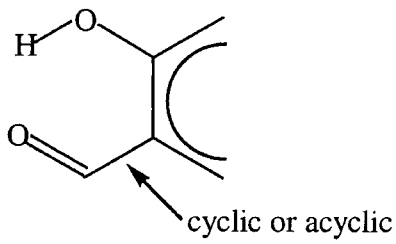

Figure 14.17 - Fragment definition, TEST 1.

TEST 2 : as TEST 1, but also requiring an additional intermolecular hydrogen bond from O-H to any nitrogen or oxygen atom, within an H --- O/N distance limit of 2.6Å. This gives the probability of formation of an intermolecular hydrogen bond, given that the hydrogen atom is involved in an intramolecular hydrogen bond.

TEST 3 : fragment search for a truncated version of the model system in Figure 14.18 but without specifically specifying the C=O acceptor group. See Figure 14.20.

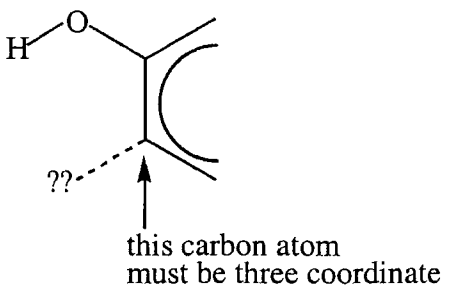

Figure 14.18 - Fragment definition, TEST 3

TEST 4 : as TEST 3 but with one intermolecular hydrogen bond from O-H to an oxygen or nitrogen atom. H --- O/N separation < 2.6Å.

TEST 5 : as TEST 4 but with two intermolecular hydrogen bonds from the hydroxyl hydrogen atom.

The results of TEST 5 provide a realistic estimate of the probability of formation of an additional intermolecular hydrogen bond, given that the hydrogen atom is already involved in one intermolecular hydrogen bond.

From the five CSD searches, the following statistics can be obtained:

3.35% of fragments that form one intermolecular hydrogen bond, form an additional intermolecular hydrogen bond.

20.0% of fragments that form one intramolecular hydrogen bond, form an additional intermolecular hydrogen bond.

29.9% of fragments form one intermolecular hydrogen bond only.

One can conclude that the formation of an intramolecular hydrogen bond does have a detrimental affect on the probability of that hydrogen atom forming an intermolecular hydrogen bond. However, bifurcation is more likely to occur if one of the hydrogen bonds formed is intramolecular rather than intermolecular.

14.9.2 Bifurcation at the acceptor

A similar series of CSD searches were performed to investigate the affect of intramolecular hydrogen bond formation on the likelihood of bifurcation at the acceptor site. The tests were carried out using the data subset as used for the donor bifurcation analysis, a combination of motifs **5** and **12**.

TEST 6 : as TEST 1 (i.e. one intramolecular hydrogen bond) but with one intermolecular hydrogen bond involving the carbonyl group and a separate donor group. C=O --- H-O/N with O --- H <2.6Å.

TEST 7 : as TEST 6 but with two intermolecular hydrogen bonds involving the carbonyl oxygen atom.

TEST 8 : fragment model for systems containing no intramolecular hydrogen bond.

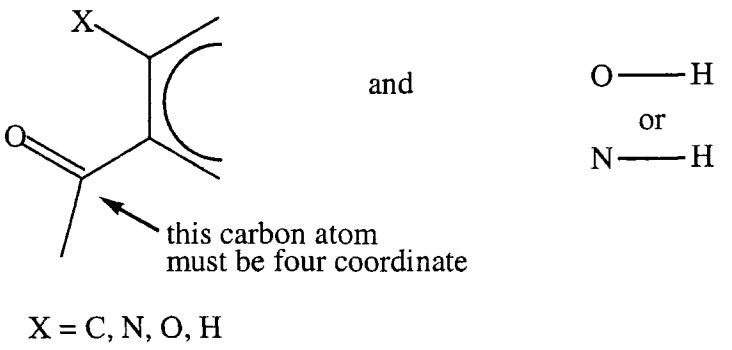

X = C, N, O, H

Figure 14.19 - Model for systems containing no intramolecular hydrogen bond

TEST 9 : as TEST 8 but with an intermolecular hydrogen bond C=O --- H-O/N with O --- H <2.6Å.

TEST 10 : as TEST 9 but with two intermolecular hydrogen bonds from the carbonyl oxygen atom.

The results of TESTS 6 and 9 and 7 and 10 can be compared to contrast the affect of the presence of an intramolecular hydrogen bond on the formation of one and two intermolecular hydrogen bonds respectively. Search statistics are as follows:

27% of fragments from one intermolecular hydrogen bond, given the presence of one intramolecular hydrogen bond.

2.8% of fragments form one intermolecular hydrogen bond, given the presence of an additional intermolecular hydrogen bond.

7.6% of fragments form one intermolecular hydrogen bond only.

The probability of formation of an intermolecular hydrogen bond is higher if the acceptor is already involved in an intramolecular hydrogen bond than if it is not. This observation is in contrast to the results of the hydrogen atom bifurcation searches. Also, bifurcation is more likely to occur if one of the hydrogen bonds formed is an intra- rather than an intermolecular interaction.

For both the acceptor and donor moieties, the probability of formation of two intermolecular hydrogen bonds is lower that that of an inter- and an intramolecular interaction. One could surmise that the formation of an intramolecular hydrogen bond makes the parties involved more 'attractive' for the participation in further interactions, but more extensive analysis is needed to substantiate this observation. Another possible explanation for these observations involves the geometry of intramolecular interactions. Intramolecular interactions tend to form at the edges of a molecule where the local geometry is more flexible. The hydrogen atoms involved are thus more likely to be free to also participate in intermolecular interactions.

14.10 Summary

Intramolecular hydrogen bonds are an integral part of the overall hydrogen bonding observed in molecular structures, but unfortunately they receive very little attention. This study has shown them to be very predictable, probably even more robust than intermolecular motifs. A series of factors have been identified which are common to the motifs which occur with high probability. The ideal motif size is a six-membered

ring, although several five-membered species were observed, they were found to have far lower probability of formation. Planarity of the ring atoms is favourable. Resonance assistance in ring formation is very important and this correlates with the high number of C=O acceptor groups observed. The formation of an intramolecular interaction has a tangible affect on the ability of the donor and acceptor to participate in intermolecular interactions. The affects on the donor and acceptor moieties are different but in both cases, an intra- and intermolecular hydrogen bond are preferable to two intermolecular hydrogen bonds. The results of this study have consequences for both crystal engineers and those involved in crystal structure prediction.

REFERENCES

Allen, F. H., (1986). *Acta Cryst., B***42,** 515-22.

Allen, F. H., Kennard, O., Watson, D. G., Brammer, L., Orpen, A. G. & Taylor, R., (1987). *J. Chem. Soc. Perkin Trans. 2*, S1.

Allen, F.H. & Kennard, O., (1993). *Chemical Design Automation News*, **8** (1), pp 1 & 31-37.

Allen, F. H, Motherwell, W. D. S., Raithby, P. R., Shields, G. P. & Taylor, R., (1999). *New J. Chem.*, 25-34.

Bernstein, J., Davis, R. E., Shimoni, L. & Chang, N-L., (1995). *Angew. Chem. Int. Engl.,* **34**, 1555-73.

Bernstein, J & Davis, R. E., (1999). *Implications of Molecular and Materials Structure for New Technologies.* Ed. J.A.K. Howard, F.H. Allen, G.P Shields, 275-290.

Chung, G., Kwon, O. & Kwon, Y., (1997). *J. Phys. Chem. A.*, **101**, 25, 4628-32.

Curran, B. C., (1945). *J. Am. Chem. Soc.*, 1835-46.

Desiraju, G. R., (1995*). Angew. Chem. Int. Ed. Engl.,* 34, 2311-2327.

Etter, M. C., (1990). *Acc. Chem. Res.*, **23**, 4, 120-6.

Etter. M. C. MacDonald, J. C. & Bernstein, J., (1990). *Acta Cryst.*, B**46**, 256-62.

Fakhraian, H., Cossebarbi, A. & Doucet, J. P., (1991). *Spec. Lett.*, **24**, 2, 243-253.

Furlani, T. R. & Garvey, J. F., (1997). *Mol. Phys.*, **92**, 3, 449-461.

Gilli, G., Bellucci, F., Ferretti, V. & Bertolasi, V., (1989). *J. Am. Chem. Soc.*, 111, **3**,1023-1028.

Gung, B. W., Mackay, J. A. & Zou, D., (1999). *J. Org. Chem.*, **64**, 3, 700-6.

Hamilton, W. C. & Ibers, J. A., (1968). *Hydrogen Bonding in Solids.* W.A.

Benjamin Inc. New York.

Harary, F., (1967). *Graph Theory and Theoretic Physics; Academic Press,* New York.

Harmon, K. M., Gill, S. H., Rasmussen P. G. & Hardgrove, G. L., (1999). *J. Molec. Struct.*, **478**, 1-3, 145-54.

Kovacs, A., Macsari, I. & Hargittai, I., (1999). *J. Phys. Chem. A.*, **103**, 16, 3110-4.

Kuln, L. P., (1952). *J. Am. Chem. Soc.*, 2492-99.

Luque, F. J., Lopez, J. M., de la Paz, M. L., Vicent, C. & Orozco, M., (1998). *J. Phys. Chem. A.*, **102**, 33, 6690-6.

Kuleshova, L. N. & Zorky, P. M., (1980). *Acta Cryst.*, B**36**, 2113-5.

Missopolinou, D. & Panayiotou, C., (1998). *J. Phys. Chem. A.*, 102, 20, 3574-81.

Murray-Rust, P. & Glusker, J. P., (1984). *J. Am. Chem. Soc.*, 106, 1018-25.

Palomer, J., DePaz, J. L. G. & Catalan, J., (1999). *J. Chem. Phys,* **246**, 1-3, 167-208.

Pimentel, G. C. & McClellan, A. L., (1960). *The Hydrogen Bond,* Freeman, San Franciso.

Runner, M. E., Kilpatrick, M. L. & Wagner, E. C., (1947). *J. Am. Chem. Soc.*, 1406 -10.

Schuster, P., (1976) in *The Hydrogen Bond, vol. 1.* Eds. P. Schuster, G. Zundel & C. Sandorfy, p 123-7, North-Holland Publishing Company, Amsterdam.

Shahat, M., (1952). *Acta Cryst.*, **5**, 763-8.

Sidgwick, N. V. & Callow, R. K., (1924). *J. Chem. Soc.,* **1**, 527-538.

Taylor, R. & Kennard, O., (1984). *Acc. Chem. Res.*, **17**, 320-6.

Wells, A. F., (1962). *Structural Inorganic Chemistry*; Clarendon Press: Oxford, 294-315.

Synthetic Procedure, Atomic Coordinates and Anisotropic Displacement Parameters for Structures **1** to **17**

APPENDIX A

A1 Synthesis of compounds 1 to 17

The synthesis and crystallisation described here was performed by N.N. Laxmi Madhavi at the University of Hyderabad, India.

All seventeen compounds were synthesised in two steps by the following general scheme. The synthesis was performed in an atmosphere of dry nitrogen using standard syringe-septum techniques. All solvents were dried by standard methods and distilled prior to use. Figure A.1 outlines the general synthetic procedure for one equivalent of ketone.

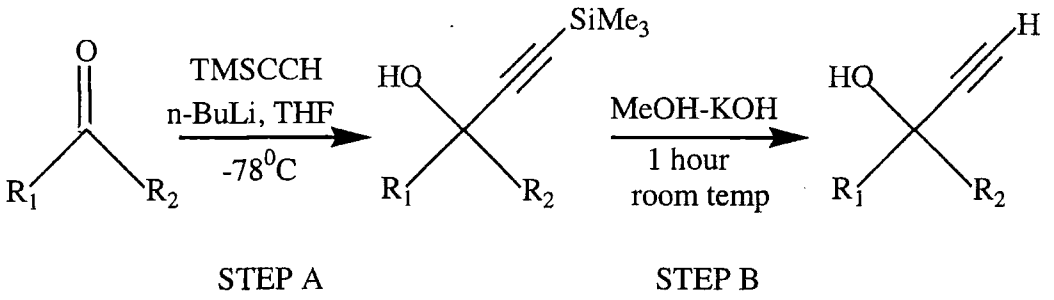

Figure A.1 - General synthetic procedure for compounds **1** to **17**.

STEP A - A solution of trimethylsilylacetylene (4.4 mmol) in 15 mL of THF was treated with n-butyllithium (4.2 mmol) at -78 °C. After stirring for 15 minutes, a solution of ketone (4 mmol) in THF was added dropwise and the stirring continued at low temperature for 30 minutes and at room temperature for 1 hour. Brine was added to the reaction mixture and was extracted with diethyl ether. The organic phase was dried over magnesium sulphate and filtered and the ether removed. The solid obtained was taken to the next step without purification.

STEP B - The solid was dissolved in methanol and a solution of methanolic KOH was added slowly and stirred for 1 hour at room temperature. Water was added to the reaction mixture and was extracted with ethylacetate. It was then dried over magnesium sulphate and solvent removed. Crystals were obtained by the purification of the crude material on column chromatography followed by recrystallisation.

Further notes on polymorphs 1 and 2

1,4-diethynyl-1,4-cyclohexanediol **1,2** was synthesised from 1,4-cyclohexanedione, the reaction product contains both the *cis*- and *trans*-isomers. The pure *trans*-isomer was separated from the amorphous *cis*-isomer by repeated recrystallisations from ethyl acetate. Further recrystallisation of the pure isomer yielded crystals of two the two polymorphs, **1** and **2**, in the same flask.

A2 Atomic Coordinates and Anisotropic Displacement Parameters for Structures 1 to 17

Table A1.1 - Atomic coordinates and equivalent isotropic displacement parameters ($Å^2$ x 10^3) for **1**

	X	y	Z	Ueq
O(1)	-3410(1)	1433(1)	6674(1)	30(1)
C(1)	-3042(3)	3971(2)	5117(1)	46(1)
C(2)	-3546(2)	2861(1)	5281(1)	33(1)
C(3)	-4107(2)	1463(1)	5468(1)	26(1)
C(4)	-6565(2)	1046(1)	5233(1)	26(1)
C(5)	-7133(2)	-425(1)	5361(1)	27(1)
O(2)	3832(1)	2665(1)	8173(1)	31(1)
C(11)	1733(2)	5650(2)	7802(1)	44(1)
C(12)	2736(2)	4923(1)	8264(1)	30(1)
C(13)	3988(2)	4044(1)	8880(1)	24(1)
C(14)	6415(2)	4547(1)	9032(1)	25(1)
C(15)	6866(2)	5953(1)	9898(1)	25(1)
O(3)	163(1)	970(1)	7904(1)	27(1)
C(21)	-2870(2)	-2128(1)	7629(1)	35(1)
C(22)	-1709(2)	-1131(1)	8112(1)	26(1)
C(23)	-347(2)	142(1)	8736(1)	22(1)
C(24)	-1557(2)	951(1)	9752(1)	23(1)
C(25)	-1840(2)	198(1)	10756(1)	23(1)

Table A1.2 - Anisotropic displacement parameters ($Å^2 \times 10^3$) for **1**

	U11	U22	U33	U23	U13	U12
O(1)	29(1)	39(1)	20(1)	5(1)	-3(1)	12(1)
C(1)	48(1)	39(1)	52(1)	14(1)	3(1)	4(1)
C(2)	31(1)	36(1)	32(1)	7(1)	0(1)	7(1)
C(3)	25(1)	32(1)	21(1)	7(1)	-1(1)	8(1)
C(4)	24(1)	33(1)	22(1)	5(1)	0(1)	10(1)
C(5)	23(1)	36(1)	24(1)	7(1)	3(1)	8(1)
O(2)	29(1)	26(1)	32(1)	-3(1)	7(1)	-5(1)
C(11)	42(1)	53(1)	41(1)	18(1)	-1(1)	8(1)
C(12)	29(1)	34(1)	27(1)	6(1)	3(1)	-2(1)
C(13)	24(1)	23(1)	23(1)	3(1)	4(1)	-2(1)
C(14)	23(1)	24(1)	25(1)	4(1)	6(1)	-2(1)
C(15)	25(1)	24(1)	25(1)	5(1)	6(1)	-4(1)
O(3)	24(1)	33(1)	28(1)	17(1)	-3(1)	-3(1)
C(21)	39(1)	34(1)	30(1)	10(1)	-6(1)	-8(1)
C(22)	26(1)	30(1)	24(1)	11(1)	-1(1)	0(1)
C(23)	20(1)	25(1)	23(1)	11(1)	-2(1)	-1(1)
C(24)	21(1)	25(1)	26(1)	10(1)	-2(1)	3(1)
C(25)	19(1)	28(1)	25(1)	10(1)	0(1)	2(1)

Table A2.1 - Atomic coordinates and equivalent isotropic displacement parameters ($Å^2$ x 10^3) for **2**

	x	y	z	Ueq
O(1)	11239(2)	6858(1)	6769(1)	22(1)
C(1)	9697(3)	4381(2)	8199(2)	35(1)
C(2)	9983(3)	4830(2)	7394(2)	24(1)
C(3)	10257(2)	5351(2)	6348(1)	19(1)
C(4)	11787(3)	4466(2)	5692(2)	21(1)
C(5)	11962(2)	4826(2)	4525(1)	20(1)
O(2)	8771(2)	8438(1)	8118(1)	21(1)
C(11)	5431(3)	6511(2)	9244(2)	36(1)
C(12)	6809(3)	7449(2)	9304(2)	24(1)
C(13)	8453(2)	8640(2)	9327(1)	18(1)
C(14)	7688(2)	10120(2)	9778(1)	20(1)
C(15)	9362(3)	11395(2)	9862(1)	20(1)
O(3)	4979(2)	8204(1)	6519(1)	21(1)
C(21)	3243(4)	11533(2)	7464(2)	43(1)
C(22)	3903(3)	10574(2)	6833(2)	27(1)
C(23)	4707(2)	9400(2)	6013(1)	19(1)
C(24)	3142(3)	8877(2)	4754(2)	21(1)
C(25)	6951(2)	9938(2)	5887(2)	21(1)

Table A2.2 - Anisotropic displacement parameters ($Å^2$ x 10^3) for **2**

	U11	U22	U33	U23	U13	U12
O(1)	24(1)	16(1)	25(1)	1(1)	11(1)	-1(1)
C(1)	50(1)	30(1)	31(1)	13(1)	18(1)	6(1)
C(2)	27(1)	20(1)	25(1)	4(1)	9(1)	2(1)
C(3)	21(1)	15(1)	21(1)	4(1)	7(1)	0(1)
C(4)	21(1)	18(1)	24(1)	5(1)	7(1)	4(1)
C(5)	18(1)	17(1)	24(1)	3(1)	8(1)	1(1)
O(2)	22(1)	27(1)	15(1)	5(1)	5(1)	4(1)
C(11)	32(1)	34(1)	38(1)	11(1)	8(1)	-5(1)
C(12)	25(1)	26(1)	20(1)	6(1)	5(1)	2(1)
C(13)	19(1)	21(1)	16(1)	6(1)	5(1)	2(1)
C(14)	16(1)	23(1)	20(1)	5(1)	5(1)	4(1)
C(15)	22(1)	20(1)	20(1)	6(1)	4(1)	5(1)
O(3)	20(1)	22(1)	24(1)	14(1)	4(1)	0(1)
C(21)	63(2)	36(1)	38(1)	11(1)	27(1)	16(1)
C(22)	34(1)	27(1)	23(1)	11(1)	11(1)	5(1)
C(23)	21(1)	18(1)	20(1)	9(1)	6(1)	2(1)
C(24)	18(1)	22(1)	22(1)	9(1)	1(1)	-4(1)
C(25)	17(1)	25(1)	22(1)	11(1)	0(1)	-1(1)

Table A3.1 - Atomic coordinates and equivalent isotropic displacement parameters ($Å^2 \times 10^3$) for **3**

	x	y	z	Ueq
O(1)	5801(3)	888(4)	8537(2)	16(1)
C(1)	3001(3)	-2507(4)	8312(2)	25(1)
C(2)	3916(2)	-1333(4)	8679(2)	16(1)
C(3)	5089(2)	38(3)	9121(1)	13(1)
C(4)	6073(2)	-1359(4)	9777(1)	15(1)
C(5)	5409(2)	-2021(3)	10471(1)	14(1)
O(2)	7598(3)	-5574(4)	8739(2)	19(1)
C(11)	10574(3)	-7927(5)	8400(2)	39(1)
C(12)	9860(3)	-6958(4)	8769(2)	24(1)
C(13)	8997(2)	-5704(3)	9216(2)	16(1)
C(14)	9528(2)	-3356(4)	9349(2)	18(1)
C(15)	9033(2)	-6780(4)	10051(2)	19(1)
O(3)	3478(3)	2265(5)	2343(2)	21(1)
HA	6079(6)	-334(8)	8222(3)	29(1)
H(1)	2194(7)	-3582(10)	7981(5)	56(2)
H(4A)	6394(6)	-2792(8)	9481(3)	33(1)
H(4B)	6998(5)	-353(8)	10031(3)	28(1)
H(5A)	6164(5)	-2963(8)	10940(3)	31(1)
H(5B)	4490(5)	-3051(8)	10232(3)	31(1)
HB	7106(5)	-7004(8)	8710(3)	30(1)
H(11)	11209(10)	-8862(18)	8088(6)	88(3)
H(14A)	9541(6)	-2630(8)	8757(3)	35(1)
H(14B)	8757(5)	-2439(8)	9601(4)	34(1)
H(15A)	8719(6)	-8473(9)	9963(4)	38(1)
H(15B)	8261(5)	-5960(9)	10322(4)	36(1)
HC	4305(6)	2810(10)	2742(4)	39(1)
HD	3101(6)	3525(9)	2017(4)	38(1)

Table A3.2 - Anisotropic displacement parameters ($Å^2 \times 10^3$) for **3**

	U11	U22	U33	U23	U13	U12
O(1)	20(1)	14(1)	16(1)	-2(1)	8(1)	-5(1)
HA	38(3)	25(2)	28(3)	-5(2)	15(2)	1(2)
C(1)	25(1)	23(1)	24(1)	-6(1)	1(1)	-9(1)
H(1)	52(4)	47(3)	59(5)	-12(3)	-2(3)	-28(3)
C(2)	17(1)	14(1)	17(1)	-3(1)	4(1)	-2(1)
C(3)	14(1)	11(1)	13(1)	-2(1)	4(1)	0(1)
C(4)	14(1)	17(1)	14(1)	-1(1)	5(1)	2(1)
H(4A)	40(3)	28(2)	33(3)	-10(2)	15(2)	10(2)
H(4B)	21(2)	26(2)	35(3)	0(2)	4(2)	-6(2)
C(5)	17(1)	12(1)	13(1)	0(1)	4(1)	1(1)
H(5A)	38(3)	27(2)	25(2)	5(2)	4(2)	10(2)
H(5B)	31(2)	30(2)	32(3)	-2(2)	7(2)	-6(2)
O(2)	13(1)	19(1)	23(1)	0(1)	-1(1)	-2(1)
HB	28(2)	25(2)	35(3)	-6(2)	3(2)	-9(2)
C(11)	38(2)	46(2)	34(2)	-12(1)	15(1)	13(1)
H(11)	82(6)	124(7)	62(6)	-22(5)	26(5)	56(6)
C(12)	25(1)	24(1)	25(1)	-7(1)	7(1)	5(1)
C(13)	15(1)	14(1)	17(1)	1(1)	3(1)	-2(1)
C(14)	17(1)	16(1)	20(1)	2(1)	3(1)	-2(1)
H(14A)	42(3)	32(3)	28(3)	11(2)	3(2)	-14(2)
H(14B)	28(2)	25(2)	48(3)	-1(2)	9(2)	5(2)
C(15)	13(1)	20(1)	24(1)	1(1)	5(1)	-4(1)
H(15A)	35(3)	32(2)	45(3)	8(2)	6(2)	-9(2)
H(15B)	20(2)	45(3)	45(4)	3(3)	11(2)	1(2)
O(3)	27(1)	18(1)	19(1)	-1(1)	7(1)	1(1)
HC	39(3)	48(3)	27(3)	-8(2)	2(2)	6(3)
HD	42(3)	32(3)	41(3)	10(2)	9(3)	8(2)

Table A4.1 - Atomic coordinates and equivalent isotropic displacement parameters ($Å^2$ x 10^3) for **4**

	x	y	z	Ueq
C(1)	3899(2)	3628(2)	6888(1)	26(1)
C(2)	4635(1)	2510(2)	6409(1)	20(1)
C(3)	5531(1)	1042(2)	5825(1)	17(1)
O(1)	7009(1)	623(2)	6201(1)	23(1)
C(4)	4761(1)	-1241(2)	5768(1)	18(1)
C(5)	4289(1)	-2161(2)	5040(1)	18(1)

Table A4.2 - Anisotropic displacement parameters ($Å^2$ x 10^3) for **4**

	U11	U22	U33	U23	U13	U12
C(1)	32(1)	22(1)	25(1)	-2(1)	5(1)	1(1)
C(2)	22(1)	18(1)	20(1)	1(1)	0(1)	-2(1)
C(3)	17(1)	16(1)	18(1)	0(1)	-1(1)	0(1)
O(1)	18(1)	25(1)	25(1)	1(1)	-3(1)	-1(1)
C(4)	19(1)	15(1)	19(1)	3(1)	2(1)	1(1)
C(5)	19(1)	14(1)	21(1)	2(1)	2(1)	-2(1)

Table A5.1 - Atomic coordinates and equivalent isotropic displacement parameters ($Å^2 \times 10^3$) for **5**

	x	y	z	Ueq
O(1)	2854(1)	1731(1)	508(1)	31(1)
O(21)	-58(1)	1884(1)	-1343(2)	33(1)
O(2)	1774(2)	1255(1)	-4907(1)	33(1)
O(22)	-5311(1)	1217(1)	-2987(2)	35(1)
C(23)	-1175(2)	1660(1)	-1077(2)	25(1)
C(30)	-4177(2)	1410(1)	-3255(2)	26(1)
C(10)	1399(2)	1349(1)	-3773(2)	25(1)
C(3)	3262(2)	1601(1)	-583(2)	24(1)
C(4)	2827(2)	975(1)	-1167(2)	23(1)
C(24)	-1653(2)	1057(1)	-1770(2)	23(1)
C(2)	4820(2)	1635(1)	145(2)	28(1)
C(33)	-3652(2)	2002(1)	-2559(2)	29(1)
C(9)	1999(2)	857(1)	-2643(2)	23(1)
C(29)	-3045(2)	939(1)	-2765(2)	25(1)
C(13)	1857(2)	1957(1)	-3146(2)	28(1)
C(11)	-160(2)	1325(1)	-4476(2)	29(1)
C(31)	-4835(2)	1478(1)	-4857(2)	30(1)
C(21)	4(2)	1578(1)	1815(2)	38(1)
C(22)	-532(2)	1615(1)	523(2)	28(1)
C(34)	-2337(2)	2110(1)	-1595(2)	29(1)
C(25)	-664(2)	601(1)	-1399(2)	31(1)
C(12)	-1393(2)	1317(1)	-4965(2)	37(1)
C(8)	1701(2)	268(1)	-3109(2)	33(1)
C(14)	2679(2)	2068(1)	-1753(2)	28(1)
C(1)	6057(2)	1658(1)	655(2)	36(1)
C(32)	-5363(2)	1536(1)	-6138(2)	38(1)
C(5)	3303(2)	503(1)	-182(2)	32(1)
C(28)	-3427(2)	372(1)	-3345(2)	36(1)
C(6)	2980(2)	-70(1)	-650(2)	39(1)

C(7)	2183(2)	-190(1)	-2132(2)	40(1)
C(26)	-1044(2)	49(1)	-2001(2)	38(1)
C(27)	-2444(2)	-72(1)	-2976(2)	41(1)

Table A5.2 - Anisotropic displacement parameters ($Å^2$ x 10^3) for **5**

	U11	**U22**	**U33**	**U23**	**U13**	**U12**
O(1)	28(1)	48(1)	15(1)	-5(1)	10(1)	5(1)
O(21)	29(1)	47(1)	23(1)	4(1)	13(1)	-7(1)
O(2)	27(1)	59(1)	14(1)	0(1)	10(1)	1(1)
O(22)	25(1)	60(1)	21(1)	-1(1)	11(1)	-3(1)
C(23)	22(1)	35(1)	17(1)	2(1)	9(1)	-3(1)
C(30)	21(1)	40(1)	16(1)	1(1)	7(1)	1(1)
C(10)	25(1)	37(1)	12(1)	2(1)	8(1)	2(1)
C(3)	25(1)	32(1)	15(1)	-3(1)	11(1)	1(1)
C(4)	21(1)	30(1)	17(1)	0(1)	8(1)	1(1)
C(24)	24(1)	31(1)	15(1)	5(1)	9(1)	2(1)
C(2)	32(1)	31(1)	20(1)	-4(1)	11(1)	0(1)
C(33)	31(1)	35(1)	20(1)	3(1)	10(1)	7(1)
C(9)	21(1)	31(1)	17(1)	-1(1)	9(1)	0(1)
C(29)	26(1)	33(1)	16(1)	1(1)	10(1)	1(1)
C(13)	30(1)	31(1)	24(1)	8(1)	13(1)	2(1)
C(11)	29(1)	40(1)	17(1)	3(1)	10(1)	1(1)
C(31)	24(1)	42(1)	20(1)	0(1)	8(1)	4(1)
C(21)	37(1)	51(1)	21(1)	0(1)	9(1)	-5(1)
C(22)	25(1)	36(1)	20(1)	0(1)	8(1)	-4(1)
C(34)	35(1)	29(1)	21(1)	0(1)	13(1)	0(1)
C(25)	28(1)	41(1)	25(1)	8(1)	12(1)	4(1)
C(12)	30(1)	53(1)	25(1)	4(1)	11(1)	2(1)

C(8)	33(1)	36(1)	27(1)	-9(1)	12(1)	-4(1)
C(14)	30(1)	26(1)	25(1)	0(1)	11(1)	0(1)
C(1)	27(1)	46(1)	30(1)	-7(1)	10(1)	-3(1)
C(32)	37(1)	54(1)	21(1)	3(1)	11(1)	9(1)
C(5)	33(1)	37(1)	23(1)	5(1)	11(1)	4(1)
C(28)	38(1)	39(1)	26(1)	-5(1)	11(1)	-3(1)
C(6)	40(1)	35(1)	40(1)	12(1)	17(1)	6(1)
C(7)	41(1)	29(1)	46(1)	-4(1)	18(1)	-3(1)
C(26)	47(1)	35(1)	37(1)	10(1)	23(1)	12(1)
C(27)	57(1)	33(1)	36(1)	-4(1)	23(1)	0(1)

Table A6.1 - Atomic coordinates and equivalent isotropic displacement parameters ($Å^2$ x 10^3) for **6**

	x	y	z	Ueq
C(1)	2626(3)	-2681(3)	455(3)	34(1)
C(2)	3852(3)	-1105(3)	951(2)	30(1)
C(3)	3410(2)	283(3)	941(2)	26(1)
C(4)	1736(2)	129(2)	463(2)	19(1)
C(5)	1330(2)	1706(2)	485(2)	19(1)
O(1)	2148(2)	3180(2)	1972(2)	28(1)
C(6)	2069(2)	2237(2)	-505(2)	25(1)
C(7)	2679(3)	2669(3)	-1283(3)	33(1)
C(8)	-513(2)	1439(2)	7(2)	20(1)
C(9)	-974(3)	2856(3)	23(2)	28(1)
C(21)	8055(3)	2958(3)	3612(3)	36(1)
C(22)	7475(3)	4286(3)	3655(2)	30(1)
C(23)	6262(2)	4628(2)	4319(2)	21(1)
C(24)	5697(2)	6133(2)	4337(2)	21(1)
O(2)	5129(2)	5911(2)	2834(2)	26(1)
C(25)	7171(2)	7758(2)	5189(2)	25(1)
C(26)	8354(3)	9037(3)	5925(2)	33(1)
C(27)	4359(2)	6393(2)	5062(2)	21(1)
C(28)	3738(3)	7721(3)	5092(2)	29(1)
C(29)	2540(3)	8040(3)	5739(3)	36(1)

Table A6.2 - Anisotropic displacement parameters ($Å^2 \times 10^3$) for **6**

	U11	U22	U33	U23	U13	U12
C(1)	37(1)	33(1)	44(1)	24(1)	15(1)	21(1)
C(2)	23(1)	41(1)	34(1)	20(1)	11(1)	18(1)
C(3)	18(1)	29(1)	27(1)	12(1)	8(1)	6(1)
C(4)	20(1)	21(1)	18(1)	10(1)	9(1)	7(1)
C(5)	19(1)	17(1)	19(1)	8(1)	6(1)	2(1)
O(1)	29(1)	22(1)	23(1)	7(1)	5(1)	3(1)
C(6)	23(1)	24(1)	28(1)	13(1)	8(1)	7(1)
C(7)	37(1)	37(1)	43(1)	27(1)	23(1)	16(1)
C(8)	20(1)	21(1)	23(1)	13(1)	10(1)	7(1)
C(9)	29(1)	24(1)	37(1)	19(1)	13(1)	10(1)
C(21)	32(1)	40(1)	40(1)	17(1)	18(1)	17(1)
C(22)	26(1)	35(1)	32(1)	17(1)	15(1)	8(1)
C(23)	20(1)	20(1)	19(1)	9(1)	6(1)	4(1)
C(24)	21(1)	23(1)	19(1)	13(1)	7(1)	4(1)
O(2)	26(1)	30(1)	21(1)	16(1)	5(1)	1(1)
C(25)	26(1)	28(1)	23(1)	16(1)	8(1)	6(1)
C(26)	31(1)	32(1)	31(1)	17(1)	6(1)	1(1)
C(27)	21(1)	21(1)	19(1)	10(1)	6(1)	4(1)
C(28)	32(1)	27(1)	32(1)	17(1)	10(1)	10(1)
C(29)	34(1)	33(1)	42(1)	16(1)	12(1)	17(1)

Table A7.1 - Atomic coordinates and equivalent isotropic displacement parameters ($Å^2$ x 10^3) for 7

	x	y	z	Ueq
Br(1)	14550(1)	2358(1)	14453(1)	34(1)
Br(2)	9556(1)	1747(1)	6020(1)	37(1)
O(1)	3788(3)	1795(2)	10575(2)	28(1)
C(10)	6726(4)	2554(2)	9690(2)	21(1)
C(15)	8996(4)	3258(2)	9790(2)	25(1)
C(14)	9833(4)	3029(2)	8698(2)	26(1)
C(3)	5921(4)	2826(2)	10935(2)	22(1)
C(2)	5352(4)	4170(2)	11473(2)	24(1)
C(12)	6082(4)	1394(2)	7376(2)	26(1)
C(11)	5266(4)	1636(2)	8476(2)	24(1)
C(5)	9410(4)	3879(2)	12966(2)	28(1)
C(1)	4884(4)	5239(3)	11907(3)	31(1)
C(4)	7950(4)	2749(2)	11894(2)	22(1)
C(13)	8365(4)	2090(2)	7505(2)	25(1)
C(7)	11801(4)	2507(2)	13444(2)	26(1)
C(8)	10325(4)	1356(2)	12387(2)	27(1)
C(6)	11362(4)	3768(2)	13750(2)	30(1)
C(9)	8406(4)	1481(2)	11613(2)	26(1)

Table A7.2 - Anisotropic displacement parameters ($Å^2$ x 10^3) for **7**

	U11	U22	U33	U23	U13	U12
Br(1)	35(1)	38(1)	30(1)	18(1)	3(1)	10(1)
Br(2)	36(1)	53(1)	25(1)	15(1)	13(1)	18(1)
O(1)	24(1)	25(1)	30(1)	11(1)	9(1)	-2(1)
C(10)	21(1)	19(1)	23(1)	10(1)	5(1)	4(1)
C(15)	21(1)	27(1)	22(1)	10(1)	3(1)	1(1)
C(14)	20(1)	33(1)	25(1)	13(1)	6(1)	5(1)
C(3)	21(1)	19(1)	24(1)	9(1)	6(1)	1(1)
C(2)	20(1)	26(1)	25(1)	11(1)	6(1)	4(1)
C(12)	28(1)	22(1)	20(1)	6(1)	-1(1)	5(1)
C(11)	21(1)	19(1)	28(1)	10(1)	3(1)	1(1)
C(5)	34(1)	23(1)	25(1)	8(1)	5(1)	7(1)
C(1)	26(1)	28(1)	37(1)	12(1)	8(1)	8(1)
C(4)	26(1)	21(1)	22(1)	11(1)	9(1)	4(1)
C(13)	28(1)	28(1)	24(1)	13(1)	9(1)	14(1)
C(7)	27(1)	32(1)	23(1)	15(1)	7(1)	8(1)
C(8)	30(1)	23(1)	31(1)	15(1)	8(1)	6(1)
C(6)	34(1)	25(1)	22(1)	6(1)	2(1)	4(1)
C(9)	29(1)	21(1)	25(1)	9(1)	5(1)	2(1)

Table A8.1 - Atomic coordinates and equivalent isotropic displacement parameters ($Å^2$ x 10^3) for **8**

	x	y	z	Ueq
C(1)	10066(3)	-266(2)	3027(2)	31(1)
C(2)	9579(3)	815(2)	3503(2)	24(1)
C(3)	9001(3)	2175(2)	4091(2)	21(1)
O(1)	11132(2)	3188(1)	4463(1)	27(1)
C(4)	8200(3)	2472(1)	5389(2)	20(1)
C(5)	9651(3)	3416(2)	6653(2)	24(1)
C(6)	8855(3)	3666(2)	7808(2)	27(1)
C(7)	6591(3)	2960(2)	7680(2)	25(1)
Cl(1)	496(1)	2648(1)	584(1)	37(1)
C(8)	5132(3)	2003(2)	6431(2)	27(1)
C(9)	5949(3)	1763(2)	5293(2)	25(1)
C(10)	6949(3)	2260(2)	3111(2)	21(1)
C(11)	6523(3)	3537(2)	3395(2)	25(1)
C(12)	4577(3)	3664(2)	2604(2)	28(1)
C(13)	3042(3)	2502(2)	1525(2)	27(1)
Cl(2)	5543(1)	3270(1)	9111(1)	38(1)
C(14)	3448(3)	1231(2)	1216(2)	29(1)
C(15)	5417(3)	1112(2)	2013(2)	26(1)

Table A8.2 - Anisotropic displacement parameters ($Å^2$ x 10^3) for **8**

	U11	U22	U33	U23	U13	U12
C(1)	24(1)	27(1)	41(1)	15(1)	11(1)	8(1)
C(2)	16(1)	27(1)	27(1)	13(1)	6(1)	3(1)
C(3)	18(1)	20(1)	25(1)	10(1)	6(1)	0(1)
O(1)	21(1)	25(1)	32(1)	12(1)	10(1)	-2(1)
C(4)	18(1)	19(1)	25(1)	12(1)	6(1)	5(1)
C(5)	21(1)	21(1)	27(1)	10(1)	4(1)	2(1)
C(6)	29(1)	23(1)	25(1)	8(1)	4(1)	5(1)
C(7)	26(1)	29(1)	26(1)	15(1)	10(1)	14(1)
Cl(1)	34(1)	45(1)	35(1)	23(1)	3(1)	13(1)
C(8)	19(1)	35(1)	31(1)	19(1)	8(1)	6(1)
C(9)	18(1)	30(1)	25(1)	12(1)	4(1)	1(1)
C(10)	21(1)	22(1)	23(1)	11(1)	8(1)	3(1)
C(11)	27(1)	21(1)	28(1)	12(1)	7(1)	3(1)
C(12)	30(1)	25(1)	33(1)	18(1)	10(1)	8(1)
C(13)	26(1)	36(1)	25(1)	18(1)	9(1)	9(1)
Cl(2)	37(1)	54(1)	30(1)	20(1)	18(1)	19(1)
C(14)	29(1)	28(1)	24(1)	9(1)	3(1)	5(1)
C(15)	28(1)	22(1)	27(1)	10(1)	6(1)	5(1)

Table A9.1 - Atomic coordinates and equivalent isotropic displacement parameters ($Å^2$ x 10^3) for **9**

	x	y	z	Ueq
C(1)	7141(3)	-109(2)	2949(1)	34(1)
C(2)	6603(2)	926(2)	2564(1)	27(1)
C(3)	5790(2)	2139(2)	2048(1)	23(1)
O(1)	3614(2)	1466(2)	1640(1)	28(1)
C(4)	6155(2)	3937(2)	2967(1)	22(1)
C(5)	4550(2)	4686(2)	3196(1)	28(1)
C(6)	4927(3)	6303(2)	4049(1)	30(1)
C(7)	6903(2)	7200(2)	4682(1)	26(1)
C(8)	7306(3)	8924(2)	5623(2)	36(1)
C(9)	8508(2)	6444(2)	4431(1)	28(1)
C(10)	8142(2)	4830(2)	3584(1)	27(1)
C(11)	6815(2)	2350(2)	1076(1)	22(1)
C(12)	5842(2)	2984(2)	282(1)	26(1)
C(13)	6724(3)	3212(2)	-604(1)	28(1)
C(14)	8597(2)	2830(2)	-727(1)	27(1)
C(15)	9529(3)	3045(2)	-1703(2)	36(1)
C(16)	9569(2)	2214(2)	76(1)	27(1)
C(17)	8691(2)	1973(2)	967(1)	25(1)

Table A9.2 - Anisotropic displacement parameters ($Å^2$ x 10^3) for **9**

	U11	U22	U33	U23	U13	U12
C(1)	44(1)	28(1)	35(1)	15(1)	10(1)	11(1)
C(2)	29(1)	22(1)	26(1)	6(1)	7(1)	3(1)
C(3)	22(1)	20(1)	25(1)	7(1)	3(1)	4(1)
O(1)	23(1)	23(1)	32(1)	5(1)	3(1)	1(1)
C(4)	27(1)	20(1)	22(1)	8(1)	6(1)	5(1)
C(5)	24(1)	25(1)	31(1)	7(1)	4(1)	5(1)
C(6)	31(1)	26(1)	36(1)	9(1)	10(1)	11(1)
C(7)	35(1)	22(1)	23(1)	9(1)	8(1)	6(1)
C(8)	46(1)	25(1)	31(1)	3(1)	11(1)	7(1)
C(9)	28(1)	26(1)	25(1)	6(1)	2(1)	2(1)
C(10)	25(1)	25(1)	29(1)	6(1)	6(1)	7(1)
C(11)	24(1)	16(1)	23(1)	4(1)	3(1)	3(1)
C(12)	25(1)	24(1)	28(1)	8(1)	3(1)	7(1)
C(13)	34(1)	24(1)	25(1)	9(1)	2(1)	7(1)
C(14)	33(1)	17(1)	24(1)	2(1)	7(1)	1(1)
C(15)	49(1)	28(1)	30(1)	6(1)	16(1)	5(1)
C(16)	24(1)	22(1)	31(1)	5(1)	7(1)	6(1)
C(17)	25(1)	21(1)	26(1)	6(1)	2(1)	5(1)

Table A10.1 - Atomic coordinates and equivalent isotropic displacement parameters ($Å^2$ x 10^3) for **10**

	x	y	z	Ueq
C(1)	423(4)	-743(3)	2980(2)	35(1)
C(2)	1443(4)	348(2)	3067(1)	30(1)
C(3)	2633(4)	1735(2)	3165(1)	28(1)
O(1)	883(3)	2659(2)	3279(1)	33(1)
C(4)	3638(4)	1901(2)	2402(1)	28(1)
C(5)	2812(6)	2778(3)	1946(2)	51(1)
C(6)	3804(7)	2913(4)	1265(2)	66(1)
C(7)	5632(4)	2191(2)	1030(2)	39(1)
C(8)	6933(12)	2569(7)	337(4)	44(2)
C(9)	7488(13)	1532(8)	-184(4)	48(2)
C(11)	8695(17)	1854(10)	-857(6)	70(2)
C(10)	9392(17)	3032(10)	-909(6)	79(2)
C(12)	9046(16)	4169(8)	-341(5)	76(2)
C(13)	7765(13)	3910(7)	277(4)	61(2)
C(8A)	6508(10)	2181(6)	279(3)	35(1)
C(9A)	8893(16)	1860(9)	183(5)	31(2)
C(10A)	9840(20)	1971(11)	-516(7)	45(2)
C(11A)	7760(30)	2539(14)	-1172(8)	51(4)
C(12A)	5950(20)	2654(12)	-1054(7)	51(3)
C(13A)	5090(19)	2510(11)	-363(7)	42(2)
C(9B)	7550(20)	1131(15)	-142(9)	47(3)
C(10B)	8428(18)	1373(12)	-838(6)	32(2)
C(11B)	8570(20)	2489(10)	-1105(6)	24(2)
C(12B)	7580(20)	3675(13)	-672(8)	54(3)
C(13B)	6540(20)	3512(11)	-1(7)	44(2)
C(14)	6400(5)	1299(3)	1487(2)	41(1)
C(15)	5424(5)	1155(3)	2167(2)	42(1)
C(16)	4697(4)	2080(2)	3876(1)	27(1)
C(17)	5842(4)	1103(2)	4191(1)	30(1)

C(18)	7747(4)	1467(2)	4825(1)	29(1)
C(19)	8535(3)	2812(2)	5161(1)	25(1)
C(20)	10514(3)	3190(2)	5849(1)	25(1)
C(21)	12571(4)	2522(2)	5880(1)	29(1)
C(22)	14380(4)	2851(2)	6535(2)	34(1)
C(23)	14181(5)	3860(3)	7168(2)	41(1)
C(24)	12180(4)	4552(3)	7141(2)	39(1)
C(25)	10358(4)	4217(2)	6488(1)	30(1)
C(26)	7358(4)	3784(2)	4842(1)	26(1)
C(27)	5500(4)	3425(2)	4201(1)	27(1)

Table A10.2 - Anisotropic displacement parameters ($Å^2$ x 10^3) for **10**

	U11	U22	U33	U23	U13	U12
C(1)	34(1)	36(1)	37(1)	8(1)	9(1)	1(1)
C(2)	26(1)	35(1)	28(1)	5(1)	7(1)	5(1)
C(3)	25(1)	29(1)	30(1)	4(1)	5(1)	6(1)
O(1)	27(1)	35(1)	37(1)	6(1)	8(1)	11(1)
C(4)	24(1)	29(1)	27(1)	1(1)	2(1)	1(1)
C(5)	59(2)	70(2)	39(2)	24(1)	21(1)	39(2)
C(6)	79(2)	96(3)	48(2)	40(2)	29(2)	55(2)
C(14)	38(1)	43(1)	46(2)	7(1)	19(1)	10(1)
C(15)	41(1)	41(1)	53(2)	19(1)	21(1)	17(1)
C(16)	25(1)	29(1)	27(1)	4(1)	7(1)	5(1)
C(17)	31(1)	24(1)	36(1)	3(1)	6(1)	6(1)
C(18)	30(1)	25(1)	33(1)	6(1)	5(1)	9(1)
C(19)	24(1)	27(1)	26(1)	6(1)	8(1)	4(1)
C(20)	23(1)	27(1)	26(1)	9(1)	7(1)	3(1)
C(21)	27(1)	31(1)	31(1)	7(1)	9(1)	6(1)
C(22)	27(1)	39(1)	40(1)	12(1)	6(1)	8(1)
C(23)	33(1)	52(2)	35(1)	3(1)	-4(1)	8(1)
C(24)	37(1)	44(1)	31(1)	-1(1)	3(1)	8(1)
C(25)	27(1)	32(1)	32(1)	7(1)	8(1)	6(1)
C(26)	28(1)	23(1)	29(1)	5(1)	8(1)	4(1)
C(27)	29(1)	26(1)	29(1)	8(1)	7(1)	6(1)

Table A11.1 - Atomic coordinates and equivalent isotropic displacement parameters ($Å^2$ x 10^3) for **11**

	x	y	z	Ueq
Cl(1)	7713(1)	6181(1)	-25(1)	64(1)
Cl(2)	6132(1)	7190(1)	-152	81(1)
O(1)	8923(1)	7288(1)	-1540(3)	53(1)
C(4)	7560(1)	6912(1)	-1362(3)	38(1)
C(5)	6900(1)	7342(2)	-1411(3)	40(1)
C(2)	8457(2)	6249(2)	-3155(3)	46(1)
C(3)	8265(1)	7018(1)	-2419(3)	36(1)
C(1)	8625(2)	5634(2)	-3678(3)	71(1)

Table A11.2 - Anisotropic displacement parameters ($Å^2$ x 10^3) for **11**

	U11	U22	U33	U23	U13	U12
Cl(1)	77(1)	58(1)	58(1)	23(1)	-5(1)	9(1)
Cl(2)	70(1)	78(1)	96(1)	19(1)	47(1)	11(1)
O(1)	35(1)	31(1)	93(2)	-10(1)	-26(1)	3(1)
C(4)	40(1)	35(1)	39(1)	3(1)	-5(1)	0(1)
C(5)	34(1)	39(1)	47(1)	1(1)	6(1)	0(1)
C(2)	42(1)	39(1)	58(2)	-7(1)	-5(1)	3(1)
C(3)	27(1)	31(1)	51(1)	-4(1)	-6(1)	1(1)
C(1)	90(3)	50(2)	74(2)	-18(2)	-4(2)	12(2)

Table A12.1 - Atomic coordinates and equivalent isotropic displacement parameters ($Å^2$ x 10^3) for **12**

	x	y	z	Ueq
Br(32)	2339(1)	1710(1)	9345(1)	30(1)
Br(21)	2697(1)	3854(1)	11304(1)	28(1)
Br(22)	4039(1)	4260(1)	8534(1)	33(1)
Br(11)	7856(1)	4375(1)	6235(1)	31(1)
Br(31)	4074(1)	-973(1)	8640(1)	28(1)
Br(1)	7908(1)	-1845(1)	5943(1)	34(1)
Br(2)	8422(1)	-876(1)	3347(1)	36(1)
Br(12)	4867(1)	6832(1)	6784(1)	25(1)
O(3)	-988(4)	3802(3)	11712(3)	23(1)
O(1)	10803(5)	-1357(3)	6498(3)	27(1)
C(34)	1752(5)	-377(3)	9406(3)	19(1)
C(25)	1746(5)	4672(3)	9417(4)	18(1)
C(4)	9092(5)	-793(4)	5363(4)	22(1)
C(13)	6262(5)	3856(3)	4816(3)	19(1)
C(3)	9714(5)	-412(3)	6199(3)	19(1)
C(5)	9306(6)	-423(4)	4334(4)	22(1)
C(35)	1068(5)	694(3)	9688(3)	19(1)
C(14)	6176(5)	4770(4)	5572(3)	18(1)
C(15)	5043(5)	5748(4)	5760(3)	18(1)
C(23)	-620(5)	4806(3)	11266(3)	18(1)
C(33)	778(5)	-1231(3)	9671(3)	16(1)
C(24)	1214(5)	4505(3)	10519(3)	19(1)
O(4)	960(4)	-1677(3)	8614(2)	21(1)
O(2)	7898(4)	3546(3)	3984(3)	20(1)
C(22)	-946(5)	5578(3)	12199(4)	20(1)
C(2)	8281(6)	123(4)	7218(4)	24(1)
C(32)	1482(6)	-2131(4)	10344(4)	22(1)
C(21)	-1280(6)	6166(4)	12985(4)	27(1)
C(12)	5913(6)	2906(4)	5515(4)	23(1)

C(1)	7190(7)	528(5)	8056(4)	33(1)
C(11)	5609(7)	2152(5)	6053(5)	39(1)
C(31)	2033(8)	-2869(5)	10836(5)	37(1)

Table A12.2 - Anisotropic displacement parameters ($Å^2$ x 10^3) for **12**

	U11	**U22**	**U33**	**U23**	**U13**	**U12**
Br(32)	24(1)	20(1)	43(1)	-3(1)	-5(1)	-10(1)
Br(21)	28(1)	33(1)	25(1)	1(1)	-17(1)	-2(1)
Br(22)	18(1)	51(1)	24(1)	0(1)	-4(1)	-7(1)
Br(11)	23(1)	45(1)	26(1)	-7(1)	-17(1)	1(1)
Br(31)	18(1)	24(1)	36(1)	-9(1)	-3(1)	-5(1)
Br(1)	45(1)	37(1)	27(1)	4(1)	-7(1)	-27(1)
Br(2)	48(1)	47(1)	28(1)	4(1)	-20(1)	-27(1)
Br(12)	26(1)	27(1)	25(1)	-8(1)	-7(1)	-9(1)
O(3)	33(2)	21(2)	14(2)	2(1)	-2(1)	-12(1)
O(1)	38(2)	24(2)	18(2)	0(1)	-11(2)	-2(1)
C(34)	17(2)	22(2)	15(2)	-2(2)	-5(2)	-5(2)
C(25)	15(2)	19(2)	20(2)	-1(2)	-5(2)	-4(2)
C(4)	20(2)	22(2)	22(2)	-2(2)	-3(2)	-9(2)
C(13)	21(2)	20(2)	15(2)	1(2)	-6(2)	-6(2)
C(3)	20(2)	18(2)	18(2)	1(2)	-8(2)	-5(2)
C(5)	24(2)	24(2)	19(2)	-1(2)	-9(2)	-8(2)
C(35)	22(2)	20(2)	16(2)	-1(2)	-7(2)	-8(2)
C(14)	17(2)	24(2)	13(2)	1(2)	-6(2)	-7(2)
C(15)	19(2)	22(2)	16(2)	-2(2)	-5(2)	-9(2)
C(23)	22(2)	18(2)	16(2)	2(2)	-8(2)	-6(2)

C(33)	19(2)	13(2)	17(2)	-3(2)	-7(2)	-3(2)
C(24)	19(2)	19(2)	19(2)	-1(2)	-8(2)	-6(2)
O(4)	31(2)	15(2)	17(1)	0(1)	10(1)	-7(1)
O(2)	18(2)	21(2)	17(2)	-1(1)	-2(1)	-4(1)
C(22)	21(2)	18(2)	22(2)	3(2)	-9(2)	-6(2)
C(2)	24(2)	29(2)	21(2)	0(2)	-10(2)	-8(2)
C(32)	22(2)	22(2)	23(2)	0(2)	-8(2)	-7(2)
C(21)	29(2)	27(2)	25(2)	-5(2)	-11(2)	-7(2)
C(12)	22(2)	23(2)	21(2)	3(2)	-6(2)	-4(2)
C(1)	26(3)	45(3)	24(2)	-6(2)	-5(2)	-7(2)
C(11)	35(3)	33(3)	37(3)	10(2)	-4(2)	-8(2)
C(31)	40(3)	33(3)	43(3)	15(2)	-25	-9(2)

Table A13.1 - Atomic coordinates and equivalent isotropic displacement parameters ($Å^2$ x 10^3) for **13**

	x	y	z	Ueq
F(1)	1314(1)	3281(1)	8582(1)	30(1)
F(2)	1028(1)	8223(1)	9901(1)	29(1)
F(21)	-4540(1)	-54(1)	7856(1)	29(1)
F(11)	5468(1)	5837(1)	12383(1)	31(1)
O(21)	-7063(1)	-2590(1)	5778(1)	24(1)
F(22)	-1849(1)	1523(1)	6678(1)	29(1)
O(11)	2485(1)	5362(1)	13441(1)	23(1)
F(12)	1825(1)	3291(1)	15495(1)	30(1)
O(1)	927(1)	6013(1)	7638(1)	25(1)
C(24)	-4726(1)	-1(1)	6463(1)	20(1)
C(3)	1303(1)	5853(1)	9100(1)	20(1)
C(5)	502(1)	6642(1)	9969(1)	20(1)
C(13)	3470(1)	4489(1)	13798(1)	20(1)
C(23)	-6518(1)	-912(1)	5668(1)	20(1)
C(12)	2727(1)	2986(1)	12779(1)	24(1)
C(25)	-3413(1)	760(1)	5881(1)	21(1)
C(14)	5277(1)	5459(1)	13677(1)	21(1)
C(15)	3402(1)	4098(1)	15282(1)	21(1)
C(4)	647(1)	4098(1)	9285(1)	21(1)
C(22)	-7616(1)	-275(1)	6225(1)	25(1)
C(1)	4628(2)	7305(2)	9972(1)	37(1)
C(2)	3153(1)	6656(1)	9559(1)	25(1)
C(21)	-8507(2)	247(2)	6635(2)	34(1)
C(11)	2162(2)	1771(2)	11989(1)	31(1)

Table A13.2 - Anisotropic displacement parameters ($Å^2 \times 10^3$) for **13**

	U11	U22	U33	U23	U13	U12
F(1)	31(1)	32(1)	32(1)	-1(1)	12(1)	17(1)
F(2)	31(1)	19(1)	33(1)	6(1)	6(1)	8(1)
F(21)	35(1)	36(1)	16(1)	6(1)	6(1)	15(1)
F(11)	31(1)	41(1)	21(1)	12(1)	7(1)	13(1)
O(21)	30(1)	18(1)	26(1)	6(1)	13(1)	9(1)
F(22)	21(1)	32(1)	27(1)	2(1)	-1(1)	6(1)
O(11)	24(1)	24(1)	23(1)	1(1)	-1(1)	14(1)
F(12)	19(1)	36(1)	33(1)	10(1)	8(1)	7(1)
O(1)	21(1)	35(1)	17(1)	8(1)	5(1)	9(1)
C(24)	25(1)	21(1)	16(1)	4(1)	4(1)	10(1)
C(3)	19(1)	23(1)	17(1)	5(1)	5(1)	8(1)
C(5)	21(1)	18(1)	21(1)	3(1)	3(1)	8(1)
C(13)	19(1)	20(1)	20(1)	3(1)	2(1)	10(1)
C(23)	21(1)	18(1)	21(1)	5(1)	7(1)	8(1)
C(12)	22(1)	25(1)	25(1)	3(1)	3(1)	12(1)
C(25)	20(1)	20(1)	20(1)	2(1)	2(1)	7(1)
C(14)	23(1)	23(1)	19(1)	6(1)	6(1)	10(1)
C(15)	18(1)	21(1)	23(1)	5(1)	6(1)	8(1)
C(4)	21(1)	22(1)	19(1)	1(1)	5(1)	11(1)
C(22)	24(1)	22(1)	28(1)	5(1)	9(1)	9(1)
C(1)	22(1)	50(1)	32(1)	13(1)	5(1)	8(1)
C(2)	22(1)	30(1)	21(1)	8(1)	6(1)	9(1)
C(21)	35(1)	32(1)	45(1)	8(1)	18(1)	18(1)
C(11)	31(1)	28(1)	31(1)	-1(1)	3(1)	13(1)

Table A14.1 - Atomic coordinates and equivalent isotropic displacement parameters ($Å^2$ x 10^3) for **14**

	x	y	z	Ueq
C(1)	2182(1)	4696(1)	8364(3)	39(1)
C(2)	1623(1)	4498(1)	9514(3)	53(1)
C(3)	1180(1)	4027(1)	8754(4)	60(1)
O(17)	4105(1)	4581(1)	4600(1)	24(1)
C(4)	1297(1)	3742(1)	6856(4)	60(1)
C(5)	1862(1)	3928(1)	5693(3)	44(1)
C(6)	2311(1)	4408(1)	6444(2)	31(1)
C(7)	2924(1)	4615(1)	5211(2)	26(1)
C(8)	3594(1)	4282(1)	5919(2)	22(1)
C(9)	3590(1)	3515(1)	5628(2)	23(1)
C(10)	3691(1)	3072(1)	7265(2)	31(1)
C(11)	3706(1)	2378(1)	6934(2)	41(1)
C(12)	3618(1)	2119(1)	4967(3)	40(1)
C(13)	3519(1)	2556(1)	3332(2)	36(1)
C(14)	3506(1)	3249(1)	3653(2)	31(1)
C(15)	3745(1)	4473(1)	8071(2)	25(1)
C(16)	3882(1)	4642(1)	9763(2)	33(1)
C(21)	3048(1)	-23(1)	-2367(2)	36(1)
C(22)	3690(1)	162(1)	-3045(3)	44(1)
C(23)	4114(1)	530(1)	-1773(3)	43(1)
O(37)	953(1)	194(1)	635(1)	25(1)
C(24)	3894(1)	728(1)	143(3)	41(1)
C(25)	3249(1)	553(1)	810(2)	33(1)
C(26)	2819(1)	170(1)	-429(2)	26(1)
C(27)	2130(1)	-29(1)	347(2)	25(1)
C(28)	1541(1)	400(1)	-537(2)	23(1)
C(29)	1681(1)	1152(1)	-215(2)	25(1)
C(30)	1884(1)	1565(1)	-1831(2)	31(1)
C(31)	2031(1)	2244(1)	-1465(3)	39(1)

C(32)	1983(1)	2507(1)	494(3)	39(1)
C(33)	1786(1)	2098(1)	2112(2)	37(1)
C(34)	1635(1)	1419(1)	1773(2)	30(1)
C(35)	1408(1)	231(1)	-2724(2)	26(1)
C(36)	1244(1)	66(1)	-4409(2)	32(1)

Table A14.2 - Anisotropic displacement parameters ($Å^2$ x 10^3) for **14**

	U11	**U22**	**U33**	**U23**	**U13**	**U12**
C(1)	34(1)	31(1)	53(1)	5(1)	14(1)	6(1)
C(2)	44(1)	44(1)	70(1)	18(1)	28(1)	15(1)
C(3)	33(1)	48(1)	100(2)	31(1)	22(1)	8(1)
O(17)	22(1)	26(1)	23(1)	2(1)	2(1)	0(1)
C(4)	28(1)	42(1)	110(2)	22(1)	-7(1)	-8(1)
C(5)	29(1)	36(1)	67(1)	7(1)	-9(1)	-3(1)
C(6)	22(1)	25(1)	45(1)	8(1)	2(1)	4(1)
C(7)	24(1)	26(1)	30(1)	2(1)	-1(1)	2(1)
C(8)	21(1)	23(1)	21(1)	1(1)	1(1)	-1(1)
C(9)	20(1)	24(1)	26(1)	-2(1)	2(1)	-1(1)
C(10)	41(1)	26(1)	27(1)	2(1)	7(1)	0(1)
C(11)	54(1)	27(1)	42(1)	7(1)	12(1)	-1(1)
C(12)	41(1)	25(1)	54(1)	-6(1)	10(1)	-5(1)
C(13)	35(1)	35(1)	38(1)	-11(1)	-2(1)	-2(1)
C(14)	31(1)	31(1)	30(1)	-4(1)	-4(1)	0(1)
C(15)	26(1)	24(1)	26(1)	2(1)	2(1)	0(1)
C(16)	42(1)	34(1)	25(1)	-2(1)	0(1)	-3(1)
C(21)	31(1)	38(1)	39(1)	-4(1)	0(1)	-1(1)
C(22)	37(1)	47(1)	48(1)	-2(1)	11(1)	-1(1)

C(23)	29(1)	38(1)	63(1)	1(1)	6(1)	-4(1)
O(37)	23(1)	25(1)	26(1)	2(1)	0(1)	1(1)
C(24)	30(1)	34(1)	59(1)	-3(1)	-5(1)	-6(1)
C(25)	30(1)	30(1)	40(1)	-2(1)	-4(1)	0(1)
C(26)	24(1)	22(1)	33(1)	3(1)	-3(1)	3(1)
C(27)	24(1)	23(1)	28(1)	3(1)	-2(1)	1(1)
C(28)	22(1)	23(1)	23(1)	1(1)	0(1)	0(1)
C(29)	20(1)	23(1)	30(1)	1(1)	-3(1)	1(1)
C(30)	32(1)	28(1)	34(1)	3(1)	-1(1)	-1(1)
C(31)	39(1)	28(1)	49(1)	10(1)	-4(1)	-5(1)
C(32)	38(1)	23(1)	57(1)	0(1)	-12(1)	-3(1)
C(33)	38(1)	32(1)	40(1)	-8(1)	-10(1)	2(1)
C(34)	29(1)	28(1)	33(1)	-1(1)	-4(1)	1(1)
C(35)	25(1)	25(1)	28(1)	2(1)	0(1)	-1(1)
C(36)	35(1)	35(1)	26(1)	1(1)	-1(1)	-4(1)

Table A15.1 - Atomic coordinates and equivalent isotropic displacement parameters ($Å^2$ x 10^3) for **15**

	x	y	z	Ueq
C(1)	4469(3)	1878(2)	2958(1)	41(1)
C(2)	4521(2)	1585(1)	2299(1)	32(1)
C(3)	4614(2)	1229(1)	1459(1)	25(1)
O(1)	4551(2)	2066(1)	955(1)	32(1)
C(4)	3264(2)	609(1)	1247(1)	28(1)
C(5)	1791(3)	1093(2)	1329(2)	39(1)
C(6)	3409(2)	-293(1)	993(1)	28(1)
C(7)	2113(3)	-940(2)	771(2)	47(1)
C(8)	4884(2)	-706(1)	904(1)	26(1)
O(2)	5005(2)	-1517(1)	623(1)	35(1)
C(9)	6232(2)	-149(1)	1136(1)	27(1)
C(10)	7680(3)	-656(2)	1050(2)	41(1)
C(11)	6119(2)	751(1)	1400(1)	27(1)
C(12)	7428(2)	1378(2)	1626(2)	42(1)
C(21)	-34(2)	2773(2)	2748(1)	34(1)
C(22)	-59(2)	3384(1)	2258(1)	26(1)
C(23)	-118(2)	4123(1)	1621(1)	23(1)
O(21)	24(2)	5033(1)	2026(1)	30(1)
C(24)	-1634(2)	4060(1)	1176(1)	25(1)
C(25)	-2928(3)	4230(2)	1689(2)	36(1)
C(26)	-1790(2)	3869(1)	385(1)	25(1)
C(27)	-3273(2)	3797(2)	-78(1)	39(1)
C(28)	-462(2)	3739(1)	-78(1)	25(1)
O(22)	-620(2)	3624(1)	-819(1)	34(1)
C(29)	1033(2)	3762(1)	327(1)	25(1)
C(30)	2294(3)	3562(2)	-200(1)	35(1)
C(31)	1215(2)	3968(1)	1115(1)	24(1)
C(32)	2695(2)	4060(2)	1575(1)	34(1)

Table A15.2 - Anisotropic displacement parameters ($Å^2$ x 10^3) for **15**

	U11	U22	U33	U23	U13	U12
C(1)	58(2)	39(1)	27(1)	-5(1)	6(1)	-1(1)
C(2)	39(1)	25(1)	30(1)	0(1)	3(1)	1(1)
C(3)	32(1)	20(1)	22(1)	1(1)	2(1)	2(1)
O(1)	46(1)	23(1)	26(1)	3(1)	5(1)	6(1)
C(4)	29(1)	32(1)	21(1)	1(1)	4(1)	0(1)
C(5)	29(1)	47(2)	42(1)	-5(1)	7(1)	6(1)
C(6)	31(1)	30(1)	22(1)	1(1)	4(1)	-5(1)
C(7)	49(1)	45(1)	48(2)	-8(1)	10(1)	-20(1)
C(8)	42(1)	21(1)	17(1)	5(1)	4(1)	0(1)
O(2)	57(1)	22(1)	26(1)	-1(1)	6(1)	2(1)
C(9)	31(1)	28(1)	20(1)	3(1)	0(1)	6(1)
C(10)	38(1)	41(1)	44(1)	-5(1)	-5(1)	16(1)
C(11)	30(1)	27(1)	23(1)	2(1)	-1(1)	2(1)
C(12)	33(1)	38(1)	53(2)	-8(1)	-3(1)	-5(1)
C(21)	47(1)	29(1)	27(1)	4(1)	1(1)	-7(1)
C(22)	30(1)	27(1)	21(1)	-3(1)	2(1)	-2(1)
C(23)	30(1)	20(1)	20(1)	-2(1)	3(1)	-1(1)
O(21)	43(1)	22(1)	25(1)	-4(1)	6(1)	-3(1)
C(24)	27(1)	21(1)	27(1)	2(1)	5(1)	2(1)
C(25)	32(1)	41(1)	36(1)	1(1)	10(1)	2(1)
C(26)	29(1)	19(1)	28(1)	1(1)	-1(1)	-2(1)
C(27)	35(1)	43(1)	38(1)	2(1)	-6(1)	-5(1)
C(28)	40(1)	13(1)	23(1)	-1(1)	4(1)	0(1)
O(22)	52(1)	28(1)	22(1)	-4(1)	2(1)	-1(1)
C(29)	33(1)	17(1)	27(1)	1(1)	7(1)	3(1)
C(30)	39(1)	35(1)	33(1)	1(1)	14(1)	9(1)
C(31)	28(1)	17(1)	26(1)	3(1)	3(1)	1(1)
C(32)	28(1)	36(1)	37(1)	1(1)	0(1)	1(1)

Table A16.1 - Atomic coordinates and equivalent isotropic displacement parameters ($Å^2$ x 10^3) for **16**

	x	y	z	Ueq
O(1)	4972(2)	3851(1)	-5079(2)	27(1)
O(2)	2961(2)	4510(1)	1289(2)	22(1)
C(1)	925(3)	4120(1)	-1794(3)	22(1)
C(2)	2469(3)	4480(1)	-3163(3)	23(1)
C(3)	4263(3)	3945(1)	-3407(3)	19(1)
C(4)	5206(3)	3543(1)	-1475(3)	21(1)
C(5)	3612(3)	3209(1)	-117(3)	20(1)
C(6)	1996(3)	3833(1)	280(3)	18(1)
C(7)	450(3)	3514(1)	1602(3)	23(1)
C(8)	-786(4)	3306(2)	2714(4)	31(1)

Table A16.2 - Anisotropic displacement parameters ($Å^2$ x 10^3) for **16**

	U11	U22	U33	U23	U13	U12
O(1)	27(1)	40(1)	16(1)	-1(1)	5(1)	1(1)
O(2)	26(1)	23(1)	15(1)	-3(1)	1(1)	-2(1)
C(1)	21(1)	27(1)	17(1)	-1(1)	1(1)	3(1)
C(2)	27(1)	28(1)	14(1)	3(1)	3(1)	4(1)
C(3)	21(1)	20(1)	16(1)	-2(1)	4(1)	-4(1)
C(4)	21(1)	25(1)	16(1)	1(1)	1(1)	4(1)
C(5)	25(1)	19(1)	15(1)	1(1)	1(1)	1(1)
C(6)	20(1)	20(1)	15(1)	-1(1)	3(1)	-1(1)
C(7)	24(1)	28(1)	17(1)	0(1)	0(1)	0(1)
C(8)	29(1)	41(1)	23(1)	1(1)	4(1)	-5(1)

Table A17.1 - Atomic coordinates and equivalent isotropic displacement parameters ($Å^2$ x 10^3) for **17**

	x	y	z	Ueq
Br(1)	5877(1)	2317(1)	1194(1)	21(1)
C(1)	4246(1)	754(1)	4092(1)	27(1)
C(2)	4308(1)	692(1)	2727(1)	17(1)
C(3)	4318(1)	682(1)	1051(1)	11(1)
O(1)	3553(1)	1447(1)	595(1)	15(1)
C(4)	5410(1)	996(1)	472(1)	12(1)
O(2)	3453(1)	1547(1)	-2475(1)	22(1)
H(1A)	3520(1)	1480(1)	-533(2)	27(1)
H(2A)	3639(2)	2202(2)	-2936(2)	44(1)
H(1)	4197(2)	803(2)	5303(2)	58(1)

Table A17.2 - Anisotropic displacement parameters ($Å^2$ x 10^3) for **17**

	U11	U22	U33	U23	U13	U12
Br(1)	20(1)	15(1)	29(1)	-7(1)	1(1)	-4(1)
C(1)	35(1)	35(1)	12(1)	-2(1)	2(1)	0(1)
C(2)	20(1)	20(1)	10(1)	0(1)	0(1)	0(1)
C(3)	12(1)	12(1)	10(1)	0(1)	0(1)	1(1)
O(1)	15(1)	15(1)	16(1)	0(1)	0(1)	4(1)
C(4)	12(1)	12(1)	13(1)	-1(1)	0(1)	0(1)
O(2)	24(1)	24(1)	19(1)	3(1)	-3(1)	-5(1)
H(1A)	29(1)	29(1)	22(1)	2(1)	-2(1)	5(1)
H(2A)	52(1)	35(1)	46(1)	8(1)	1(1)	-11(1)
H(1)	78(1)	78(1)	17(1)	-3(1)	3(1)	3(2)

Lectures, Meetings and Conferences Attended

APPENDIX B

B1 Meetings and conferences attended

The following meetings and conferences were attended during the period of tuition for this thesis:

14/11/96	BCA CCG Autumn meeting. Daresbury Laboratory, Manchester.
6/4/97 - 14/4/97	BCA Intensive Teaching School in X-ray Structure Analysis. University of Durham, Durham.
14/4/97 - 17/4/97	BCA Spring meeting. University of Leeds, Leeds. Presented poster entitled : Azides as Hydrogen Bond Acceptors.
24/8/97 - 28/8/97	ECM-17. I. S. T. Lisboa, Portugal. Presented poster entitled : Azides as Hydrogen Bond Acceptors.
5/4/98 - 8/4/98	BCA Spring Meeting, University of St. Andrews, St. Andrews. Presented poster entitled : C-H --- O and C-H --- π in the Presence of O-H --- O. Designing Supramolecular Synthons.
28/5/98 - 7/6/98	International School of Crystallography 27th Course - Implications of Molecular and Materials Structure for New Technologies, Erice, Sicily. Presented poster entitled : C-H --- O and C-H --- π in the Presence of O-H --- O. Designing Supramolecular Synthons.
15/10/98 - 16/10/98	UK Neutron and Muon Young researchers meeting, Coesners House, Abingdon. Presented lecture entitled : Weak Hydrogen Bonding, Database Analysis and Structural Studies.

16/10/98 - 17/10/98	UK Neutron and Muon Users Meeting, Rutherford Appleton Laboratories, Chilton.
18/11/98	BCA CCG Autumn meeting, ISIS, Chilton.
3/8/99 - 14/8/99	IUCr XVIII Congress and General Assembly, Glasgow. Presented poster entitled Analysis of Probability of Formation of Intramolecular Hydrogen Bonded Rings.

B2 Departmental seminars

The following is a list of colloquia given by invited speakers at the Department of Chemistry at the University of Durham during the tuition period of this thesis. Those marked with an asterisk were attended by the author.

1996

October 9 Professor G. Bowmaker, University Aukland, NZ
Coordination and Materials Chemistry of the Group 11 and Group 12 Metals : Some Recent Vibrational and Solid State NMR Studies.

October 14 Professor A. R. Katritzky, University of Gainesville, University of Florida, USA. Recent Advances in Benzotriazole Mediated Synthetic Methodology.

October 16 Professor Ojima, Guggenheim Fellow, State University of New York at Stony Brook. Silylformylation and Silylcarbocyclisations in Organic Synthesis.*

October 22 Professor Lutz Gade, Univ. Wurzburg, Germany. Organic transformations with Early-Late Heterobimetallics: Synergism and Selectivity.

October 22 Professor B. J. Tighe, Department of Molecular Sciences and Chemistry, University of Aston. Making Polymers for Biomedical Application - can we meet Nature's Challenge? Joint lecture with the Institute of Materials.

October 23 Professor H. Ringsdorf (Perkin Centenary Lecture), Johannes Gutenberg-Universitat, Mainz, Germany. Function Based on Organisation.

October 29 Professor D. M. Knight, Department of Philosophy, University of Durham. The Purpose of Experiment - A Look at Davy and Faraday.

October 30 Dr Phillip Mountford, Nottingham University. Recent Developments in Group IV Imido Chemistry.*

November 6 Dr Melinda Duer, Chemistry Department, Cambridge. Solid-state NMR Studies of Organic Solid to Liquid-crystalline Phase Transitions.*

November 12 Professor R. J. Young, Manchester Materials Centre, UMIST. New Materials - Fact or Fantasy? Joint Lecture with Zeneca & RSC.

November 13 Dr G. Resnati, Milan. Perfluorinated Oxaziridines: Mild Yet Powerful Oxidising Agents.

November 18 Professor G. A. Olah, University of Southern California, USA. Crossing Conventional Lines in my Chemistry of the Elements.

November 19 Professor R. E. Grigg, University of Leeds. Assembly of Complex Molecules by Palladium-Catalysed Queueing Processes.

November 20 Professor J. Earnshaw, Department of Physics, Belfast. Surface Light Scattering: Ripples and Relaxation.*

November 27 Dr Richard Templer, Imperial College, London. Molecular Tubes and Sponges.

December 3 Professor D. Phillips, Imperial College, London. "A Little Light Relief".

December 4 Professor K. Muller-Dethlefs, York University. Chemical Applications of Very High Resolution ZEKE Photoelectron Spectroscopy.

December 11 Dr Chris Richards, Cardiff University. Sterochemical Games with Metallocenes.

1997

January 15 Dr V. K. Aggarwal, University of Sheffield. Sulfur Mediated Asymmetric Synthesis.*

January 16 Dr Sally Brooker, University of Otago, NZ. Macrocycles: Exciting yet Controlled Thiolate Coordination Chemistry.

January 21 Mr D. Rudge, Zeneca Pharmaceuticals. High Speed Automation of Chemical Reactions.

January 22 Dr Neil Cooley, BP Chemicals, Sunbury. Synthesis and Properties of Alternating Polyketones.

January 29 Dr Julian Clarke, UMIST. What can we learn about polymers and biopolymers from computer-generated nanosecond movie-clips?

February 4 Dr A. J. Banister, University of Durham. From Runways to Non-metallic Metals - A New Chemistry Based on Sulphur.

February 5 Dr A. Haynes, University of Sheffield. Mechanism in Homogeneous Catalytic Carbonylation.

February 12 Dr Geert-Jan Boons, University of Birmingham. New Developments in Carbohydrate Chemistry.

February 18 Professor Sir James Black, Foundation/King's College London. My Dialogues with Medicinal Chemists.

February 19 Professor Brian Hayden, University of Southampton. The Dynamics of Dissociation at Surfaces and Fuel Cell Catalysts.*

February 25 Professor A. G. Sykes, University of Newcastle. The Synthesis, Structures and Properties of Blue Copper Proteins.

February 26 Dr Tony Ryan, UMIST. Making Hairpins from Rings and Chains.*

March 4 Professor C. W. Rees, Imperial College. Some Very Heterocyclic Chemistry.

March 5 Dr J. Staunton FRS, Cambridge University. Tinkering with biosynthesis: towards a new generation of antibiotics.

March 11 Dr A. D. Taylor, ISIS Facility, Rutherford Appleton Laboratory. Expanding the Frontiers of Neutron Scattering.*

March 19 Dr Katharine Reid, University of Nottingham. Probing Dynamical Processes with Photoelectrons.*

October 8 Professor E Atkins, Department of Physics, University of Bristol. Advances in the control of architecture for polyamides: from nylons to genetically engineered silks to monodisperse oligoamides.

October 15 Dr R M Ormerod, Department of Chemistry, Keele University. Studying catalysts in action.*

October 21 Professor A F Johnson, IRC, Leeds. Reactive processing of polymers: science and technology.

October 22 Professor R J Puddephatt (RSC Endowed Lecture), University of Western Ontario. Organoplatinum chemistry and catalysis.*

October 23 Professor M R Bryce, University of Durham, Inaugural Lecture. New Tetrathiafulvalene Derivatives in Molecular, Supramolecular and Macromolecular Chemistry: controlling the electronic properties of organic solids.*

October 29 Professor R Peacock, University of Glasgow. Probing chirality with circular dichroism.

October 28 Professor A P de Silva, The Queen's University, Belfast. Luminescent signalling systems".

November 5 Dr M Hii, Oxford University. Studies of the Heck reaction.

November 11 Professor V Gibson, Imperial College, London. Metallocene polymerisation.

November 12 Dr J Frey, Department of Chemistry, Southampton University. Spectroscopy of liquid interfaces: from bio-organic chemistry to atmospheric chemistry.

November 19 Dr G Morris, Department of Chemistry, Manchester Univ. Pulsed field gradient NMR techniques: Good news for the Lazy and DOSY.*

November 20 Dr L Spiccia, Monash University, Melbourne, Australia. Polynuclear metal complexes.

November 25 Dr R Withnall, University of Greenwich. Illuminated molecules and manuscripts.

November 26 Professor R W Richards, University of Durham, Inaugural Lecture. A random walk in polymer science.*

December 2 Dr C J Ludman, University of Durham. Explosions.*

December 3 Professor A P Davis, Department. of Chemistry, Trinity College Dublin. Steroid-based frameworks for supramolecular chemistry.*

December 10 Sir G Higginson, former Professor of Engineering in Durham and retired Vice-Chancellor of Southampton Univ. 1981 and all that.

December 10 Professor M Page, Department of Chemistry, University of Huddersfield. The mechanism and inhibition of beta-lactamases.

1998

January 14 Professor D Andrews, University of East Anglia. Energy transfer and optical harmonics in molecular systems

January 20 Professor J Brooke, University of Lancaster. What's in a formula? Some chemical controversies of the 19th century

January 21 Professor D Cardin, University of Reading.

January 27 Professor R Jordan, Dept. of Chemistry, Univ. of Iowa, USA. Cationic transition metal and main group metal alkyl complexes in olefin polymerisation.

January 28 Dr S Rannard, Courtaulds Coatings (Coventry). The synthesis of dendrimers using highly selective chemical reactions.

February 3 Dr J Beacham, ICI Technology. The chemical industry in the 21st century

February 4 Professor P Fowler, Department of Chemistry, Exeter University. Classical and non-classical fullerenes

February 11 Professor J Murphy, Dept of Chemistry, Strathclyde University

February 17 Dr S Topham, ICI Chemicals and Polymers. Perception of environmental risk; The River Tees, two different rivers

February 18 Professor G Hancock, Oxford University. Surprises in the photochemistry of tropospheric ozone

February 24 Professor R Ramage, University of Edinburgh. The synthesis and folding of proteins

February 25 Dr C Jones, Swansea University. Low coordination arsenic and antimony chemistry.

March 4 Professor T C B McLeish, IRC of Polymer Science Technology, Leeds University. The polymer physics of pyjama bottoms (or the novel rheological characterisation of long branching in entangled macromolecules).

March 11 Professor M J Cook, Dept of Chemistry, UEA. How to make phthalocyanine films and what to do with them.*

March 17 Professor V Rotello, University of Massachusetts, Amherst. The interplay of recognition & redox processes - from flavoenzymes to devices.

March 18 Dr J Evans, Oxford University. Materials which contract on heating (from shrinking ceramics to bullet proof vests).*

October 7 Dr S Rimmer, Ctr Polymer, University of Lancaster. New Polymer Colloids.

October 9 Professor M F Hawthorne, Department Chemistry & Biochemistry, UCLA, USA. RSC Endowed Lecture.

October 21 Professor P Unwin, Department of Chemistry, Warwick University. Dynamic Electrochemistry: Small is Beautiful.

October 23 Professor J C Scaiano, Department of Chemistry, University of Ottawa, Canada. In Search of Hypervalent Free Radicals, RSC Endowed Lecture.

October 26 Dr W Peirs, University of Calgary, Alberta, Canada. Reactions of the Highly Electrophilic Boranes HB(C6F5)2 and B(C6F5)3 with Zirconium and Tantalum Based Metallocenes.

October 27 Professor A Unsworth, University of Durham. What's a joint like this doing in a nice girl like you? In association with The North East Polymer Association.

October 28 Professor J P S Badyal, Department of Chemistry, University of Durham. Tailoring Solid Surfaces, Inaugural Lecture.*

November 4 Dr N Kaltscoyannis, Department of Chemistry, UCL, London. Computational Adventures in d & f Element Chemistry.*

November 3 Dr C J Ludman, Chemistry Department, University of Durham. Bonfire night Lecture

November 10 Dr J S O Evans, Chemistry Department, University of Durham. Shrinking Materials.*

November 11 Dr M Wills, Department of Chemistry, University of Warwick. New Methodology for the Asymmetric Transfer Hydrogen of Ketones.

November 12 Professor S Loeb, University of Windsor, Ontario, Canada. From Macrocycles to Metallo-Supramolecular Chemistry.*

November 17 Dr J McFarlane. Nothing but Sex and Sudden Death!

November 18 Dr R Cameron, Department of Materials Science & Metallurgy, Cambridge University. Biodegradable Polymers.*

November 24 Dr B G Davis, Department of Chemistry, University of Durham. Sugars and Enzymes.

December 1 Professor N Billingham, University of Sussex. Plastics in the Environment - Boon or Bane. In association with The North East Polymer Association.

December 2 Dr M Jaspers, Department of Chemistry, University of Aberdeen. Bioactive Compounds Isolated from Marine Inverterates and Cyanobacteria.*

December 9 Dr M Smith Department. of Chemistry, Warwick University. Multinuclear solid-state magnetic resonance studies of nanocrystalline oxides and glasses.

January 19 Dr J Mann, University of Reading. The Elusive Magic Bullet and Attempts to find it?.

January 20 Dr A Jones, Department of Chemistry, University of Edinburgh. Luminescence of Large Molecules: from Conducting Polymers to Coral Reefs.

January 27 Professor K Wade, Department of Chemistry, University of Durham. Foresight or Hindsight? Some Borane Lessons and Loose Ends.

February 3 Dr C Schofield, University of Oxford. Studies on the Stereoelectronics of Enzyme Catalysis.

February 9 Professor D J Cole-Hamilton, St. Andrews University. Chemistry and the Future of life on Earth.

February 10 Dr C Bain, University of Oxford. Surfactant Adsorption and Marangoni Flow at Expanding Liquid Surfaces.

February 17 Dr B Horrocks, Department of Chemistry, Newcastle University. Microelectrode techniques for the Study of Enzymes and Nucleic Acids at Interfaces.

February 23 Dr C Viney, Heriot-Watt. Spiders, Slugs And Mutant Bugs.

February 24 Dr. A-K Duhme, University of York. Bioinorganic Aspects of Molybdenum Transport in Nitrogen-Fixing Bacteria.*

March 3 Professor B Gilbert, Department of Chemistry, University of York. Biomolecular Damage by Free Radicals: New Insights through ESR Spectroscopy.

March 9 Dr Michael Warhurst, Chemical Policy issues, Friends of the Earth. Is the Chemical Industry Sustainable?

March 10 Dr A Harrison, Department of Chemistry, The University of Edinburgh. Designing model magnetic materials.*

March 17 Dr J Robertson, University of Oxford. Recent Developments in the Synthesis of Heterocyclic Natural Products.*

May 11 Dr John Sodeau, University of East Anglia. Ozone Holes and Ozone Hills.

May 12 Dr Duncan Bruce, Exeter University. The Synthesis and Characterisation of Liquid-Crystalline Transition Metal Complexes.